CO-REMOVAL OF PHENOL AND CYANIDE FROM WASTEWATER BY SIMULTANEOUS ADSORPTION AND BIODEGRADATION

A DISSERTATION

Submitted in the partial fulfillment of the

requirements for the award of the degree

of

MASTER OF TECHNOLOGY

in

CHEMICAL ENGINEERING

(With specialization in Industrial Pollution Abatement)

By

PRIYA SENGUPTA

Under the guidance of

Dr. C. Balomajumder

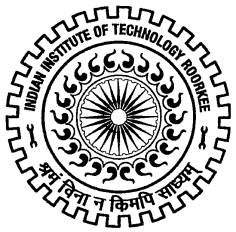

DEPARTMENT OF CHEMICAL ENGINEERING

INDIAN INSTITUTE OF TECHNOLOGY ROORKEE

ROORKEE – 247667 (INDIA)

INDIAN INSTITUTE OF TECHNOLOGY ROORKEE

ROORKEE

CANDIDATE'S DECLARATION

I hereby declare that the work, which is being presented in this seminar report entitled **"CO-REMOVAL OF PHENOL AND CYANIDE FROM WASTEWATER BY SIMULTANEOUS ADSORPTION AND BIODEGRADATION"** in partial fulfilment of the requirements for the award of the degree of Master of Technology in Chemical Engineering with specialization in **Industrial Pollution Abatement (IPA),** and submitted in the Department of Chemical Engineering of Indian Institute of Technology Roorkee, India, is an authentic record of my own work carried out during the period from June 2013 to june 2014, under the supervision of **Dr. C. Balomajumder**, Professor, Department of Chemical Engineering, Indian Institute of Technology Roorkee India.

The matter embodied in this dissertation has not been submitted by me for the award of any other degree of this or any other Institute/University.

Date:

Place: Roorkee (**PRIYA SENGUPTA)**

CERTIFICATE

This is to certify that the above statement made by the candidate is correct to the best of my knowledge and belief.

DR. C. BALOMAJUMDER
Professor
Department of Chemical Engineering
Indian Institute of Technology Roorkee
Roorkee-247667, India

ACKNOWLEDGEMENTS

I would like to express my deep sense of gratitude, thankfulness and indebtedness to my revered guide **Dr. C. Balomajumder**, Professor, Department of Chemical Engineering, Indian Institute of Technology Roorkee, India, who provided whole hearted co-operation, never ending inspirations and guidance, all blended with the personal touch throughout the duration of this work. His invaluable suggestions and through discussions have immensely contributed towards the completion of this work.

I take this opportunity to put on record my respects to **Dr. V.K. Agarwal**, Head of Department of Chemical Engineering, Indian Institute of Technology Roorkee, for providing various facilities during course of the present investigation.

I am greatly indebted to my seniors **Mrs. Bhumica Agarwal, Ms. Mousumi Saha Podder, Mrs. Neetu Sharma, Mr. Ankur Gupta, Mr. Tej Pratap Singh** and my friends **Mr. Mandeep Sharma, Mr. Aash Mohammad, Mr. Ashutosh Kumar** and all others for their enthusiastic support, encouragement and help, made me come up with this report.

I would also like to thank my hostel mates **Ms. Priya Yadav, Ms. Anjali Payal, Ms. Susmita Singh** for their valuable emotional support. The last but not least I am grateful to my family members and my sister **Mrs. Jaya Sen** for her love, suggestions and moral support without which I would not have achieved this goal.

PRIYA SENGUPTA

ABSTRACT

Recent industrial advances has led to an increase in pollution be it air, water or any other kind of pollution. Industries like iron and steel plant, electroplating, coke industries discharge a good deal of phenol and cyanide. These pollutants cause many kinds of skin problems, gastrointestinal disorders and even death. The present work concentrates on treatment of industrial discharge containing phenol and cyanide by simultaneous adsorption and biodegradation. The simulated synthetic wastewater is treated by various biosorbents in batch as well as continuous reactors for the co-removal of phenol and cyanide using simultaneous adsorption and biodegradation. Influence of various experimental parameters like pH, adsorbent dose, contact time, temperature and initial concentration have been studied and these parameters have also been optimised for increase in removal percentage.

The mathematical modelling has also been done for the simultaneous adsorption and biodegradation process by using different adsorption isotherms, kinetic and thermodynamic models. The experimental data has been modelled using various multicomponent isotherm models. SAB process of phenol and cyanide are dependent of pH of the process. The optimum pH for the process for all the adsorbents comes out to be 7. The bacteria showed no visible growth in extreme acidic and extreme alkaline pH. Both pseudo first order and second order models were best fitted to the SAB process with all the three adsorbents. The equilibrium isotherms that were best fit were either non modified Langmuir or extended Langmuir for phenol adsorption onto the three adsorbents and the isotherms that best fitted cyanide data was modified Langmuir isotherm. There is not much change in the SAB process with increase in temperature. ΔG^{o} ***is negative showing the feasibility of the process. For rice husk SAB of phenol is an endothermic process with an increase in randomness at the solid/liquid interface but SAB of cyanide is an exothermic process with decrease in randomness at the solid/liquid interface. For corn husk leaves and egg shells SAB of both phenol and cyanide is an exothermic process with a decrease of randomness at the solid/liquid interface.***

RTD studies were also performed on the reactor which showed its behaviour to be close to plug flow. Column studies were carried out taking rice husk and granular activated carbon. Effective bed contact time of 5 h showed a higher removal percentage and column capacity for simultaneous adsorption and biodegradation in the GAC column. The

percentage removal of phenol and cyanide for the continuous GAC column by simultaneous adsorption and biodegradation was estimated as 99.99 %and 98.85 %. The percentage removal for co-adsorption of phenol and cyanide by regenerated GAC columns were 64.24 % and 73.12 %. The breakthrough curve obtained showed a better fit to the Adams Bohart and Wolborska Model. The percentage removal of phenol and cyanide for the continuous rice husk column by simultaneous adsorption and biodegradation was estimated as 81.43 % and 90.80 %.

CONTENTS

LIST OF FIGURES

LIST OF TABLES

NOMENCLATURE

SYMBOLS

A_i	Area under the curve plotted between normalized concentration and time for component 'i'
B	Langmuir Constant
C_0	Initial Concentration of the pollutant (mg/L)
C_a	adsorbed pollutant concentration per litre (mg/L)
C_e	Concentration of pollutant at equilibrium (mg/L)
D	axial diffusion coefficient (m^2/min)
E	exit age distribution, $time^{-1}$
ΔG^0	standard free energy change of sorption (J/mol)
ΔH^0	standard enthalpy change (kJ/mol)
k_1	Rate constant for pseudo first order kinetic model (h^{-1})
k_2	Rate constant for pseudo second order kinetic model (mg g^{-1} h^{-1})
k_{AB}	kinetic constant (L/ mg min)
K_F	Freundlich Constant
k_{Th}	Thomas Constant
k_{YN}	rate constant (min^1)
M	Mass of adsorbent (g)
M	units of tracer introduced (g or moles)
$m_{i,total}$	Total amount of component 'i' sent to the column, mg
N	Number of observations
n	Freundlich Constant
q_e	Uptake capacity of the adsorbent at equilibrium (mg/g)
$q_{eq,i}$	Equilibrium capacity for component 'i'
$q_{e,i}$	Equilibrium monolayer capacity for 'i' component, (mg/g)
$q_{i,total}$	Total amount of component 'i' adsorbed by the column, mg
Q	volumetric flow rate of the fluid, m^3/min or mL/min
Q_0	Langmuir Constant
R_L	separation factor
R	gas constant (J/ mol. K)
R^2	Correlation Constant
ΔS^0	standard entropy change (kJ /mol. K)
T	Temperature (K)
t_{total}	Total flow time, (min)
U_0	superficial velocity (m/ min)
V	Volume of the solution (L)
V	working volume of the reactor, m^3 or mL
V_{eff}	Effluent Volume, (mL)
X	Mass of packing material in the column (g)
x_i	Freundlich constants for 'i' component
y_i	Freundlich constants for 'i' component

Z	**height of the column (m)**
z_i	**Freundlich constants for 'i' component**

GREEK SYMBOLS

η_i	**Correction factor for 'i' component.**
σ^2	**Variance**
β_a	**Kinetic coefficient of external mass transfer (min^{-1})**
β_0	**external mass transfer coefficient with negligible D (min^{-1})**
τ	**Mean residence time, min or h**

SUBSCRIPTS

o,i **Initial**

e **Equilibrium**

a **Adsorbed**

CHAPTER 1

INTRODUCTION

Dawn of industrialization and mechanization of human life has paved a road towards the end of peace between the Mother Nature and its children. Industrial effluents and waste discharged from human activities does produces bodily wastes which not only is the causes water pollution by entering in rivers, lakes and other surface waters but also cause air, soil and other types of pollution. The increase in solids suspended in water (turbidity), increases the concentration of microorganisms e.g. viruses and bacteria which leads to potential health impacts as well as nutrient loading which causes eutrophication leading to water pollution thereby destroying the aesthetics of surroundings. Organic waste and farm waste such as sewage does impose high oxygen demands on the receiving water which causes oxygen depletion that has severe impacts on the whole eco-system. Industries do discharge a large variety of pollutants in their wastewater which includes heavy metals, oils, organic toxins, solids and nutrients. Discharges also do have thermal effects, especially those from power stations, and these also reduce the availability of oxygen. Variety of pollutants are also discharged in water bodies which includes suspended solids, , organics , heavy metals inorganic pollutants etc. thereby causing a good deal of water pollution. Phenols and cyanides

discharged in the environment also have serious impacts on the humans as well as flora and fauna.

Phenols which are weakly biodegradable pollutants reach human life by bio accumulation in food chain. Exposure to phenol can cause skin problems, , headache, gastrointestinal disorders eye injuries, , lung, kidney central nervous system, liver and heart damage which finally leads to death. Cyanides are a type of inorganic pollutants that are generally used in mining, , iron and steel industries metal electroplating. An exposure to even small amount of highly toxic cyanide causes, thyroid gland enlargement, headache, heart attacks, breathing problems and is even fatal to humans.

Various industries that discharge phenol and cyanide are:

- Electroplating anodizing industry
- Petroleum Oil Refinery
- Integrated Iron and Steel plant
- Textile, woollen and dye industry
- Common Effluent Treatment Plan

1.1GENERAL:

1.1.1PHENOL:

1.1.1.1PROPERTIES AND NATURAL OCCURRENCE:

Listed in the Priority Pollutants by the US Environmental Protection Agency (US EPA), phenol is a colourless, crystalline substance, possesses a characteristic odour and is soluble in water and organic solvents. It is extracted from coal tar and is formed by high quantities of plant cumene transformation. It is also obtained by reacting chlorobenzene and sodium hydroxide, oxidation of toluene and synthesis from benzene and propylene. Hydroxybenzene (phenol) is also formed as the result of chemical reactions occurring in the atmosphere in condensed water vapour that forms clouds and is formed during natural processes like biosynthesis in plants or organic matter decomposition. These components also penetrate the ecosystem through the drainage off industrial sewage and municipal water to surface water.

In the recent years the phenol concentration is rapidly increasing in the environment which is a serious matter of concern as the toxic influence of phenols and its derivatives cause histopathological changes, mutagenicity and carcinogenicity (Phenols-Sources and Toxicity).According to Michalowicz (Phenols-Sources and Toxicity), increased daily exposure of phenol from 10-240 mg per person caused diarrhoea, dark urine, mouth sores,

pain in mouth. Therefore phenol treatment is mandatory before discharging phenol containing industrial effluent in water bodies.

Table 1.1 Properties of Phenol

PROPERTY	
Molecular weight	94.111 g/mol
Density	1.0545 g/cm^3 at 20°C
Physical state	Crystalline solid liquid (8% H_2O by wt)
Colour	Colourless to pink
Boiling point	181.7°C
Melting point	40.98°C
Odour	Distinct aromatic, somewhat sickening sweet
Solubility	1. In water at 25°C – 8.28x10^4 mg/l. 2. Somewhat soluble in water and ethanol, very soluble in ether, miscible with acetone

1.1.2 CYANIDE:

1.1.2.1 PROPERTIES AND NATURAL OCCURRENCE:

Wastewaters generated from electroplating, mining, petroleum industries generally contain free and metal complexes of cyanide. Cyanide generally refers to compounds which have CN group. Natural cyanides are generally produced by some plants, some soil bacteria etc. Cyanide has the property of readily combining with major and trace metals which is why it is used for ore extraction. It also reacts with other chemical elements thereby forming toxic cyanide related compounds. As cyanide is carbon based it also reacts with other carbon based matter including living beings.

FREE CYANIDE:

The cyanide ion (CN^-) and sometimes HCN is termed as free cyanide. Both of these if ingested are very toxic to humans and animals. CN^- ion is the stable form of cyanide, at a pH less than 6 i.e. in acidic range; CN^- readily forms HCN (Adams 1994). HCN readily converts into a gas and is released in the air which is a very noxious gas. Free cyanides also react with other chemical elements to form cyanide complexes.

Free cyanides do form:

- Simple Cyanides: Potassium Cyanide, Sodium Cyanide.
- Complex Cyanides: Iron, cobalt and gold cyanides.

Cyanides are highly harmful to mammals as well as aquatic life. According to Dr. Gerry Heningson (USEPA) HCN concentration above 40- 200 mg/l can prove very harmful to humans, other mammals and to the aquatic life. Cyanide is also included in CERCLA list of priority pollutants [1]. Due to the toxic nature of cyanide it cannot be discharged into the environment without prior treatment. Chronic exposure of humans to cyanide effects primarily on the central nervous system (CNS). Other effects include cardiovascular and respiratory effects, enlarged thyroid gland, and irritation to the eyes and skin. Oral exposure to cassava (a cyanide-containing vegetable) in animals may be associated with malformations in the foetus and low foetal body weights. EPA has classified cyanide as a Group D, not classifiable as to human carcinogenicity.

Table 1.2 Properties of Sodium Cyanide (NaCN)

PROPERTY	
Molecular weight	49.0072 g/mol
Density	1.595 g/cm^3
Physical state	Solid
Colour	White
Boiling point	1496^{0}C
Melting point	563.7^{0}C
Odour	Faint Almond like
Solubility	In water ➢ 48 g/100 ml (10 °C) ➢ 82 g/100 ml (34.7 °C)

1.2 INDUSTRIAL SOURCES:

Phenols and cyanides are found in effluents of a number of industries where they are either used or are generated as waste. Following are the few industries that discharge phenol and cyanide as effluents along with the standards of their discharge as per The Environment (Protection) Rules, 1986 and Ministry of Environment and Forests.

1.2.1 PETROLEUM OIL REFINERY:

Table 1.3 Standards for effluent from petroleum oil refinery: The Environment (Protection) Rules, 1986

EFFLUENT	
pH	6.0-8.5
Oil & Grease	5.0
$BOD_{3\ days,\ 27^oC}$	15.0
COD	125.0
Suspended Solids	20.0
Phenols	0.35
Sulphides	0.5
CN	0.20
TKN	40.0
P	3.0

1.2.2 ELECTROPLATING ANODIZING INDUSTRY:

Table 1.4 Standards for cyanide effluent from electroplating industry, Ministry of Environment and Forests

INDUSTRY	CN^- (mg/l)
Zinc Plating	0.2
Cadmium Plating	0.2
Copper and Tin Plating	0.2
Precious Metal plating	0.2

1.2.3 TEXTILE WOOLLEN AND DYE INDUSTRY:

Table 1.5: Standards for phenol effluent from woollen and dye industry, The Environment (Protection) Rules 1986

INDUSTRY	PHENOL (mg/l)
Composite	5.0

Woollen Mill	
Dye and Dye intermediate	1.0
Textile	1.0

1.2.4 INTEGRATED IRON AND STEEL PLANT:

Table 1.6: Standards for phenol and cyanide discharge from integrated iron and steel plant, Ministry of Environment and forest

	PHENOL(mg/l)	CYANIDE(mg/l)
Coke Oven	1.0	0.2
Blast Furnace	-	0.2

1.2.5 COMMON EFFLUENT TREATMENT PLANT:

Table 1.7: Standards for phenol and cyanide discharge from common effluent treatment plant, Environment (Protection) Rules 1986

PLANT	PHENOL(mg/l)	CYANIDE(mg/l)
Primary Treatment	5.0	2.0
Treated Effluent	1.0	0.2

1.2.6 COKE PLANT EFFLUENT:

Table 1.8: Characteristics and standards of coke plant effluent, M.K. Ghose (2002)

Parameter	Avg.	Tolerance Limit Drinking Water Standards	Tolerance Limit Effluent Water standard
pH	8.28	5.5-8.5	5.5-9
Temperature	30.40	-	40

BOD	80.60	-	30
Phenols	92.82	0.001	1
COD	692.11	-	250
Dissolved Solids	1122.65	500	2100
Ammonical Nitrogen	454.95	-	50
Cyanide	10.3	0.05	0.2

1.3 USES:

1.3.1 PHENOL:

Phenols are used in various industries. It has a wide range of applications. Some of them are listed in the table:

Table 1.9: Applications of phenol

USES	EXAMPLES
Synthetic Resins	➢ Cresols ➢ Resorcinol ➢ Phenol formaldehyde resins ➢ Thermoplastic Resins (Novolacs) ➢ Thermosetting Resins(Resols).
Dyestuff	➢ Anthraquinone dye ➢ Bromophenol blue ➢ Bromocresol green ➢ Cresol Red.
Medical	➢ **Antiseptic**: Inhibits microbe growth. ➢ **Topical Anesthetic**: It numbs skin on contact, Sooth rashes and minor skin irritation.

	➢ **Antipruritic:** Itch reliever ➢ **Blemish Removal:** Removes Scars ➢ **Cosmetic Surgery:** For peeling of face ➢ **Skin Lightening:** Reduces pigmentation
Pesticides	➢ **MALLINCKRODT Phenol (Crystals):** Used as disinfectant ➢ **ACID CARBOLIC PHENOL (Crystals):** Used as disinfectant. ➢ **SUPERTOX:** disinfectant ➢ **CRESOTE DIP:** Insecticide, Miticide ➢ **MOSQUITO LARVAECIDE:**Insecticide, Miticide
Perfumes	➢ Tar like and acrid. ➢ Contains carbolic acid and phenic acid. ➢ Possess very pungent, smoky and acrid scent that is very dry.
Lubricating Oils	As antioxidant additive in oils

1.3.2 CYANIDE:

Cyanide also has a varied application in many industries. Some of them are listed below:

Table 1.10 Industrial applications of cyanide

USES	EXAMPLES
Pesticides and fumigants	Hydrogen Cyanide (HCN)
Electroplating	➢ Zinc Plating ➢ Cadmium Plating ➢ Copper Plating ➢ Precious Metal Plating ➢ Tin Plating
Mining	Gold mining
Dyes	Prussian blue
Synthetic fibres and resins	Acrylonitrile(vinyl cyanide)

1.4 HEALTH HAZARDS:

1.4.1 EXPOSURE ROUTES:

Phenols easily enter the body of an organism via mouth i.e. oral pathway by consuming contaminated ground water supplies, via nose i.e. inhalation by breathing tobacco smoke, via skin i.e. dermal contact by exposure with contaminated water or by many products like lotions, ointments, nose drops etc.

Cyanides basically enter by smoking i.e. via inhalation. Cyanides also enter by drinking or eating cyanide containing water i.e. oral pathway. Dermal pathways are less common in case of cyanides.

1.4.2 EFFECTS OF EXPOSURE ON HUMANS:

1.4.2.1 PHENOL:

1.4.2.1.1 ACUTE EXPOSURE EFFECTS:

Short term exposure of phenol may cause anorexia, dark urine, headache, gastrointestinal effects, inflammation, erythema, cough, wheezing, vomiting.

1.4.2.1.2 CHRONIC EXPOSURE EFFECTS:

Long term exposure of phenol may cause weight loss, salivation, muscle weakness, lung and kidney failure sore throat, mouth ulcers, necrosis, carcinogenic (except humans)

1.4.2.2 CYANIDE:

After exposure, cyanide quickly enters the bloodstream. Small cyanide doses in the body can be changed into thiocyanate, which being less harmful is excreted in urine. Heavy cyanide doses avert cells from using oxygen and eventually the cells die.

1.4.2.2.1 ACUTE EXPOSURE EFFECTS:

Short term exposure of cyanide may cause

- Inhalation exposure to 100 mg/m^3 of cyanide causes death.
- 6 to 49 mg/m^3 of cyanide causes weakness, eye and skin irritation.
- Headache
- Nausea

1.4.2.2.2 CHRONIC EXPOSURE EFFECTS:

Long term exposure of cyanide causes:

- Effects on Central Nervous System: Headaches, numbness, loss of vision acuity.
- Cardiovascular effects on both humans and animals
- Respiratory effects on both human and animals
- Enlargement of thyroid gland
- Oral exposure to Cassava (cyanide containing vegetable) causes malformations in foetus and underdeveloped babies.
- Not classifiable to humans as carcinogenic

1.5 MAXIMUM CONTAMINANT LIMIT (MCL):

1.5.1 PHENOL:

MCL for phenol for industrial effluent discharge is set to be 0.5 mg/l by USEPA, WHO, CPCB India (B. Agarwal et.al).

1.5.2 CYANIDE:

MCL for cyanide for industrial effluent discharge is set to be 0.2 mg/l or 200 ppb by EPA.

CHAPTER 2

THEORY AND EQUATIONS USED

2.1 BATCH STUDIES:

2.1.1 EQUILIBRIUM ISOTHERM:

After a sufficiently long time of contact between adsorbent and waste stream equilibrium is established between the amount of pollutant adsorbed and amount of pollutant remaining in the solution. At equilibrium, the amount of material adsorbed onto the media is estimated using Equation 1.

$$q_e = \frac{(C_0 - C_e)V}{M} \quad (1)$$

Where q_e= Uptake capacity of the adsorbent at equilibrium (mg/g)

C_0= Initial Concentration of the pollutant (mg/L)

C_e= Concentration of pollutant at equilibrium (mg/L)

V= Volume of the solution (L)

M= Mass of adsorbent (g)

The single component models used in this present study are

- Langmuir Isotherm
- Freundlich Isotherm

2.1.1.1 LANGMUIR ISOTHERM:

The Langmuir isotherm is the model representing monolayer chemisorption on the identical sites. Basic assumptions of Langmuir isotherms are:

- It is used for predicting both physisorption and chemisorption
- Each site can adsorb only one pollutant molecule
- Surface molecule have constant heat of adsorption
- Molecules on the surface do not interact with each other.

Basic Langmuir isotherm equation:

$$q_e = \frac{Q_0 b C_e}{1 + b C_e} \quad (2)$$

Where q_e= Equilibrium monolayer uptake (mg/g)

Q_0= Langmuir Constant

b = Langmuir Constant

C_e= Equilibrium concentration of the pollutant (mg/L)

Langmuir constant 'b' also shows the favourability of adsorption by determination of dimensionless separation factor R_L which is estimated by equation 3 (Shen et al. 2009, Liu et al. 2009).

$$R_L = {}^{1}/_{(1 + bC_0)} \quad (3)$$

The nature of adsorption is indicated as

$R_L > 1$ (Unfavorable)

$R_L < 1$ (Favorable)

$R_L = 0$ (irreversible) (S.Kumar et al 2011).

2.1.1.2 FREUNDLICH ISOTHERM:

The Freundlich adsorption isotherm holds good for both multilayer adsorption and heterogeneous adsorption. It simply assumes that there are multiple sets of adsorption sites on the surface of the adsorbent but all the sets behave in accordance to Langmuir isotherm.

The basic equation for Freundlich isotherm is given by equation 4.

$$q_e = K_F C_e^{\,1/n} \quad (4)$$

Where K_F and n are the constant for Freundlich isotherm and K_F shows the adsorption capacity and 1/n is the measure of reaction's intensity, Favourable adsorption conditions exist when n>1.

2.1.2 MULTICOMPONENT ADSORPTION ISOTHERM:

Single component adsorption isotherms are not sufficient for the multicomponent adsorption from a binary solution. As in the case of more than one component in a solution one component can provide competition to the other component for adsorption on the active sites. The multicomponent adsorption isotherms used in this study are Non-modified Langmuir, Modified Langmuir, Extended Langmuir and Extended Freundlich adsorption isotherm. The constants for these multicomponent models are estimated single component modelling of the individual component for the adsorption of the component from their individual solution.(Wuster et al. 2000, S.Kumar et al. 2011, Nouri et al. 2002).

2.1.2.1 NON MODIFIED LANGMUIR ISOTHERM:

The general equation for Non-modified Langmuir Isotherm is given by equation 5 (S.Kumar et al. 2011, Nouri et al. 2002, Aksu et al. 2002, Agarwal et. al).

$$q_{e,i} = \frac{Q_{0,i} b_i C_{e,i}}{1+\sum_{j=1}^{N} b_j C_{e,j}} \quad (5)$$

Where $q_{e,i}$= Equilibrium monolayer capacity for 'i' component, (mg/g)

$Q_{0,i}$ and b_i are the Langmuir constants for individual components.

$C_{e,i}$= Equilibrium concentration for the 'i' component (mg/L)

2.1.2.2 MODIFIED LANGMUIR ISOTHERM:

The general equation for Modified Langmuir isotherm is given by equation 6. (S.Kumar et al. 2011, Nouri et al. 2002, Aksu et al. 2002, Agarwal et. al.2013).

$$q_{e,i} = \frac{Q_{0,i} b_i \frac{C_{e,i}}{\eta_i}}{1+\sum_{j=1}^{N} b_j \frac{C_{e,j}}{\eta_j}} \quad (6)$$

Where η_i= Correction factor for 'i' component.

2.1.2.3 EXTENDED LANGMUIR ISOTHERM:

The general equation for extended Langmuir isotherm is given by equation 7.(Agarwal et. al. 2013)

$$q_{e,i} = {(Q_{0,i} b_i C_{e,i})}\Big/{(1 + \sum_{j=1}^{N} b_j C_{e,j})} \quad (7)$$

2.1.2.4 EXTENDED FREUNDLICH ISOTHERM:

The equation of extended Freundlich isotherm is given by equation 8 and equation 9. (Agarwal et. al. 2013).

$$q_{e,1} = {(K_{F,1} C_{e,1}^{1/(n_1+x_1)})}\Big/{(C_{e,1}^{x_1} + y_1 C_{e,2}^{z_1})} \quad (8)$$

$$q_{e,2} = {(K_{F,2} C_{e,2}^{1/(n_2+x_2)})}\Big/{(C_{e,2}^{x_2} + y_2 C_{e,1}^{z_2})} \quad (9)$$

Where $K_{F,i}$= Freundlich isotherm constant for 'i' component

x_i ,y_i, z_i = Freundlich constants for 'i' component

2.1.3 KINETIC MODELS:

The rate of adsorption as well as the mechanism of adsorption can be explained by carrying out kinetic studies for the contact time data. Many kinetic models generally used for modelling contact time data are first order, pseudo first order, second order, pseudo second order and intraparticle diffusion. The models considered generally are pseudo first order, pseudo second order, intrapartcle diffusion (Agarwal et.al. 2013). The equations for these models are given below from equation 10 to

Pseudo first order kinetics:

$$q_t = q_e(1 - \exp(-k_1 t)) \quad (10)$$

Pseudo second order kinetics:

$$q_t = {k_2 q_e^2 t}\Big/{(1 + k_2 q_e t)} \quad (11)$$

Intraparticle diffusion:

$$q_t = k_{id} t^{0.5} \quad (12)$$

Where k_1= Rate constant for pseudo first order kinetic model (h^{-1})

k_2 = Rate constant for pseudo second order kinetic model (mg g^{-1} h^{-1})

2.1.4 THERMODYNAMIC MODELLING:

Temperature also has an influence on the simultaneous adsorption and biodegradation of phenol and cyanide, but affects only to a limited extent under a certain range of temperature. Temperature also affects the growth rate of bacteria. Process is usually not carried out at extremely high and low temperature as bacterial growth is not very prominent.

Thermodynamic parameters i.e. standard free energy change of sorption (ΔG^0 (kJ/mol)), the standard enthalpy change (ΔH^0 (kJ/mol)) and the standard entropy change (ΔS^0 (kJ /mol. K)) are determined for studying the thermodynamic feasibility of simultaneous adsorption and biodegradation of phenol and cyanide.

$$\Delta G^0 = -RT lnK \quad (13)$$

$$lnK = \frac{C_a}{C_e} \quad (14)$$

where, C_a = adsorbed pollutant concentration per litre (mg/L)

C_e = equilibrium pollutant concentration (mg/L)

R = gas constant (8.314 J/ mol. K)

T = temperature (K)

$$lnK = \frac{\Delta S^0}{R} - \frac{\Delta H^0}{RT} \quad (15)$$

The thermodynamic parameters ΔH0 (kJ/mol) and ΔS0 (kJ/mol. K) can be obtained from slope and intercept of plot of ln K vs 1/T (Kamsonlian et al., 2011).

2.1.5 ERROR FUNCTIONS:

The error function utilized to show the fit between experimental and predicted value for both kinetic models and equilibrium isotherms is Average Relative Error (ARE). The equation for ARE is given below

$$ARE\ \% = 100/N \times \sqrt[2]{\sum(\frac{q_{e,i}^{exp} - q_{e,i}^{cal}}{q_{e,i}^{exp}})^2} \quad (16)$$

Where N= number of observations

2.2 CONTINUOUS STUDIES:

2.2.1 RESIDENCE TIME DISTRIBUTION STUDIES:

The residence time distribution or RTD studies are carried out to estimate the flow pattern of a reactor. RTD studies are carried out using a tracer which is easily detectable, is non-reactive to the carrier fluid, there is not much density difference with the tracer and the carrying fluid and it should not get adsorbed or absorbed by the packing material or the walls of the reactor.

E-CURVE:

All fluid elements in the reactor do not take the same time to appear in the outlet stream. The study of different time duration taken by different fluid element is called Exit age studies and the curve thus obtained between exit age and time is called E-curve or exit age distribution curve.

$$\int_0^\infty Edt = 1 \quad (17)$$

Where *E(t)dt* = fraction of material in exit stream with ages between (t, t+dt)

E= exit age distribution, time^{-1}

F-CURVE:

The fluid element that have age less than any time 't_1' is represented by F (t_1), which is also called fluid fraction's "cumulative distribution".

$$\int_0^{t_1} Edt = F(t_1) \quad (18)$$

Mean value of the E-Curve or the mean residence time can be calculated as

$$t_m = \frac{\int_0^\infty tE(t)dt}{\int_0^\infty E(t)dt} \quad (19)$$

For constant density systems mean residence time is calculated as

$$\tau = V/Q \quad (20)$$

Where V = working volume of the reactor, m^3 or mL

Q = volumetric flow rate of the fluid, m^3/min or mL/min

M=units of tracer introduced (g or moles)

E-curve can be estimated from the C-curve as

$$E = \frac{C_{pulse}}{M/Q} \tag{21}$$

$$E_\theta = \tau E = \frac{V}{M} C \tag{22}$$

$$\theta = \frac{t}{\tau} \tag{23}$$

Spread of the E-curve can be measured by estimation of variance (σ^2), It has the unit of time^2

$$\sigma^2 = \frac{\int_0^\infty (t-t_m)^2 C dt}{\int_0^\infty C dt} = \frac{\int_0^\infty t^2 C dt}{\int_0^\infty C dt} - t_m^2 \tag{24}$$

DISPERSION MODEL:

Further to characterize the flow pattern of the reactor a term of dispersion number (D/uL) is defined as per dispersion model. If dispersion number is 0 the flow is more towards plug flow and if the dispersion number is infinity the flow is more towards mixed flow. D/uL is estimated as

$$\sigma_\theta^2 = 2\left(\frac{D}{uL}\right) \tag{25}$$

There is presence of low dispersion when dispersion number is less than 0.05, presence of moderate dispersion when dispersion number is between 0.05 and 0.25 and there is presence of high dispersion when dispersion number is greater than 0.25. (Levenspiel)

2.2.2 COLUMN REACTOR:

The Empty Bed Contact Time (EBCT) can be calculated as

$$EBCT = \frac{Bed\ Volume}{Volumetric\ flow\ rate\ of\ the\ liquid} \tag{26}$$

The curve obtained by plotting normalized concentration (C/C_0) versus time or effluent volume is called the breakthrough curve and is further utilized for estimation of percentage removal or the column capacity of the packed bed reactor (Aksu et. al. 2004).

Where C_0= Inlet concentration (mg/L)

C= Outlet concentration (mg/L)

$$V_{eff} = Qt_{total} \quad (27)$$

Where V_{eff}= Effluent Volume, (mL)

Q = Volumetric flow rate, (mL/min)

t_{total}= Total flow time, (min)

Percentage removal of a particular pollutant can be calculated by equation 12.

$$Removal\ \%,_i = \frac{q_{i,total}}{m_{i,total}} \times 100 \quad (28)$$

Where $q_{i,total}$= Total amount of component 'i' adsorbed by the column, mg

$m_{i,total}$= Total amount of component 'i' sent to the column, mg

$$q_{i,total} = QA_i \quad (29)$$

$$m_{i,total} = C_0\ Qt_{i,total} \quad (30)$$

Where A_i= Area under the curve plotted between normalized concentration and time for component 'i'.

Maximum column capacity can be estimated by equation 15.

$$q_{eq,i} = \frac{q_{i,total}}{X} \quad (31)$$

Where X= Mass of packing material in the column.

$q_{eq,i}$= Equilibrium capacity for component 'i'

2.2.3 KINETIC MODELS:

The dynamic behavior of the packed bed reactor is determined by different kinetic models.

ADAMS BOHART MODEL:

This model assumes that adsorption rate is directly proportional to the adsorbate and adsorbent's residual capacity. The model works better for $C/C_0<0.15$.

The general equation of this model is

$$ln\frac{C}{C_0} = k_{AB}C_0t - k_{AB}N_0\frac{Z}{U_0} \quad (32)$$

Where k_{AB} is the kinetic constant (L/ mg min), U_0 is the superficial velocity (m/ min) and Z is the height of the column (m).

A graph is plotted between $\ln(C/C_0)$ and time (t) which gives a slope equal to $k_{AB}C_0$ and an intercept equal to $-k_{AB}N_0\frac{Z}{U_0}$.

WOLBORSKA MODEL:

This model uses the same plot as for the Adams Bohart model. The general equation of the model is

$$ln\frac{C}{C_0} = \frac{\beta_a C_0}{N_0}t - \frac{\beta_a Z}{U_0} \quad (33)$$

Where β_a is the Kinetic coefficient of external mass transfer (min^{-1}), D is the axial diffusion coefficient (m^2/min) and β_0 is the external mass transfer coefficient with negligible D (min^{-1})

THOMAS MODEL:

Thomas model assumes the kinetics to be second order without any axial dispersion along with Langmuir kinetics for adsorption. The general equation of the model is

$$\frac{C}{C_0} = \frac{1}{1+\exp(\frac{k_{Th}}{Q}(q_0X - C_0V_{eff}))} \quad (34)$$

The equation is linearized and the plot of ln $((C/C_0)-1)$ versus time is utilized for the estimation of k_{Th} i.e. Thomas constant and q_0.

YOON AND NELSON MODEL:

The major assumption of this model is that the rate of adsorption is directly proportional to the probability of adsorbate adsorption. The equation of this model is

$$ln\frac{C}{C_0-C} = k_{YN}t - \tau k_{YN} \quad (35)$$

A plot of lnC / (C_0-C) versus time gives k_{YN} i.e. rate constant (min^1) from slope and τ i.e. 50 % breakthrough time (min) from intercept.

2.2.4 MASS TRANSFER ZONE ESTIMATION:

The mass transfer zone is the length of the reactor where the actual mass transfer takes place. It is estimated as

$$MTZ = \left(1 - \frac{T_v}{T_c}\right) Z \quad (36)$$

Where $T_v = \int_0^{T_{bp}} \left(1 - \frac{C}{C_0}\right) dt$ (37)

$$T_c = \int_0^{\infty} \left(1 - \frac{C}{C_0}\right) dt \quad (38)$$

The rate of movement of mass transfer zone (RMTZ) can be calculated as

$$RMTZ = \frac{MTZ \times Q}{V_{0.9} - V_{0.2}} \quad (39)$$

Where $V_{0.9}$ and $V_{0.2}$ are volume of effluent at 90 % breakthrough and 20 % breakthrough respectively.

2.2.5 ERROR FUNCTIONS:

The error functions utilized to show the fit between experimental and predicted values are given below

$$\varepsilon\% = \frac{\sum_{i=1}^{N} \left| \frac{(C/C_0)exp - (C/C_0)theo}{(C/C_0)exp} \right|}{N} \times 100 \quad (40)$$

$$\chi^2 = \left(\frac{q_{th} - q_e}{q_{th}}\right)^2 \quad (41)$$

CHAPTER 3

LITERATURE REVIEW

There are a number of techniques for removal of phenols and cyanides from the industrial effluents that are discharged in the surface waters. The choice of efficient removal technique depends on many factors like:

- Process Feasibility
- Cost effectiveness
- Waste water characteristics
- Eco-friendly

3.1 TREATMENT METHODS:

3.1.1 PHENOL:

A list of techniques used for phenol removal from waste water along with the work of authors in the respective technique is listed below:

3.1.1.1 ULTRAFILTRATION:

This method is used for treatment of industrial waste water. It is a kind of membrane filtration in which liquid is passed through the semi-permeable membrane by the application of hydrostatic pressure. The components that do not pass through the membrane are called retentate and the ones that pass the membrane are called permeate.

W.Zhang et al (2012)

Removal of phenol using Gemini micellar-enhanced Ultrafiltration (GMEUF)

In this study phenol was removed from waste water by ultrafiltration using different cationic Gemini surfactant (N1-dodecyl-N1,N1,N2,N2-tetramethyl-N2-octylethane-1,2-diaminium bromide, CG), surfactant (dodecyl trimethylmmonium bromide, DTAB), anionic surfactant (sodium dodecyl sulfate, SDS) and nonionic surfactant ((dodecyloxy)polyethoxyethanol, Brij35) concentrations. Polyethersulfone (PES) membrane was used. The effect of Feed (phenol and surfactant) concentration on the retention of phenol, Permeate flux and Membrane fouling by micelles was studied. Retention of phenol reached a peak value of 95.8 %.Gemini Surfactant has higher capacity of solubilizing phenol as compared to other surfactants.

3.1.1.2PERVAPORATION:

The process of pervaporation consists of two steps:

- Permeation through the membrane
- Evaporation of permeate into vapor phase.

This process is also used for the removal of phenol from industrial waste water.

W.Kujawski et al (2004)

Pervaporation and adsorption application for phenol removal

In this study phenol produced with cumene oxidation process was removed by the application of pervaporation and adsorption. Composite membranes PEBA, PERVAP 1060 and PERVAP 1070 were used for the pervaporation of water–acetone, water–phenol and water–phenol–acetone mixtures. All membranes were found to be selective towards phenol while the PEBA membrane showed the best selectivity. However, due to unavailability of this membrane on the commercial scale PERVAP-1060 and PERVAP-1070 were used for practical applications. Application of different Amberlite resins was also studied for the adsorption of phenol. Amongst the Amberlite resins, the Amberlite XAD-4 had the best properties of decontaminating aqueous phenol solutions.

3.1.1.3 SOLVENT EXTRACTION:

This extraction process works on the basis of solubility of substance in solvent. It is generally used for separation of organic substances from wastewaters. In this process the waste stream and solvent are mixed and the contaminant mass transfer takes place from the waste to the solvent. Gravity method is applied in separation of solvent and water. The solvent that contains contaminant is called extract whereas, the waste stream that contains no or negligible contaminants is called raffinate.

C.Yang et al. (2006)

Solvent extraction process utilization

Phenol was removed from the coal-gasification wastewater. The extracting solvent was selected by considering solvent recovery phenol and COD removal for the coal-gasification wastewater. The parameters of extraction process conditions were studied. Setting up of an on-site trial-plant of 2 t/h was done to test and for industrial verification. On-site trial results showed that more than 93% and 80% of phenol and COD respectively were removed from the wastewater.

Boyadzhiev L. et al. (1984)

Double emulsion membranes and creeping film pertraction.

In the liquid-liquid extraction method for extraction of phenol from waste waters using polar solvents there was a demand of additional operations for removal of dissolved solvent from dephenolized waters. In the liquid pertraction (liquid membrane) process, non-polar solvents like high boiling point normal paraffins were used as intermediate phase which avoided the need of additional water purification. This method of double emulsion and creeping film pertraction provided 95-99% dephenolization of low concentration waste waters.

3.1.1.4 PHOTOCATALYTIC REMOVAL:

The acceleration of a photoreaction in the presence of a catalyst is called photocatalysis. In these recations the adsorbed substrate absorbs light. The photocatalytic activity (PCA) depends on the catalyst's ability to create electron–hole pairs which then generate free radicals (e.g. hydroxyl radicals) to initiate secondary reactions.

Priya S.S. et al (2008)

Photocatalytic removal application

The present work aims at in-situ wastewater treatment and its recycling for low-grade industrial applications .Sunlight can completely destruct the contaminant s. Sunlight is an inexhaustible and a free source of energy thus the process consumes very less primary energy

for its operation. The experiments were performed in laboratory photo reactor for degradation of phenolic wastewater. Experiments were carried out using 0.2 g/l of TiO_2 catalyst for concentration of phenol in wastewater varying from 20, 50,100,200,300,400 and 600 ppm. Complete phenol degradation is possible in a time less than 5 hrs, at a phenol concentration ≤100 ppm. This study reviews the potential, opportunities and challenges of solar photocatalytic wastewater treatment for Indian environmental conditions.

M.A. Gondal et al. (2008)

Laser enhanced photo-catalytic removal by p-type NiO semiconductor catalyst

In the present study removal of phenol by waste water is done by laser induced photo-catalysis using p-type NiO semiconductor catalyst. The parameters of laser energy (100–250 mJ) and laser irradiation time (0–60 min) and their impact on the process was studied. The removal of phenol took place in a couple of minutes as compared to the conventional method that takes hours. The removal process was of first order with decay constant of 0.0125 min^{-1}

3.1.1.5 ADVANCED OXIDATION:

Advanced oxidation process is used for removal of organic waste for treatment for waste water. In the process organic waste is removed by oxidation through reactions with hydroxyl ions (OH^-).

T. Huanosta-Gutiérrez et al. (2012)

Copper slag for catalyzing advanced oxidation processes

In this work copper slag was used for catalyzation of phenol degradation in water by advanced oxidation processes (AOPs).The testing of copper slag was done with H_2O_2 and H_2O_2/UV. The complete photocatalytic degradation of phenol was done. The parameters studied were Slag characteristics, biodegradability and acute toxicity. There was a reduction of almost 50 % TOC from the slag. The toxicity peaks indicated formation of more toxic compounds during the treatment process which can be minimized by controlling the reaction time.

3.1.1.6 CHEMICAL OXIDATION:

Both ozone and chlorine has proved to be effective for removal of phenol. A removal efficiency of 48 % can be reached for phenol at pH 7 and 1000 mg/l of initial concentration by the application of ozone as an oxidant reagent. The effectiveness of the process is

influenced by ozone reactivity with the target compound, the rate at which it reacts, the demand of ozone for achieving a desired degree of treatment, the incidental stripping associated with the dispersion of ozone along with effect of treatment variables like pH and temperature. For instance, in treatment of phenol by, the rate of treatment is twice at pH 11 then at pH 7 (Metcalf and Eddy, 2003).

3.1.1.7 BIOLOGICAL TREATMENT(BIODEGRADATION):

The action of living microorganisms on the pollutants is the basis of biodegradation or biological treatment. Microorganisms convert the waste material into simpler substances by natural metabolic process by utilizing it as food material. Phenol is also biodegraded by the use of certain micro-organisms including bacteria, yeast etc. Initial phenol concentrations up to 500 mg/L can be easily treated by biological treatment techniques.

Djokic L. et al. (2013)

Phenol removal by Bacillus sp.PS11.

This study concerns with the biodegradation of phenol in four natural soils (loamy sand, sandy loam, sandy clay loam and loam) by microorganism Bacillus sp. PS11.A total removal of 2 g of phenol/ kg of soil was achieved in laboratory experiments for all soil types in 6 to 21 days. In comparison to other soil samples loamy woodland soil which contained least amount of sand (42.5 %) and maximum amount of silt and clay (57.5 %) showed maximum phenol removal. However, increasing the clay in sandy loam sample (13.5 % to 30 %) decreased the phenol removal rate, while changing sand content (from 74.4% to 90%) resulted in the removal rate to be twice in comparison to natural soil type. Bacillus sp. PS11in the presence of soil microorganisms bio remediated phenol within 9 days, whereas Bacillus sp. PS11 improved the phenol removal by 20%.

Banerjee A. et al. (2011)

Phenol degradation by Bacillus cereus immobilized in alginate.

In this study phenol was degraded by Bacillus cereus AKG1 MTCC9817 and AKG2 MTCC 9818 and the degradation kinetics for the free and Ca-alginate gel-immobilized systems were reported. For maximum phenol degradation by immobilized AKG1 and AKG2 the optimal pH were reported to be 6.7 and 6.9, respectively, and for both the strains 3% alginate was optimum. At lower concentrations of phenol (100-1000 mg/ l) phenol biodegradation by both free as well as immobilized cells was comparable. While immobilized strains showed higher degradation rate than that of the free strains at phenol concentrations (1500-2000 mg/ l) and hence indicates the improved phenol toxicity tolerance of the immobilized cells. In 26 and 36 days respectively AKG1 and AKG2 could degrade 50% and even more 2000 mg/ l phenol concentration.

Fialova A. et al. (2004)

Biodegradation of phenol by the yeast Candida maltose.

This study is based on the degradation of phenol by the soil-borne yeast Candida maltosa. The study revealed that C. maltose uses phenol and catechol as sole sources of carbon and energy at concentrations up to 1.7 g/land 1.5 g/l, respectively, remains unaffected by resorcinol, even at 2 g/ l. It also has the ability to co-metabolise p-cresol, but is unable to utilise benzoate or salicylate. Maximum levels of phenol hydroxylase activity reached at the beginning of the exponential phase during cultivation on phenol. After the complete utilization of phenol the enzyme was slowly degraded.

3.1.1.8 PHYTOREMEDIATION:

Phytoremediation is the technology that uses plants to degrade, integrate, digest, or decontaminate metals, hydrocarbons and other pollutants. The remediation of these compounds can be done by in situ, in vivo and in vitro methods. Various phytoremediation process include

- Phytoaccumulation
- Phytoextraction
- Phytostabilization
- Phytotransformation
- Phytovolatilization
- Rhizodegradation

Phytoremediation has the potential for providing an economical and optimum resource utilization approach for remediation of hazardous chemicals contaminated sites. (S.Susarla et al., 2002).

Gonz´alez P.S. et al. 2006

Phytoremediation by peroxidases of tomato hairy root cultures.

This study describes the removal of phenol from waste water by using tomato hairy root cultures as source of enzymes especially peroxidases, which are capable of oxidising these compounds. Roots removed phenol from 100 mg/l phenol containing solutions in the presence of 5 mM H_2O_2. Within 1 h, in a pH range of (4.0–9.0) and at a temperature between 20–60 ◦C, maximum removal was reached. Peroxidase activity of hairy root extracts and isoenzyme patterns were affected after removal of phenol. Basic peroxidase isoenzymes were the main peroxidases associated with the removal processes and their inactivation was possible during the treatment. Acidic peroxidase isoenzymes participated a little while retaining their activities.

Singh S. et al. 2008

Vetiver (Vetiveria zizanoides L. Nash) for phenol phytoremediation.

This paper evaluated the potential of aseptically grown Vetiveria zizanoides for phenol phytoremediation from Murashige and Skoog's liquid medium. Complete removal of phenol from incubation medium was seen at the end of 4 days, when the initial concentration was 50 and 100 mg/l. While a removal of 89%, 76% and 70% was seen when the initial concentrations were 200, 500, and 1000mg/ l respectively. Phenol was removed due to inherent production of peroxidase and hydrogen peroxide. After coupling with H_2O_2 formation, the antioxidant enzymes levels like superoxide dismutase and peroxidase enhanced. The results of the study indicated that Vetiver plant can adapt to the phenolic environment without affecting its ability to degrade phenols but it shows a slight decrease in the plant growth in the phenolic environement.

3.1.1.9 ADSORPTION:

The widely used method for waste water treatment from organic as well as inorganic waste till date remains adsorption. In the process of adsorption the pollutants are adsorbed on the surface of the adsorbent, which is a surface phenomenon. Adsorption takes place either by physisorption or by chemisorption. When the adsorbate adsorbs on the adsorbent surface by weak vander walls forces thereby forming multilayer then the process is called physisorption and it is reversible in nature. If the adsorbate adsorbs by ion exchange method or is attached by ionic forces and forms a monolayer, the process is called chemisorption and this process is irreversible. The process of adsorption has been generally used as it is easy to execute, cost

effective and eco-friendly. Phenol has also been widely removed by adsorption. The work of different authors on different adsorbents is given below:

ACTIVATED CARBON:

Da browski A. et al. 2005

Adsorption by activated carbon.

This study is concerned with the adsorption of phenol and its derivatives on activated carbons. The effect of various parameters like pH of solution and heterogeneity effects accompanying adsorption of phenolic compounds are studied on the adsorption process. This paper also discussed the important aspects referring to irreversible adsorption of phenols along with the impact of different phenolic compound substituents on their uptake by activated carbons.

FLY ASH:

Srivastava V.C. et al 2006

Using bagasse fly ash and activated carbon.

Phenol is adsorbed on bagasse fly ash (BFA), activated carbon-commercial grade (ACC) and activated-carbon laboratory grade (ACL). The influence of various parameters like initial pH, contact time, adsorbent dose and initial concentration were evaluated on the removal of phenol. Initial concentration was varied between 75 to 300 mg/l .Optimum parameters for maximum phenol removal were found as pH 6.5, adsorbent dose ≈10 g/l of solution and an equilibrium time ≈5 h. The adsorption rates were found to be highest for ACL followed by BFA and ACC. The effective phenol diffusion coefficient was of the order of 10^{-10} m^2/s. The adsorption process is feasible and spontaneous in case on BFA.

BENTONITE:

Senturk H.B.at al 2009

Adsorption onto organomodified Tirebolu bentonite.

The present study deals with the application of natural bentonite modified with a cationic surfactant, cetyl trimethylammonium bromide (CTAB) as an adsorbent for phenol removal from aqueous solutions. Experimental parameters effects like effect of solution pH, contact time, initial phenol concentration, organobentonite concentration, and temperature were studied on the process. Maximum phenol was removed at a pH 9.0 and process attained equilibrium after contact time of 1 h. Organobentonite was found to have a monolayer

adsorption capacity of 333mg/ g. Phenol desorption from the loaded adsorbent was achieved by the application of 20% acetone solution.

GRANULAR SILICA AEROGELS:

Qin G et al (2013)

Using hydrophobic granular silica aerogels.

In the present study the aerogels prepared via sol-gel synthesis followed by drying were used for phenol adsorption from water. The effects of parameters like degree of hydrophobicity, initial phenol concentration, and contact time were studied. The process of phenol adsorption involved both boundary layer diffusion and intraparticle diffusion. At the phenol equilibrium concentration of 290 mg/ l, phenol adsorption on the aerogel was 142 m/g.

NANOPOWDERS:

Lina K., Pana J., Chena Y., Chenga R. and Xua X. (2009)

Adsorption on hydroxyapatite nanopowders.

In this research, the adsorbent used was hydroxyapatite (HAp) nanopowders prepared by chemical precipitation for phenol adsorption from aqueous solution. The effect of experimental parameters like contact time, initial pollutant concentration, pH, dose of adsorbent , temperature of solution and adsorbent calcining temperature on the phenol adsorption were reported. The equilibrium was achieved in 2 h of contact time. Increase in initial phenol concentration, pH and HAp doses increased phenol adsorption capacity while high calcining temperature decreased the adsorption capacity. A maximum phenol adsorption capacity of 10.33 mg/g was obtained for 400 mg/L initial phenol concentration at pH 6.4 and 60 ^{0}C.

Further the work of various authors is listed below:

Table 3.5: Work of various authors on the removal of phenol by adsorption

Adsorbent	Initial Concentration	Adsorbent Dose	Adsorption Capacity	Contact Time (H)	Temperature ^0C	% Removal	pH	Process	Isotherm	Reference
Activated carbon by biomass material	25-200 mg/l	-	149.29 mg/g	4 h	30	-	3-10	Batch	Langmuir	Hameed et.al. (2007)
A natural bentonite modified with a cationic surfactant, cetyl trimethylammonium bromide (CTAB)	105 mg/l	-	333 mg/g	1 h	0-40	56.2	9	Batch	Langmuir and Freundlich	Senturk et.al. (2009)
Carbonised beet pulp	25-500 mg/dm^3	-	89.5 mg/g	-	60	-	6	Batch	Langmuir and Freundlich	Dursun et.al. (2005)
Granular silica aerogels	290 mg/l	-	142 mg/g	40 h	-	-	5.5	Batch	Freundlich	Qin et.al. (2013)
Hydroxyapatite	400	-	10.33	2 h	60	-	6.4	Batch	Freundlich	Lin et.al.

nanopowders	mg/l		mg/g							2009
Lignite	100 mg/l	-	10 mg/g	200 h	25	100 %	-	Batch	-	Polat et.al. 2006
Three agro based carbons Black gram husk(BGH) Green gram husk(GGH) Rice Husk(RH)	100 mg/l	0.5 g/l	-	6 h	25	-	5.1	Batch	Redlich-Peterson	Srihari et.al. 2008
Palm seed coated activated carbon	25 mg/l	-	18.3 mg/g	3 h	-	-	4-9	Batch	Freundlich	Rengaraj et.al. (2001)
Bagasse fly ash (BFA) activated carbon commercial scale (ACC) Activated carbon laboratory scale(ACL)	75-300 mg/l		6 g/l	5 h	30	-	6.5	Batch	Redlich-Peterson	Srivastava et. al. (2006)
Peat, fly ash and bentonite	1 mg/l		0.015-0.1 mg/g	16 h (peat) 5 h (fly ash) 16 h	21±1	46.1% (peat) 41.6% (fly ash) 42.5%	4-5	Batch	Fruendlich And Langmuir	Viraraghavan et.al. (1997)

				(bentonite)		(bentonite)				
Chitin	300 mg/dm³	-	21.5 mg/g	-	40	-	1	Batch	Freundlich	Dursun and Kalayci 2005
Banana Peel	13.45 g/l	1-5 g Banana Peel dosage 30 g/l	689 mg/g Equilibrium reached at 82.33 mg/g	3 h	30	60-88 %	2-11	Batch	Freundlich and Langmuir	Achak et. al 2008
Activated carbon from wood particle board waste	300 ppm	-	500 mg/g	-	25	-	-	Batch	Type II isotherm	Girods et al 2009
Bentonite	25-500 mg/ml	-	1 mg/g	6 h	-	-	5-11	Batch	Langmuir and Freundlich	Banat et al 2000
Surfactant modified bentonite	10 mg/l	100 mg	SMB-H 0.93±0.09 mg/g SMB-B 1±0.14	48 h	25	-	6	Batch	Freundlich	Diaz- Nava et al. 2011

				mg/g						

Table 3.6: Works of different authors on phenol biodegradation

Bacteria	Degradation Rate (Dr)/Yield	Support Material/ Medium	Cell Adsorption Ratio	Initial Concentration	pH	Temperature ^0C	Process	Time	Decay Coefficient H^{-1}	Reference
***Pseudomonas putida* 50026**	DR- 0.042g/l h	Zr-activated Pumice	91 % 99 %	1 g/l 1.25 g/l	-	28	Batch Continuous	22 h	-	Pazarlioglu and Telefoncu 2004
***Pseudomonas Putida* MTCC 1194**	YIELD-0.65 mg/g YIELD-0.50 mg/g	Basal Salt Medium (BSM)	-	1000 mg/l phenol 500 mg/l Catechol	7.1	29.9±0.3	Batch	162h 94 h	0.0056 0.0067	Kumar et. al 2004
Pseudomonas	-	-	-	Cell Concentrati	7	30	Batch	-	-	Juang-Tsi 2006

***Putida* CCRC 14365**				on 0.025g/l Substrate Level 0-4.25 mM						
Yeast ***Candida tropicalis***	-	-	100 %	2000 mg/l 280 mg/l	-	-	Batch	66 h 52 h	-	Yan et.al., 2006
***Pseudomonas* sp. SA01 isolated from pharmaceutical wastewater.**	-	Ammonium Chloride 1g/l	100 %	0.7 g/l	6.5	30	Batch	30 h	-	Shourian et,al.,2009.

Table 7.3: Works of author on phenol removal by phytoremediation

Pollutant	Plant	Initial Concentration	Duration	Temperature ^0C	pH	In the presence of	Process	Removal %	Reference
Phenol from waste water	Tomato hairy root cultures that act as enzymes	100 mg/l	1 h	20-60	4-9	H_2O_2 5 mM	Oxidation by peroxidase	80-95	Gonzalez et.al 2005
Phenol from Murashige and Skoog's	Vetiver *Vetiveria zizanoides* L.Nash	50 mg/l 100 mg/l 200 mg/l 500 mg/l 1000 mg/l	4 days	-	-	H_2O_2	Oxidation	- - 89 76 70	Singh et. al 2007
Three Azo dyes from waste water • **Bismark browny**	Sunflower	100 mg/l	4 days	-	-	-	-	99.96	Huicheng et.al 2012

• **Evans Blue**	61.26
• **Orange G**	26.7

3.1.2 CYANIDE:

A list of techniques used for cyanide removal from waste water is:

3.1.2.1MEMBRANES:

In this method cyanide is separated from water using membranes with either reverse osmosis or electrodialysis. The process of electrodialysis consists of two electrodes across which a potential is applied and is separated by a membrane permeable to cyanide. The cyanide solution which requires purification is placed in the cathode or negative electrode half of the cell. Being negatively charged cyanide diffuses through the membrane and concentrates in the positive half of the cell. In reverse osmosis, water is forced by applying pressure through a membrane which is impermeable to cyanide.

Murthy Z.V.P, Gupta S.K. (1999)

Application of reverse osmosis using thin film composite polyamide membrane.

In this work sodium cyanide is separated from synthetic waste water using a commercial thin film composite polyamide reverse osmosis membrane. The effects of mass transfer coefficients and membrane transport parameters were simultaneously estimated. The cyanide separation data was analysed with a combined film theory-solution-diffusion (CFSD) model and a combined film theory-Spiegler-Kedem (CFSK) model. The predictions of CFSK model were found to be more accurate.

Han b. et al. (2009)

Using gas membranes.

The present work removes cyanide from four industrial wastewaters using hollow fibre gas membranes. There were 10 hollow fibre modules in the plant that had a total membrane surface area of 180m^2. The strip stream had 10% NaOH. The feed as well as the membrane mass transfer coefficients do contribute to the overall mass transfer coefficient. The volatile species contained in the real wastewaters also get transferred to the strip solution. If there is no reaction in the volatile species in the strip stream then all the three individual mass transfer coefficients contribute to the overall mass transfer coefficient. Water vapour transport occurs from lower to higher osmolarity solution due to osmotic distillation.

3.1.2.2 SOLVENT EXTRACTION:

Solvent extraction is also used for cyanide removal from waste water. But the application of solvent extraction to all the cyanide species is still unknown.

Alonso-González O. et al. (2010)

Quaternary ammonium salts to remove copper–cyanide complexes by solvent extraction.

This work aims at the use of solvent extraction for the removal of copper–cyanide species from a synthetic solution so that recycling of the solution into the process can be done. For this purpose the extractants used were quaternary ammonium salts like Quartamin TPR, Adogen 464 and Aliquat 336. From the experiments it was found that for a synthetic solution of initial copper and cyanide concentration of 710 mg/l copper and 1100 mg/l respectively, a copper extraction of 99% can be obtained by using 0.033 mol/l of the extractant Adogen 464 (organic/aqueous volume ratio (O/A) = 1) and a pH range of 9–11.

3.1.2.3 BIOLOGICAL TREATMENT (BIODEGRADATION):

Barclay M. et al. 1998

Biodegradation by fungi.

The study focuses on the application of isolated mixed fungal cultures to utilize iron or nickel cyanide as the sole source of nitrogen at either acidic or neutral pH. Two mixed cultures were obtained at pH 4 by enrichment of tetracyanonickelate which comprised of Fusarium solani and Trichoderma polysporum and one consisting of Fusarium oxysporum, Scytalidium thermophilum, and Penicillium miczynski which was isolated on hexacyanqferrare. A minimum of 50% of the total cyanide was reported to be degraded. At a pH 7 it required 5 days for cyanide degradation as compared to 28 days.

Ezzi M.J., Lynch J.M 2005

Biodegradation by Trichoderma spp. and Fusarium spp.

The research evaluated the degradation rate of cyanide by certain strains of the Trichoderma spp. Two Fusarium spp. were also studied for comparing the results. Cyanide was considered as the sole source of carbon. Cyanide biodegradation and co-metabolism were reported from the studies where glucose was taken as a co-substrate. The degradation rate of 2000 ppm CN^- became thrice in the presence of glucose.

Dash R.R. et al 2008

Treatment using simultaneous adsorption and biodegradation (SAB).

Biodegradation and adsorption alone were comparatively studied with simultaneous adsorption and biodegradation (SAB) process by the application of Pseudomonas fluorescens. Ferrocyanide solutions of initial CN^- concentrations of 50, 100, 200 and 300 mg/L with an initial pH of 6 were used. Biodegradation efficiency alone with pseudomonas fluorescens was observed as 96.4, 94.1, 86.2 and 69.3%, respectively after 60 h of agitation. In case of only adsorption with granular activated carbon (GAC) the removal percentage were found to be

85.6, 80.1, 70.2 and 50.2%, respectively. But SAB removes only in 36 h more than 70% for all concentrations and achieves a removal efficiency of 99.9% for 50 and 100 mg CN^-/l. Hence SAB is better than biodegradation or adsorption alone.

3.1.2.4 PHYTOREMEDIATION:

Larsen M. et al 2004

Phytoremediation by woody plants.

The present research tested the toxicity of potassium cyanide (KCN) to basket willow trees (Salix viminalis).The trees showed 50 % depressed transpiration after 72 h at a concentration of 2 mg CN/1 as KCN. At 0.4 mg CN^-/1 the trees showed an initial depression of transpiration, but then it recovered. At the doses of 8 and 20 mg CNl/1 the trees died. Finally cyanide disappears from the solutions.

3.1.2.5 ADSORPTION:

Adsorption is also one of the widely used techniques for cyanide removal from waste water.

A few works of authors on different adsorbents are given below:

ZEOLITES:

Ning P. et al 2013

Metal loaded zeolite adsorbent

The authors concerned about application of metal (Cu, Co, or Zn) loaded zeolite Y and ZSM-5 as adsorbents for toxic gas hydrogen cyanide (HCN) adsorption. It was found that Cu loaded zeolites showed enhanced HCN breakthrough capacity. HCN adsorption capacity was analysed for adsorbent's different physical and chemical properties. Maximal breakthrough capacities of HCN were almost in case of both zeolites when HCN concentration was 2.2 mol of HCN/mol of Cu. CN^- formed in Cu^+/Cu^{2+} and oxygen gas presence is found to be easily adsorbed onto Cu/ZSM-5 zeolite.

PRESSMUD:

Gupta N. et al 2012

Application of pressmud surface

Keeping in view the cost effectiveness of adsorption the authors utilized pressmud, a waste from sugar industry as a potential adsorbent for cyanide ion adsorption from aqueous solution. Among many conventional models tested specific uptake was accurately predicted by Langmuir type I, Temkin and (three parameter) Redlich–Peterson model. Pseudo second-order and Elovich model were acceptable for explaining the cyanide ion adsorption kinetics.

NANO-PORE SUBSTRATES:

Si-Hyun D., et al 2012

Potential of iron composites on nano-pore substrates.

Two nano-pore substrates, waste-reclaimed (WR) and soil mineral (SM) modified with irons (i.e. Fe (II):Fe(III) = 1:2) i.e. Fe-WR and Fe-SM were used as adsorbents for cyanide removal. BET surface area and PZC of the original substrates were decreased whereas pore diameter and the cation exchange capacity (CEC) were increased by modification. The results showed better cyanide adsorption for Fe-WR than Fe-SM. 97 % cyanide was removed by Fe-WR without any pH adjustment, but HCN was formed as pH descended to 7.5. 54% cyanide adsorption took place on Fe-WR at a pH 12. The first-order cyanide removal rate constant was found to be 0.49(±0.081) h^{-1}.

ACTIVATED CARBON:

Behnamfard A. and Salarirad M.M. 2009

Free cyanide adsorption by activated carbon

Free cyanide adsorption onto activated carbon was studied. Effects of parameters like contact time (1–72 h) and initial pollutant concentrations (102–532 mg/l) were also investigated. From the results it was found that, three-parameter were more efficient in fitting of data than the two-parameter models. Koble–Corrigan model best represented equilibrium data. The results brought forth that free cyanide adsorption is a two-step process. Fast cyanide adsorption takes place in the first step followed by slowing down of the process.

Table 3.8: Different works of authors based on cyanide removal by adsorption

Adsorbent	Initial Concentration	Adsorbent Dose	Adsorption Capacity	Contact Time (H)	Temperature ^{0}C	% Removal	pH	Process	Isotherm	Reference
Lignite activated carbon (LAC) Iron-Impregnated activated carbon (FeAC) From Golbasi lignite	100 mg/l	1.5g BET surface area LAC-921 m^2/g FeAC-667 m^2/g	-	72 h Stirring speed 100 rpm	25	LAC-60.18 % FeAC-67.82% LAC-64.10 % FeAC-68.02%	7-7.5 10-10.5	Batch	Langmuir Pseudo second order rate reaction	Tolga Depci 2012
Acid-washed activated carbon	172.96 mg/l	-	5.5 mg/g	24 h	23	-	7	Batch	Freundlich	Wei and Cao (1993)
Activated Carbon	102-532 mg/l	1.5 g	-	1-72 h	25±2	-	10	Batch	Three parameter Koble-Corrigan	Behnamfard et.al 2009

									model	
Metal loaded granular activated carbon	TCN-2-7 mg/l	20-100 mg of pulverised carbon	-	6 h	-	≈ 100 %	6-7	Batch	-	Zhang et. al 2010
Activated Carbon And copper impregnated activated carbon	0.5 g/l	25 g/l activated carbon 0.5 % Cu was impregnate.	-	8 h 2 h	-	50 % 99 %	10.2	Batch	-	M.D. Adams 1994
Activated carbon from olive oil mill	260-1000 mg/l	10-30 g/l	11 mg/g	-	20	-	11	Batch	-	Yeddou et.al 2010
Impregnated activated carbon with Silver and nickel on srfaces.	40 mg/l	3 g activated carbon 40-2800 mg/l Ag 40-1200 mg/l Ni	Ag-26.5 mg/l Ni-15.4 mg/l Carbon-7 mg/l	-	25	-	-	Batch	Langmuir	Adhoum et. al 2012

Granular activated carbon Metal impregnated granular activated carbon(Cu and Ag)	100 mg/l	0.2-4.5 g/l	19.7 mg/g plain carbon 22.4 mg/g Cu impregnated 29.6 mg/g Ag impregnated	72 h	Room Temperature	AC-Ag 5.7-92.3% AC 1.5-14.3% AC-Cu 4.4-35.4%	10.5-11	Batch	Langmuir isotherm and pseudo second order kinetics	Deveci et. al 2006.
Powdered pistachio Hull (PHP) Powdered activated carbon (PAC)	Cr-85.5 mg/l Cyanide-36 mg/l	2 g/l PHP PAC	PHP-117.6 mg/g Cr 151.5 mg/g Cyanide PAC-47.6	1 h	Room Temperature	100 % 69.2 % Cr 77.8 % Cyanide	3.5	Batch	Langmuir isotherm And second order kinetics	Moussavi et. al 2012

			mg/g Cr 39.4 mg/g Cyanide							
Pistachio green hull waste	100 mg/l	1.5 g/l	156.2 mg/g	1 h	24±3	99 %	10	Batch	Langmuir Isotherm and pseudo second order kinetics	Moussavi and Khosravi 2010
Pressmud	100-1000 ppm of 100 ml cyanide solution	5 g	-	12 h	30	-	7± 0.1	Batch	Empirical polynomial isotherm and pseudo second order elovich model	N. Gupta, C.B.Majumder, V.K. Agarwal 2012

Table 3.9: Biological degradation of cyanide

Bacteria	Pollutant	Degradation Rate (Dr)/Yield	Support Material/ Medium	Initial Concentration	pH	Temperature ^{0}C	Process	Time	Reference
Rhodococcus **UKMP-5M**	Cyanide KCN	-	Glucose and yeast medium	0.1 mM	6.3	30	Batch	24 h	Nallapan et al 2013
Burkholderia cepacia **strain C-3**	Cyanide	1.85 mg/h	Cu^{2+} and Fe^{2+} medium	1 mM	10	30	Batch	48 h	Adjei and Ohta 1999
Pseudomonas fluorescens **NCIB 11764**	Cyanide	100 % degradation	zeolite	26 mg/l	-	-	Batch Continous	10 h 2 days	Suh et al 1994
Klebsiella oxytoca	Cyanide KCN	100 % degradation	alginate and cellulose triacetate	3 mM	7	30	Batch	20 h	Chen et al. 2008

			immobilized beads were 0.224 and 0.192 mM h^{-1}						
Cyanide degrading microbes enriched from the Fairbanks, Alaska municipal wastewater treatment plant.	Cyanide	0.5 mg/l h cyanide	156 mg/l glucose substrate	20 mg/l	-	-	Sequencing batch biofilm reactor	48 h	White D.M. et al 2000

Table 3.10: Works of authors on cyanide removal by phytoremediation

Pollutant	Plant	Initial Concentration	Duration	Reference
Cyanide	Water hyacinths *(Eichhornia crassipes)*	5-50 mg/l	96 h	Ebel et al.,2006
Cyanide	Woody plants	2 mg/l	72 h	Larsen et al.,2004
Iron cyanide complex	Barley (Hordeum vulgare L.), oat (Avena sativa L.) wild cane (Sorghum bicolor L.)	-	16 h	Samiotakis 2004

3.1.2 SIMULTANEOUS ADSORPTION AND BIODEGRADATION:

Simultaneous adsorption and biodegradation is the method that utilizes the potential of both adsorption and biodegradation. The method has efficiency quite higher as compared to both adsorption and biodegradation. In this process the pollutant gets adsorbed on the adsorbent surface and then biologically degraded by the microorganisms. A few cases of simultaneous adsorption and biodegradation have been reported below:

Table 3.11: Works of authors based on simultaneous adsorption and biodegradation

Pollutant	Adsorbent	Bacteria	Initial Concentration mg/L	Temperature (^{0}C)	Time (h)	pH	% Removal/ Adsorption Capacity	Isotherm	Kinetic Model	Reference
Phenol	Pineapple peels	*P. aeruginosa* NCIB 950	100-500	30	72	7	193.3 mg/g	Langmuir and Redlich Peterson	First order rate kinetics	Agarry et. al. 2012
Cyanide	Granular activated carbon	*P.fluorescens*	100	30	36	6	99.9	Langmuir	-	Dash et. al. 2008
Phenol and Resorcinol	Granular activated carbon	*P.putida* MTCC 1194	200	28	5	6.24	90	Langmuir	-	Mondal et. al. 2007
Phenol	Iron	*Serratia Sp.*	200 –Phenol	30	-	8	99	Extended	Pseudo	Agarwal

and Cyanide	impregnated Granular activated carbon		20- Cyanide					Langmuir isotherm	first order and pseudo second order kinetics	et. al. 2013
Cyanide	Granular activated carbon	*R.oryzae and S.loti*	150	30	-	5.6 7.2	95.3 and 98.6	-	-	Dash et. al.2006
Textile dye stuff	Activated Sludge		200	25	20 days	5	82	-	-	Kapdan et. al. 2001

3.2 COLUMN STUDIES:

A few works on column study are given below

Table 3.12: Works of authors on continuous studies

Pollutant	Packing material	Initial Concentration (mg/L)	% Removal/ Adsorption Capacity	Kinetic Model	Reference
Phenol and Chromium(VI)	Activated Sludge	50-500	9.0 mg/g phenol 18.5 mg/g chromium (VI)	Yoon and Nelson model	Aksu et. al. 2006
Basic dye	Activated carbon from palm oil seeds	100	40.86 mg/g	-	Tan et.al. 2007
Methylene Blue	Rice Husk	50	4.41 mg/g	Thomas Model	Han et. al. 2007
Acid dyes	Activated Carbon	-	-	-	Walker et. al. 1997
Methylene Blue	Palm oil mill	100	-	Thomas and Yoon Nelson model	Kanadasan et.al.

Azo dyes	Granular activated carbon	100	39.02 mg/g	Thomas and Yoon Nelson model	Ahmad et.al. 2010
Cationic dyes	Coconut Husk	50-500	99	-	Low et.al. 1990
Lead	Granular activated Carbon	20 to 60	2.0132 mg/g	-	Dwivedi et.al. 2008

From the detailed literature survey on treatment processes on phenol and cyanide, following objectives were made to carry out the present work.

1. Simultaneous removal of phenol and cyanide from its aqueous solution using different bioadsorbents.
2. Preparation of phenol and cyanide containing synthetic waste water and different adsorbents in laboratory.
3. Characterization of adsorbents using various analytical techniques.
    - ✓ Surface area, pore volume
    - ✓ XRD, SEM, TGA and proximate analysis
4. Identifying the potential of a suitable micro-organism for simultaneous degradation of phenol and cyanide by simultaneous adsorption and biodegradation (SAB).
5. Batch experimentation to study the effects of parameters such as adsorbent dose, pH, contact time and initial concentration on simultaneous adsorption and biodegradation process on selected adsorbents.
6. Studying the equilibrium and kinetic behaviour utilizing different isotherm and kinetic models to understand the mechanism of the process.
7. Application of various error functions to select the most appropriate isotherm and kinetic model representing the equilibrium data.
8. Column studies on the suitable potential biosorbents based on the results of batch studies.
9. Studying the dynamic behaviour of the reactor by various kinetic models.

CHAPTER 4

EXPERIMENTAL SET-UP AND INSTRUMENTATION

The present study concentrates on co-removal of phenol and cyanide from waste water by simultaneous adsorption and biodegradation. This process was carried out in batch and continuous mode. This chapter is all about the analytical and auxiliary equipment used in the present work along with the experimental setup.

4.1 BATCH STUDIES:

Optimization of process parameters is the prerequisite to efficient removal of phenol and cyanide from wastewater. Process parameters optimization can be done using batch studies. Batch studies for simultaneous adsorption and biodegradation of phenol and cyanide were carried out using powdered activated carbon (PAC), egg shells, rice husk and corn husk leaves.

4.1.1 EXPERIMENTAL SETUP FOR SIMULTANEOUS ADSORPTION AND BIODEGRADATION OF PHENOL AND CYANIDE IN BATCH STUDIES:

All the batch experiments were carried out in flat bottom flasks of 250 mL tightly enclosed with cotton plug at the mouth. Bacteria growth was also conducted in the same 250 mL flat bottom flask. Batch reactors i.e. the flasks were agitated in orbital incubator cum shaker (Metrex MO-250, India). At a max 12 batch reactors were agitated at a time. The phenol: cyanide ratio was taken as 10:1 according to the ratio in which it is discharged from coke waste water (Agarwal et. al. 2013).

4.2 CONTINUOUS STUDIES:

Industrial approach to co-removal of phenol and cyanide from waste water by simultaneous adsorption and biodegradation utilizes continuous studies. The continuous studies were carried out using granular activated carbon (GAC) and rice husk.

4.2.1 EXPERIMENTAL SETUP FOR SIMULTANEOUS ADSORPTION AND BIODEGRADATION OF PHENOL AND CYANIDE IN CONTINUOUS STUDIES:

Column studies were carried out in packed bed continuous plug flow reactor. The entire continuous reactor setup consists of an inlet tank, with a tank height of 60 cm and a diameter

of 30 cm, an initial feed pump (peristaltic pump) to regulate the flow of the feed and also the output flow rate from the reactor along with a plug flow reactor. The peristaltic pump used was Miclins pump of PP series, pp-20-EX with a flow range between 2 mL/h to 10 L/h. The continuous reactor used had a length of 100 cm or 1 m, a width of 8.0 cm. There are 6 exit ports to the reactor placed at heights as shown in table 4.1. The samples were collected from all the 5 exit ports except exit port 6 which was used to empty the reactor completely. The phenol: cyanide is the same as taken in batch studies i.e. 10:1.

Table 4.13 Specifications of the Column reactor

Reactor Segments	
Length of reactor	1.0 m or 100.0 cm
Diameter of reactor	8.0 cm
Exit ports of reactor	Base Height (cm)
Port 6	0.0
Port 5	12.5
Port 4	37.5
Port 3	62.5
Port 2	87.5
Port 1	100

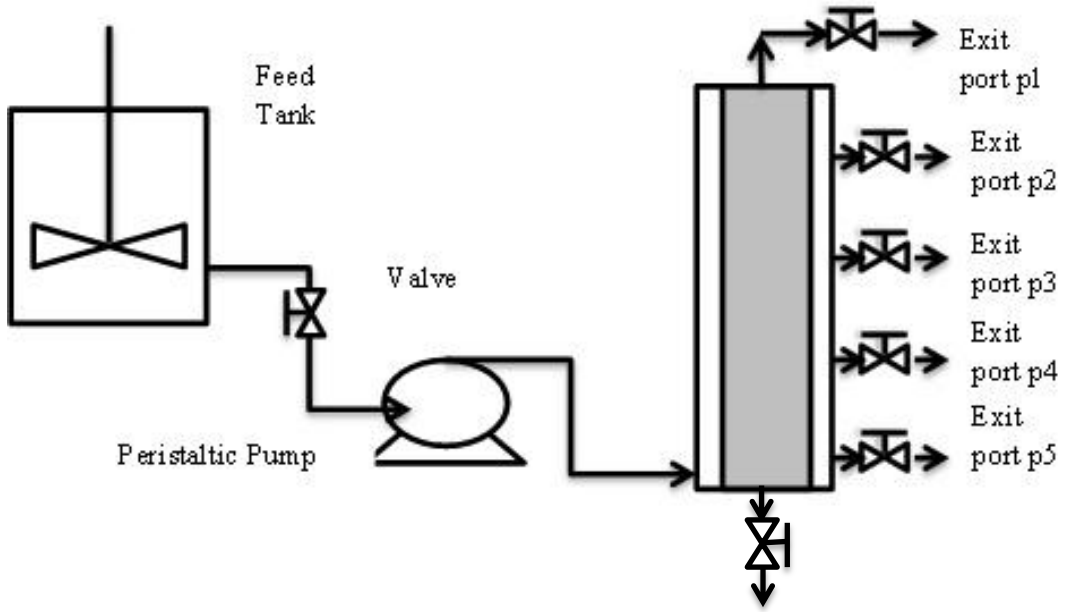

Figure 4.1 Schematic diagram of the experimental setup used for continuous studies

Figure 4.2 Inlet Feed Tank

Figure 4.3 Peristaltic Pump (Micilin Pump pp-20-EX)

Figure 4.4 Complete reactor setup for column studies

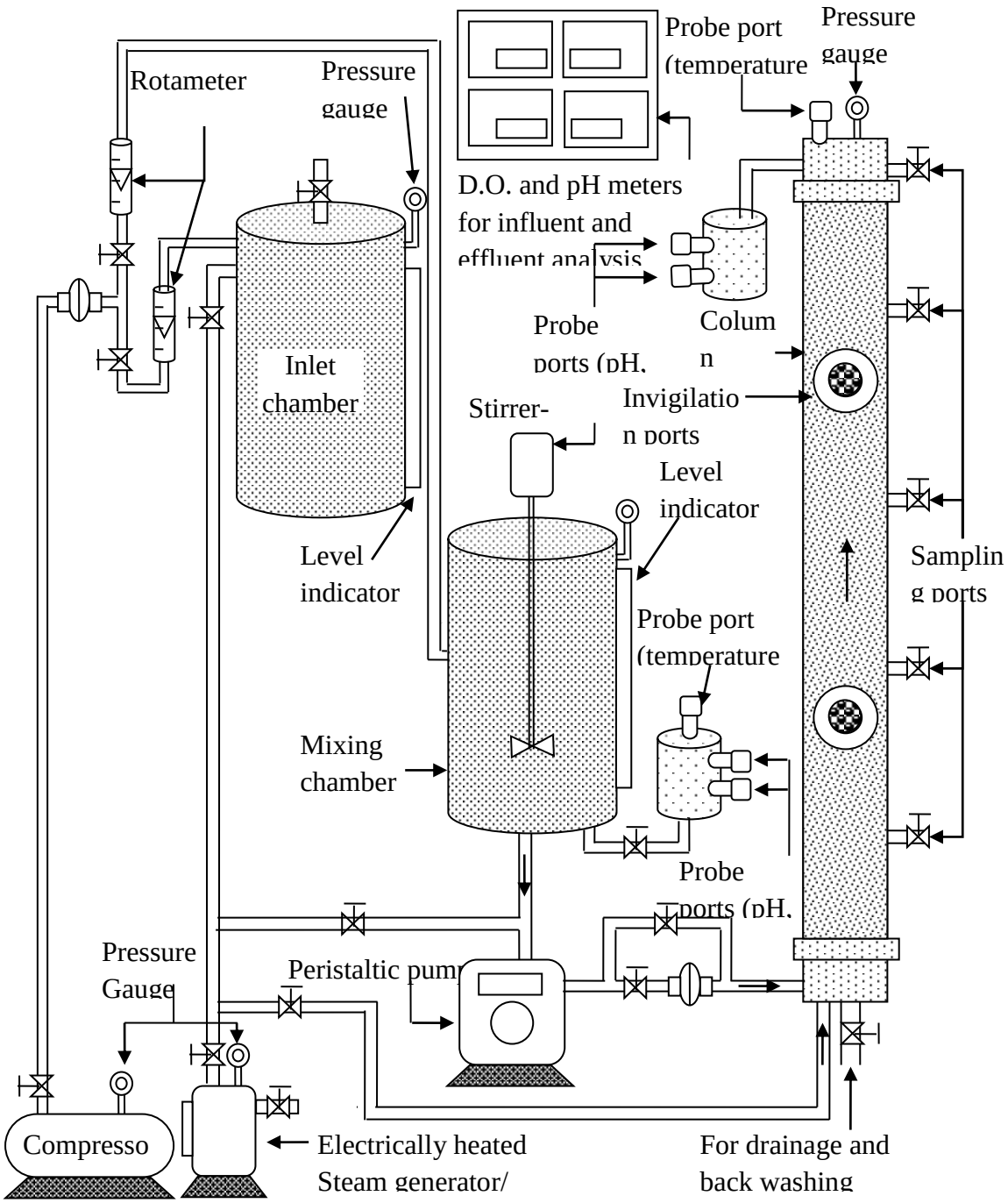

Figure 4.5: Reactor system set-up

4.3 ANALYTICAL INSTRUMENTS USED IN THIS STUDY:

The Analytical instruments used in this study were

- UV spectrophotometer
- Dissolved Oxygen Meter
- Fourier transform infrared spectroscopy (FTIR)
- X-Ray diffractometer (XRD)

- Scanning electron microscope (FeSEM)
- Surface area analyser

Following analytical instruments are shown from figure 3.5 to 3.9. For measuring the pH of the solution a pH/Redox electrode of Toshcon Pvt. Ltd was used which was calibrated with standard buffer solutions. Phenol concentration in the solution was determined by colorimetric method using 4-aminoantipyrene, buffer solution and potassium ferricyanide. Cyanide concentration in the sample was also determined by colorimetric method using picric acid reagent and nickel solution. DR-4000 UV-VIS spectrophotometer (Hach® USA) was used for all spectrophotometric measurements. The dissolved oxygen estimation was done by DO meter. The type of functional groups present on the adsorbents surface before and after adsorption was determined using FTIR (FTIR, Nicolet 6700, USA) spectrometer. Adsorbent pellets were made with 1% KBR and 4,000 to 400 cm−1 wavelength was used. The texture of the adsorbents before and after SAB were studied by Scanning electron microscopic (SEM; Leo electron microscopy Ltd. England) which gives qualitative idea about the porosity of the adsorbents. Loss of weight of adsorbent with change in temperature was analysed by Thermogravimetric analysis of the adsorbents (PerkinElmer, Japan). Procedures of all used analytical instruments are given in APPENDIX B.

Figure 4.6 SEM, LEO Electron Microscopy Ltd., England

Figure 4.7 TGA, Perkin Elmer, Japan

Figure 4.8 FT-IR, Nicholet 6700, Thermo Scientific

Figure 4.9 Surface Area Analyser, Micrometrics, Chemisorb 2720

Figure 4.10 UV-VIS Spectrophotometer

Figure 4.11 Dissolved Oxygen meter

4.4 AUXILIARY EQUIPMENT USED IN THE PRESENT WORK:

The auxiliary equipment used in this study were:

- Hot air Oven
- Centrifuge
- Autoclave
- Muffle furnace
- pH meter
- Orbital incubating shaker etc

These instruments are also shown in the following figures below:

Figure 4.12 pH meter (Toschon Pvt. Ltd., India) **Figure 4.13 Hot air oven**

Figure 4.14 Orbital shaking incubator (METREX SCIENTIFIC LTD., India)

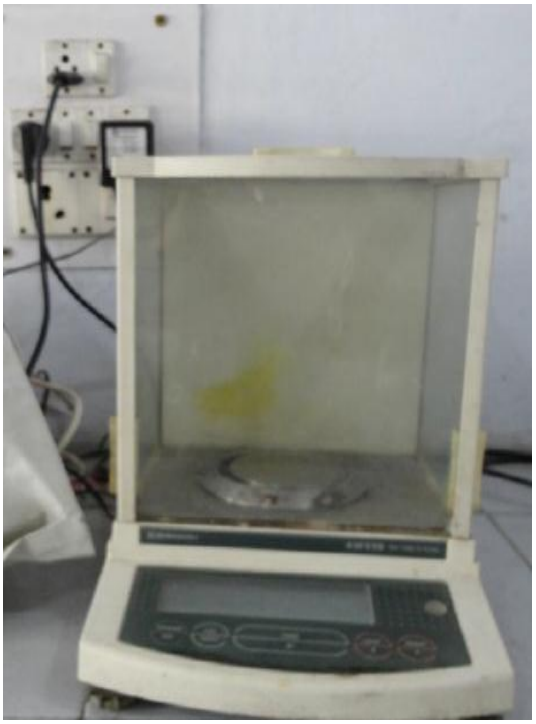

Figure 4.15 Weighing Balance

Figure 4.16 REMI Research Centrifuge

Figure 4.17 Autoclave (LEQUITRON)

Figure 4.18 Direct- Q 3 Millipore water

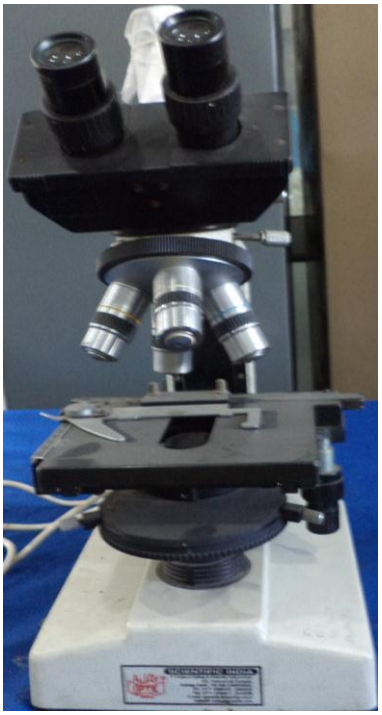

Figure 4.19 Microscope

Figure 4.20 Laminar Workstation

Figure 4.21 Vortex Shaker

CHAPTER 5

EXPERIMENTAL PROCEDURE

The method of co-removal of phenol and cyanide by simultaneous adsorption and biodegradation were performed in as batch and continuous process. This chapter deals with the adsorbent preparations, experimental procedures for both batch and continuous experiments conducted and the data analysis of phenol and cyanide for both batch and continuous processes.

5.1 ADSORBENTS AND CHEMICALS:

Granular activated carbon and powdered activated carbon were purchased from Himedia Laboratories Pvt. Ltd. Mumbai, India. Rice Husk, egg shells and corn husk leaves were obtained from local market of Roorkee, India. The chemicals used in all the studies were of analytical grade and were obtained from Himedia Laboratories Pvt. Ltd. Mumbai India, Loba Chemie Pvt. Ltd. Mumbai, India, RFCL Ltd. New Delhi and E. Merck India Ltd. Mumbai, India.

5.2 PREPARATION OF ADSORBENTS AND THEIR PRE-TREATMENT:

Simultaneous adsorption and biodegradation of phenol and cyanide were carried out using the following adsorbents:

- Activated Carbon
- Rice Husk
- Egg shells
- Corn Husk Leaves

5.2.1 ACTIVATED CARBON:

Activated Carbon both powdered and granular was obtained from Himedia Laboratories Pvt. Ltd. Mumbai, India. Powdered activated carbon was used for batch studies due to its high surface area as compared to granular activated carbon whereas granular activated carbon was used in continuous studies as a comparatively less amount of Granular activated carbon will be required in column studies as compared to powdered activated carbon which in turn increases the economy of the process.

5.2.2 RICE HUSK:

Rice Husk was obtained as a waste product from the local market of Roorkee, India. The rice husk was washed 3-4 times with tap water to remove the dust and dirt particles present in the husk. The washed rice husk was then again washed with Millipore water. Then it was dried at 100 ^{0}C for 5 h in a hot air oven. The adsorbent prepared was now stored in air tight packets.

5.2.3 EGG SHELLS:

Egg shells were also obtained as waste from a local egg vendor at Roorkee, India. Egg shells were washed several times with tap water to clean them properly and to free them from the remaining egg white in the shells. The shells were then washed with Millipore water twice to further clean it and make it fit for bacterial use. The shells were then dried at 100 ^{0}C for 24 h. The dried egg shells were then crushed to a size of 1.4 mm. The crushed and sieved egg shells to a size of 1.4 mm were collected and stored in air tight bags as the third adsorbent.

5.2.4 CORN HUSK LEAVES:

Corn caps were acquired as waste from a local shop at Roorkee, India. Corn husk leaves were obtained by removing the fibres from corn caps. The husk leaves then obtained were washed several times with tap water and then was twice washed with Millipore water. The washed husk leaves were dried at 50 ^{0}C for 24 h. The dried husk leaves were crushed to a size of 1.7 mm. The crushed and sieved husk leaves now obtained were stored in air tight polybags and stored as adsorbent for further use.

5.3 CHARACTERIZATION OF ADSORBENTS:

Characterization of adsorbents was done by estimating surface area, pore volume, thermal stability, degree of crystallinity and the functional groups present in the adsorbent before and after simultaneous adsorption and biodegradation process by FTIR, studying the surface texture by SEM studies along with proximate analysis.

Figure 5.1 Rice Husk

Figure 5.2 Corn Husk Leaves

Figure 5.3 Egg Shells

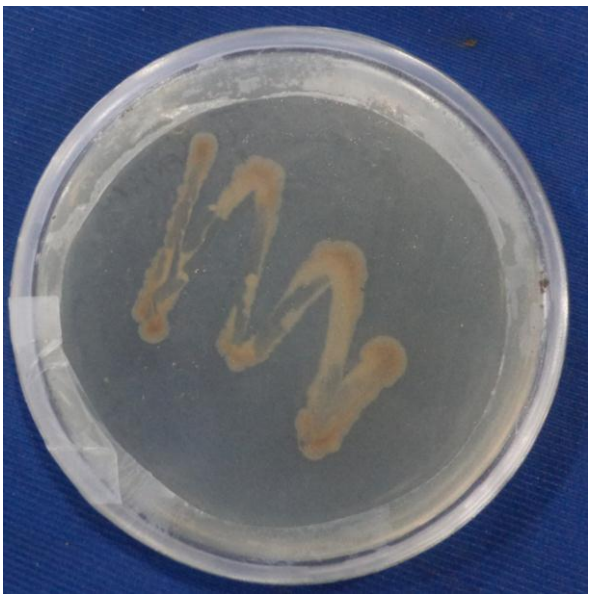

Figure 5.4 Petri plates containing cultured bacteria

5.4 PREPARATION OF SIMULATED SYNTHETIC WASTEWATER CONTAINING PHENOL AND CYANIDE:

0.189 g of NaCN (Sodium Cyanide) was dissolved in 1L of millipore water (Q-H_2O, Millipore Corp. with resistivity of 18.2 MX-cm) to prepare a stock solution of cyanide concentration of 100 mg/L. The pH of the cyanide stock solution was adjusted to 10 using 1 N NaOH. The phenol stock solution, with the concentration of 1000 mg/L, was prepared by adding 1 g of pure phenol crystals to 1 L of millipore water.

5.5 STERILIZATION:

All the glassware used i.e. flat bottom flasks, petridishes and test tubes for the bacteriological studies were properly washed and rinsed with distilled water, then oven dried at 110 ^{0}C. The washed and dried glassware were cotton plugged and then with their solid and liquid medium were sterilized in an autoclave at 15 psi for 20 min. Bacteria transfer and media were all done in laminar hood over the flame of spirit lamp.

5.6 BACTERIA GROWTH:

The singular bacterium of *Serratia species* i.e. *S. odorifera* was used as the bacterial species in this study. The bacterial specie used in the present study was isolated in the laboratory (Agarwal et.al. 2013). The bacteria were cultured initially in a nutrient medium and then it was stored in the agar plates and as slant culture for further use.

5.7 BACTERIA PLATING:

Bacteria were cultured in the nutrient medium and then it was stored in agar plates and as slant culture for further use. The plating procedure is as follows:

1. 50 mL of nutrient agar solution was prepared by adding 2g agar to 50 mL of Millipore water containing media components as required.
2. The nutrient agar solution was sterilized in an autoclave at 121 ^{0}C at 15 psi for 20 min.
3. The sterilized nutrient agar solution was allowed to cool for some time and then it was poured in the plates
4. The plates were covered and allowed to cool overnight.
5. Then an inoculum was taken in the inoculation loop from the cultured nutrient media and striped on the plates.
6. The plates were then incubated at 30 ^{0}C for 24 h.
7. After 24 h colonies of bacteria started to grow on the nutrient plates.
8. Then the cultured plates were stored at 4 ^{0}C for further use.

5.8 MICROORGANISMS GROWTH STUDY IN NUTRIENT MEDIUM:

Growth study of microorganism was done in 100 mL of nutrient medium in a 250 mL flask. The 250 mL flask along with the 100 mL of nutrient media was sterilized in an autoclave at 121 ^{0}C and 15 psi for 20 min. After that an inoculum using the inoculation loop from the petri plates was added to the nutrient broth in the laminar hood in presence of a spirit lamp. The culture flask was then kept at 30 ^{0}C in an orbital incubator cum shaker for 24 h to subculture the bacteria further. The media composition taken for the nutrient media of the bacteria consisted of the following components:

Table 5.14 Media composition for bacterial growth

Salt	Composition (g/L)
Na_2HPO_4	4.4
KH_2PO_4	0.6
NaCl	2.5
NH_4Cl	0.5
$MgSO_4.7H_2O$	0.0625
Glucose	5

5.9 ACCLIMATIZATION OF BACTERIA:

The bacteria were further acclimatized to a high phenol and cyanide concentration so that it could get used to phenol and cyanide as carbon and nitrogen source for survival. 100 mL of nutrient media were prepared in Millipore water containing 10 mg/L phenol and 1 mg/L cyanide. The flask along with the media replacing glucose with phenol and cyanide were sterilized in the autoclave at 121 ^{0}C and 15 psi. The revived culture was further inoculated in the media in the ratio of 1:10. The salt medium with the inoculated bacteria was now incubated in an incubator shaker at an rpm of 120 and at a temperature of 30 ^{0}C. Initially there was no growth in the flask but after 24 h significant growth was observed in the flask when the solution started getting turbid indicating microorganism growth. This microbial culture was then grown in the increasing phenol and cyanide concentration in a step of 50 mg/L phenol and 5 mg/L cyanide until the final concentration of phenol and cyanide reached 500 mg/L and 50 mg/L respectively. Solution's initial pH was maintained by adding sterile

HCl and NaOH. All the sterilization was done in an autoclave at 121 $^{\circ}$C for 20 min and all the transfers were done in a laminar hood under the burner flame.

5.10 Batch Studies on Simultaneous Adsorption and Biodegradation of Phenol and Cyanide:

Experiments for simultaneous adsorption and biodegradation of phenol and cyanide were carried out in 250 mL flat bottom flask in a 100 mL solution. All the glassware plugged with cotton with the liquid medium was sterilized in an autoclave at 121 ^{0}C and 15 psi for 20 min. The bacteria was then inoculated in the flask to a 50 mL media solution in the ratio of 1:10 and then the flasks were placed in an incubator shaker at 30 ^{0}C. After 24 h when turbidity appeared in the flask sterilised adsorbents were added in the flask in the laminar hood under the spirit lamp. Again the flasks were left in the incubator shaker at 30 ^{0}C for the bacteria to get immobilized on the adsorbent surface. After 24 h sterile 50 mL solutions of 200 mg/L phenol and 20 mg/L cyanide were added in the solution making it a 100 mL solution containing 100 mg/L phenol and 10 mg/L cyanide concentration. Different concentrations of phenol and cyanide were taken in the range of 100-1000 mg/L and 10-100 mg/L respectively. The flasks were placed further in the incubator and orbital shaker at 30 ^{0}C at an rpm of 120 for 60 h. After 60 h the samples were collected and they were first filtered by Whatman filter paper (Cat No 1001 125) to filter out the adsorbent. The filtrate was then collected and centrifuged at 10000 rpm in a centrifuge. The supernatant was then collected and analysed for phenol and cyanide concentration by colorimetric methods.

Figure 5.5: Colouring agents used for phenol and cyanide analysis Nickel Solution (left) Potassium ferricyanide (centre) and picric acid solution (right)

Figure 5.6: Sampling bottles used for phenol and cyanide analysis as phenol as highly photosensitive

5.10.1 EFFECT OF pH:

The experiments to study the effect of pH on the SAB process were carried out in 250 mL flat bottom flask. 50 mL media was prepared and sterilised at 121 ^{0}C for 20 min at 15 psi. Millipore water was used to prepare the synthetic solutions. pH of the solution was varied between 2-12 using 1 N HCl and 1 N NaOH in the laminar hood under spirit lamp. pH of the solution were tested using pH strips. The bacteria were inoculated in the media and were incubated at 30 ^{0}C for 24 h in an incubator shaker. Then a specific adsorbent dose was further introduced in the flask and the flask was incubated for 24 h at 30 ^{0}C to let the bacteria immobilize on the adsorbent surface. The synthetic simulated water with 800 mg/L phenol and 80 mg/L cyanide was prepared in Millipore water and was sterilised in an autoclave at 121 ^{0}C for 20 min. The phenol and cyanide solution was added in the flask reducing the phenol and cyanide concentration to 400 mg/L and 40 mg/L respectively. The samples after 54 h were collected and filtered by Whatman Filter Paper (Cat No 1001 125) for filtering the adsorbent and the filtrate was further centrifuged at 10000 rpm for 10 min. The supernatant was then analysed for phenol and cyanide by UV-Vis spectrophotometer.

5.10.2 EFFECT OF ADSORBENT DOSE:

The adsorbent dose experiments for the SAB process of phenol and cyanide were carried out in 250 mL flat bottom flask. 50 mL media was prepared and sterilised at 121 ^{0}C for 20 min at 15 psi. Millipore water was used to prepare the synthetic solutions. pH of the solution was maintained at the optimum pH value using 1 N HCl and 1 N NaOH in the laminar hood under spirit lamp. pH of the solution were tested using pH strips. The bacteria were inoculated in the media and were incubated at 30 ^{0}C for 24 h in an incubator shaker. Then a specific adsorbent dose was further introduced in the flask and the flask was incubated for 24 h at 30 ^{0}C to let the bacteria immobilize on the adsorbent surface. The adsorbent dose was then varied in a certain range. The synthetic simulated water with 800 mg/L phenol and 80 mg/L cyanide was prepared in Millipore water and was sterilised in an autoclave at 121 ^{0}C for 20 min. The phenol and cyanide solution was added in the flask reducing the phenol and cyanide concentration to 400 mg/L and 40 mg/L respectively. The samples after 54 h were collected and filtered by Whatman Filter Paper (Cat No 1001 125) for filtering the adsorbent and the filtrate was further centrifuged at 10000 rpm for 10 min. The supernatant was then analysed for phenol and cyanide by UV-Vis spectrophotometer.

Table 5.2 Range of adsorbent dose for biosorbents used

Adsorbent	Range
Activated Carbon	40 g/L
Rice Husk	1-6 g/L
Corn Husk leaves	2-10 g/L
Egg Shells	10-60 g/L

5.10.3 EFFECT OF TEMPERATURE:

The temperature effect studies for the SAB process of phenol and cyanide were carried out in 250 mL flat bottom flask. 50 mL media was prepared and sterilised at 121 ^{0}C for 20 min at 15 psi. Millipore water was used to prepare the synthetic solutions. pH of the solution was maintained at the optimum pH value using 1 N HCl and 1 N NaOH in the laminar hood under spirit lamp. pH of the solution were tested using pH strips. The bacteria were inoculated in the media and were incubated at a range of temperature between 25-40 ^{0}C for 24 h in an incubator shaker. Then the optimum adsorbent dose was further introduced in the flask and the flask was incubated for 24 h at different temperatures to let the bacteria immobilize on the adsorbent surface. The simulated synthetic water with concentration of 800 mg/L phenol and 80 mg/L cyanide was prepared in Millipore water and was sterilised in an autoclave at 121 ^{0}C for 20 min. The phenol and cyanide solution was added in the flask reducing the phenol and cyanide concentration of 400 mg/L phenol and of 40 mg/L cyanide. The flasks were incubated and the samples were collected after 54 h. These samples were collected and filtered by Whatman Filter Paper (Cat No 1001 125) for filtering the adsorbent and the filtrate was further centrifuged at 10000 rpm for 10 min. The supernatant was then analysed for phenol and cyanide by UV-Vis spectrophotometer.

5.10.4 EFFECT OF CONTACT TIME:

The contact time effect studies for the SAB process of phenol and cyanide were carried out in 250 mL flat bottom flask. 50 mL media was prepared and sterilised at 121 ^{0}C for 20 min at 15 psi. Millipore water was used to prepare the synthetic solutions. pH of the solution was maintained at the optimum pH value using 1 N HCl and 1 N NaOH in the laminar hood under spirit lamp. pH of the solution were tested using pH strips. The bacteria were inoculated in the media and were incubated at 30 ^{0}C for 24 h in an incubator shaker. Then the optimum adsorbent dose was further introduced in the flask and the flask was incubated for 24 h at 30 ^{0}C to let the bacteria immobilize on the adsorbent surface. The synthetic simulated water with

concentration of 800 mg/L phenol and 80 mg/L cyanide was prepared in Millipore water and was sterilised in an autoclave at 121 ^{0}C for 20 min. The phenol and cyanide solution was added in the flask reducing the phenol and cyanide concentration of 400 mg/L phenol and of 40 mg/L cyanide. The flasks were incubated for 54 h and the samples were collected after every 6 h. These samples were collected and filtered by Whatman Filter Paper (Cat No 1001 125) for filtering the adsorbent and the filtrate was further centrifuged at 10000 rpm for 10 min. The supernatant was then analysed for phenol and cyanide by UV-Vis spectrophotometer.

5.10.5 Effect of Initial Concentration:

The initial concentration effect studies for the SAB process of phenol and cyanide were carried out in 250 mL flat bottom flask. 50 mL media was prepared and sterilised at 121 ^{0}C for 20 min at 15 psi. Millipore water was used to prepare the synthetic solutions. pH of the solution was maintained at the optimum pH value using 1 N HCl and 1 N NaOH in the laminar hood under spirit lamp. pH of the solution were tested using pH strips. The bacteria were inoculated in the media and were incubated at 30 ^{0}C for 24 h in an incubator shaker. Then the optimum adsorbent dose was further introduced in the flask and the flask was incubated for 24 h at 30 ^{0}C to let the bacteria immobilize on the adsorbent surface. The synthetic simulated water with concentration between (200-1200) mg/L phenol and (20-120) mg/L cyanide was prepared in Millipore water and was sterilised in an autoclave at 121 ^{0}C for 20 min. The phenol and cyanide solution was added in the flask reducing the phenol and cyanide concentration to a range of (100-600) mg/L phenol and (10-60) mg/L cyanide. The samples after 54 h were collected and filtered by Whatman Filter Paper (Cat No 1001 125) for filtering the adsorbent and the filtrate was further centrifuged at 10000 rpm for 10 min. The supernatant was then analysed for phenol and cyanide by UV-Vis spectrophotometer.

The operating parameters for the batch study of Simultaneous Adsorption and biodegradation of phenol and cyanide using different adsorbents is given below:

Table 5.3 Range of operating parameters for all the three adsorbents

Experiment	Range of operating parameters					
	pH	**Initial Phenol Concentration (mg/L)**	**Initial Cyanide Concentration (mg/L)**	**Adsorbent Dose (g/L)**	**Contact Time (h)**	**Temperature (^{0}C)**
			Rice Husk			
Effect of pH	2-12	400	40	5	54	30
Effect of Adsorbent Dose	**6.5-7**	400	40	1-6	54	30
Effect of Temperature	**6.5-7**	400	40	**5**	54	25-40
Effect of Contact Time	**6.5-7**	400	40	**5**	6-54	**30**
Effect of initial concentration	**6.5-7**	100-600	10-60	**5**	**54**	**30**
			Corn Husk Leaves			
Effect of pH	2-12	400	40	**5**	54	30
Effect of Adsorbent Dose	**6.5-7**	400	40	2-10	54	30
Effect of Temperature	**6.5-7**	400	40	**6**	54	25-40
Effect of Contact Time	**6.5-7**	400	40	**6**	6-54	**30**
Effect of Initial Concentration	**6.5-7**	100-600	10-60	**6**	**54**	**30**
			Egg Shells			
Effect of pH	2-12	400	40	10	54	30
Effect of Adsorbent Dose	**6.5-7**	400	40	10-60	54	30

Effect of Temperature	**6.5-7**	400	40	**35**	54	25-40
Effect of Contact Time	**6.5-7**	400	40	**35**	6-54	**30**
Effect of Initial Concentration	**6.5-7**	100-600	10-60	**35**	**54**	**30**

Experiments were conducted using activated carbon at a dose of 40 g/L, with an initial phenol and cyanide concentration of 400 mg/L and 40 mg/L at a temperature of 30 ^{0}C for 54 h.

5.10.6 THERMODYNAMIC STUDY FOR SIMULTANEOUS ADSORPTION AND BIODEGRADATION OF CYANIDE AND PHENOL:

The thermodynamic study for SAB of phenol and cyanide was carried out at an initial phenol concentration of 400 mg/L an initial cyanide concentration of 40 mg/L at a pH 6.5-7 for 54 h and in a temperature range of 25-40 ^{0}C. The data was modelled for the prediction of thermodynamic parameters.

5.10.7 KINETICS STUDY FOR SIMULTANEOUS ADSORPTION AND BIODEGRADATION OF CYANIDE AND PHENOL:

The concluded experiments data was utilized for computing the kinetic data. The pseudo 1st order model and pseudo 2nd order model along with the Webber Morris Intraparticle model was used for generation of kinetic data.

5.10.8 EQUILIBRIUM ISOTHERM STUDY FOR CYANIDE AND PHENOL REMOVAL:

The adsorption isotherm for cyanide and phenol simultaneous adsorption and biodegradation was studied using initial concentration of phenol and cyanide between 100-600 mg/L and 10-60 mg/L at different adsorbent dose for different adsorbents. The data available from the concluded experiments were utilized for equilibrium isotherm calculation. Various multi-component adsorption isotherms were plotted including Non-modified Langmuir isotherm, Modified Langmuir isotherm, Extended Langmuir isotherm, Extended Freundlich model. The constants for these models were calculated using single component Langmuir and Freundlich isotherm.

5.11 CONTINUOUS STUDIES ON SIMULTANEOUS ADSORPTION AND BIODEGRADATION OF PHENOL AND CYANIDE:

The continuous simultaneous adsorption and biodegradation of phenol and cyanide is studied in a column reactor.

5.11.1 WORKING VOLUME OF THE COLUMN REACTOR:

For calculation of working volume of the column reactor used, the reactor was first fully filled with water until water appeared from port 1 and then after closing all the input and output valves i.e. by only opening exit port 6 and draining the water into a large graduated cylinder. After all the water has been drained out, the volume of the water that was emptied into the graduated cylinder was measured. This volume of water emptied is equal to the working volume of the column reactor.

5.11.2 RESIDENCE TIME DISTRIBUTION STUDIES OF THE REACTOR (PREDICTING THE FLOW BEHAVIOR OF THE REACTOR):

Before optimizing the continuous removal process of simultaneous adsorption and biodegradation of phenol and cyanide it is necessary to predict the flow pattern of the column reactor. The two edges for the flow pattern of a reactor can be either plug flow or mixed flow. The flow behavior of the present reactor was studied using Residence Time Distribution (RTD) studies on the reactor. For the RTD studies a suitable tracer was used which in this case was Sodium Hydroxide (NaOH). The packed bed reactor was filled with a packing of glass beads. Tracer used in all the trials was NaOH. The NaOH solution was first standardized by titrimetric method using 0.2 N oxalic acid solution. HCl solution was then standardized using the standardized NaOH by titrimetric method. The titrations were conducted using phenolphthalein as an indicator.

Different case studies were carried out to understand the flow pattern of the reactor. In these case studies the volumetric flow rate of the reactor was varied by changing the rpm of the peristaltic pump as well as by introducing agitation in the feed tank.

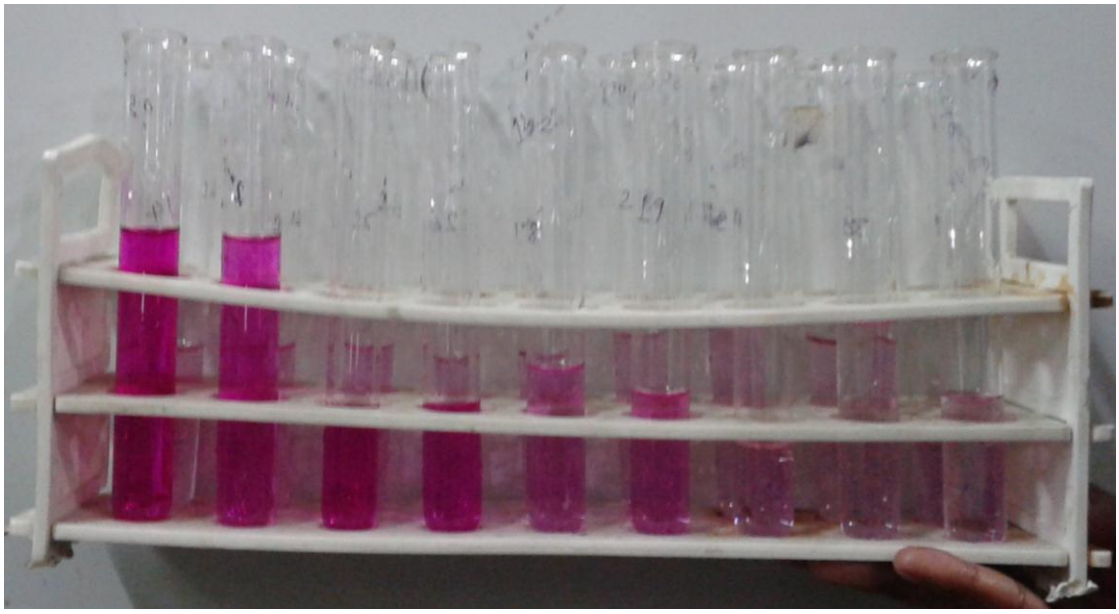

Figure 3.7 Test tubes with different tracer concentrations for the RTD studies of the column reactor

5.11.3 Suitable Adsorbent for Column Studies:

In the present study the column studies for simultaneous adsorption and biodegradation of phenol and cyanide are carried out using two adsorbents granular activated carbon and rice husk based on their batch performance.

5.11.4 Granular Activated Carbon: Packing Material of the Column:

After the Residence Time Distribution studies the column was washed 2-3 times with tap water and then the reactor was emptied of the glass beads. The empty column was again washed with tap water and then with distilled water. Then the reactor bed was packed with granular activated carbon. After filling the column completely the packing material of the reactor it was washed twice or thrice with tap water and then twice with distilled water.

5.11.4.1 Immobilization of Bacteria on the Packing Material:

15 L of bacterial solution was prepared by inoculating and incubating bacteria in 15 L of nutrient media. This bacterial solution was added in the feed tank and was made to flow in the packed bed using the peristaltic pump until the column was completely filled with bacterial solution. The liquid was passed in the column until the solution emerged from exit port 1. Then all the entry and exit ports of the reactor were closed so that neither the fluid could escape the reactor from the exit port nor could back flow in the inlet tank. The outlet

from exit port 1 was continuously analysed for bacterial growth under a high power microscope. When bacterial growth appeared from the outlet of exit port 1, all the reactor ports were closed for 48 h when the bacteria were immobilized on the adsorbent i.e. packing material of the reactor.

5.11.4.2 CONTINUOUS STUDY:

After 48 h the inlet feed tank was filled with a synthetic simulated solution of 400 mg/L phenol and 40 mg/L cyanide concentration. The rpm of the peristaltic pump was set according to the EBCT i.e. effective bed contact time. The continuous study was carried out for two EBCT of 2.5 h and 5 h. The inlet port and exit port 1 were opened and the synthetic simulated solution was made to flow in the packed bed by using the peristaltic pump at a particular rpm. After every 6 h samples were collected by exit port 1, 2, 3, 4 and 5. Those samples were centrifuged at 10000 rpm for 10 min. The supernatant was analysed for phenol and cyanide concentration whereas the biomass accumulated at the bottom of the centrifuge tube was analysed for the O.D. of the biomass by UV-Vis spectrophotometer for monitoring the bacterial growth.

5.11.4.3 BREAKTHROUGH CURVE:

The granular activated bed which is simultaneously regenerated by the simultaneous biodegradation of the adsorbed phenol and cyanide is reused for plotting the breakthrough curve i.e. the curve between normalized concentration and effluent volume or time. The bacteria immobilized on the GAC bed was starved to death and then the bed was washed 2-3 times with distilled water. The outlet from the exit port 1 was then analysed for any bacterial growth under the microscope. When the bacteria were completely dead and the remaining biomass was washed away with distilled water a binary solution of 400 mg/L and 40 mg/L of phenol and cyanide was added in the inlet tank and was made to flow in the reactor at an EBCT of 5 h. The samples were collected after every 6 h and were analyzed for phenol and cyanide concentration by colorimetric method using a UV-Vis spectrophotometer. A breakthrough curve was obtained by plotting the normalized concentration versus the flow time.

5.11.4.4 KINETIC MODELING OF BREAKTHROUGH CURVE DATA AND MASS TRANSFER ZONE (MTZ) STUDIES FOR THE PACKED COLUMN AT DIFFERENT BED HEIGHTS:

The breakthrough curve data was analyzed by different kinetic models to predict dynamic response of the packed bed reactor. The different kinetic models plotted were Adams Bohart

Model, Wolborska Model, Thomas Model and Yoon and Nelson model. Mass transfer (MTZ) zone studies were also carried out for the column for different bed heights.

5.11.5 RICE HUSK: PACKING MATERIAL OF THE COLUMN:

After the breakthrough experiment the column was cleared of the activated carbon. The column was washed several times with tap water and then several times with distilled water. Then the column was completely filled with NaOH treated rice husk. The rice husk filled packed bed was washed twice with distilled water.

5.11.5.1 IMMOBILIZATION OF BACTERIA ON THE PACKING MATERIAL:

15 L of bacterial solution was prepared by inoculating and incubating bacteria in 15 L of nutrient media. This bacterial solution was added in the feed tank and was made to flow in the packed bed using the peristaltic pump until the column was completely filled with bacterial solution. The liquid was passed in the column until the solution emerged from exit port 1. Then all the entry and exit ports of the reactor were closed so that neither the fluid could escape the reactor from the exit port nor could back flow in the inlet tank. The outlet from exit port 1 was continuously analysed for bacterial growth under a high power microscope. When bacterial growth appeared from the outlet of exit port 1, all the reactor ports were closed for 48 h when the bacteria immobilized on the adsorbent i.e. packing material of the reactor.

5.11.5.2 CONTINUOUS STUDY:

After 48 h the inlet feed tank was filled with a synthetic simulated solution of 400 mg/L phenol and 40 mg/L cyanide concentration. The rpm of the peristaltic pump was set according to the EBCT i.e. effective bed contact time. The continuous study was carried out for an EBCT of 5 h. The inlet port and exit port 1 were opened and the synthetic simulated solution was made to flow in the packed bed by using the peristaltic pump at a particular rpm. After every 6 h samples were collected by exit port 1, 2, 3, 4 and 5. Those samples were centrifuged at 10000 rpm for 10 min. The supernatant was analysed for phenol and cyanide concentration whereas the biomass accumulated at the bottom of the centrifuge tube was analysed for the O.D. of the biomass by UV-Vis spectrophotometer for monitoring the bacterial growth.

CHAPTER 6

RESULT AND DISCUSSION

The results of all the experiments carried out are discussed in detail in this chapter. The chapter is divided two main segments:

1. Batch studies for Simultaneous Adsorption and Biodegradation of Phenol and Cyanide
2. Column Studies or Continuous Studies for Simultaneous Adsorption and Biodegradation of Phenol and Cyanide.

These two main segments are further divided into sub segments.

6.1 BATCH STUDIES FOR SIMULTANEOUS ADSORPTION AND BIODEGRADATION OF PHENOL AND CYANIDE:

6.1.1 CHARACTERISATION OF ADSORBENT:

Characterisation of the following adsorbents is given below:

6.1.1.1 GRANULAR ACTIVATED CARBON:

6.1.1.1.1 GENERAL CHARACTERISTICS:

Table 6.15: General Characteristics of Granular Activated Carbon

Parameter	Value
Surface Area	228.6375 m^2/g
Total Pore Volume	0.1151 m^3/g
Moisture	8.82 %
Volatile Matter	12.47 %
Ash	11.45 %
Fixed Carbon	67.26 %

6.1.1.1.2 FT-IR SPECTRA:

The FTIR spectra of granular activated Carbon (GAC) before and after SAB are shown in figure 6.1 and 6.2 respectively. Peaks in the region of 3600-3200 cm^{-1} i.e. the peak at 3434.07

cm^{-1} show the presence of –OH or –NH functional groups. –CH stretching is shown by the peak at 2357.30 cm^{-1}. The peak at 1633.22 cm^{-1} shows the presence of secondary amines. The peaks at 1047.48 cm^{-1} and at 665.34 cm^{-1} predict the presence of aliphatic ether and –CN stretching. As seen from fig 6.2 after SAB there are some major shifts in peaks in the –OH region, -CH stretching region and amine region i.e. from 3437.07 to 3417.76 cm^{-1} , from 2357.30 to 2357.38 cm^{-1} and from 1633.22 to 1599.65 cm^{-1}. The shifts in peak in the primary alcohol region and in the –CH stretching region indicates the presence of phenol and the shifts in peak in amine region indicates the adsorption of –CN as secondary amine (Agarwal et. al., 2013).

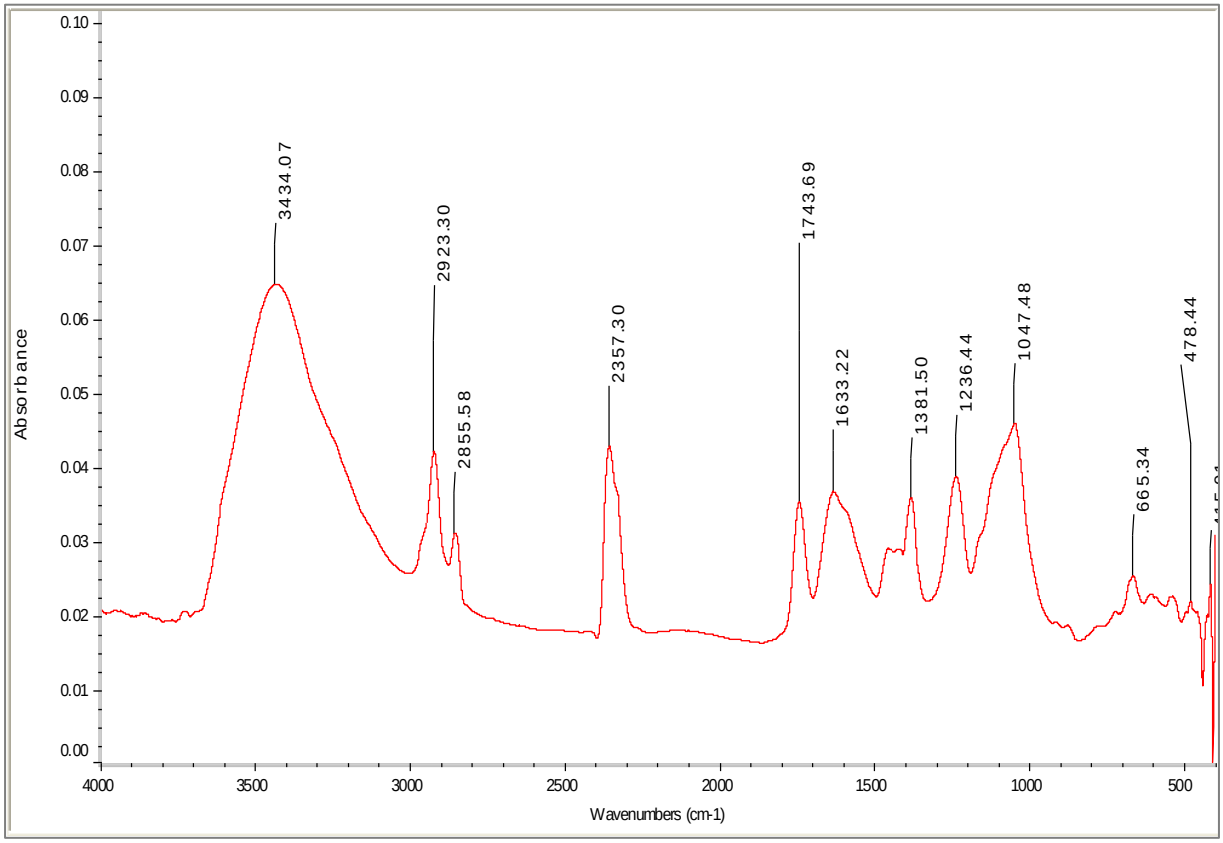

Figure 6.4: FT-IR Spectra of granular activated carbon before SAB of phenol and cyanide

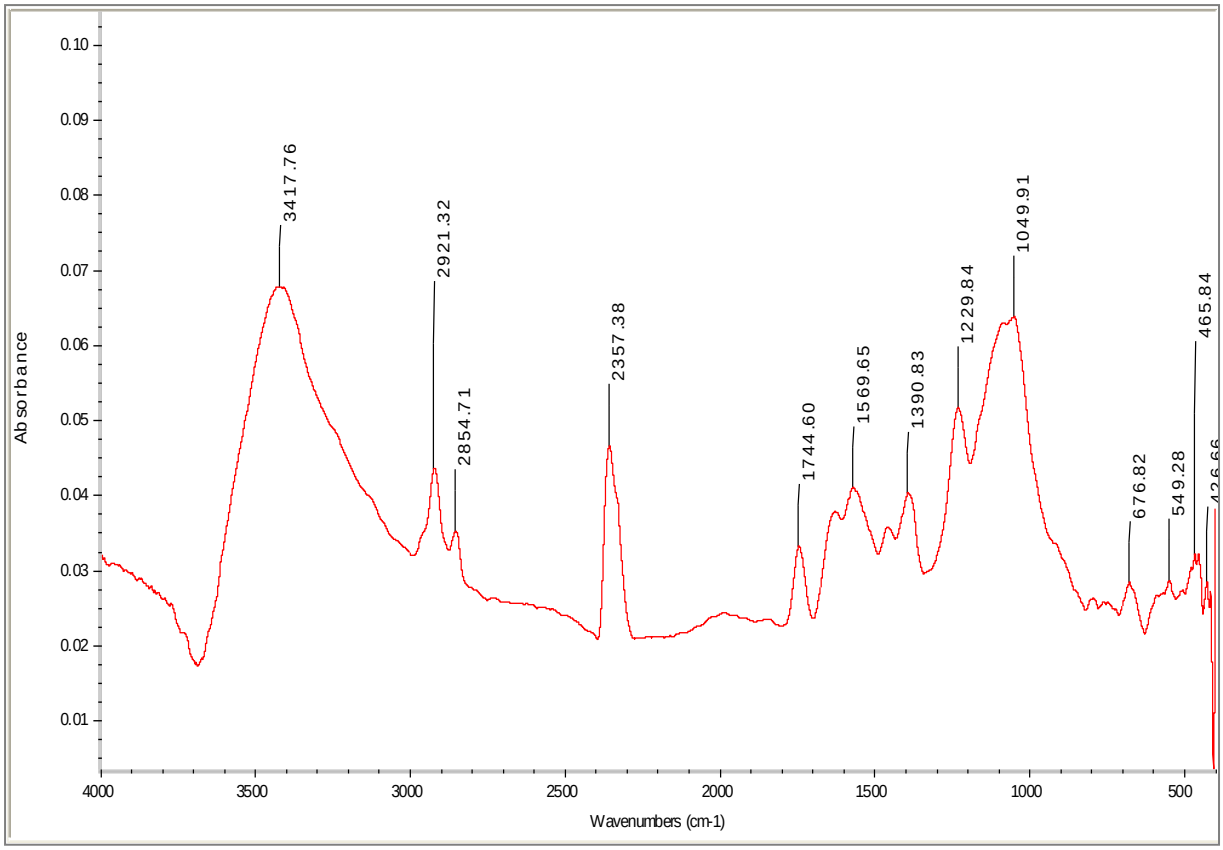

Figure 6.5: FT-IR Spectra of granular activated carbon after SAB of phenol and cyanide

6.1.1.1.3 X-RAY DIFFRACTION:

Granular activated carbon was analysed for its crystalline structure by XRD analysis before and after simultaneous adsorption and biodegradation of both phenol and cyanide. The comparative XRD analysis is given in figure 6.3.

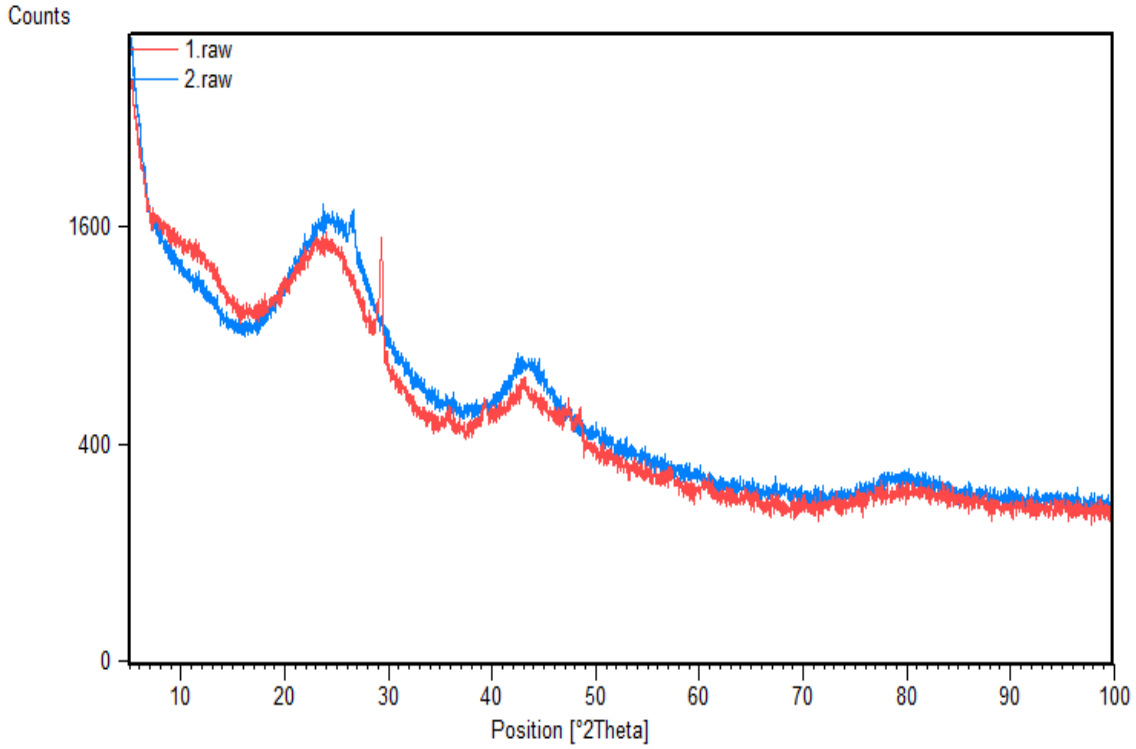

Figure 6.6: XRD pattern of granular activated carbon before SAB (red line) and after SAB (blue line)

The prominent crystalline peaks can be seen at 2θ= 8^0, 25^0, 29^0 and 45^0 The above figure shows that the degree of crystallinity of granular activated carbon is not much compromised due to simultaneous adsorption and biodegradation of both phenol and cyanide.

6.1.1.1.4 THERMOGRAVIMETRIC ANALYSIS:

The thermogravimetric analysis of granular activated carbon is shown in figure 6.4 (blue line). TGA curve shows that till 27° C there was no weight loss of adsorbent. At 97 °C a 5.2 % weight loss of adsorbent took place which is corresponding to moisture evaporation as the temperature is quite close to 100 °C. Between 97 °C and 307 °C there was weight loss of 7.4 %. A major adsorbent adsorbent weight loss of 79.7 % occurs between 393 °C and 457 °C which is due to decomposition of granular activated carbon. After 1212 °C there was no further weight loss in the adsorbent and a residue of 10.8 % remained constant.

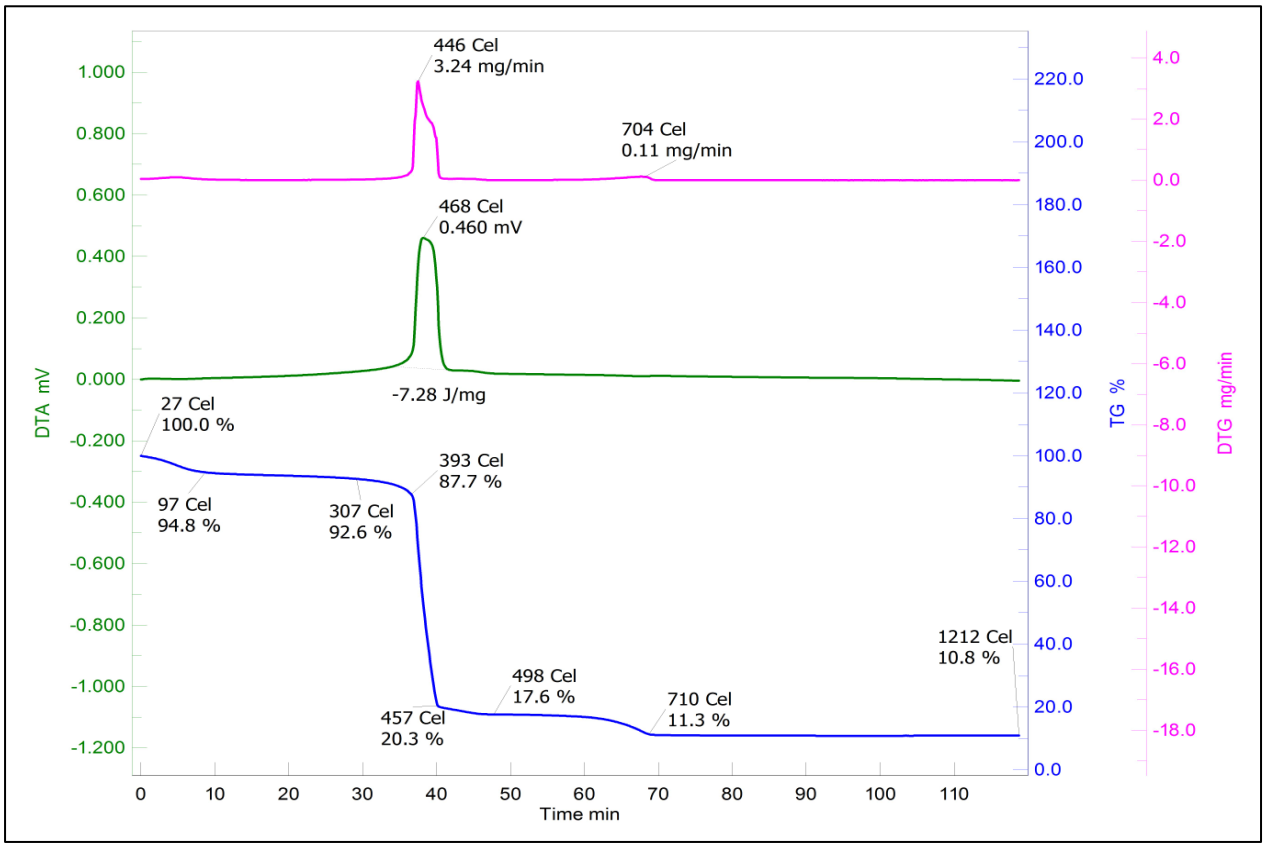

Figure 6.7: Thermogravimetric analysis of granular activated carbon

6.1.1.1.5 Fe-SEM:

SEM image of granular activated is given below showing the porous nature of the adsorbent.

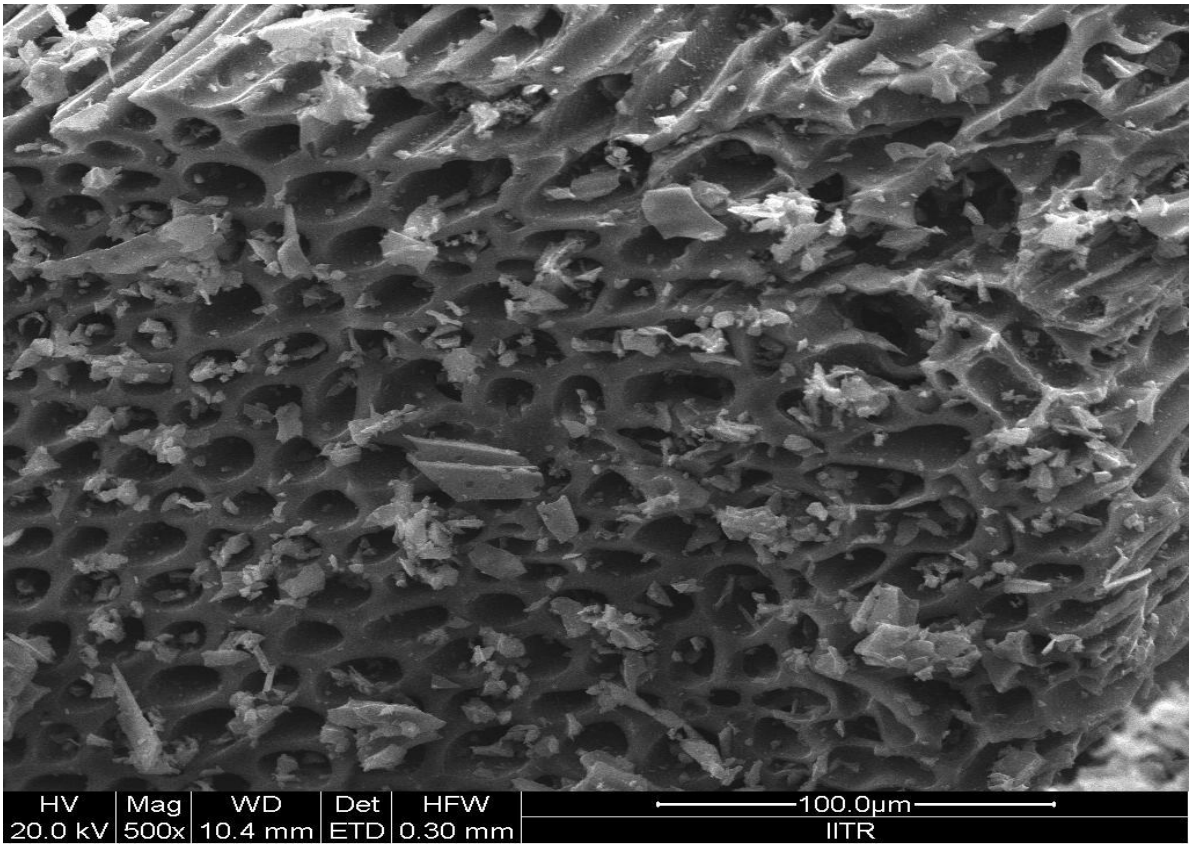

Figure 6.8: SEM Image of Granular activated carbon at 500 magnification

6.1.1.2 RICE HUSK:

6.1.1.2.1 GENERAL CHARACTERISTICS:

Table 6.16: General Characteristics of Rice Husk

Parameter	Value
Surface Area	47.9554 m^2/g
Total Pore Volume	0.0241 m^3/g
Monolayer Volume	11.016 cm^3/g
Moisture	12.45 %
Volatile Matter	65.37 %
Ash	17.45 %

6.1.1.2.2 FT-IR SPECTRA:

The FTIR spectra of rice husk before and after SAB is shown in figure 6.6 and 6.7 respectively. The FTIR spectra shows peaks at 3431.89 cm^{-1}, 2356.23 cm^{-1}, 1640.63 cm^{-1} reveal the presence of –OH or –NH groups, along with –CH stretching and presence of secondary amines. The spectra also show the presence of aliphatic ethers and –CN stretching through the peaks of 1049.67 cm^{-1} and 664.82 cm^{-1}.

As seen from figure 6.7 after SAB the major shifts in peaks are in the –OH region, -CH stretching region and amine region i.e. from 3437.89 to 3428.78 cm^{-1} , from 2356.23 to 2358.04 cm^{-1} and from 1640.63 to 1641.48 cm^{-1}. The shifts in peak in the primary alcohol region and in the –CH stretching region indicates the presence of phenol and the shifts in peak in amine region indicates the adsorption of –CN as secondary amine(Genieva et. al. 2008).

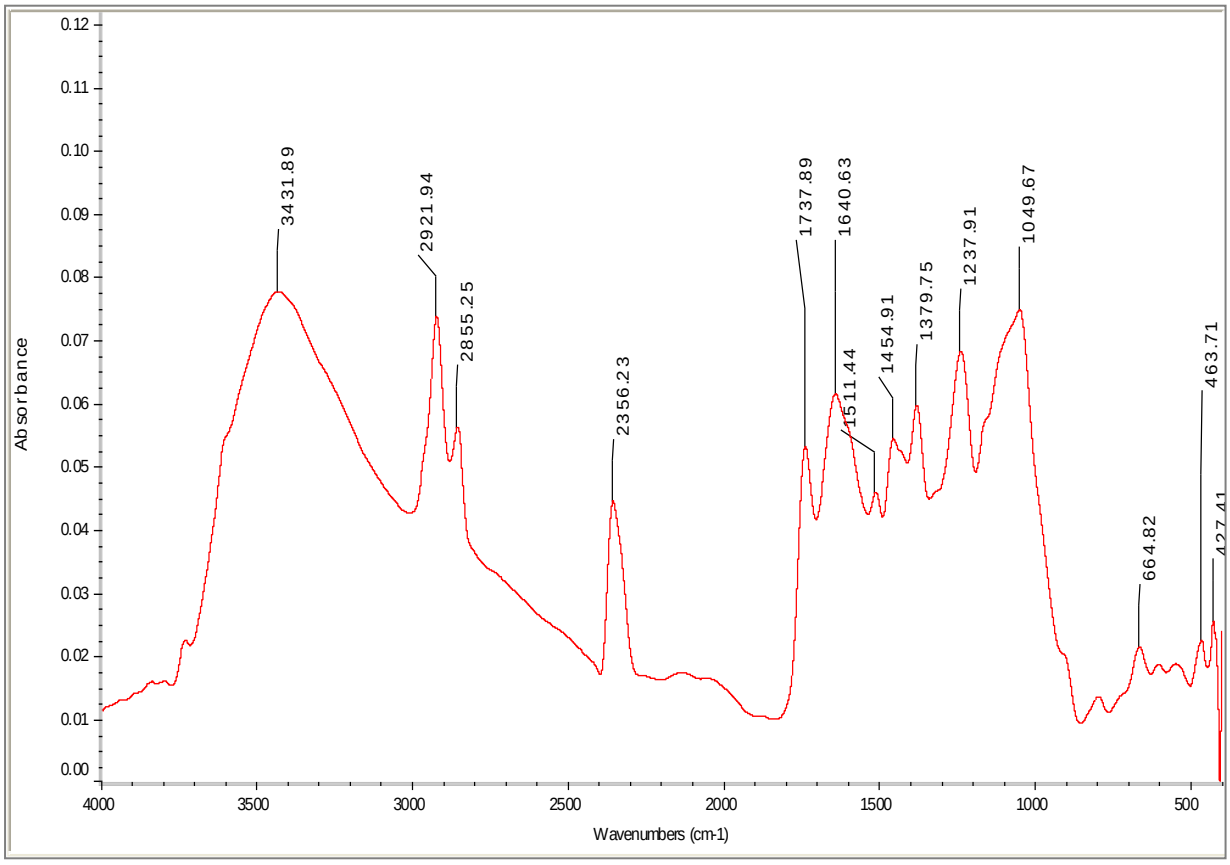

Figure 6.9: FT-IR Spectra of rice husk before SAB of phenol and cyanide

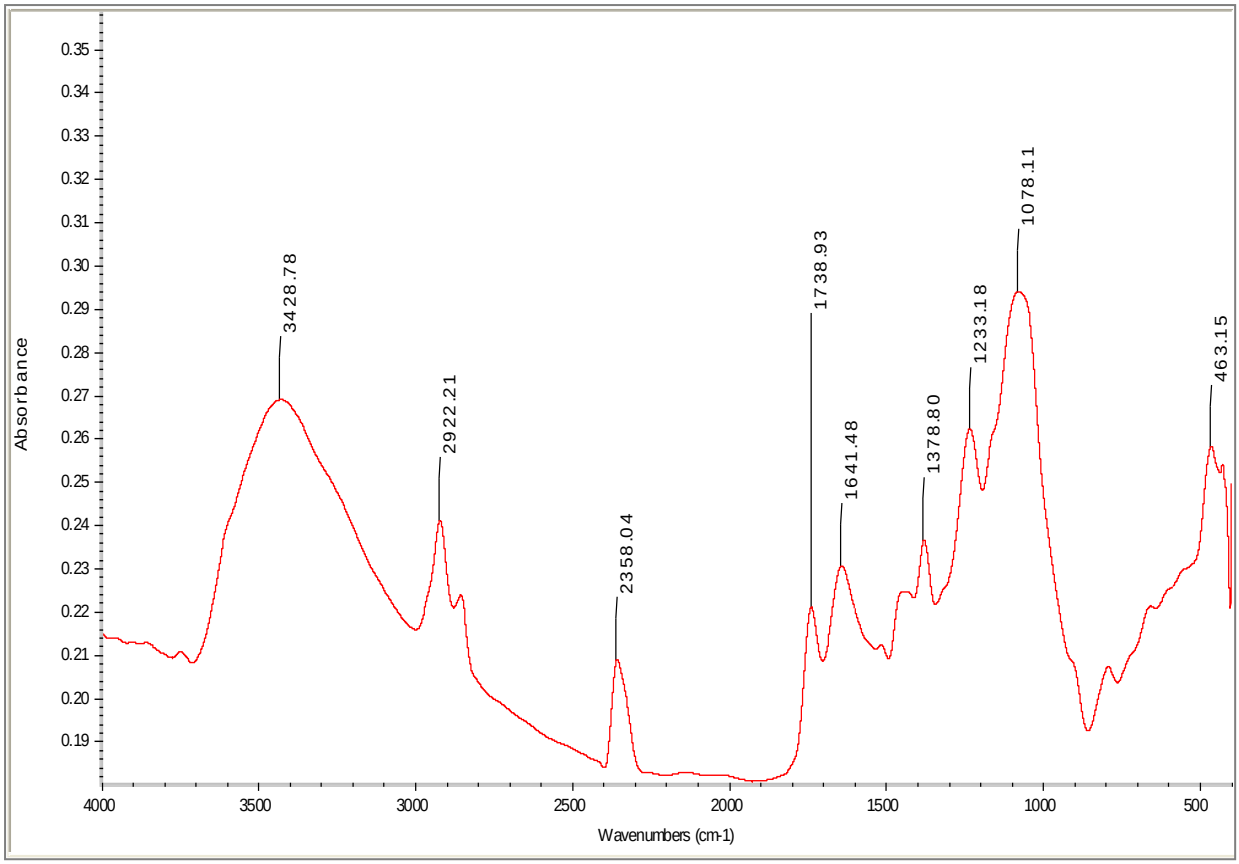

Figure 6.7: FT-IR Spectra of rice husk after SAB of phenol and cyanide

6.1.1.2.3 X-RAY DIFFRACTION:

Rice husk structure analysis by XRD before and after is shown in figure 6.8. The characteristic peaks for rice husk are visible at $2\theta = 5^0$, 15^0, 22^0. This figure also shows that there is not much change in crystallinity of rice husk before and after SAB of phenol and cyanide.

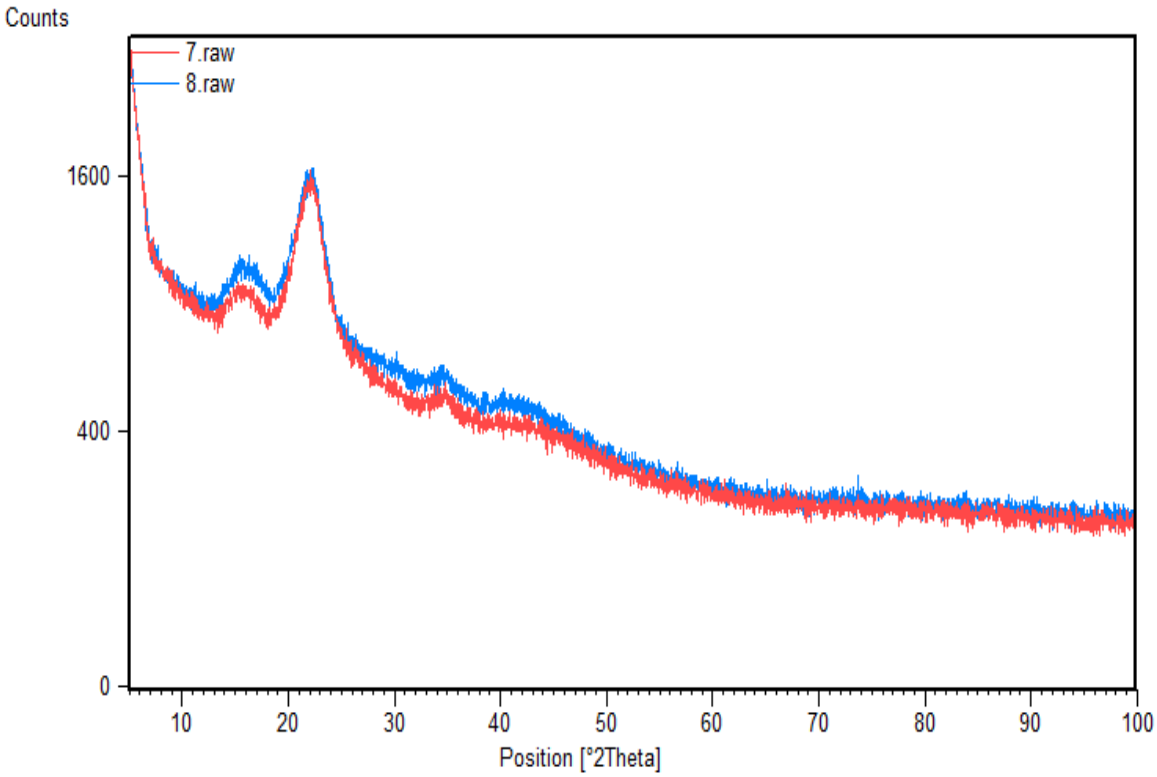

Figure 6.8: XRD pattern of rice husk before SAB (red line) and after SAB (blue line)

6.1.1.2.4 THERMOGRAVIMETRIC ANALYSIS:

The thermogravimetric analysis of rice husk is shown in figure 6.9 (blue line). TGA curve shows that till 24° C there was no weight loss of adsorbent. At 98 °C an adsorbent weight loss of 8.3 % took place which is corresponding to moisture evaporation as the temperature is quite close to 100 °C. At 247 °C there was a weight loss of about 13.3 %. A major adsorbent weight loss of 82.3 % occurs between 247 °C and 415 °C which is due to decomposition of rice husk. After 1214 °C there was no further weight loss in the adsorbent and a residue of 14.8 % remained constant.

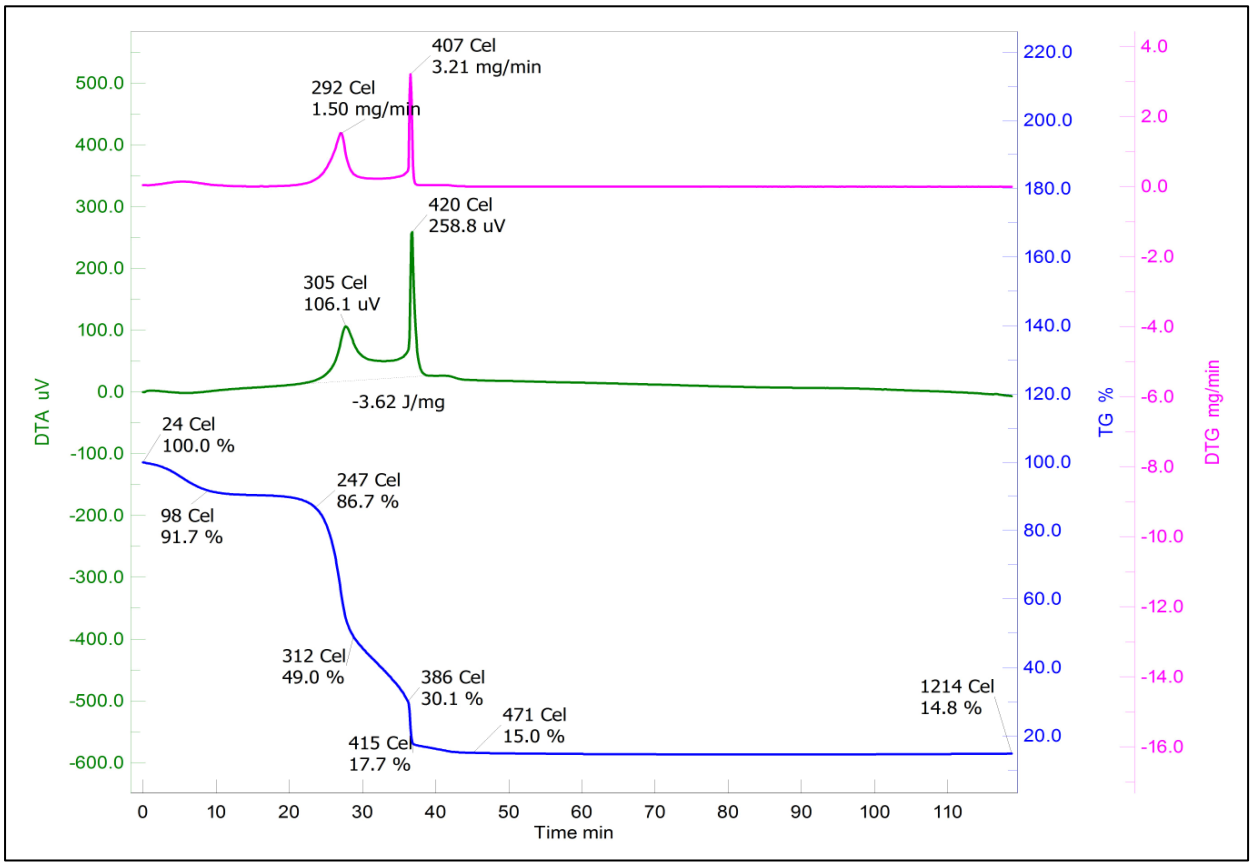

Figure 6.9: Thermogravimetric analysis of rice husk

6.1.1.2.5 FE-SEM:

The surface morphologies of only rice husk as well as rice husk along with the immobilized bacteria before and after SAB are shown in figure 6.10, 6.11and 6.12 respectively.

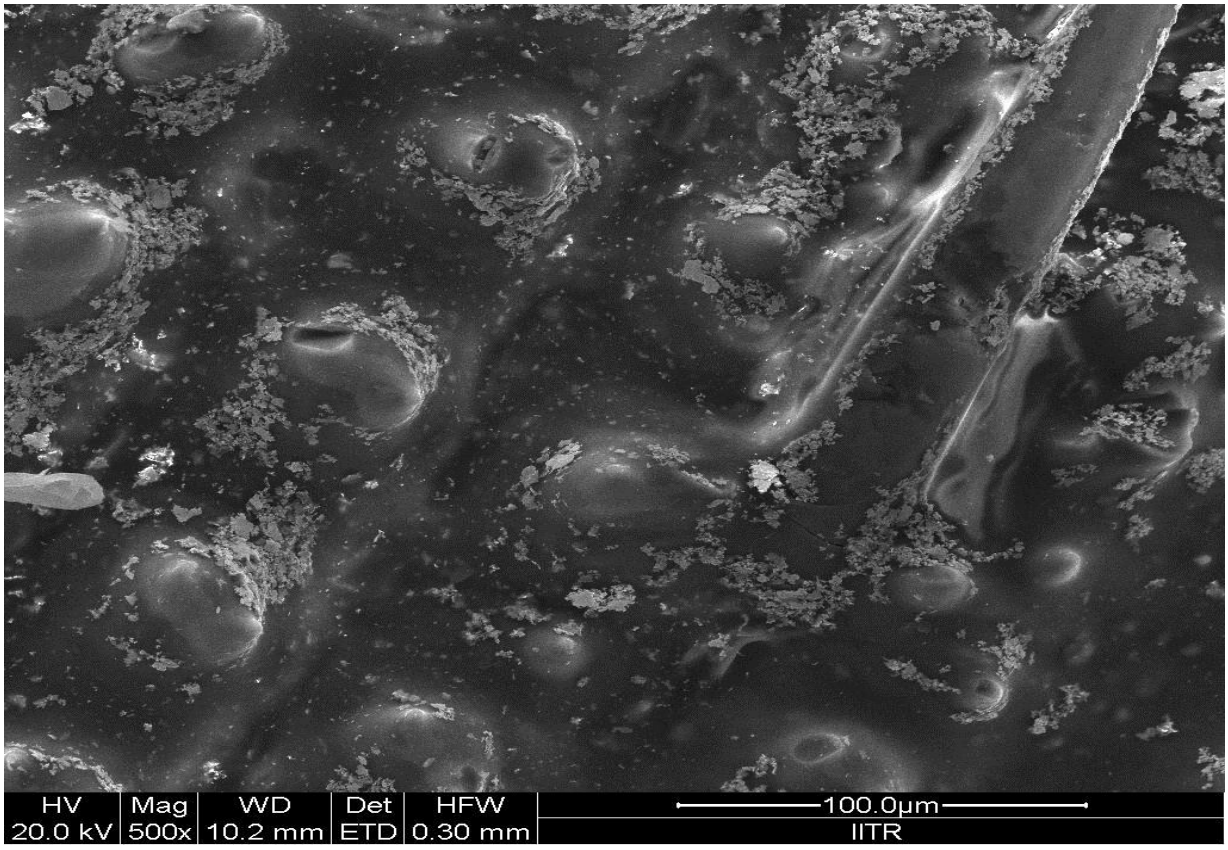

Figure 6.10: SEM image of Rice Husk showing its slightly porous nature

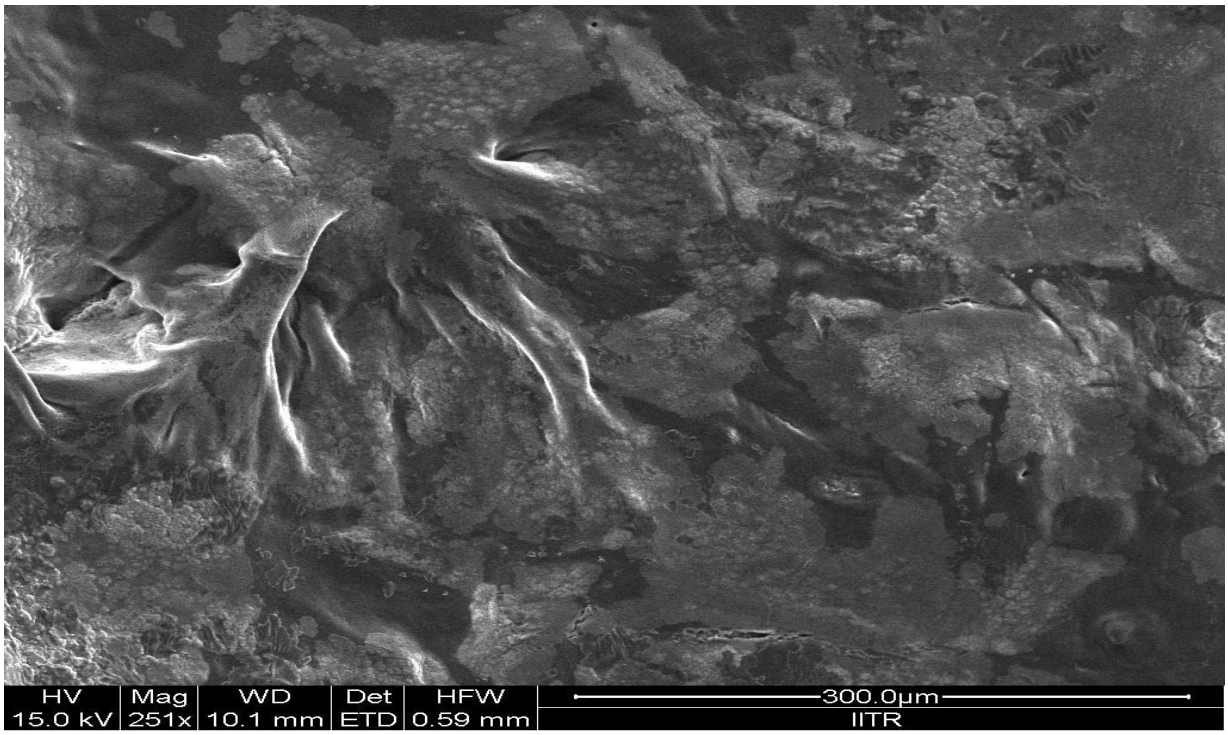

Figure 6.11: SEM image of rice husk with immobilized bacteria before SAB of phenol and cyanide

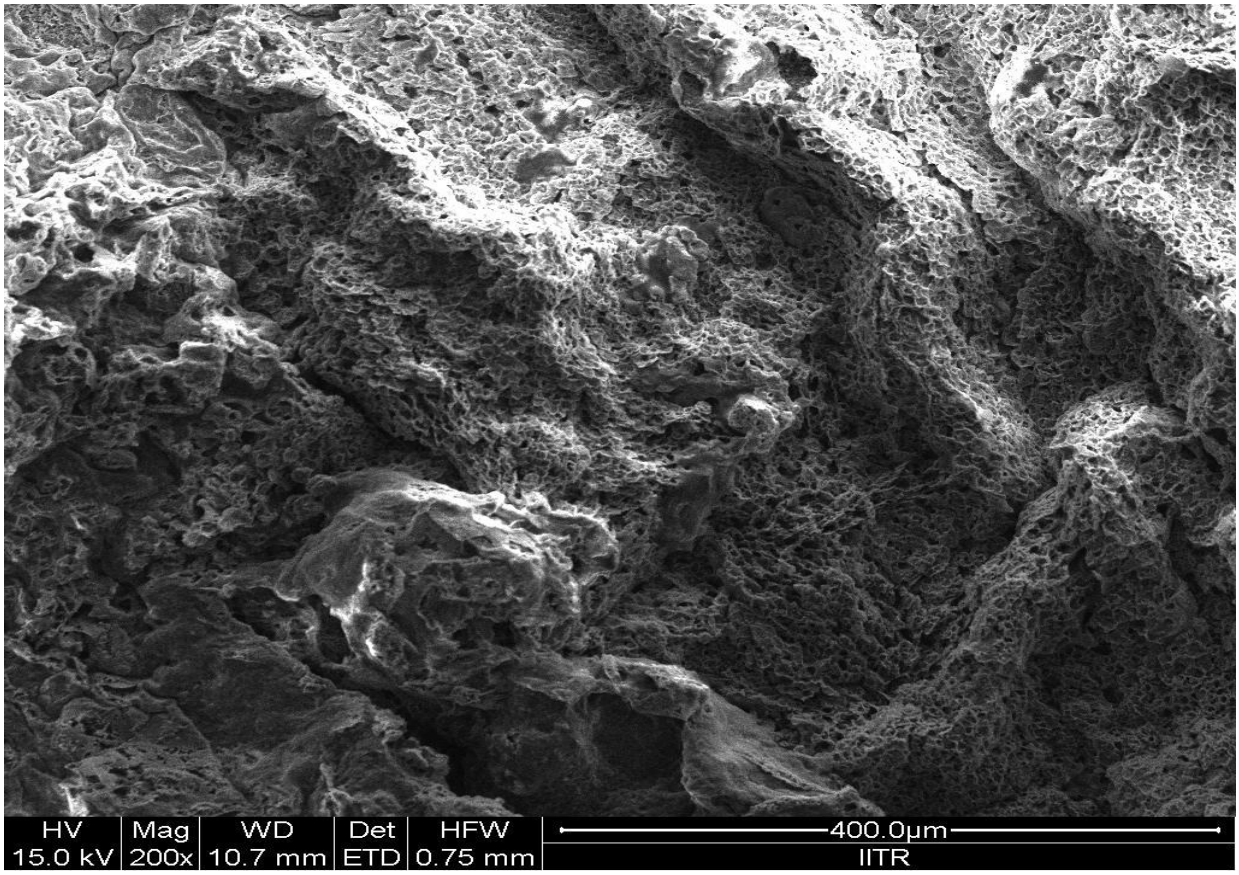

Figure 6.12: SEM image of rice husk with immobilized bacteria after SAB of phenol and cyanide

6.1.1.3 CORN HUSK LEAVES:

6.1.1.3.1 GENERAL CHARACTERISTICS:

Table 6.17 General Characteristics of Corn Husk Leaves

Parameter	Value
Surface Area	51.8880 m^2/g
Total Pore Volume	0.0261 m^3/g
Monolayer Volume	11.920 cm^3/g
Moisture	12.95 %
Volatile Matter	87.81 %
Ash	5.702 %

6.1.1.3.2 FT-IR SPECTRA:

The FTIR spectra of corn husk leaves before and after SAB is shown in figure 6.13 and 6.14 respectively. The FTIR spectra shows peaks at 3437.24 cm^{-1}, 2357.19 cm^{-1}, 1638.88 cm^{-1} reveal the presence of –OH or –NH groups, along with –CH stretching and presence of secondary amines. The spectra also show the presence of aliphatic ethers and –CN stretching through the peaks of 1048.77 cm^{-1} and 553.56 cm^{-1}.

As seen from figure 6.14 after SAB the major shifts in peaks are in the –OH region, -CH stretching region and amine region i.e. from 3437.24 to 3430.89 cm^{-1} , from 2357.19 to 2358.63 cm^{-1} and from 1638.88 to 1642.92 cm^{-1}. The shifts in peak in the primary alcohol region and in the –CH stretching region indicates the presence of phenol and the shifts in peak in amine region indicates the adsorption of –CN as secondary amine.

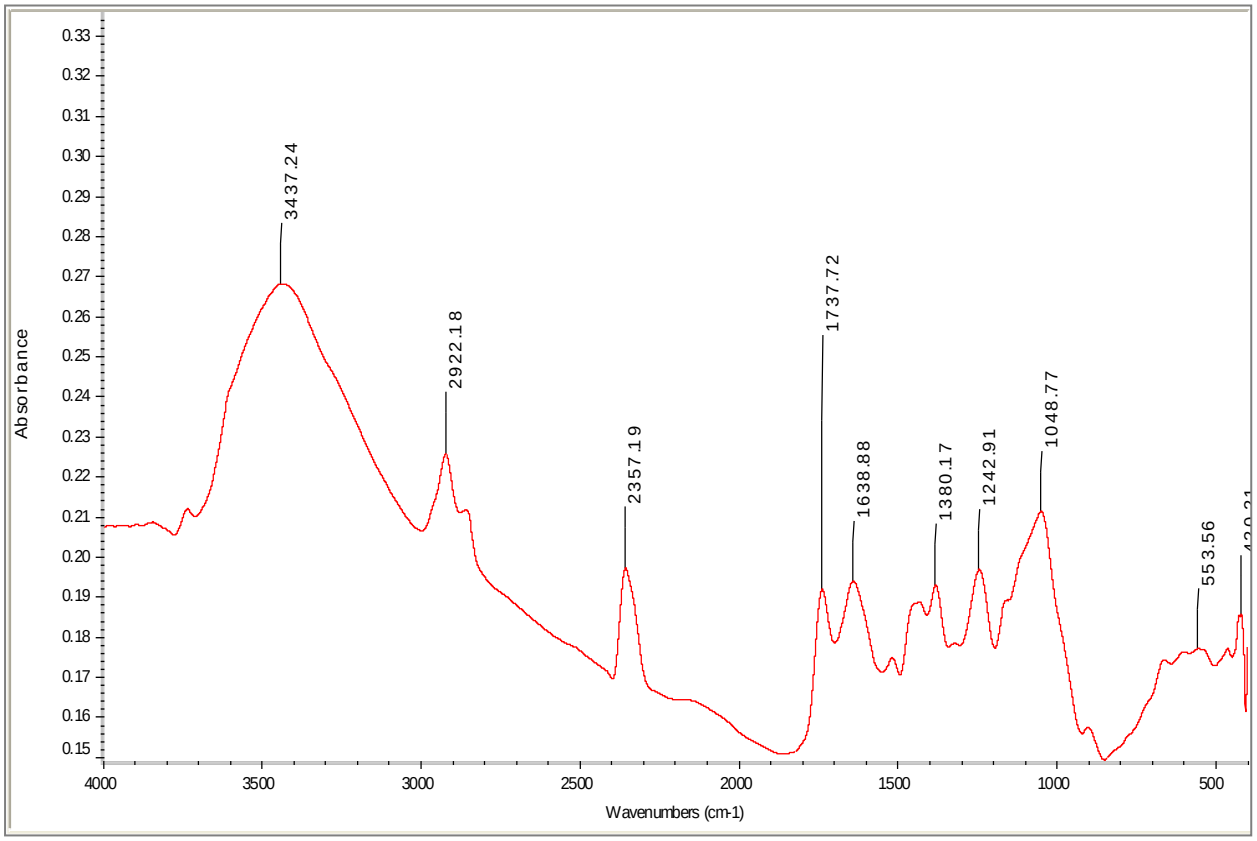

Figure 6.13: FT-IR Spectra of Corn husk leaves before SAB of phenol and cyanide

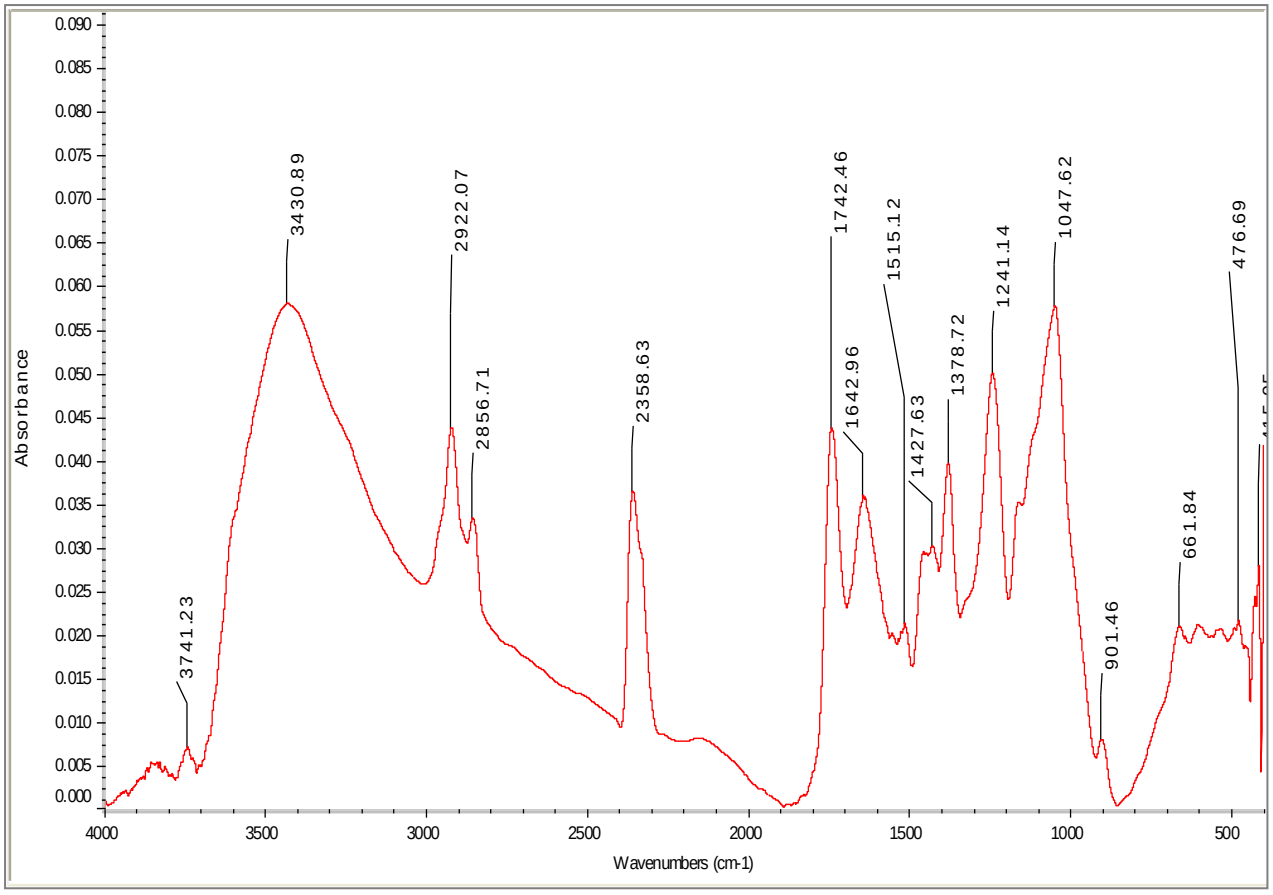

Figure 6.14: FT-IR Spectra of Corn husk leaves after SAB of phenol and cyanide

6.1.1.3.3 X-RAY DIFFRACTION:

XRD pattern of corn husk leaves before and after SAB of phenol and cyanide is shown in figure 6.15. Prominent peaks are visible at $2\theta = 5^0$, 15^0, 22^0. The figure shows almost overlapping patterns before and after SAB showing not much difference in the crystalline structure.

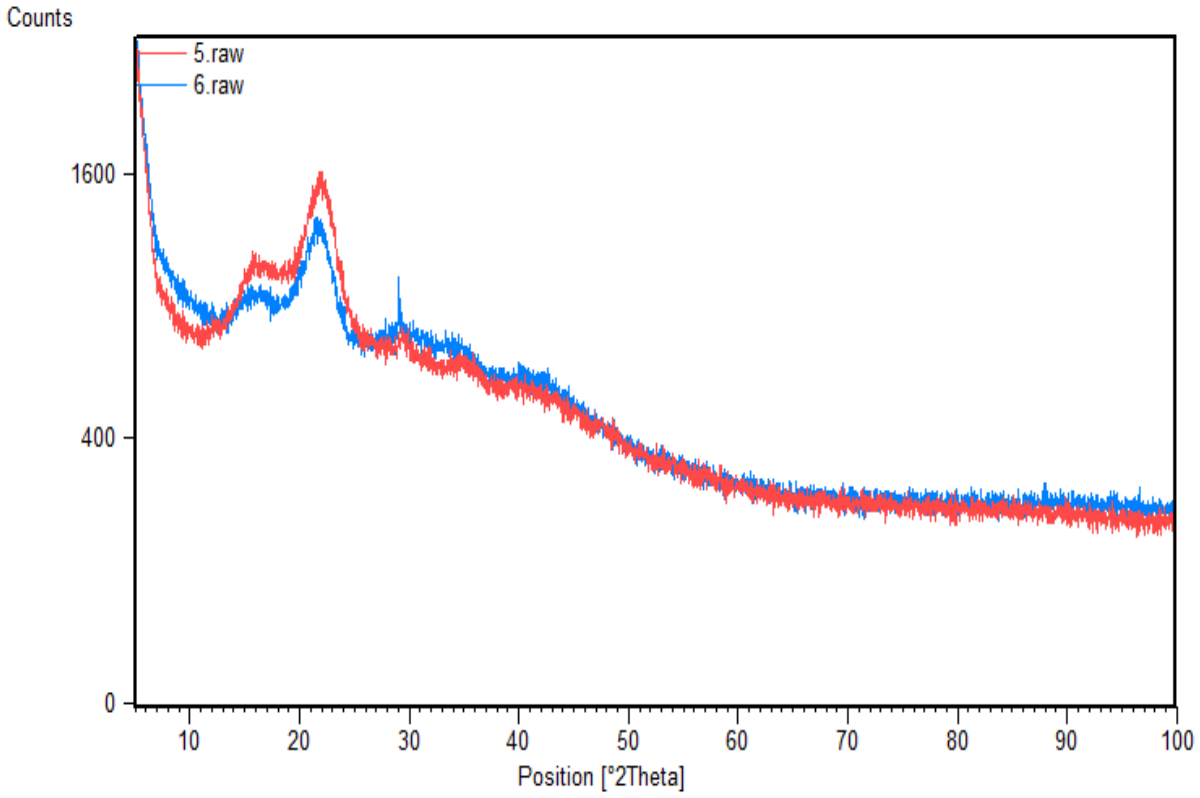

Figure 6.15: XRD pattern of corn husk leaves before SAB (red line) and after SAB (blue line)

6.1.1.3.4 THERMOGRAVIMETRIC ANALYSIS:

The thermogravimetric analysis of corn husk leaves is shown in figure 6.16 (blue line). TGA curve shows that till 27 ^{0}C there was no weight loss of adsorbent. At 103 ^{0}C an adsorbent weight loss of 6.4 % took place which is corresponding to moisture evaporation as the temperature is quite close to 100 ^{0}C. At 240 ^{0}C there was a weight loss of about 13.1 %. A major adsorbent weight loss of 78.6 % occurs between 240 ^{0}C and 349 ^{0}C which is due to decomposition of corn husk leaves. After 1212 ^{0}C there was no further weight loss in the adsorbent and a residue of 11 % remained constant.

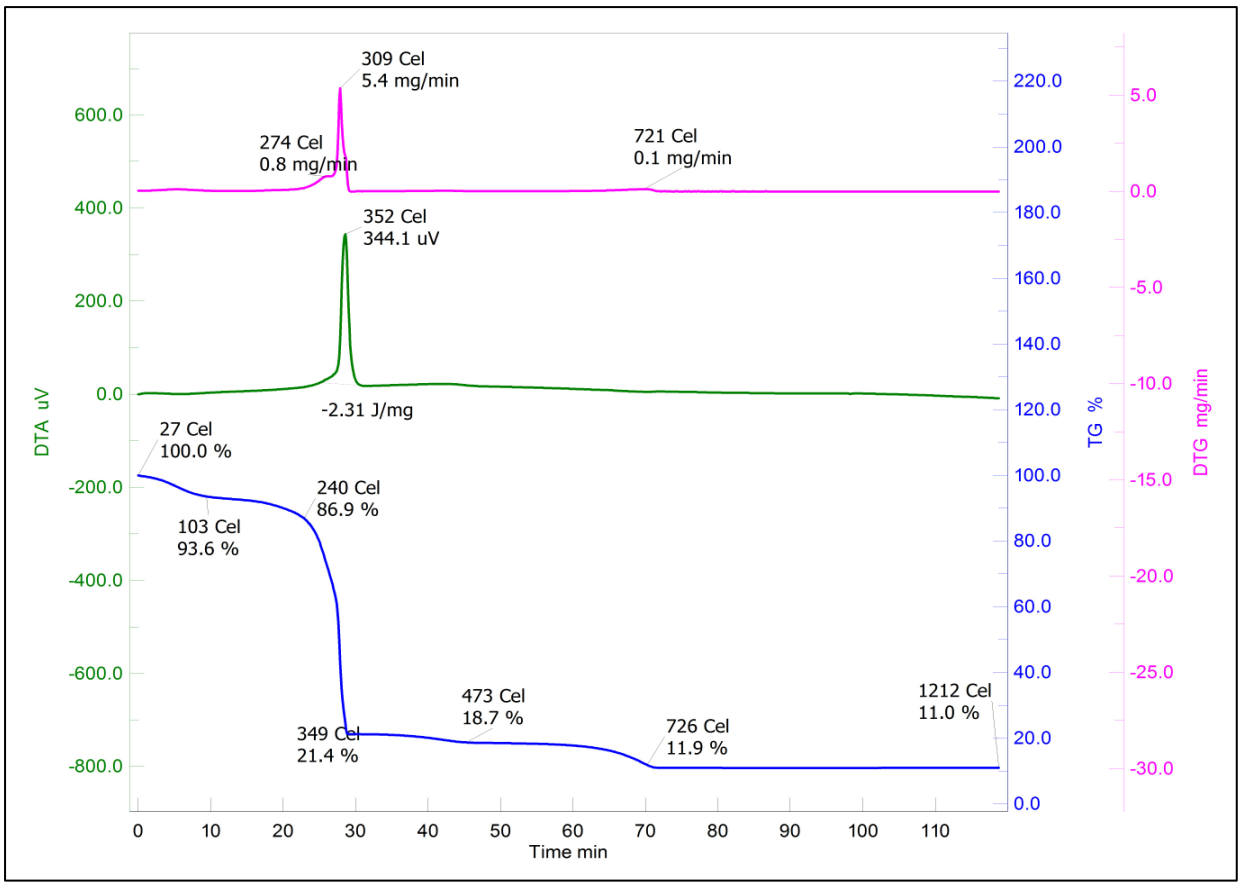

Figure 6.16: Thermogravimetric analysis of corn husk leaves

6.1.1.3.5 Fe-SEM:

The surface morphologies of only corn husk leaves as well as corn husk leaves along with the immobilized bacteria before and after SAB are shown in figure 6.17, 6.18 and 6.19 respectively.

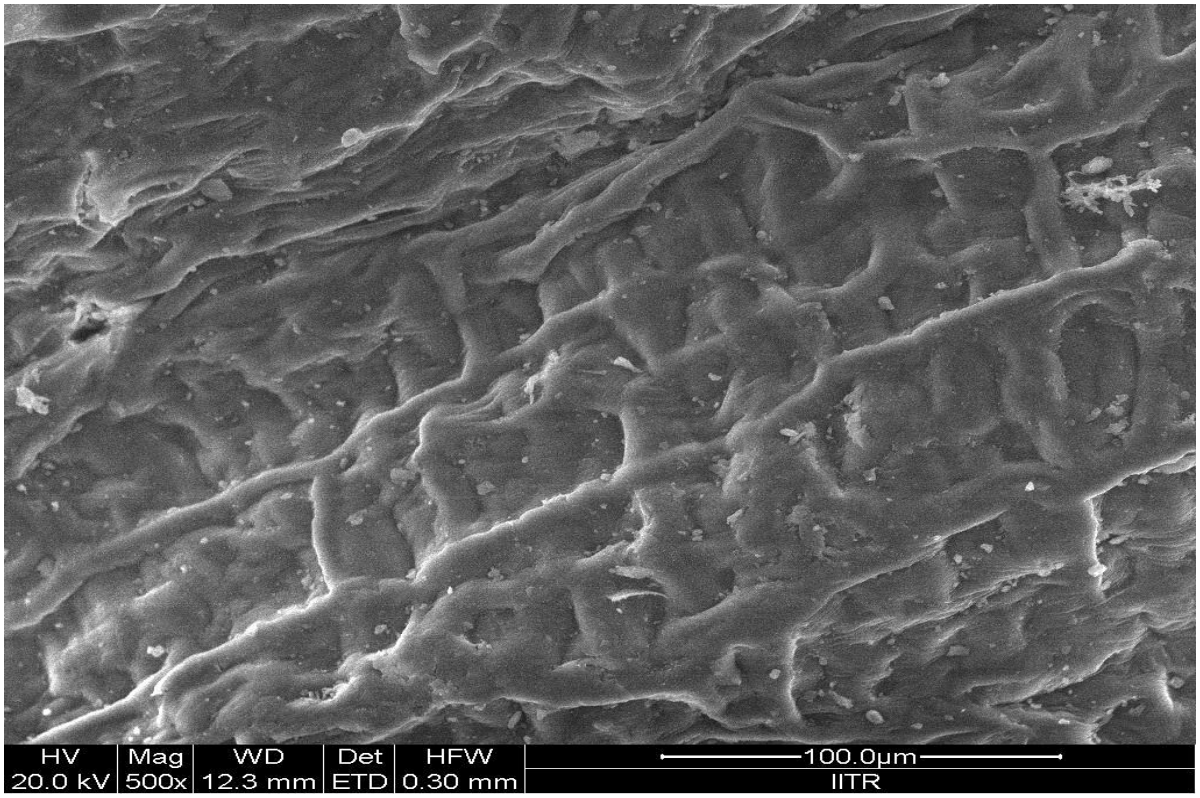

Figure 6.17: SEM image of corn husk leaves showing its fibrous nature

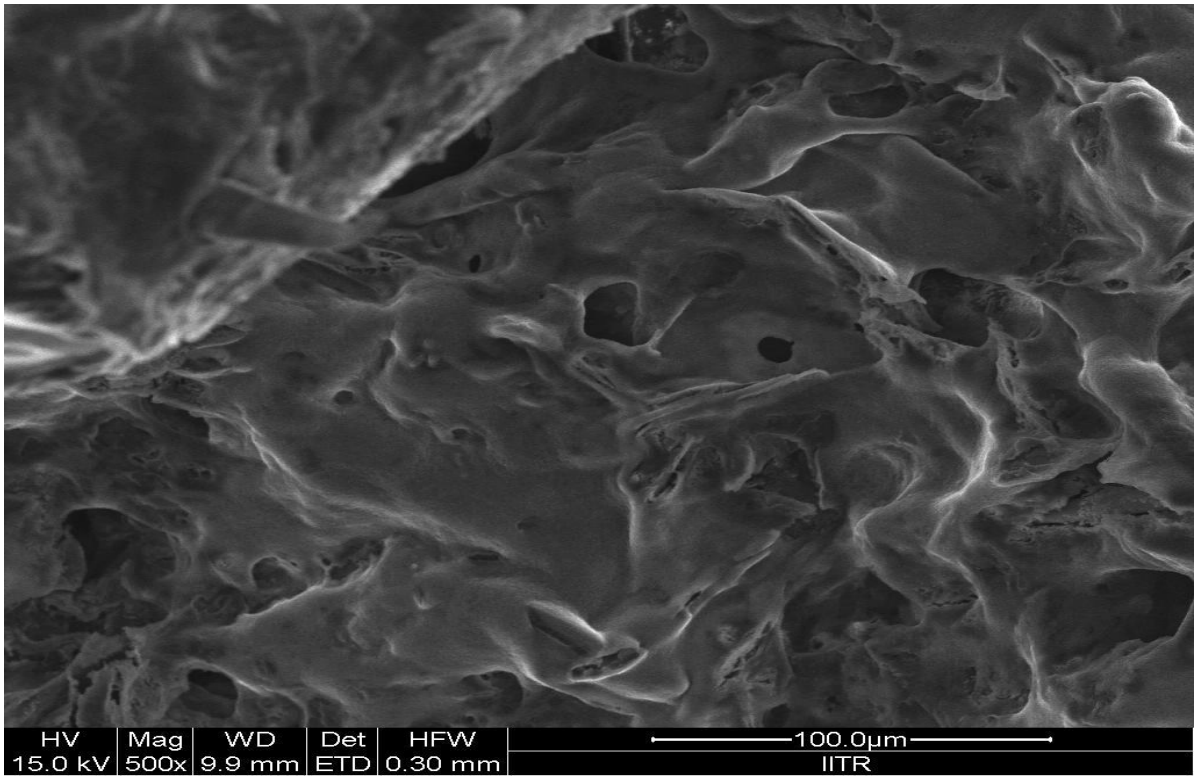

Figure 6.108: SEM image of corn husk leaves with immobilised bacteria before SAB of phenol and cyanide

Figure 6.19: SEM images of corn husk leaves with immobilised bacteria after SAB of phenol and cyanide

6.1.1.4 EGG SHELLS:

6.1.1.4.1 GENERAL CHARACTERISTICS:

Table 6.18: General Characteristics of Egg Shells

Parameter	Value
Surface Area	30.5434 m^2/g
Total Pore Volume	0.0154 m^3/g
Monolayer Volume	7.016 cm^3/g
Moisture	1.13 %
Volatile Matter	12.35 %
Ash	52.83 %

6.1.1.4.2 FT-IR SPECTRA:

The FTIR spectra of egg shells before and after SAB is shown in figure 6.20 and 6.21 respectively. The FTIR spectra shows peaks at 3416.77 cm^{-1}, 2357.59 cm^{-1} reveal the presence of –OH or –NH groups, along with –CH stretching. The spectra also show the presence of aliphatic ethers and –CN stretching through the peaks of 874.12 cm^{-1} and 707.66 cm^{-1}.

As seen from figure 6.21 after SAB the major shifts in peaks are in the –OH region, -CH stretching region i.e. from 3416.77 to 3429.26 cm^{-1} , from 2357.59 to 2357.77 cm^{-1}. The shifts in peak in the primary alcohol region and in the –CH stretching region indicates the presence of phenol. There is also an additional peak at 1641.91 cm^{-1} in peak in amine region that indicates the adsorption of –CN as secondary amine (Tsai et. al. 2006).

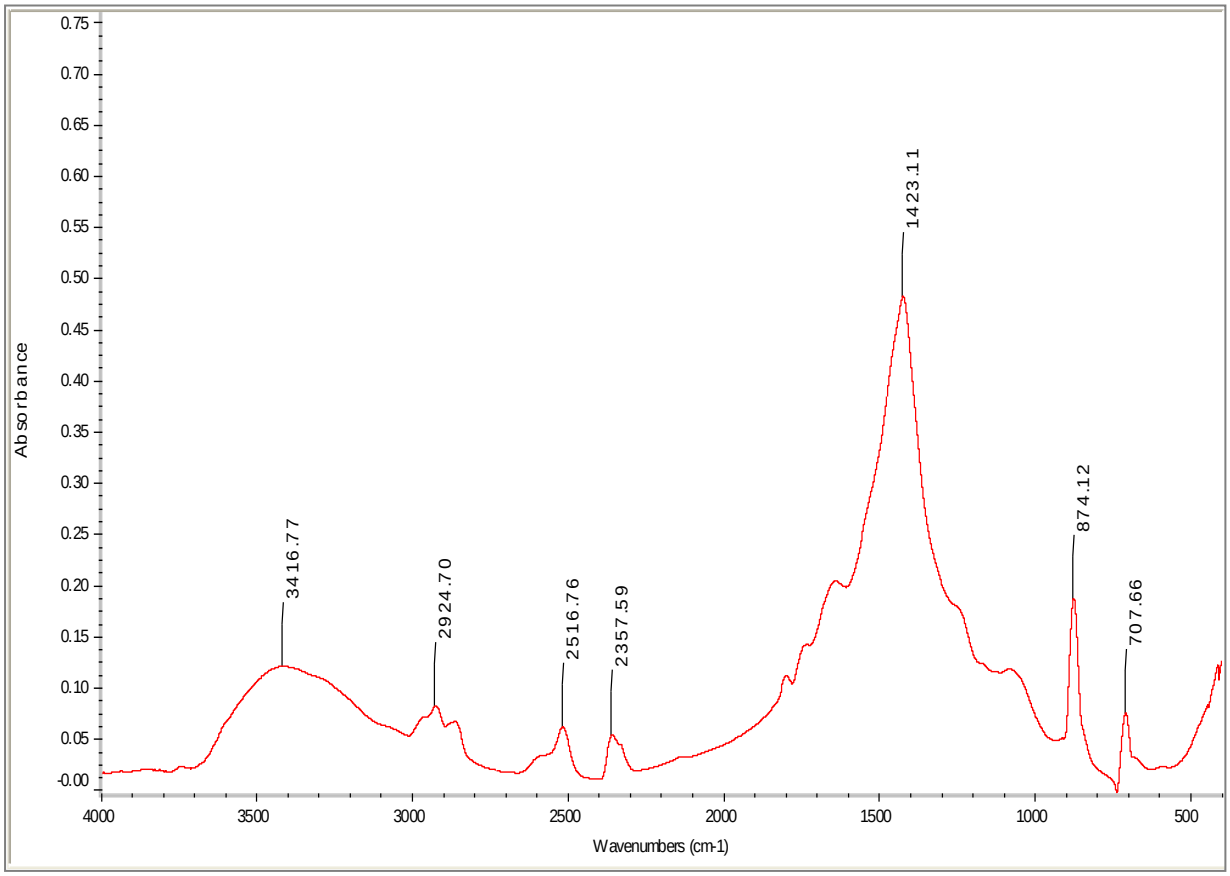

Figure 6.20: FT-IR Spectrum of egg shells before SAB

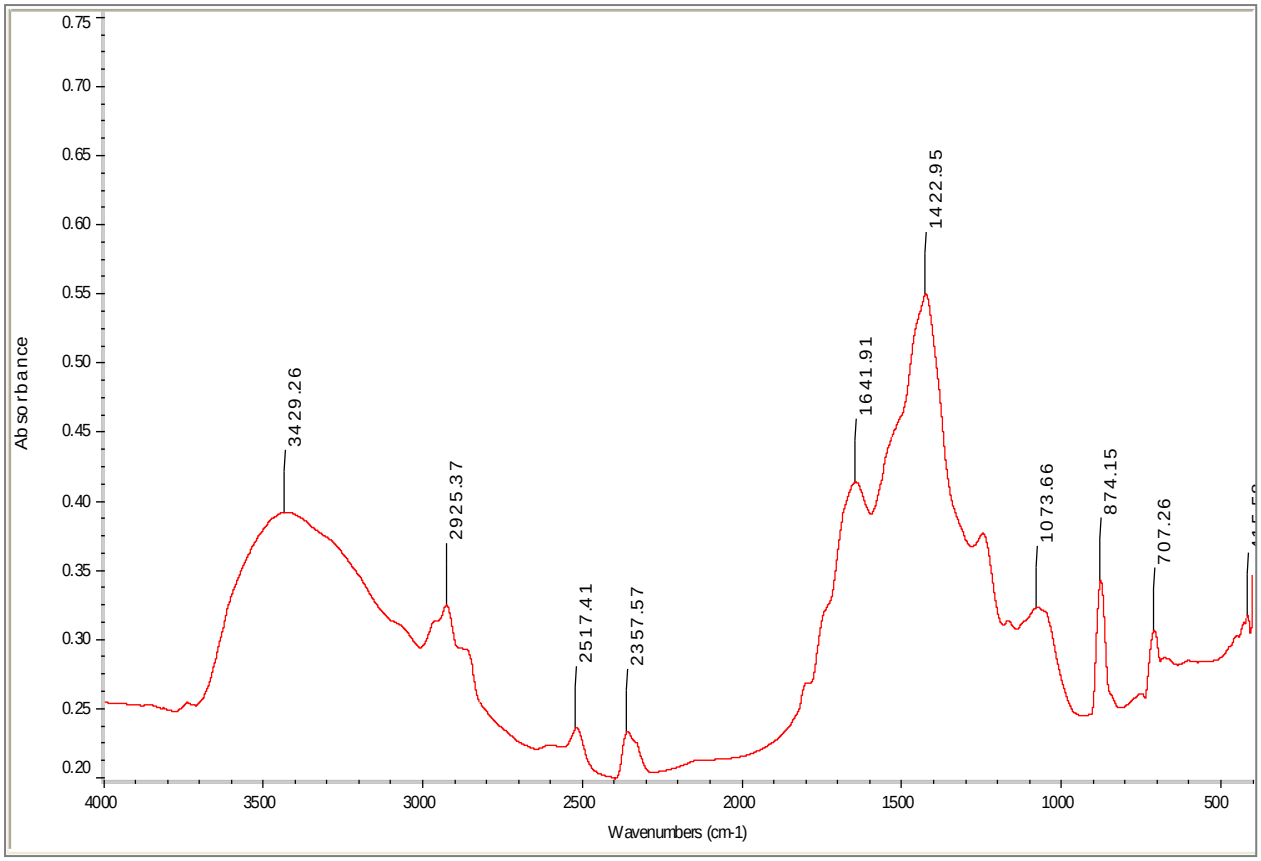

Figure 6.21: FT-IR Spectrum of egg shells after SAB of phenol and cyanide

6.1.1.4.3 X-RAY DIFFRACTION:

Figure 6.22 shows the comparative XRD pattern for egg shells before and after SAB. Prominent peaks can be seen at $2\theta = 5^0, 30^0, 32^0, 40^0, 45^0, 49^0, 50^0$ etc. For the case of egg shells also it can be seen that much variation does not take place in the crystalline structure of egg shells before and after SAB.

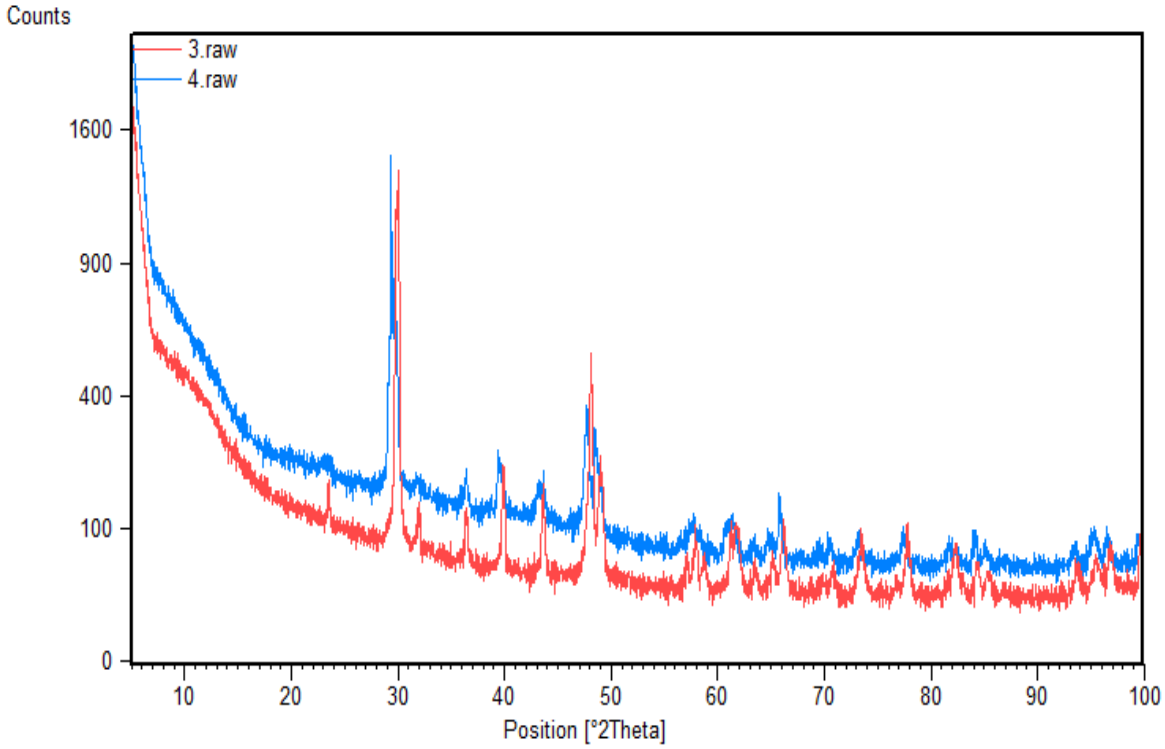

Figure 6.22: XRD pattern for egg shells before SAB (red line) and after SAB (blue line)

6.1.1.4.4 THERMOGRAVIMETRIC ANALYSIS:

The thermogravimetric analysis of egg shells is shown in figure 6.23 (blue line). TGA curve shows that till 27 ^{0}C there was no weight loss of adsorbent. At 132 ^{0}C an adsorbent weight loss of 0.6 % took place which is corresponding which shows very less moisture content in the adsorbent i.e. egg shells. Till 626 ^{0}C there is a weight loss of about 5 % showing that egg shells are quite thermal resistant. An adsorbent weight loss of 47.7 % occurs between 626 ^{0}C and 796 ^{0}C which is due to decomposition of egg shells. After 1213 ^{0}C there was no further weight loss in the adsorbent and a residue of 52.4 % remained constant.

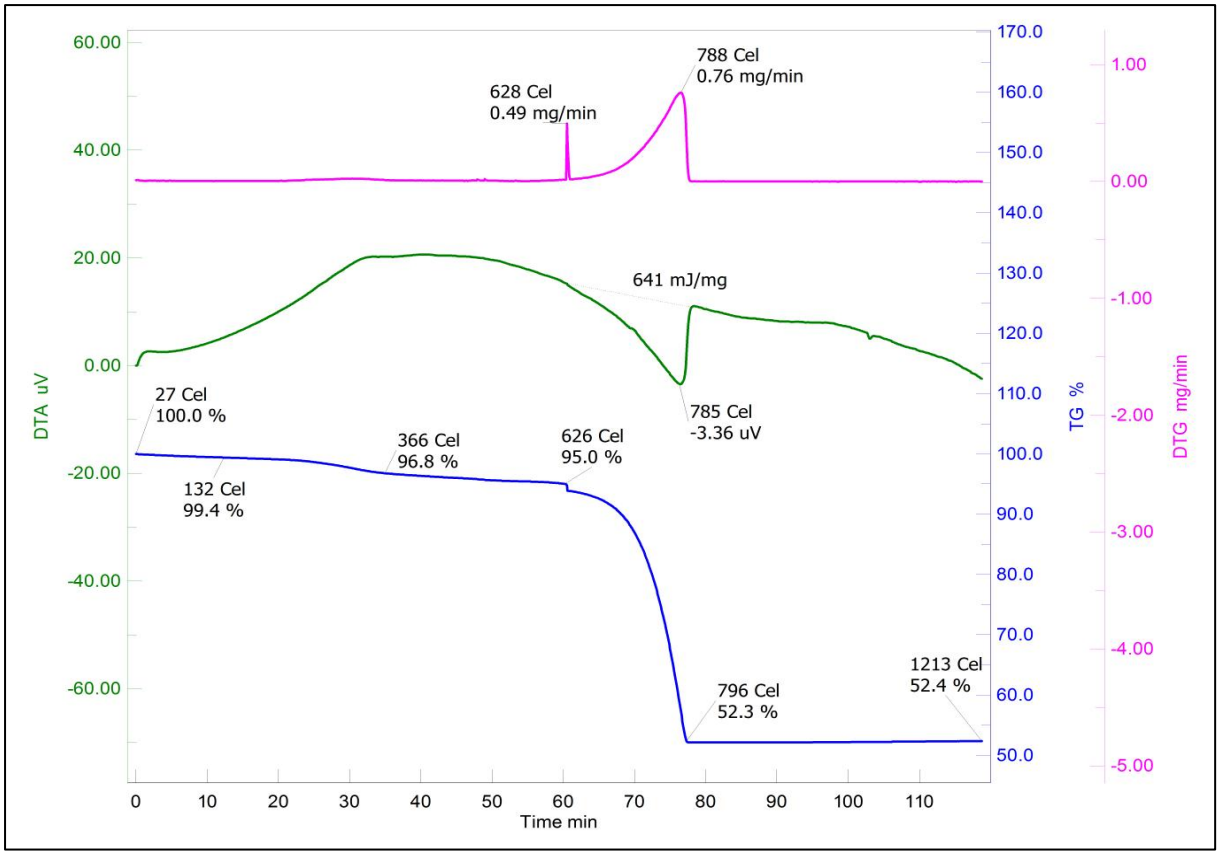

Figure 6.23: Thremogravimetric analysis of egg shells

6.1.1.4.5 Fe-SEM:

The surface morphologies of egg shells and egg shells along with the immobilized bacteria before and after SAB are shown in figure 6.24, 6.25 and 6.26.

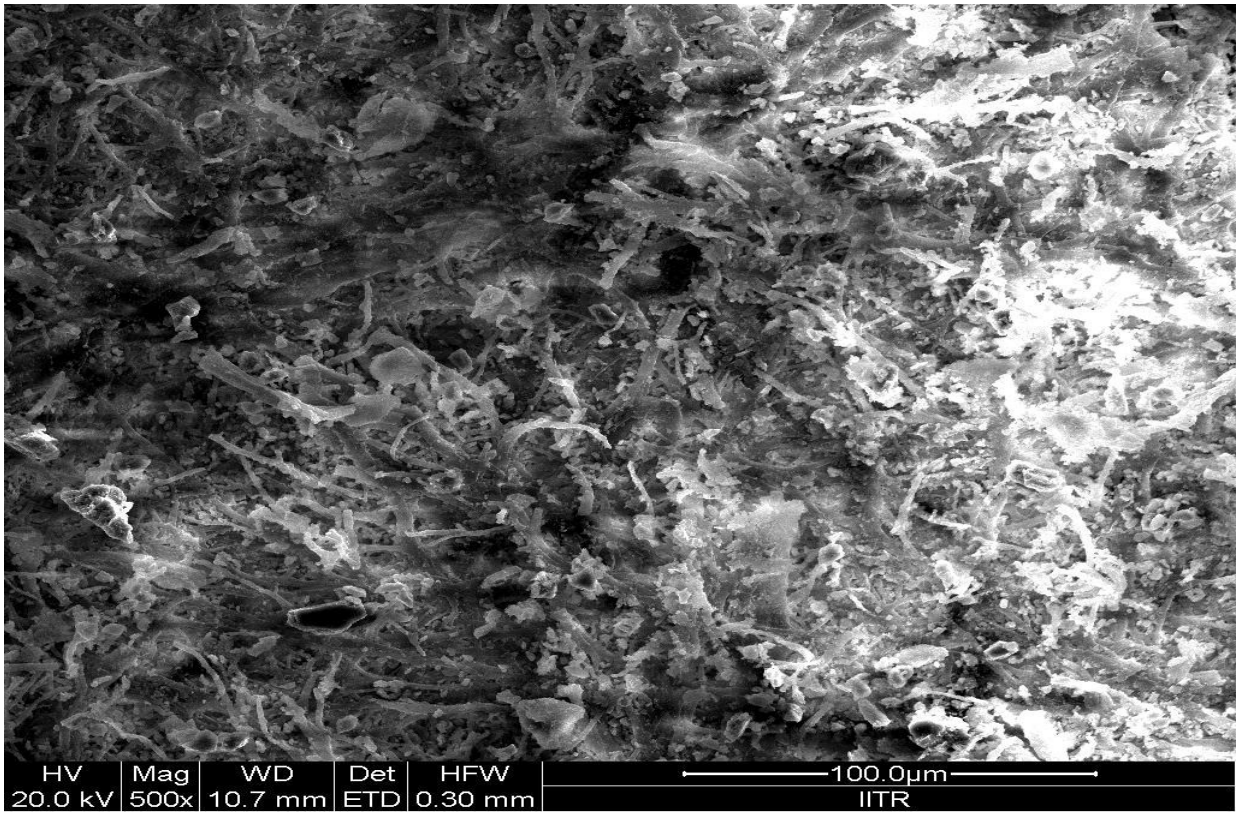

Figure 6.24: SEM image of Egg shells showing it's not very porous nature

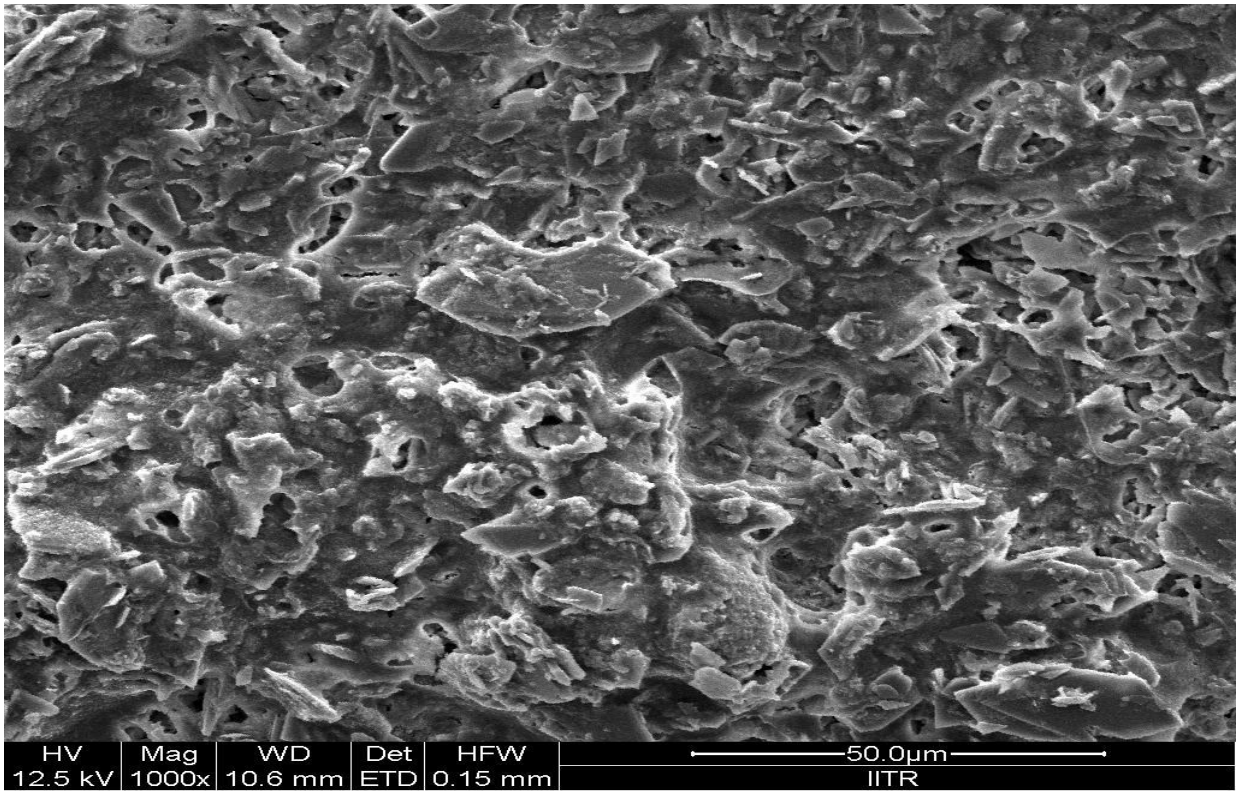

Figure 6.25: SEM image of egg shells along with immobilised bacteria before SAB of phenol and cyanide

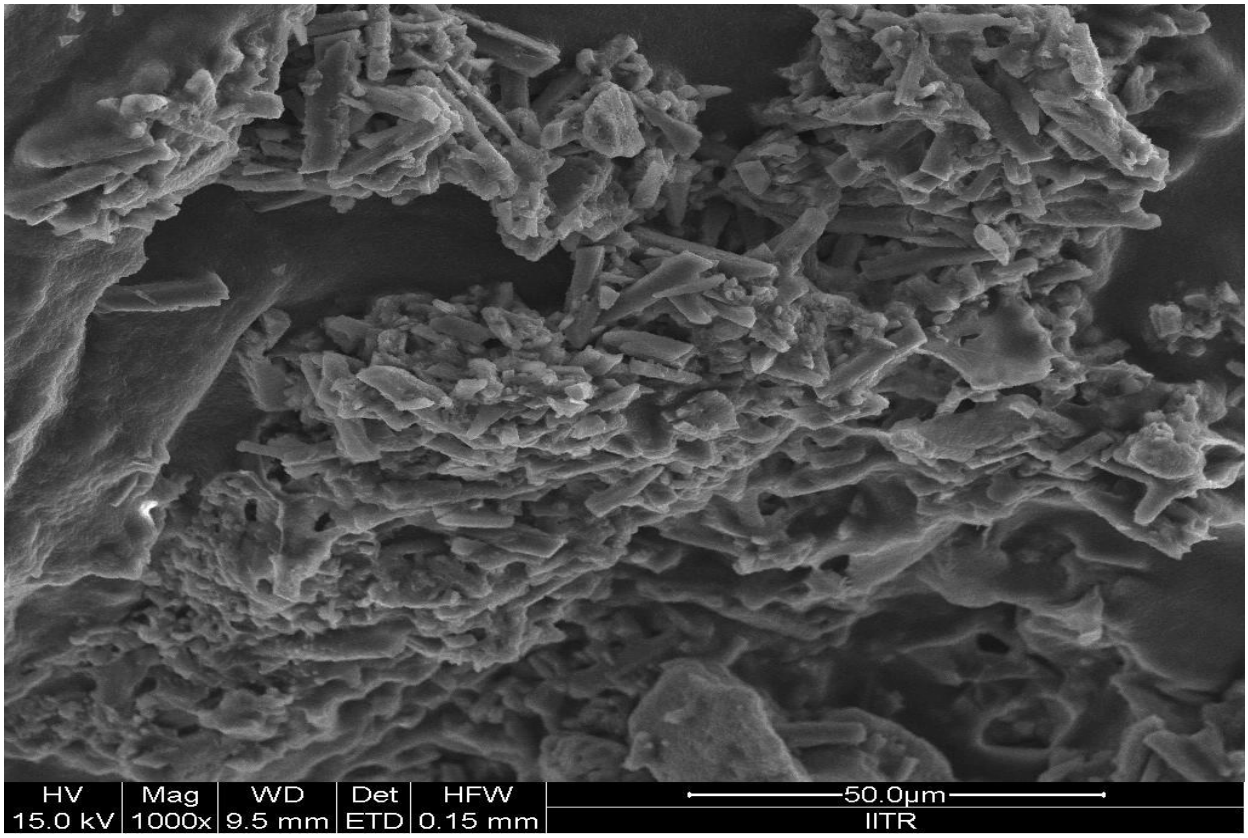

Figure 6.26: SEM image of egg shells along with immobilised bacteria after SAB of phenol and cyanide

From the above characterisation data it can be inferred that Egg shells are the most thermally stable out of all the biosorbents used. The surface of corn husk leaves is more porous as compared to rice husk and egg shells. The crystallinity of all the adsorbents is not changing after SAB process of phenol and cyanide.

6.1.2 BACTERIAL GROWTH CURVE:

Microbial strain was inoculated in the growth media as mentioned in the previous chapter at an optimum pH 7 and 30 °C temperature. The growth curve obtained for Seratia Sp. by plotting optical density at 600 nm for a time interval of 3 hr. is shown in figure 6.27.

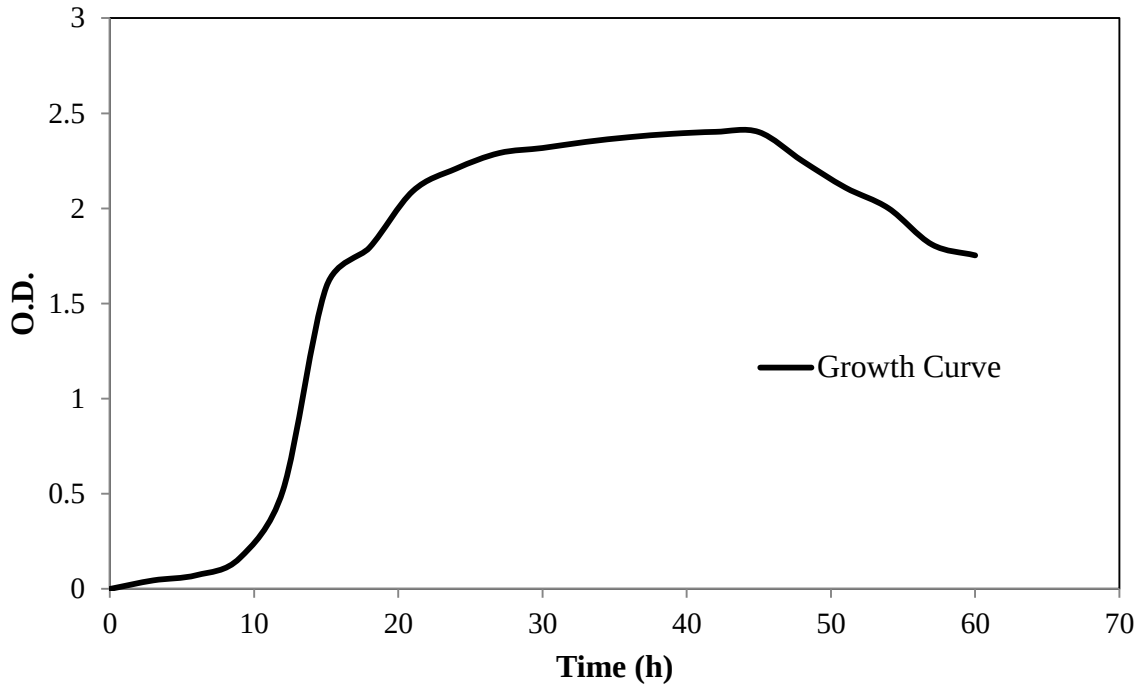

Figure 6.117: Growth Curve of S. *odorifera* at pH 7 and temperature= 30 ^{0}C

The growth curve shows that the optimum growth time for S. *odorifera* is between 12 h to 24 h. After 24 h the stationary phase arrives and death phase starts after 45 h.

6.1.3 Simultaneous Adsorption and Biodegradation of Phenol and Cyanide:

In this section the simultaneous adsorption and biodegradation of phenol and cyanide from synthetic simulated waste water is studied using three adsorbents, rice husk, corn husk leaves and egg shells. The effect of operating parameters i.e. pH, time, adsorbent dose and initial concentration is studied on the process. The optimum value of operating parameters is also studied for different adsorbents.

6.1.3.1 Effect of pH:

Studying effect of pH is necessary as it affects the adsorption mechanism by changing the surface charge of adsorbents along with the degree of ionisation. The effect of pH was studied in the range of 2-12. At extreme acidic conditions i.e. at a pH less than 4 there was no visible bacterial growth similarly at extreme alkaline conditions i.e. at a pH greater than 10 there was no visible growth therefore the SAB studies were conducted at a pH range of 5-10. The figures given below i.e. figures 6.28, 6.29 and 6.30 show the effect of pH on SAB

process of phenol and cyanide using rice husk, corn husk leaves and egg shells. In case of phenol it can be seen that phenol shows a maximum removal of 77.98 %, 76 % and 75 % for rice husk, corn husk leaves and egg shells respectively at a pH 7. Similarly for Cyanide a maximum removal of 87.9 %, 96 % and 94.15 % for rice husk, corn husk leaves and egg shells respectively at a pH 7. At extremely low pH, the surface of adsorbent is positively charged but phenol adsorption is highly favourable as phenolate ion gets adsorbed on the surface of the adsorbent. At a pH of about 6.5 the adsorbent surface is also positively charged and the phenol ion is also in partially dissociated form which increases the adsorption whereas at extremely alkaline pH the adsorbent surface is negatively charged and so is the phenolate ion which causes a repulsion thereby decreasing adsorption of phenol on the adsorbent (Srivastava et.al. and Mondal et.al.). For both phenol and cyanide it can be seen that adsorption takes place at undissociated forms as the pK_a for phenol and cyanide is 9.96 and 9.39 respectively under which both the components remain in their undissociated form. Phenol and cyanide adsorption shows a slight decrease with the increase in pH for all the three adsorbents which is in accordance to the results obtained by Agarwal et.al. 2013 for simultaneous adsorption and biodegradation of phenol and cyanide using Iron impregnated Granular Activated Carbon.

Cyanide ion is neucleophilic in nature which attracts it towards positively charged surface. At an extremely acidic pH i.e. at a pH less than 6 due to reduced pressure there is an evolution of HCN as seen by Adams et.al. Since HCN is hydrophilic in nature it does not get adsorbed on the adsorbent surface. Whereas at extremely alkaline pH cyanide acts as an ion exchanger exchanging OH^- ion from the adsorbent (Moussavi et. al.). Since there is no bacterial growth at extreme acidic and alkaline pH therefore in this case the optimum pH is selected as 7 which at which both phenol and cyanide show a maximum removal percentage. pH of 7 was also considered best for removal of phenol and cyanide (Dash et.al. and Mondal et.al.).

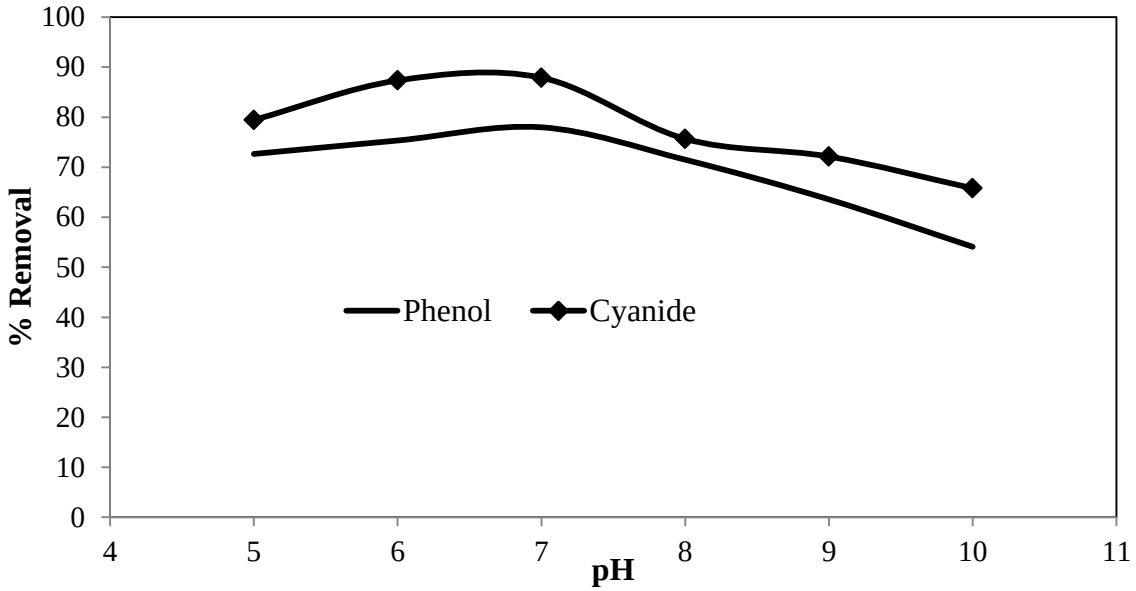

Figure 6.28: Effect of pH on the SAB of phenol and cyanide using rice husk(RH) as an adsorbent at Initial phenol concentration 400 mg/L, initial cyanide concentration 40 mg/L, temperature: 30 ^{0}C and for 54 h

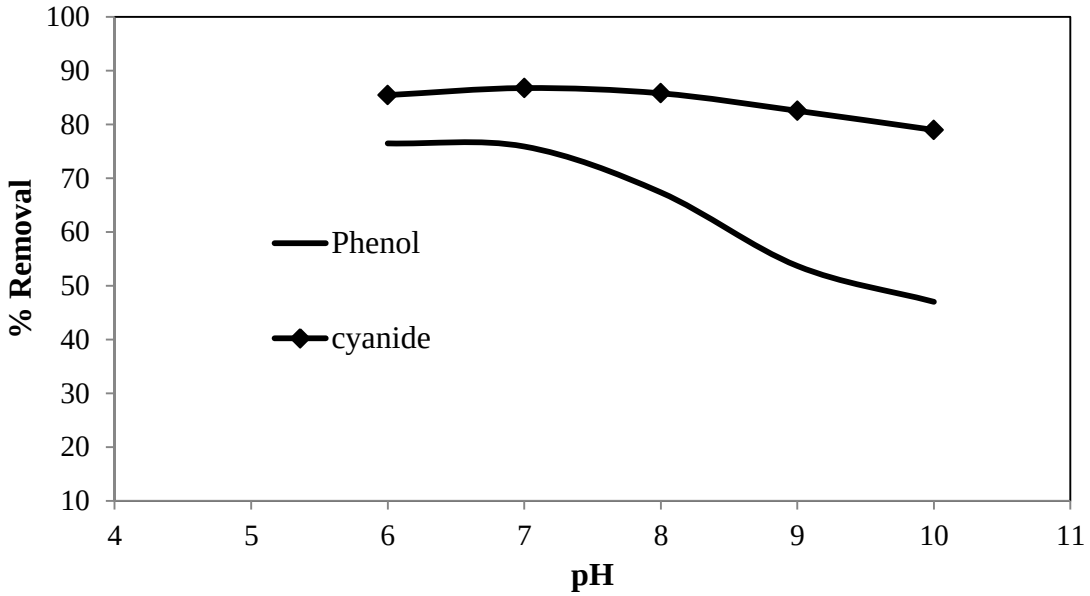

Figure 6.29: Effect of pH on the SAB of phenol and cyanide using corn husk leaves(CHL) as an adsorbent at Initial phenol concentration 400 mg/L, initial cyanide concentration 40 mg/L, temperature: 30 ^{0}C and for 54 h

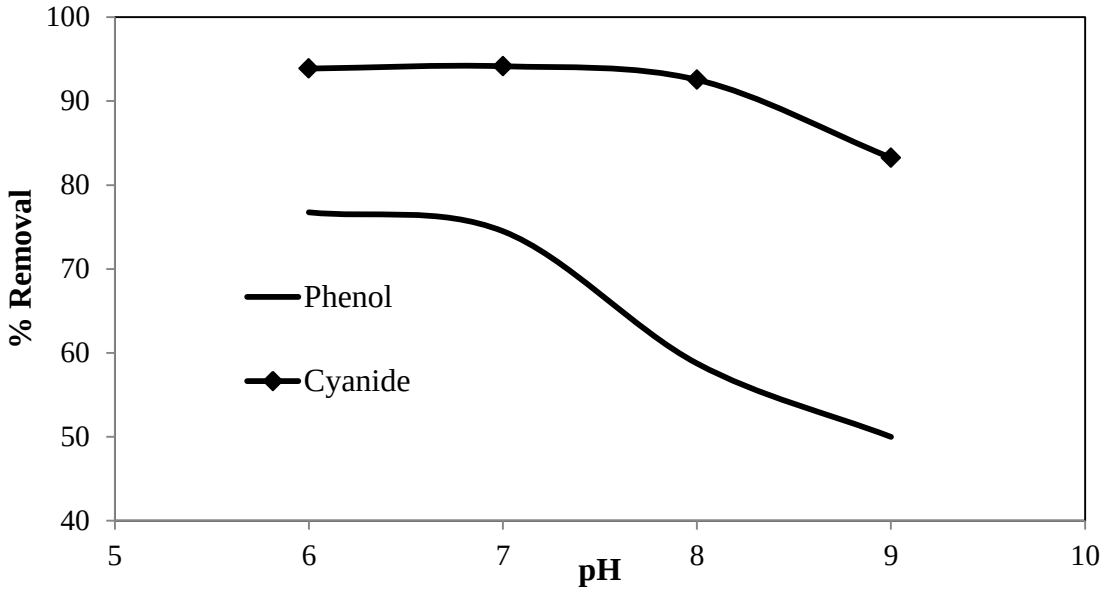

Figure 6.12: Effect of pH on the SAB of phenol and cyanide using Egg Shells(ES) as an adsorbent at Initial phenol concentration 400 mg/L, initial cyanide concentration 40 mg/L, temperature: 30 ^{0}C and for 54 h

6.1.3.2 EFFECT OF ADSORBENT DOSE:

Adsorbent dose is also an important parameter that has an impact on the SAB process of phenol and cyanide from its synthetic simulated solution. For three different adsorbents the studies were carried out for different range of adsorbent dose. Figure 6.31, 6.32 and 6.33 show the impact of varying adsorbent dose on the SAB process for rice husk, corn husk leaves and egg shells respectively. From figure 6.31 it can be seen that for phenol there is not much increase in removal percentage after a dose of 5 g/L i.e. the plot reaches an asymptotic value. Whereas for cyanide there is a slight increase in removal percentage from 5 g/L to 6 g/L. Therefore for rice husk the optimum adsorbent dose is taken as 5 g/L.

For Corn husk i.e. from figure 6.32 it can be inferred that after 6 g/L there is not much increase in the removal percentage for both phenol and cyanide i.e. both the plots reach their asymptotic value. Therefore optimum adsorbent dose for corn husk leaves is taken as 6 g/L.

From the figure 6.33 it is clearly visible that the percentage removal increases with adsorbent dose till 30 g/L and then it becomes constant. Optimum removal of 80 % phenol and 82 % cyanide occurs at 35 g/L therefore it is taken as optimum adsorbent dose for the egg shells.
For all the three adsorbents the increase in active sites explains the initial increase in percentage removal with increase in adsorbent dose. However above certain dose removal

percentage assumes an asymptotic value. As observed by [5] there can be an overlapping of active sites which decreases the surface area on the adsorbent there by making the removal percentage to reach an asymptotic value.

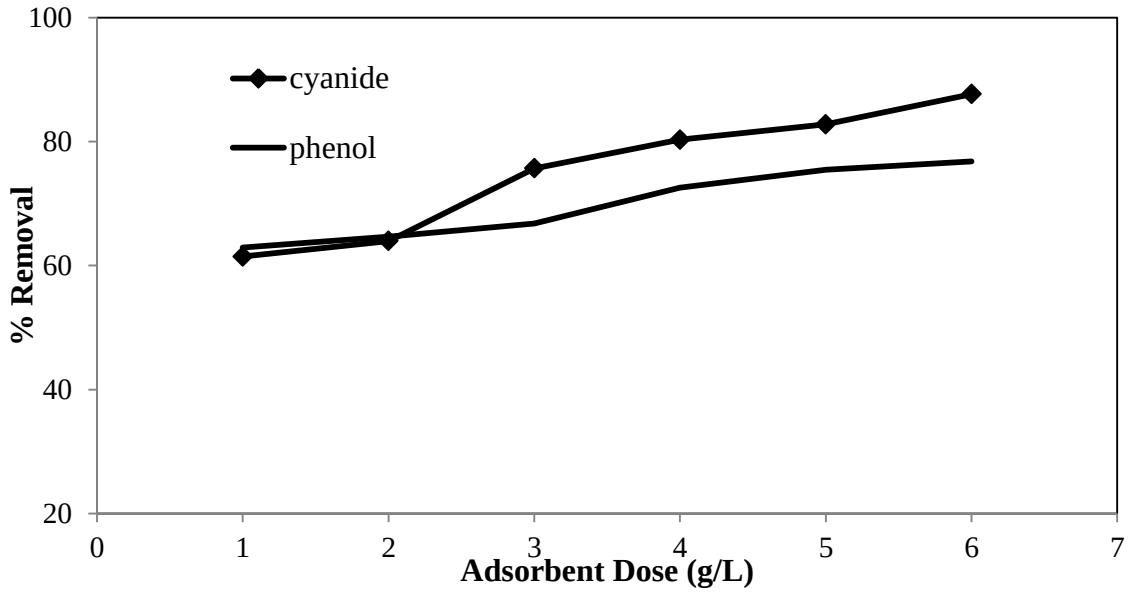

Figure 6.31: Effect of adsorbent dose on the SAB of phenol and cyanide using Rice Husk(RH) as an adsorbent at Initial phenol concentration 400 mg/L, initial cyanide concentration 40 mg/L, pH:6.5-7, temperature: 30 ^{0}C and for 54 h

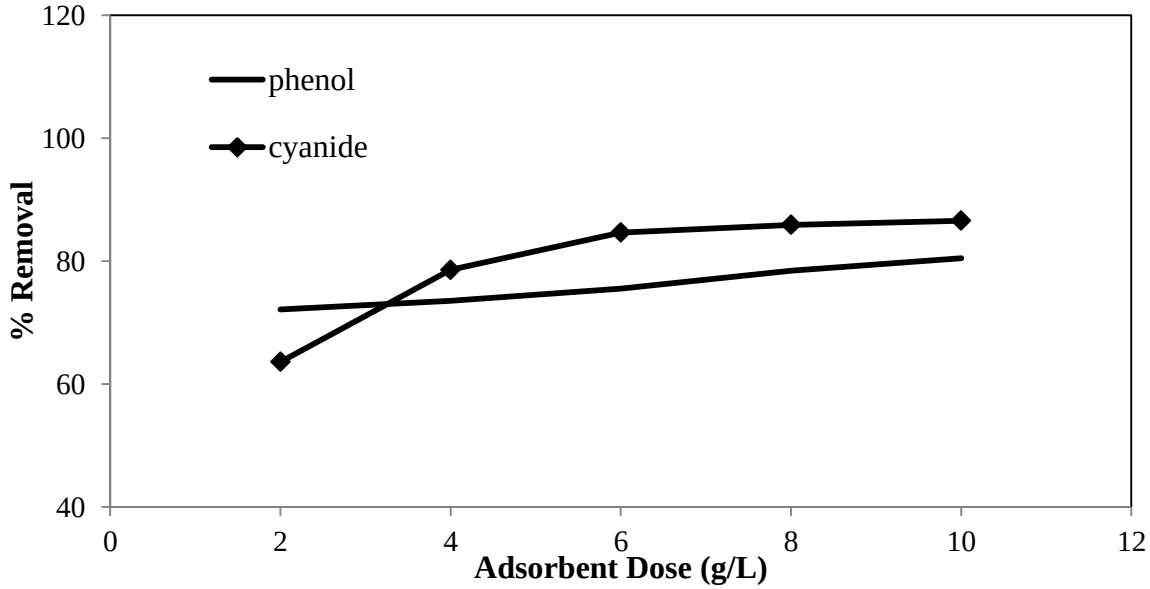

Figure 6.32: Effect of adsorbent dose on the SAB of phenol and cyanide using Corn Husk Leaves(CHL) as an adsorbent at Initial phenol concentration 400 mg/L, initial cyanide concentration 40 mg/L, pH:6.5-7, temperature: 30 ^{0}C and for 54 h

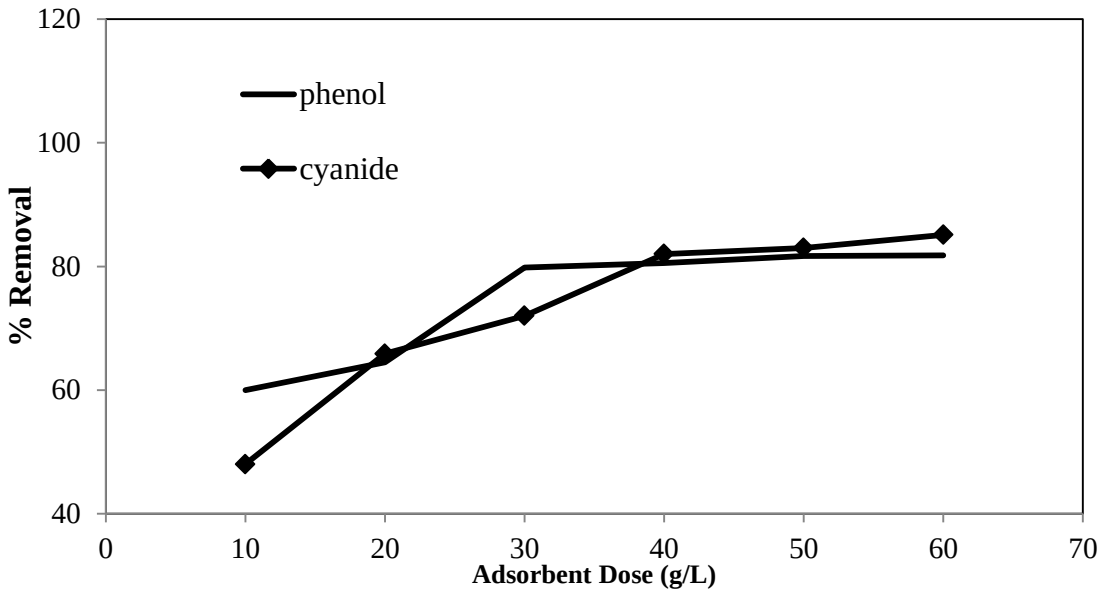

Figure 6.133: Effect of adsorbent dose on the SAB of phenol and cyanide using Egg Shells(ES) as an adsorbent at Initial phenol concentration 400 mg/L, initial cyanide concentration 40 mg/L, pH: 6.5-7, temperature: 30 ^{0}C and for 54 h

6.1.3.3 EFFECT OF TEMPERATURE:

The effect of temperature is also studied on the SAB studies of phenol and cyanide for all the three adsorbents and the plots are shown in figure 6.34, 6.35 and 6.36.

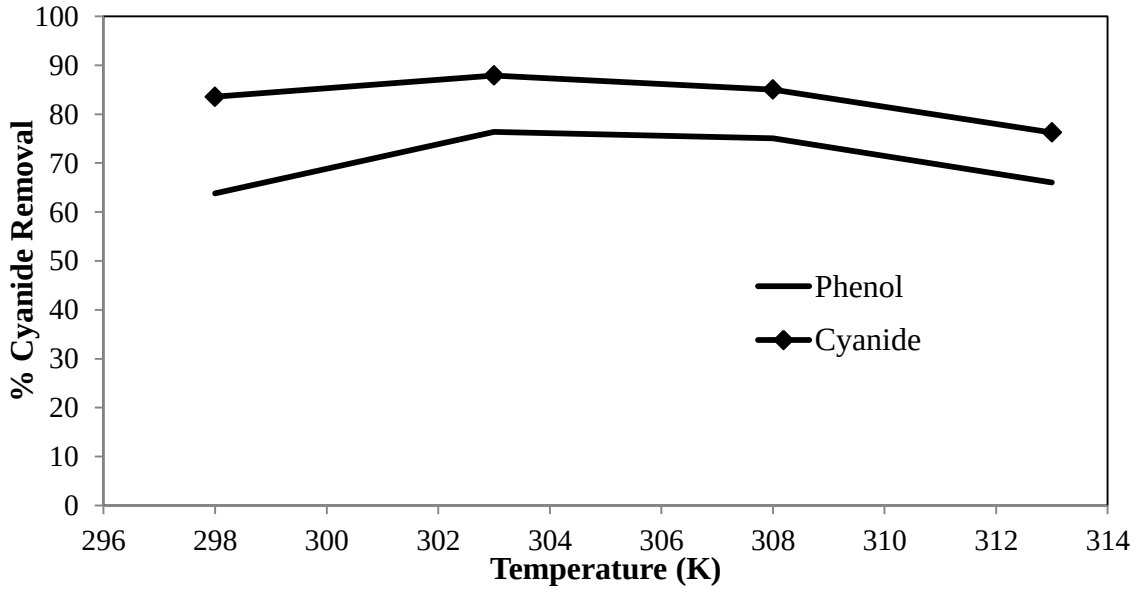

Figure 6.34: Effect of temperature(25-40) ^{0}C on the SAB of phenol and cyanide using Rice Husk(RH) as an adsorbent at Initial phenol concentration 400 mg/L, initial cyanide concentration 40 mg/L, pH: 6.5-7, adsorbent dose: 5 g/L and for 54 h

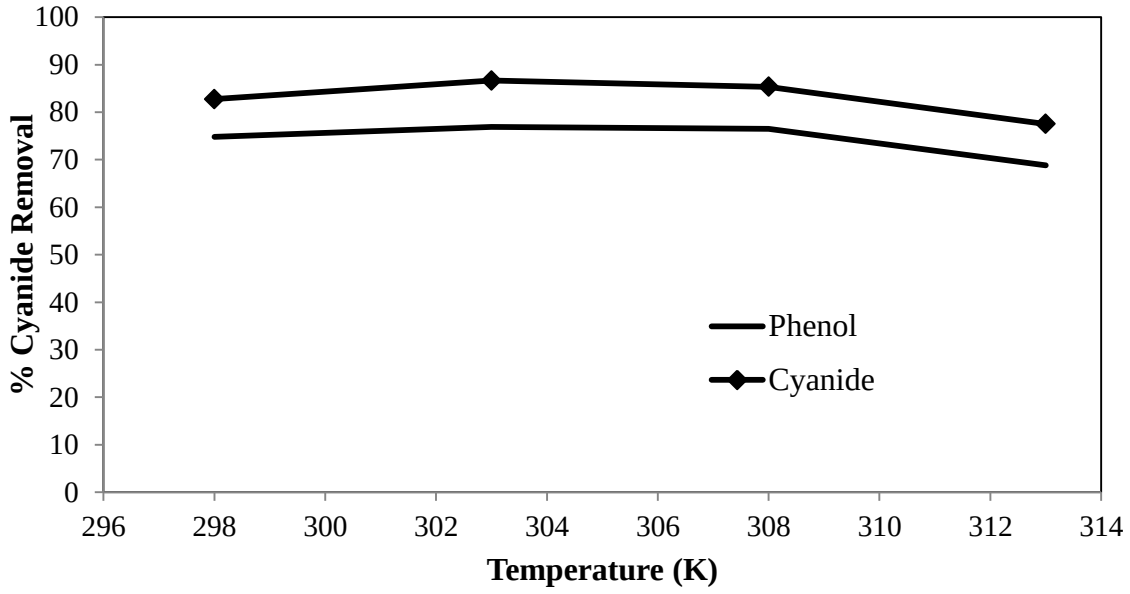

Figure 6.145: Effect of temperature(25-40) ^{0}C on the SAB of phenol and cyanide using Corn Husk Leaves(CHL) as an adsorbent at Initial phenol concentration 400 mg/L, initial cyanide concentration 40 mg/L, pH: 6.5-7, adsorbent dose: 6 g/L and for 54 h

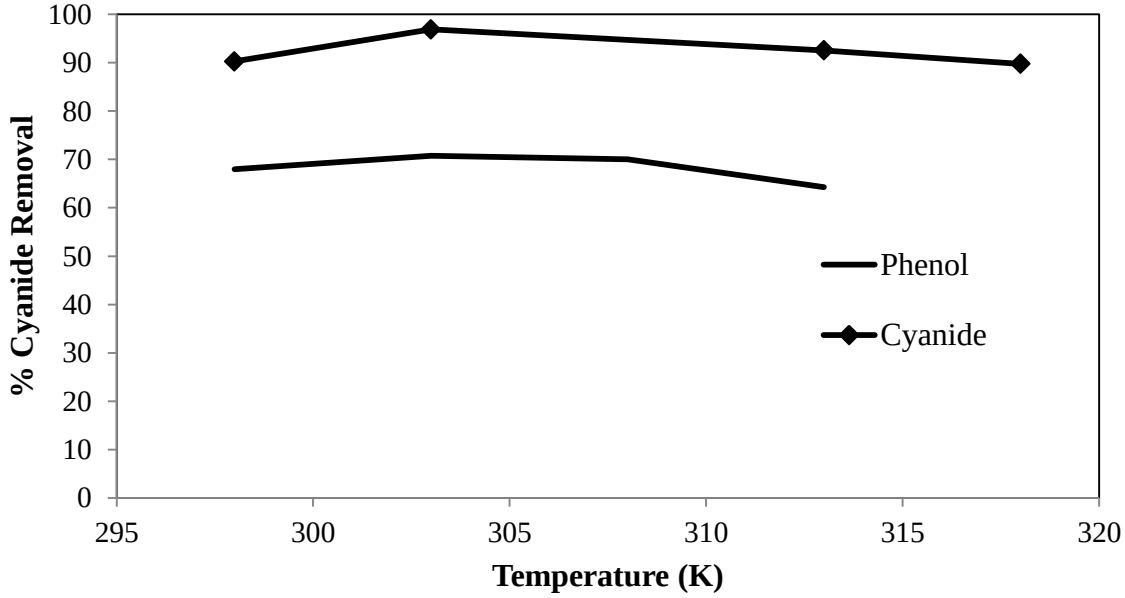

Figure 6.36: Effect of temperature(25-40) ^{0}C on the SAB of phenol and cyanide using Egg Shells(ES) as an adsorbent at Initial phenol concentration 400 mg/L, initial cyanide concentration 40 mg/L, pH: 6.5-7, adsorbent dose: 35 g/L and for 54 h

The above plots show that percentage removal for SAB of both phenol and cyanide using all the three adsorbents is not very much dependent on temperature between the range of (25-40) ^{0}C. There is no visible bacterial growth at a temperature less than 25 ^{0}C or above 40 ^{0}C.

6.1.3.4 EFFECT OF CONTACT TIME:

Equilibrium time of adsorption process can be determined by the contact time study of the SAB process. The effect of contact time on the SAB process is studied by plotting the percentage removal versus time. Figures 6.37, 6.38 and 6.39 are the plots of percentage removal versus time for rice husk, corn husk leaves and egg shells respectively.

For rice husk the removal for both phenol and cyanide increases with time. For phenol there is an abrupt increase after 24 h which is due to biodegradation that frees the occupied active sites of the adsorbent. Further for both corn husk leaves and egg shells there is an increase in percentage removal with time for both phenol as well as for cyanide.

In case of all the three adsorbents for both phenol and cyanide the initial removal takes place by simple adsorption and then the further increase in removal is adhered to the fact the occupied sites are freed due to biodegradation (Agarwal et.al. 2013).

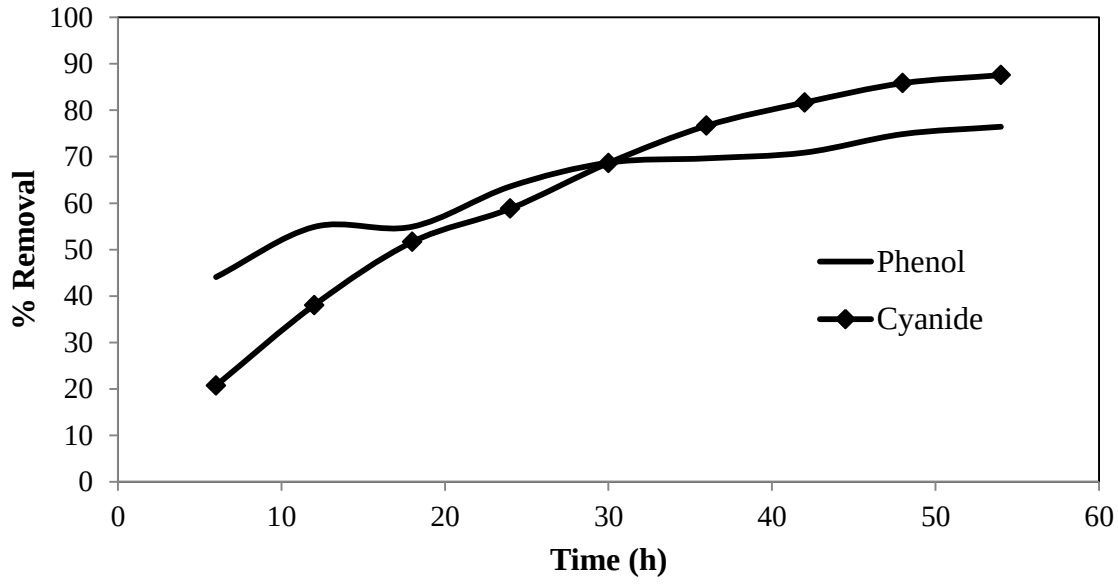

Figure 6.157: Effect of time (6-54) h on the SAB of phenol and cyanide using Rice Husk(RH) as an adsorbent at Initial phenol concentration 400 mg/L, initial cyanide concentration 10-40) mg/L, pH: 6.5-7, adsorbent dose 5 g/L, temperature: 30 ^{0}C

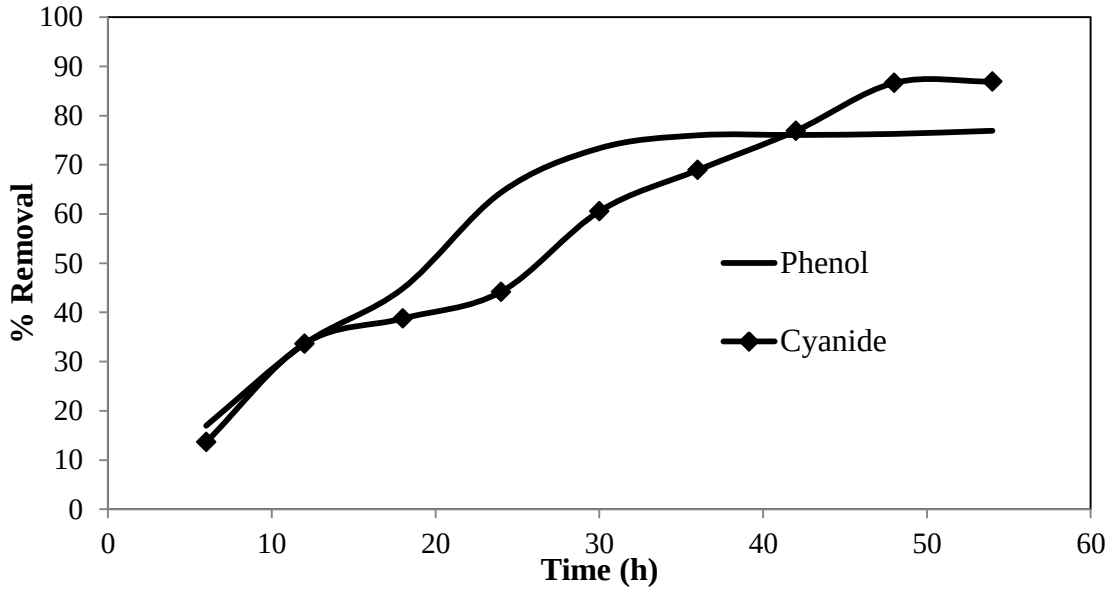

Figure 6.168: Effect of time (6-54) h on the SAB of phenol and cyanide using Corn Husk Leaves(CHL) as an adsorbent at Initial phenol concentration 400 mg/L, initial cyanide concentration 40 mg/L, pH: 6.5-7, adsorbent dose 6 g/L, temperature: 30 ^{0}C

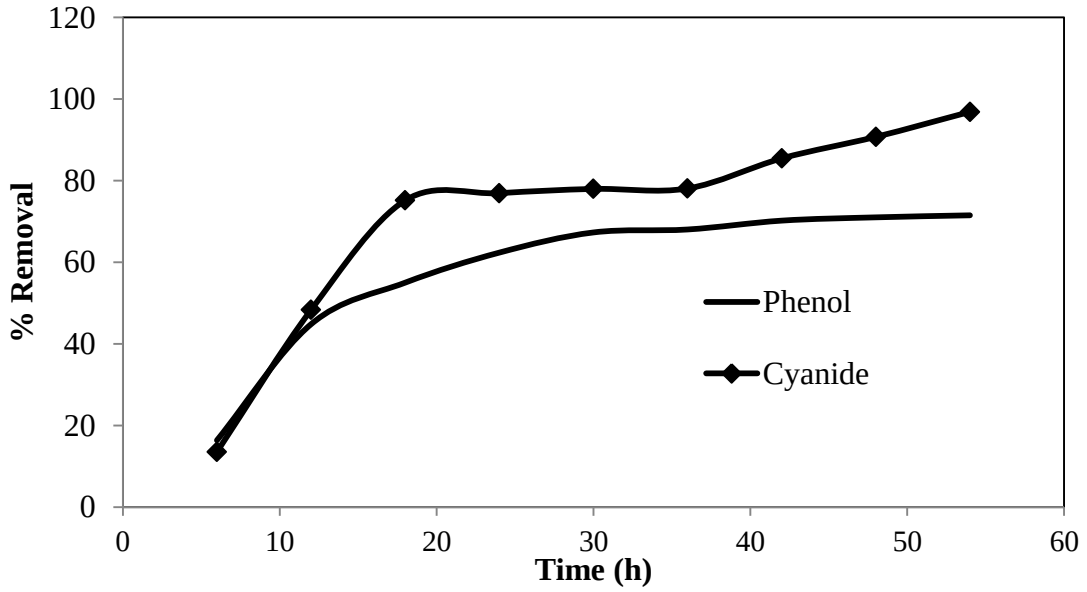

Figure 6.39: Effect of time (6-54) h on the SAB of phenol and cyanide using Egg Shells(ES) as an adsorbent at Initial phenol concentration 400 mg/L, initial cyanide concentration 40 mg/L, pH: 6.5-7, adsorbent dose 35 g/L, temperature: 30 ^{0}C

6.1.3.5 EFFECT OF INITIAL CONCENTRATION:

The efficiency of phenol and cyanide removal by SAB process also depends on the initial concentration of phenol and cyanide as it provides driving force to overcome the mass

transfer limitations between adsorbate and adsorbent molecules. The graphs plotted for Removal percentage versus Initial phenol or cyanide concentration are shown below in figure 6.40 (a), (b), 6.41 (a), (b) and 6.42 (a), (b) for all the three adsorbents. From the figures shown below it can be inferred that for all the three adsorbents the percentage removal decreases with increasing concentration of phenol and cyanide.

This behaviour of the plots can be followed by the fact that at low adsorbate concentrations the active sites of the adsorbent are easily occupied by adsorbate molecules which show a high percentage removal whereas at a high concentration saturation adsorbent's binding capacity can take place which in turn can decrease removal (Vedula et.al.). With increasing concentration of pollutants the percentage removal decreases, this can also be possible due to the deaths of microorganisms due to increasing toxicity.

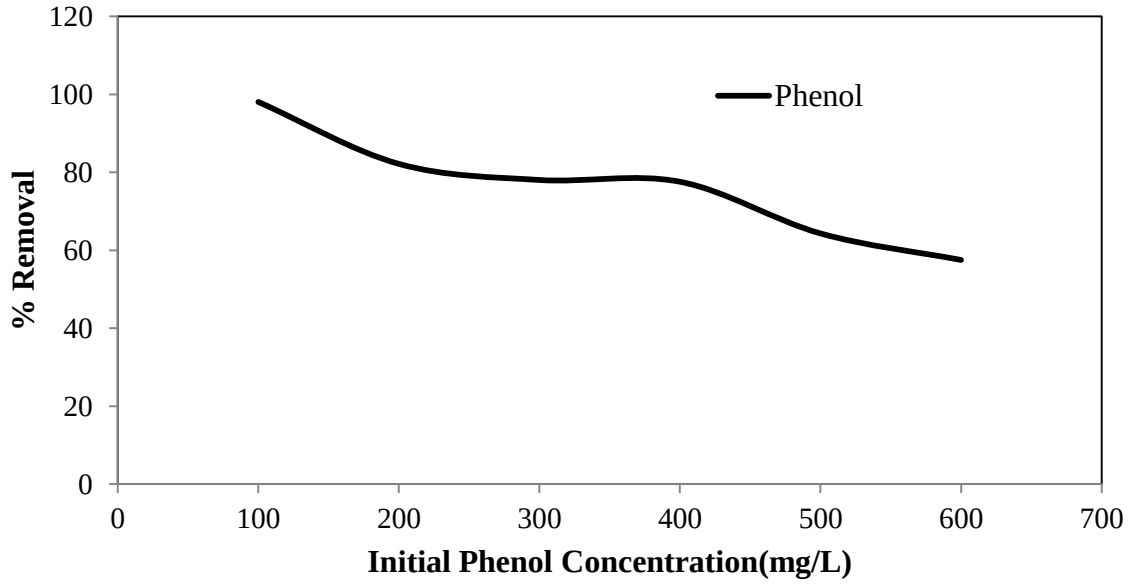

(a)

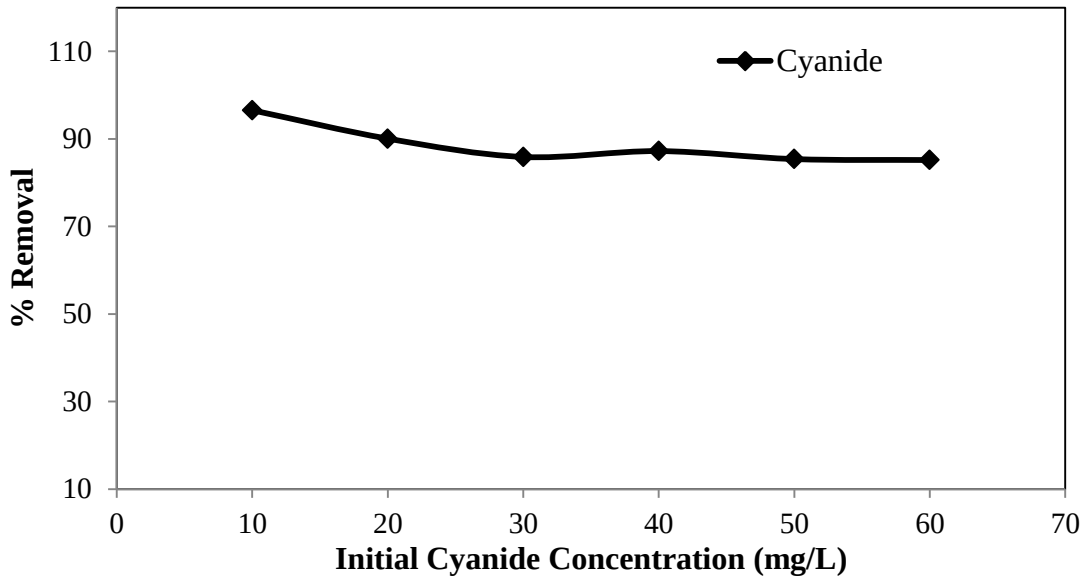

(b)

Figure 6.40: Effect of initial concentration on the SAB of phenol (a) and cyanide (b) using Rice Husk(RH) as an adsorbent at Initial phenol concentration (100-400) mg/L, initial cyanide concentration (10-40) mg/L, pH: 6.5-7, adsorbent dose 5 g/L, temperature: 30 ^{0}C and for 54 h

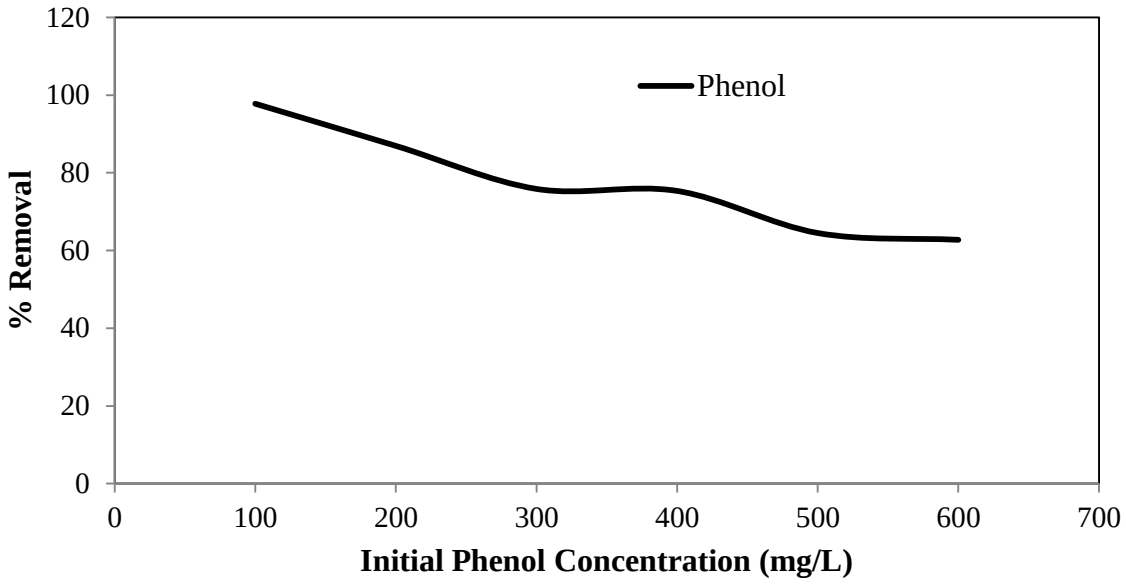

(a)

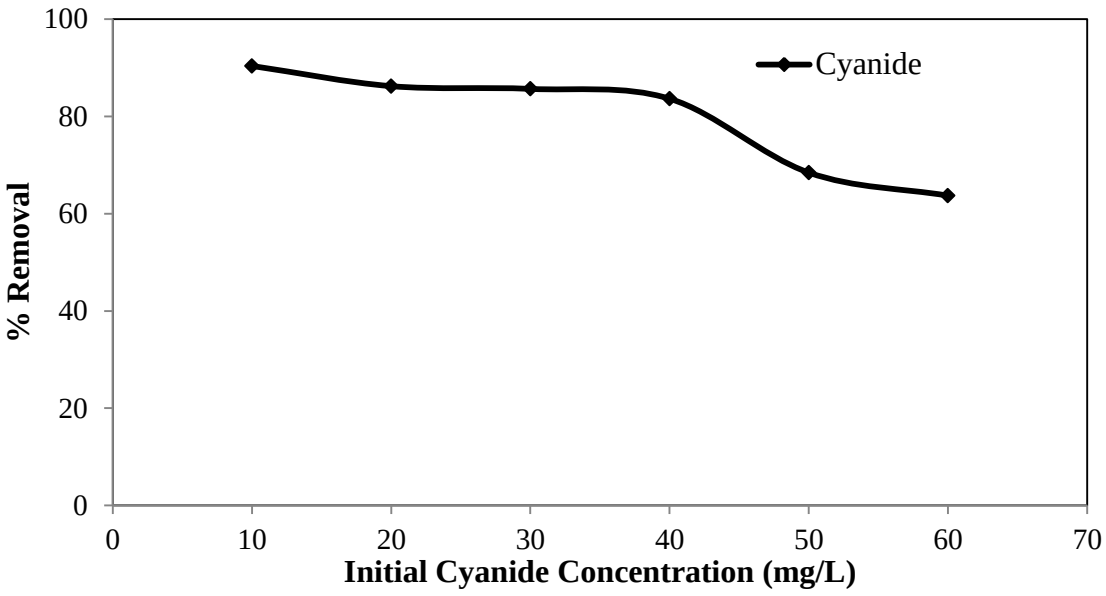

(b)

Figure 6.41: Effect of initial concentration on the SAB of phenol (a) and cyanide (b) using Corn Husk Leaves(CHL) as an adsorbent at Initial phenol concentration (100-400) mg/L, initial cyanide concentration (10-40) mg/L, pH=6.5-7, adsorbent dose 6 g/L, temperature: 30 ^{0}C and for 54 h

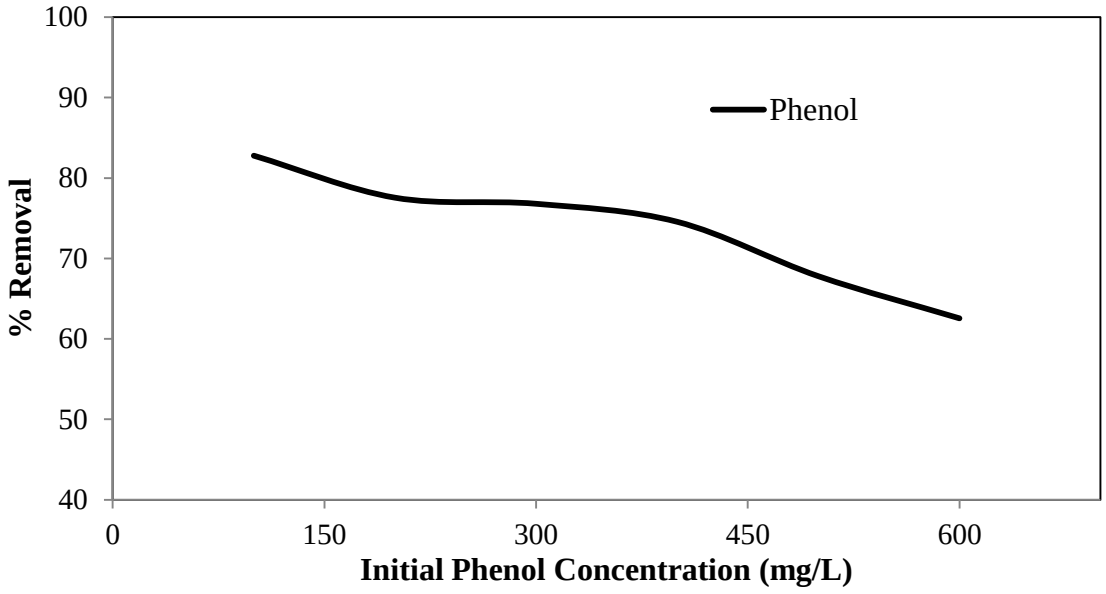

(a)

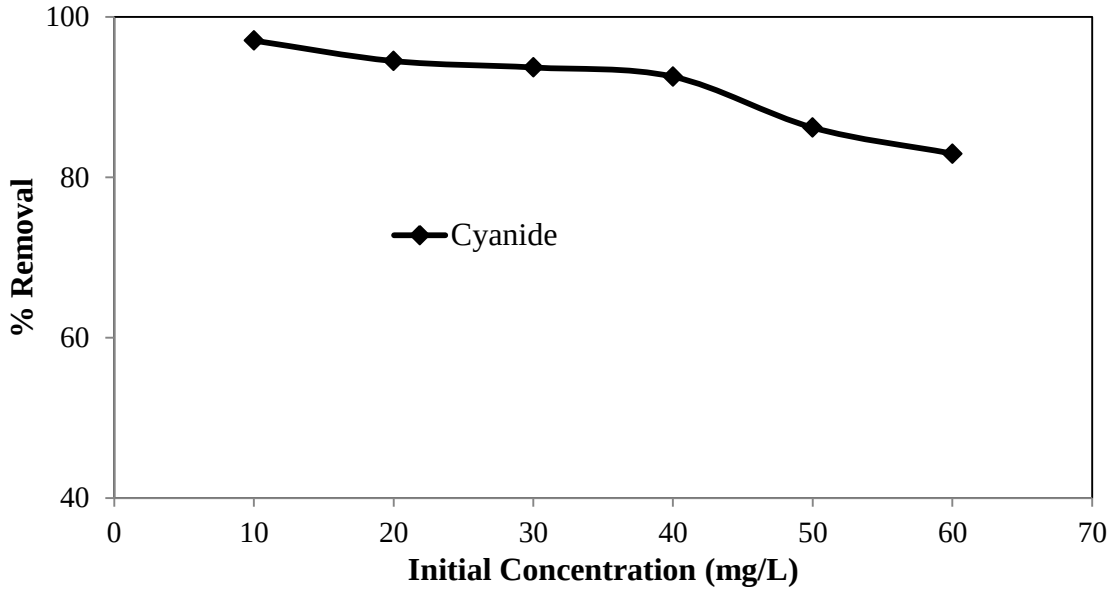

Figure 6.42: Effect of initial concentration on the SAB of phenol (a) and cyanide (b) using Egg Shells(ES) as an adsorbent at Initial phenol concentration (100-400) mg/L, initial cyanide concentration (10-40) mg/L, pH: 6.5-7, adsorbent dose 35 g/L, temperature: 30 ^{0}C and for 54 h

The optimum pH for SAB of phenol and cyanide for all the adsorbents was between 6.5-7. Optimum time was also same as 30 ^{0}C. The contact time for all the adsorbents was also optimized at 54 h with different doses for different adsorbents.

6.1.4 EQUILIBRIUM ISOTHERMS:

The data for simultaneous adsorption and biodegradation of phenol and cyanide on rice husk, corn husk leaves and egg shells were analysed using Solver function of Microsoft excel 2010. The multicomponent SAB data for both phenol and cyanide were fitted to different multicomponent isotherm models i.e. Non Modified Langmuir, Modified Langmuir, Extended Langmuir and Extended Freundlich models. The multicomponent model constants are taken from single component models. The predictability of these models were analysed using Average Relative Error (ARE). The data of different isotherm models is shown in table 6.5.

Single component models of Langmuir and Freundlich were fitted nonlinearly for the adsorption of phenol and cyanide in their individual solutions. The calculated specific uptake for different isotherm models is plotted linearly with the equilibrium concentration. The plots for Langmuir and Freundlich isotherm for different adsorbents are shown below from figure 6.43 to figure 6.48.

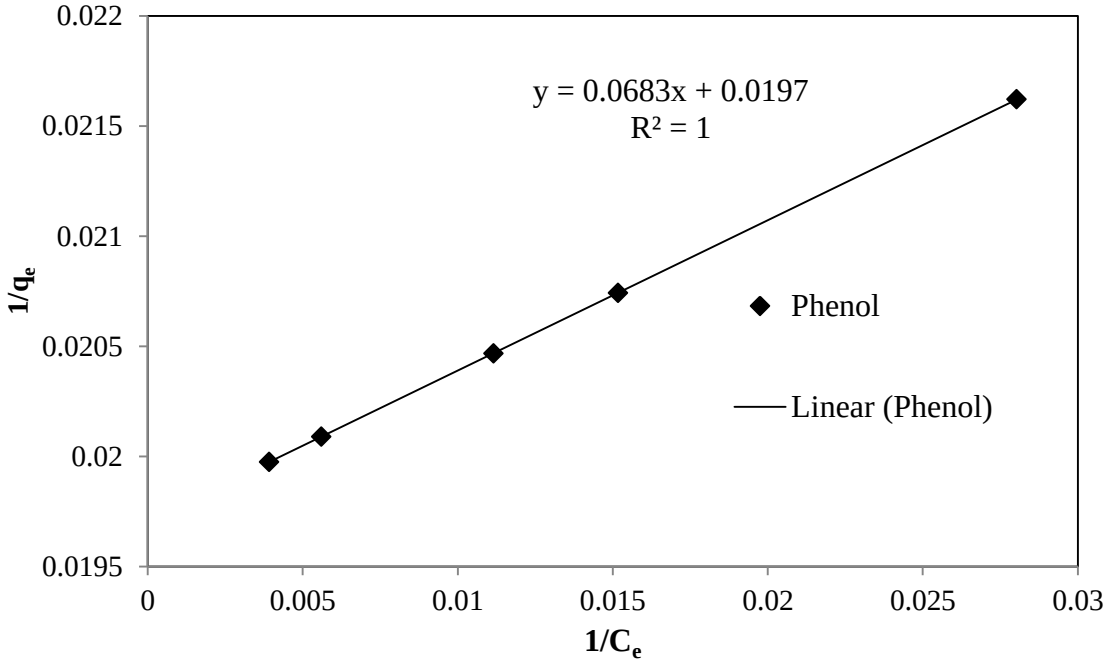

(a)

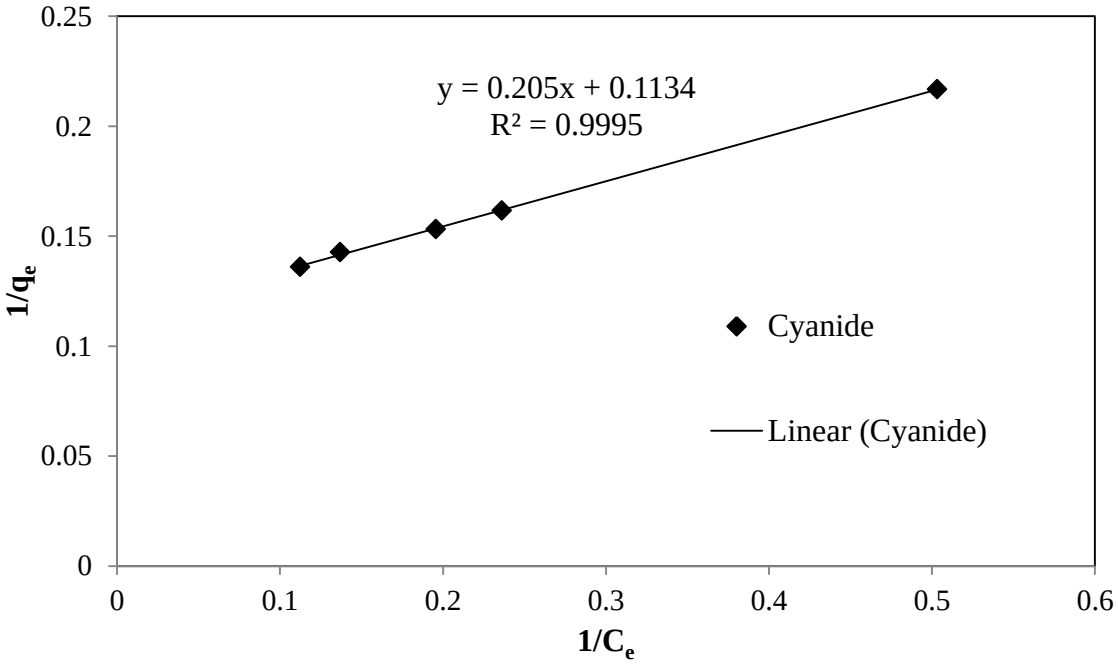

(b)

Figure 6.43: Langmuir isotherm plots for SAB of phenol (a) and cyanide (b) using Rice Husk(RH) as adsorbent

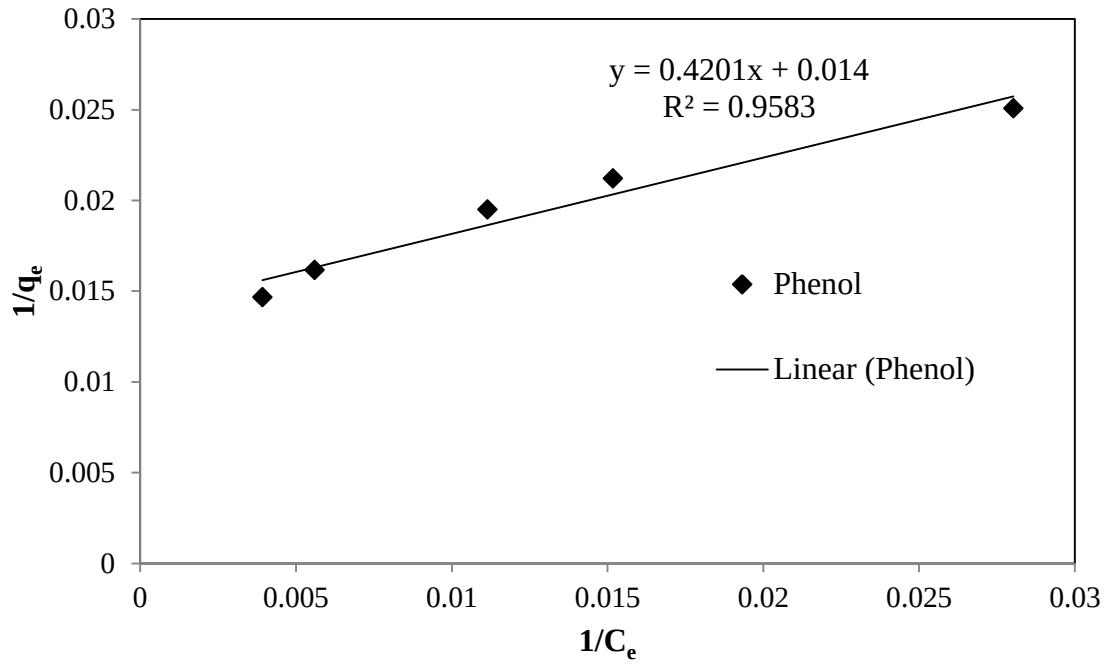

(a)

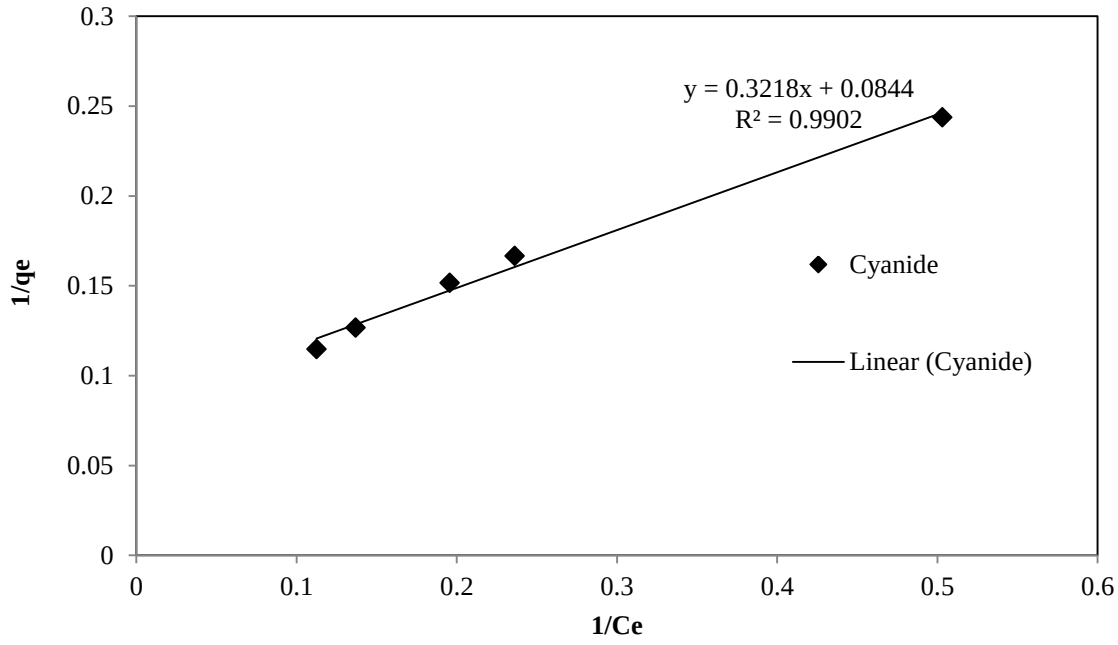

Figure 6.44: Freundlich isotherm plots for SAB of phenol (a) and cyanide (b) using Rice Husk (RH) as adsorbent

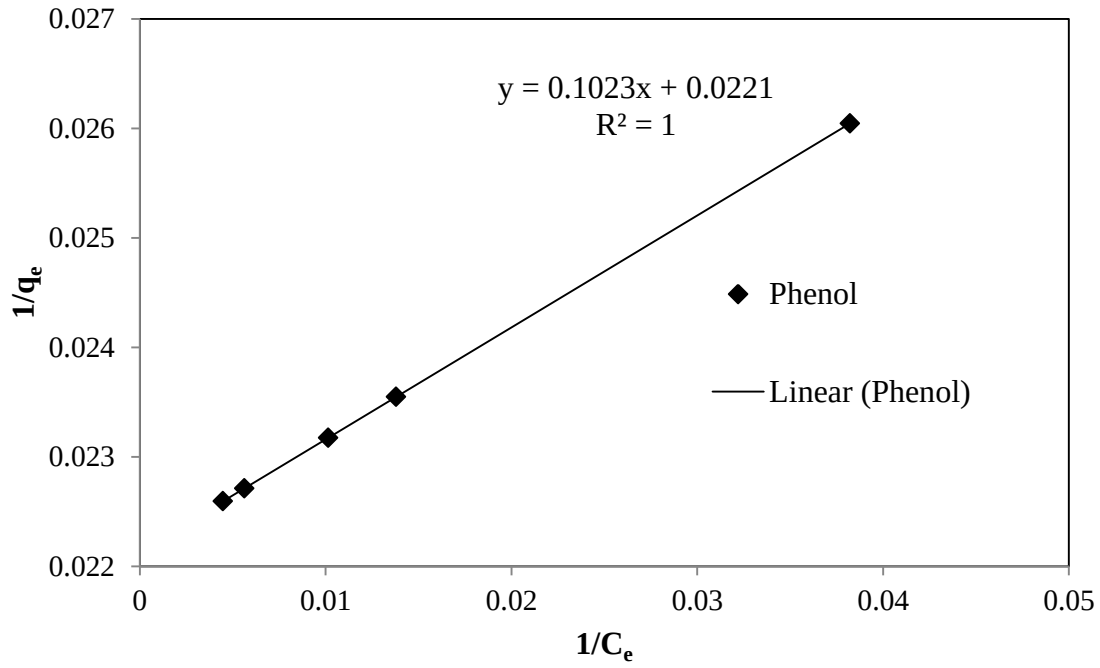

(a)

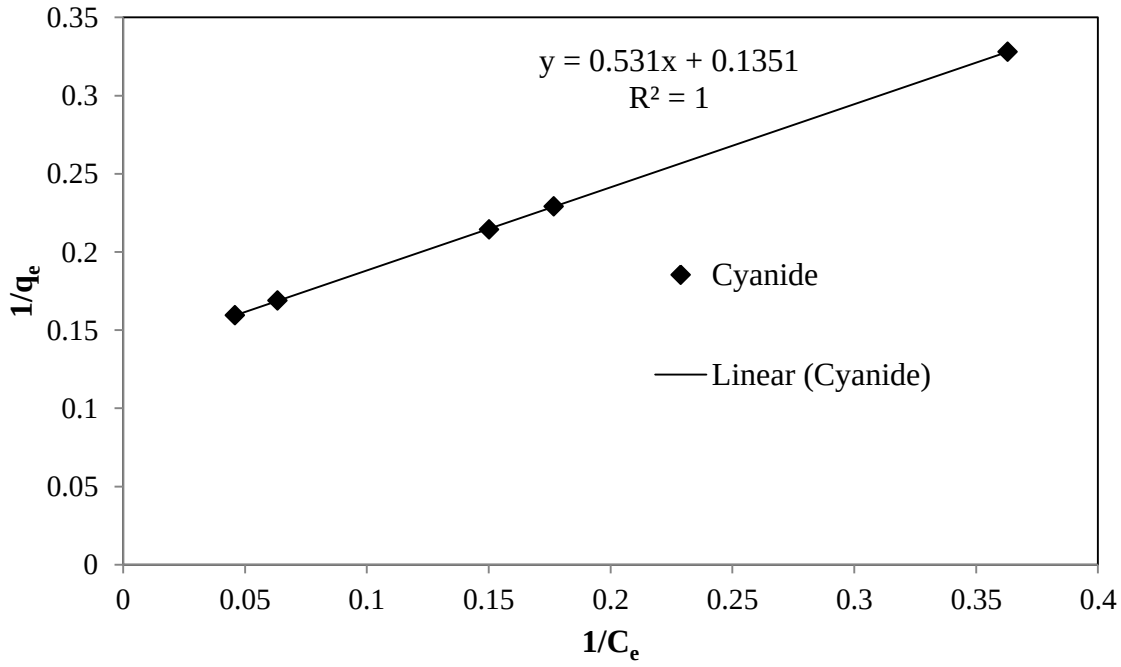

(b)

Figure 6.45: Langmuir isotherm plots for SAB of phenol (a) and cyanide (b) using Corn Husk Leaves (CHL) as adsorbent

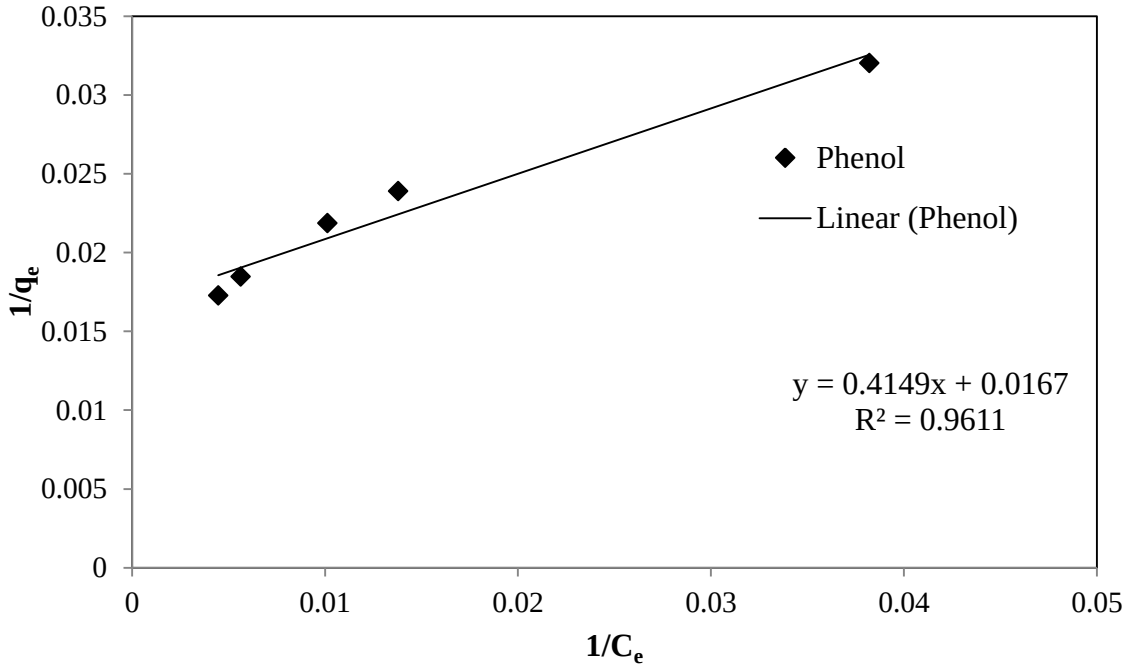

(a)

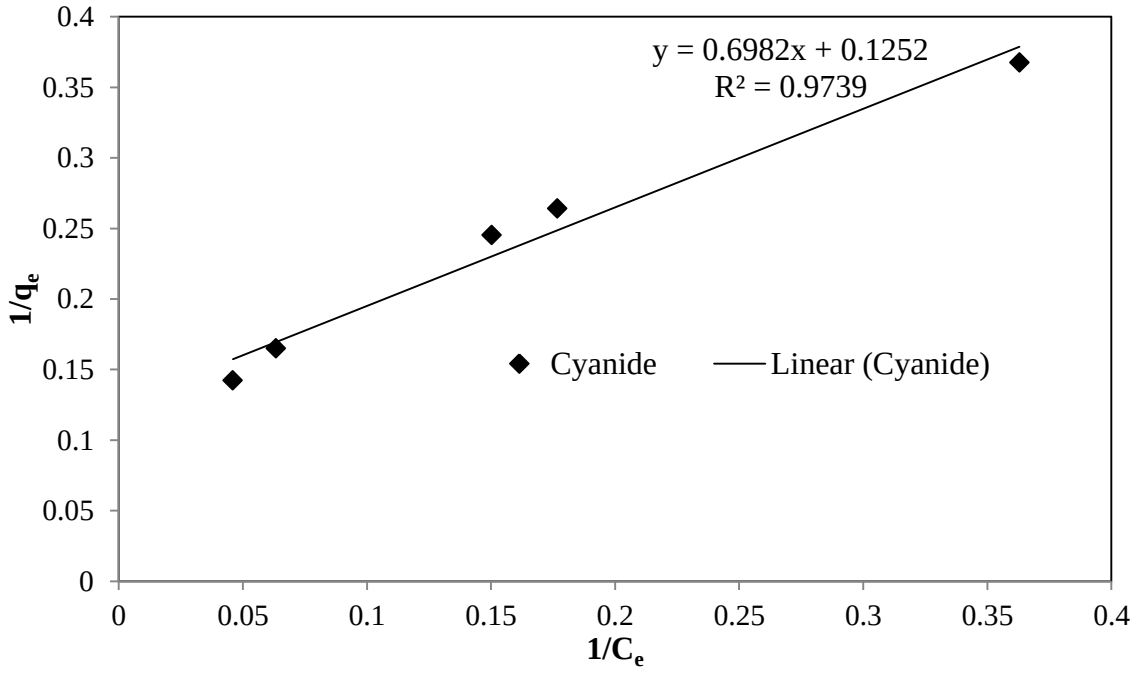

(b)

Figure 6.176: Freundlich isotherm plots for SAB of phenol (a) and cyanide (b) using Corn Husk Leaves (CHL) as adsorbent

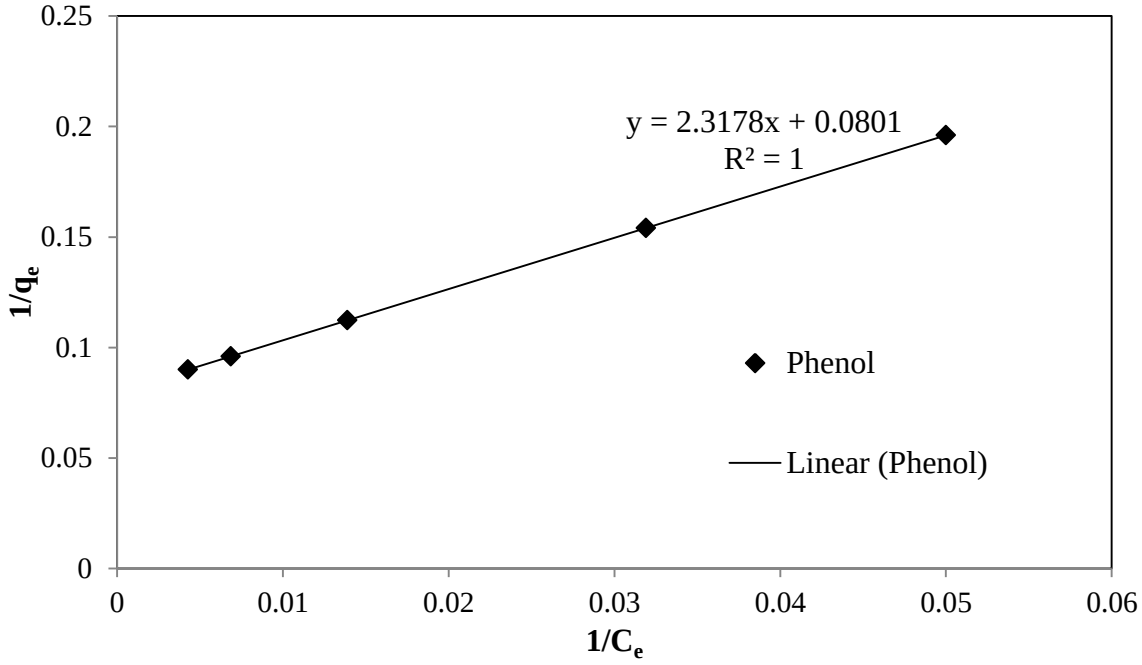

(a)

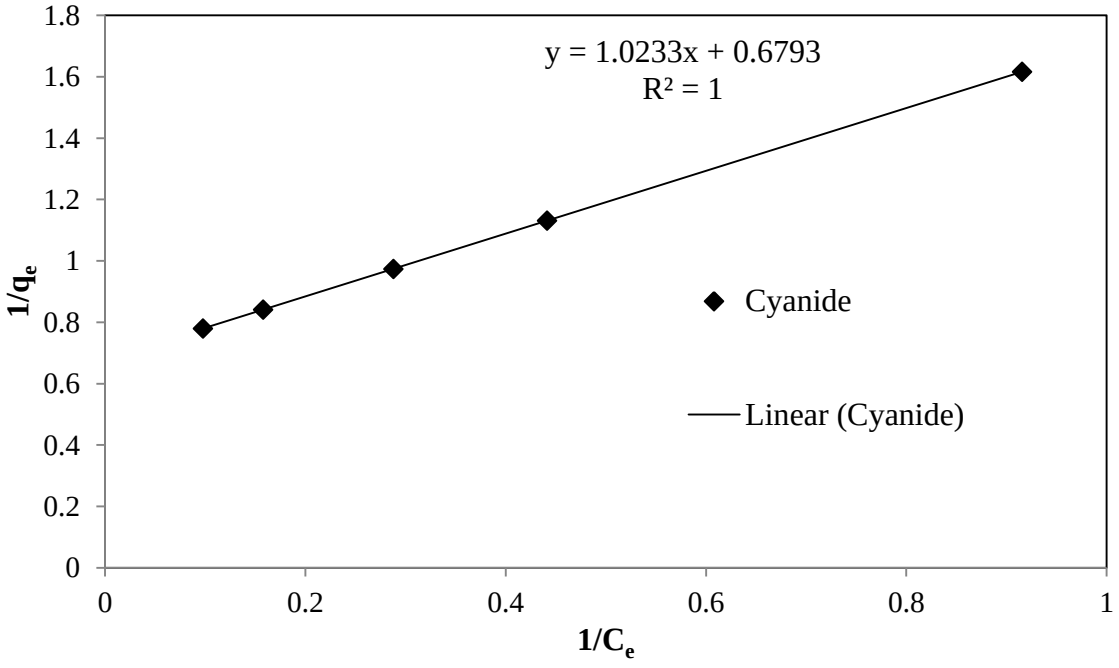

(b)

Figure 6.187: Langmuir isotherm plots for SAB of phenol (a) and cyanide (b) using Egg Shells (ES) as adsorbent

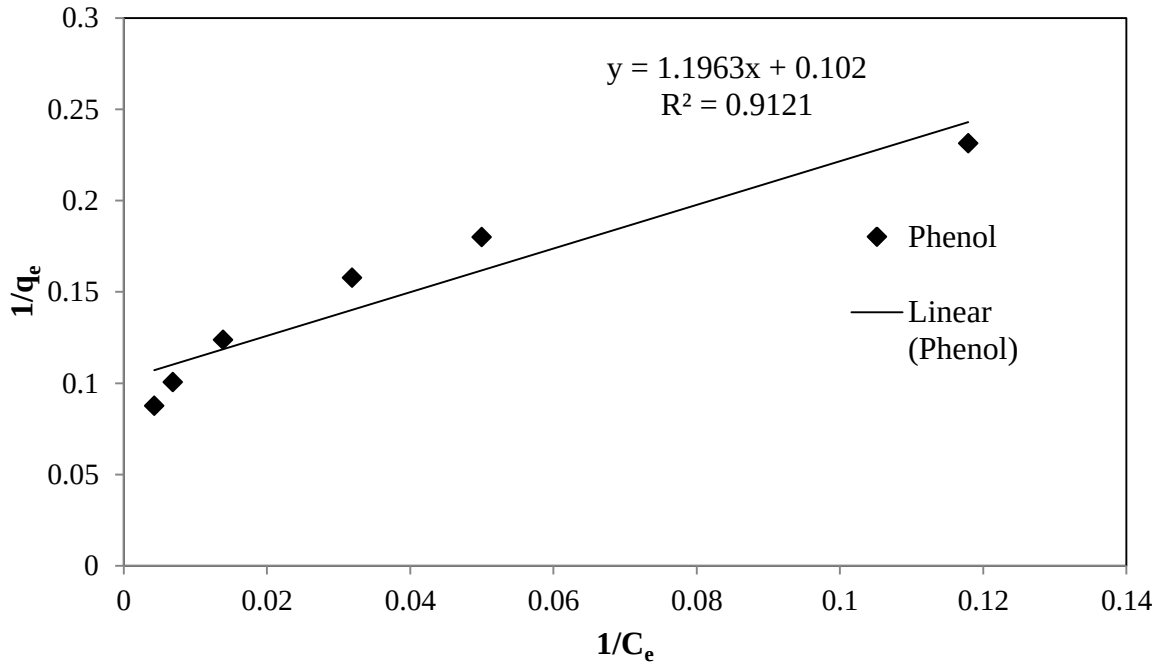

(a)

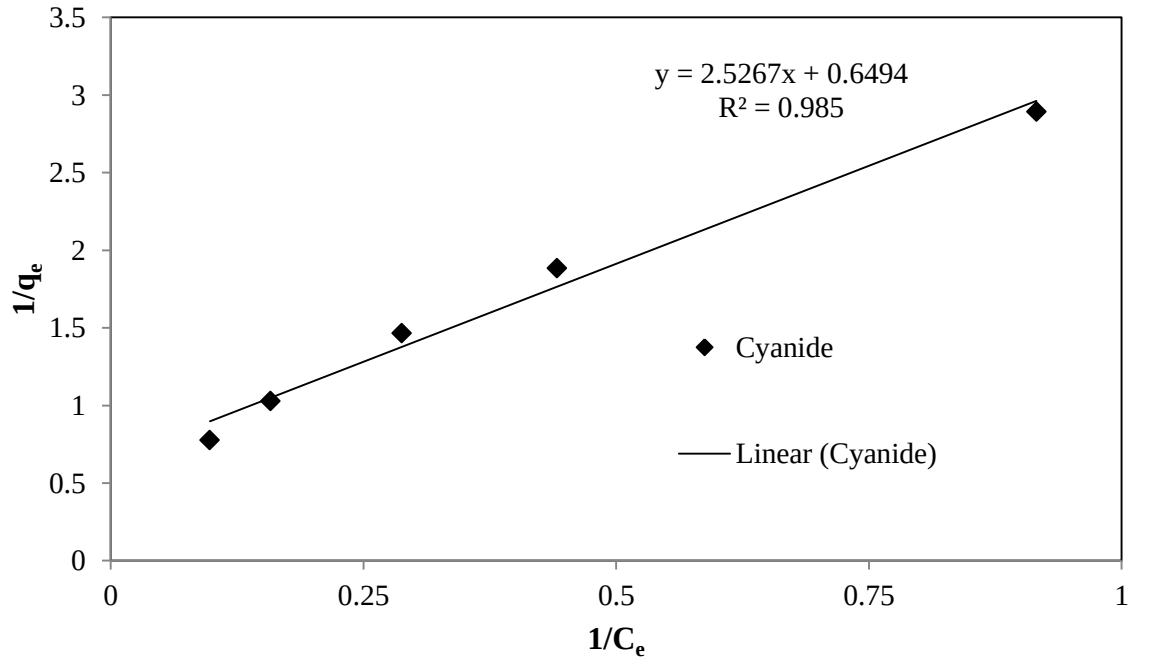

(b)

Figure 6.198: Freundlich isotherm plots for SAB of phenol (a) and cyanide (b) using Egg Shells (ES) as adsorbent

From the above plots it can be inferred that both Langmuir and Freundlich isotherms can be fairly used to fit the co-adsorption data of phenol and cyanide on all the three adsorbents i.e.

rice husk, corn husk leaves and egg shells. Thereby proving that co-adsorption of phenol and cyanide takes place both by the formation of monolayer as well as multilayer.

Table 6.19: Parameters of phenol and cyanide SAB onto GAC as estimated by multicomponent modeling

Parameters and ARE	Present Study	
	Rice Husk	
	Non-modified Langmuir Isotherm	
	Phenol (i=1)	**Cyanide (i=2)**
$Q_{0,i}$	50.741	8.871
b_i	0.289	0.545
ARE	10.237	33.668
	Modified Langmuir Isotherm	
$Q_{0,i}$	50.741	8.871
b_i	0.289	0.545
n_i	1.876	0.359
ARE	17.858	21.857
	Extended Langmuir Isotherm	
$Q_{0,i}$	78.741	113.743
b_i	0.031	0.044
ARE	13.569	12.913
	Extended Freundlich Isotherm	
$K_{F,i}$	15.052	2.907
n_i	3.669	1.990
x_i	-1.654	-1.876
y_i	2.919	0.122
z_i	6.604	0.959
ARE	136.135	36.996
	Corn Husk Leaves	
	Non-modified Langmuir Isotherm	
	Phenol (i=1)	**Cyanide (i=2)**
$Q_{0,i}$	45.172	7.393
b_i	0.216	0.255

ARE	9.597	32.353
	Modified Langmuir Isotherm	
$\mathbf{Q_{0,i}}$	45.172	7.393
$\mathbf{b_i}$	0.216	0.255
$\mathbf{n_i}$	2.595	0.522
ARE	19.028	20.790
	Extended Langmuir Isotherm	
$\mathbf{Q_{0,i}}$	99.646	2.624
$\mathbf{b_i}$	2.186	0.255
ARE	11.317	27.197
	Extended Freundlich Isotherm	
$\mathbf{K_{F,i}}$	12.213	1.709
$\mathbf{n_i}$	3.477	2.178
$\mathbf{x_i}$	-2.564	-3.545
$\mathbf{y_i}$	1.748	0.391
$\mathbf{z_i}$	1.231	0.958
ARE	15.357	37.716
	Egg Shells	
	Non-modified Langmuir Isotherm	
	Phenol (i=1)	**Cyanide (i=2)**
$\mathbf{Q_{0,i}}$	12.479	1.472
$\mathbf{b_i}$	0.0346	0.664
ARE	15.319	23.586
	Modified Langmuir Isotherm	
$\mathbf{Q_{0,i}}$	12.479	1.472
$\mathbf{b_i}$	0.0346	0.664
$\mathbf{n_i}$	0.68	0.54
ARE	16.449	12.170
	Extended Langmuir Isotherm	
$\mathbf{Q_{0,i}}$	16.486	13.168
$\mathbf{b_i}$	0.02	0.033
ARE	6.186	18.803
	Extended Freundlich Isotherm	

$\mathbf{K_{F,i}}$	2.314	0.328
$\mathbf{n_i}$	3.419	1.708
$\mathbf{x_i}$	-1.986	-3.479
$\mathbf{y_i}$	2.152	1.234
$\mathbf{z_i}$	0.456	0.007
ARE	41.131	35.875

Based on the data of table 6.5 it can be seen that in the case of rice husk non-modified Langmuir isotherm suits best the adsorption of phenol and extended Langmuir model suits best the adsorption of cyanide, owing to the low values of ARE. Similarly owing to the values of ARE non-modified Langmuir proves to be the best fit for phenol adsorption on corn husk leaves and modified Langmuir proves to be the best fit for cyanide adsorption on corn husk leaves. Whereas for phenol adsorption on egg shells extended Langmuir proves to be the best fit and for cyanide adsorption on egg shells modified Langmuir isotherm is the best fit.

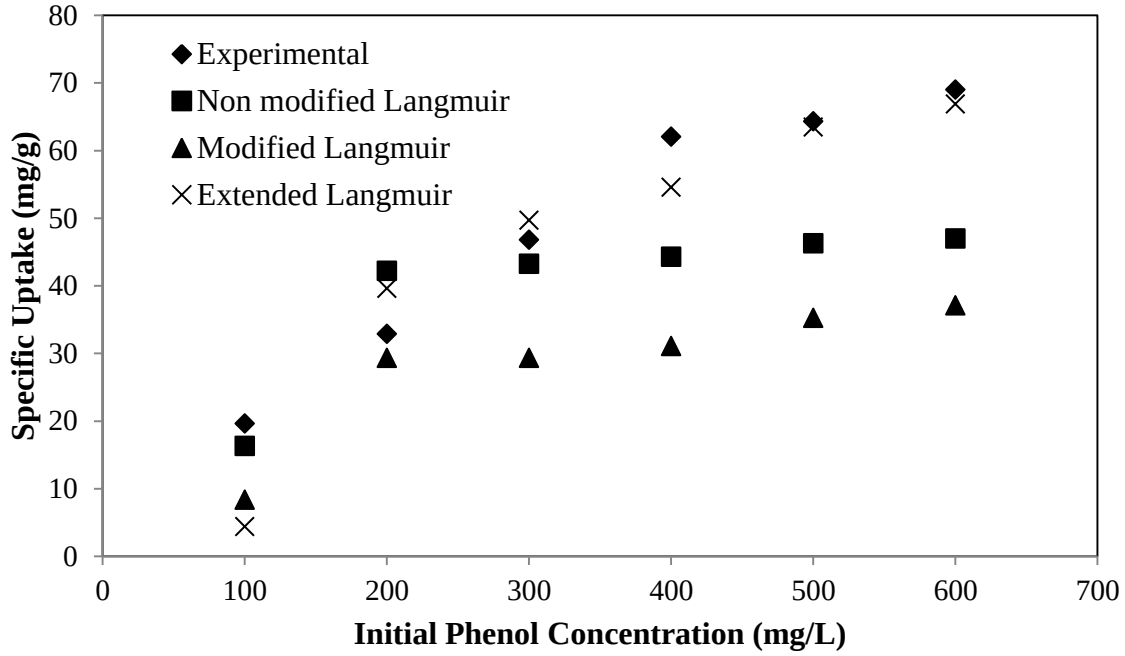

(a)

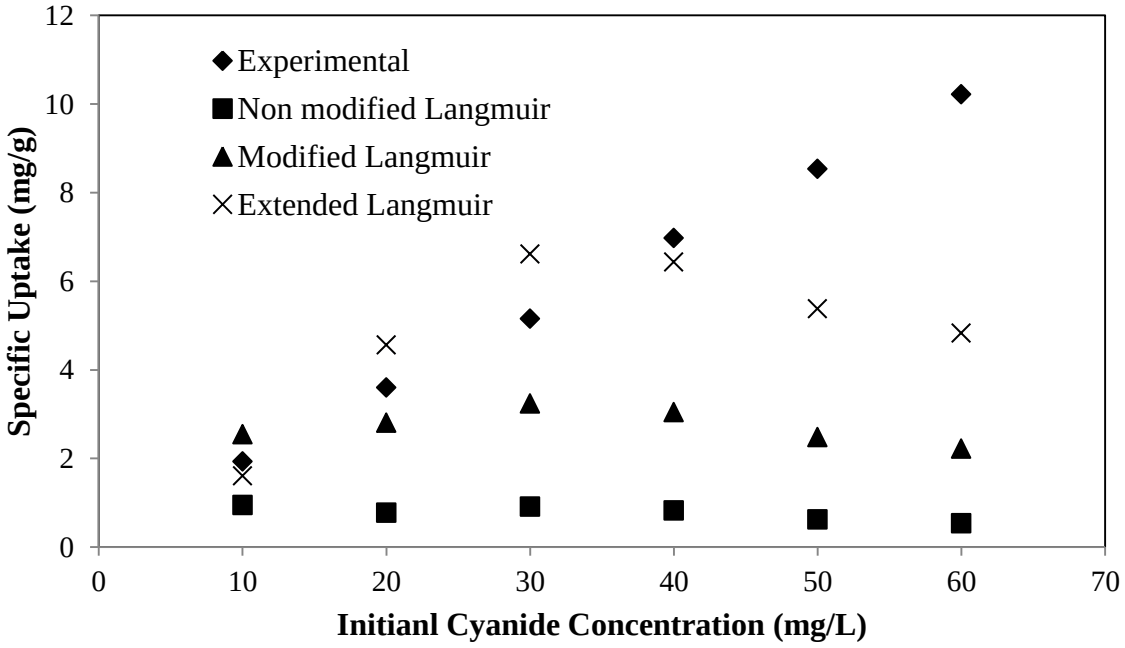

(b)

Figure 6.49: Equilibrium adsorption isotherms for SAB of (a) phenol and (b) cyanide at 30 ^{0}C and 400 mg/L phenol and 40 mg/L cyanide using Rice Husk (RH)

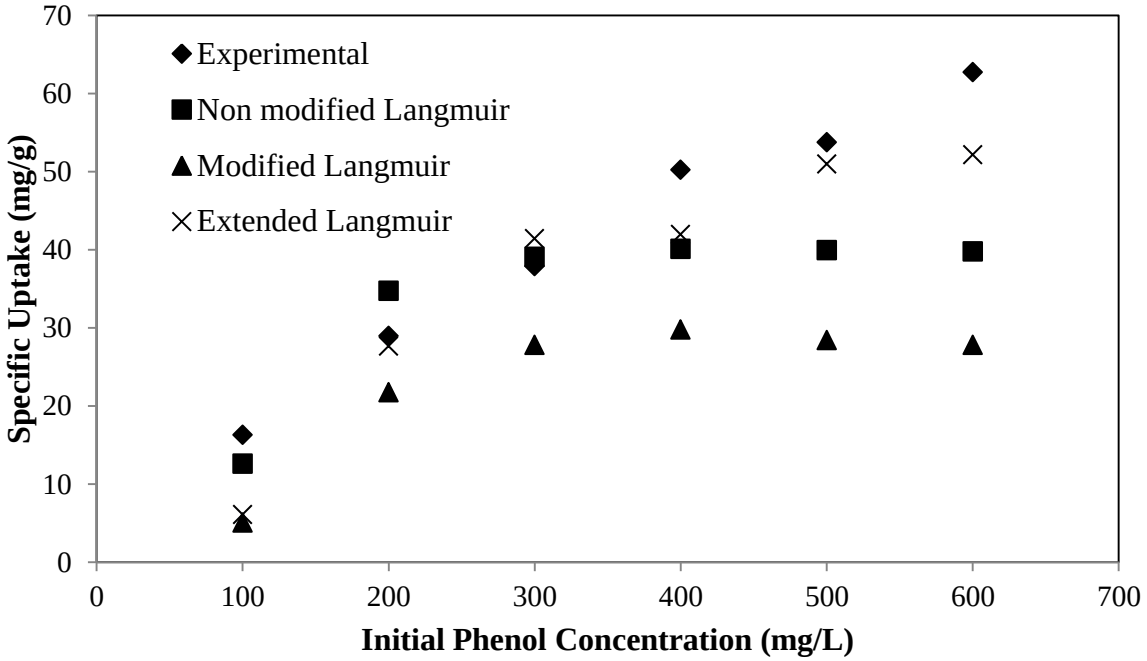

(a)

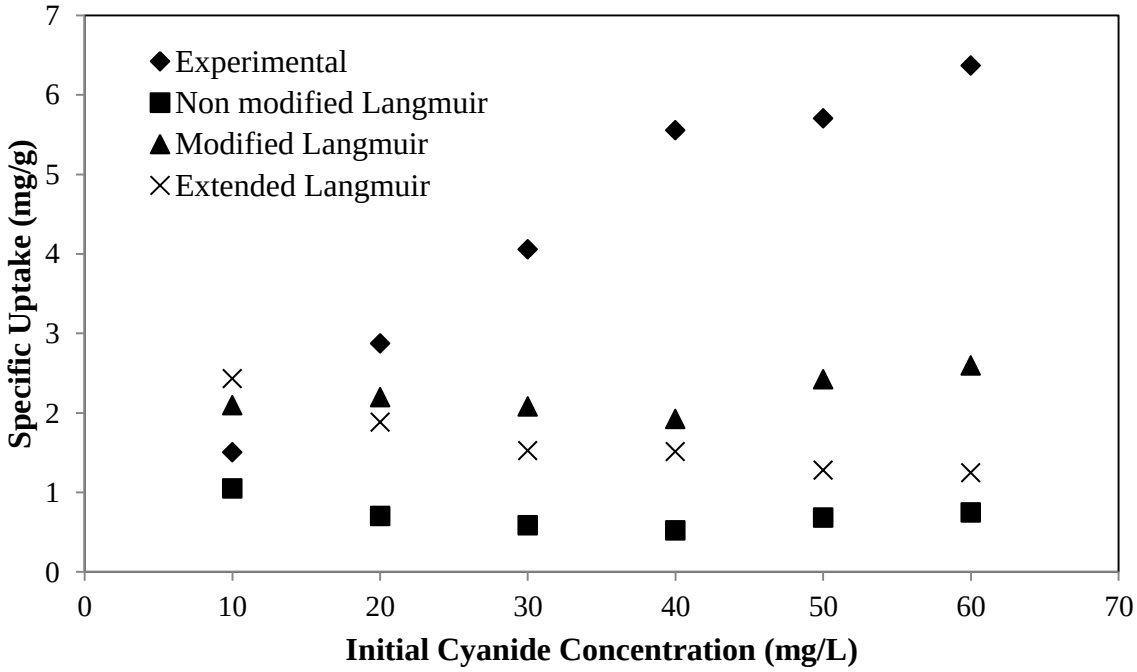

(b)

Figure 6.50: Equilibrium adsorption isotherms for SAB of (a) phenol and (b) cyanide at 30 ^{0}C and 400 mg/L phenol and 40 mg/L cyanide using Corn Husk Leaves (CHL)

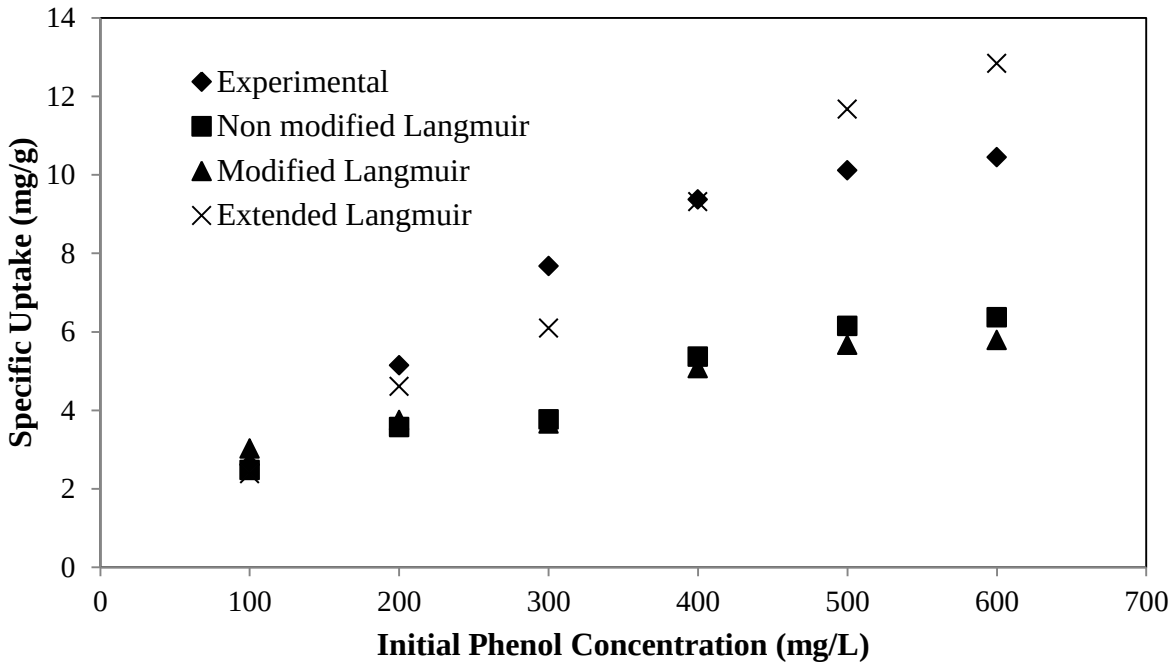

(a)

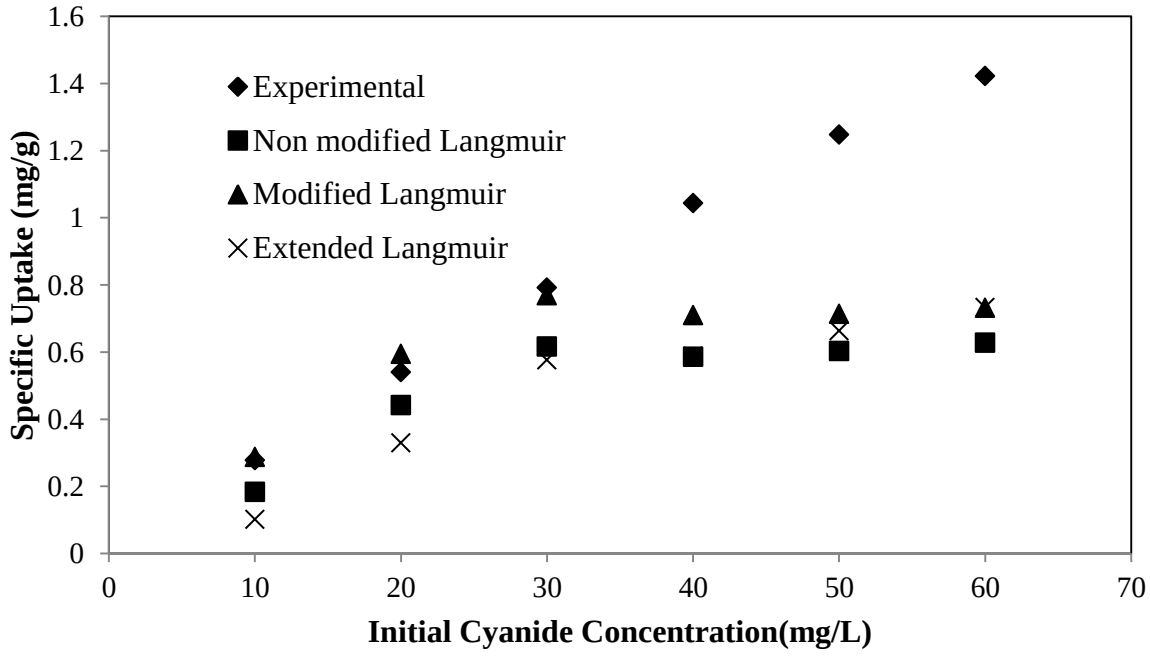

(b)

Figure 6.51: Equilibrium adsorption isotherms for SAB of (a) phenol and (b) cyanide at 30 ^{0}C and 400 mg/L phenol and 40 mg/L cyanide using Egg Shells (ES)

Figures 6.49 to 6.51 shows the comparison of specific uptake obtained experimentally and the specific uptake obtained by different equilibrium isotherms for all the three adsorbents rice husk, corn husk leaves and egg shells. Figure 6.49 (a) shows that phenol adsorption data on rice husk is best fitted by both Non-modified Langmuir isotherm and Extended Langmuir isotherm. Figure 6.49 (b) shows that cyanide adsorption data on rice husk is best fitted by both Modified Langmuir and Extended Langmuir isotherm. Adsorption data of phenol on corn husk leaves is best fitted by Non-modified and Extended Langmuir isotherm whereas adsorption data of cyanide on corn husk leaves is best fitted by Modified Langmuir isotherm as shown by figure 6.50 (a) and (b).

Figure 6.51 (a) shows adsorption data of phenol on egg shells by extended Langmuir isotherm whereas that for cyanide is shown by Modified Langmuir isotherm, figure 6.51 (b).

The equilibrium isotherms that were best fit were either non modified Langmuir or extended Langmuir for phenol adsorption onto the three adsorbents and the isotherms that best fitted cyanide data was modified Langmuir isotherm.

6.1.5 KINETIC STUDIES:

The contact time data for the simultaneous adsorption and biodegradation of phenol and cyanide by rice husk, corn husk leaves and egg shells were non linearly fitted for pseudo first order model and pseudo second order model. Kinetic data predictions either by pseudo first order (physisorption) or by pseudo second order (chemisorption) was done based on the values of ARE. The kinetic data for all the three adsorbents is shown in Table 6.6. From the data shown in table 6.6 it can be inferred that mechanism of co-adsorption of phenol and cyanide for all the three adsorbents is both by physisorption and chemisorption which is also shown by figure 6.52 (a), (b) for rice husk, 6.54 (a), (b) for corn husk leaves and 6.56 (a), (b) for egg shells respectively. The results are in accordance with the results of Agarwal et. al. 2013) for simultaneous adsorption and biodegradation of phenol and cyanide by iron impregnated granular activated carbon. The graph of q_t vs $t^{0.5}$ determines the diffusion nature of the co-adsorption process. According to Kilic et.al. 2011, for intraparticle diffusion to be involved the plot should be linear. Since the plot obtained for all the three adsorbents i.e. rice husk figure 6.53 (a) and (b), corn husk leaves figure 6.55 (a) and (b) and egg shells i.e. figure 6.57 (a) and (b) are nonlinear it also it does pass through origin therefore intraparticle diffusion is not the rate controlling step (Moussavi et.al. and Dash et. al.). From the Weber Morris plot for rice husk both phenol and cyanide show intraparticle diffusion as the

dominating step as ($R_2^2 > R_1^2$). From the Weber Morris plot for Corn Husk leaves it can be seen that for phenol ($R_1^2 > R_2^2$) showing surface diffusion to be dominating whereas for cyanide ($R_2^2 > R_1^2$) showing intraparticle diffusion to be dominating. Finally the Weber Morris plot for egg shells shows that for both phenol and cyanide ($R_2^2 > R_1^2$) showing intraparticle diffusion to be dominating for the co-adsorption and biodegradation of phenol and cyanide.

Table 6.20: Kinetic model parameters for SAB of phenol and cyanide

Parameters and ARE	**Present Study**	
	Rice Husk	
	Pseudo First Order Kinetics	
	Phenol	**Cyanide**
$q_{e,cal}$	55.568	8.059
k_1	0.140	0.039
ARE	3.934	0.832
	Pseudo Second Order	
$q_{e,cal}$	64.060	12.103
k_2	0.003	0.002
ARE	2.243	1.062
	Intraparticle	
$k_{id\ 1}$	5.446	1.212
R_1^2	0.952	0.997
$k_{id\ 2}$	3.027	0.328
R_2^2	1	1
	Corn Husk Leaves	
	Pseudo First Order Kinetics	
	Phenol	**Cyanide**
$q_{e,cal}$	66.445	10.278
k_1	0.034	0.016
ARE	4.043	4.003
	Pseudo Second Order	
$q_{e,cal}$	104.548	10.278
k_2	0.000215	0.016

ARE	4.557	4.003
		Intraparticle
$k_{id\ 1}$	11.862	1.013
R_1^2	0.9805	0.9703
$k_{id\ 2}$	0.657	0.0428
R_2^2	0.9182	1
		Egg Shells
		Pseudo First Order Kinetics
	Phenol	**Cyanide**
$q_{e,cal}$	9.666	1.761
k_1	0.045	0.0207
ARE	6.276	10.502
		Pseudo Second Order
$q_{e,cal}$	15.542	3.146
k_2	0.002	0.004
ARE	6.959	10.669
		Intraparticle
$k_{id\ 1}$	1.621	0.205
R_1^2	0.905	0.811
$k_{id\ 2}$	0.172	0.15
R_2^2	0.987	0.996

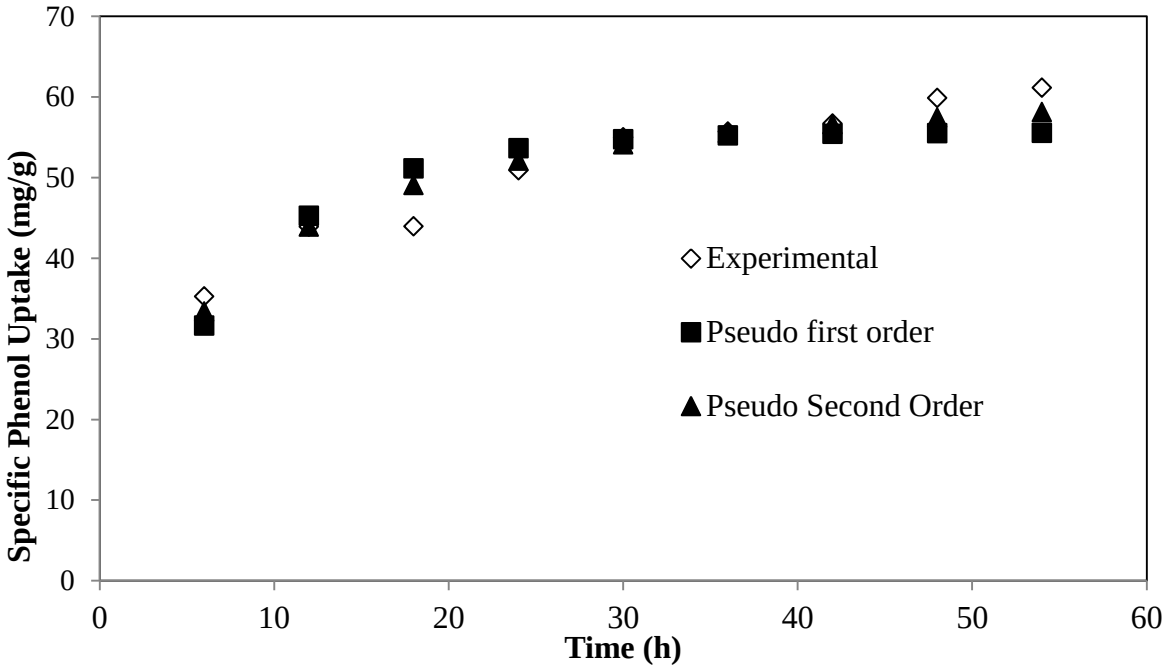

(a)

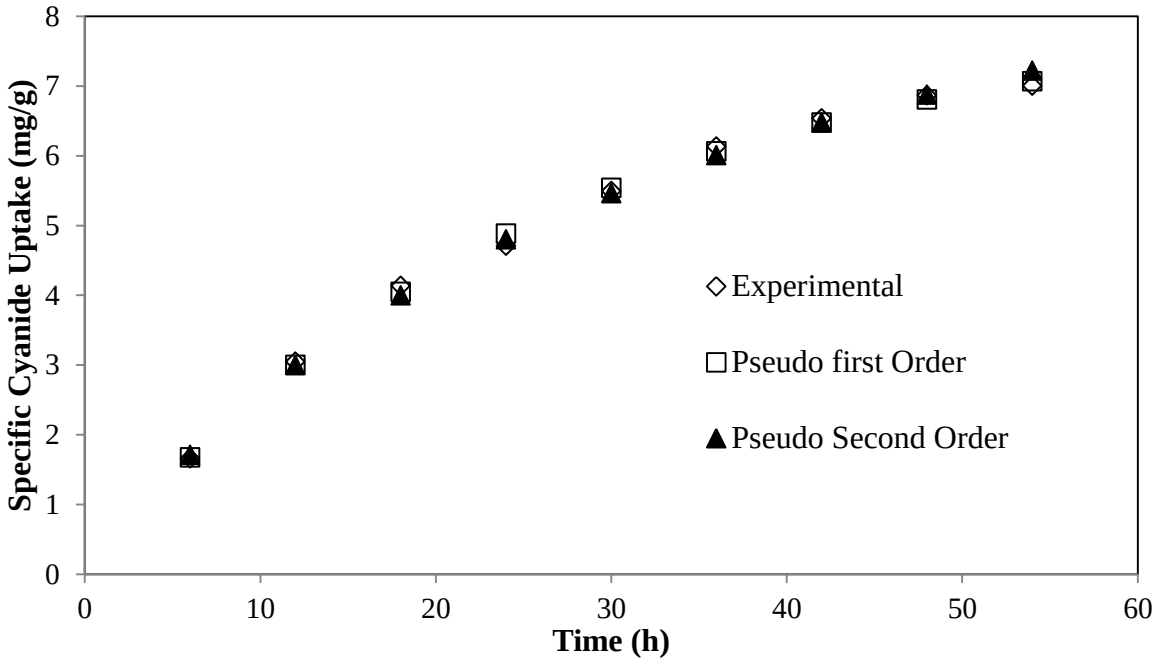

(b)

Figure 6.52: Kinetic modelling of SAB of (a) phenol and (b) cyanide at reaction conditions using Rice Husk (RH).

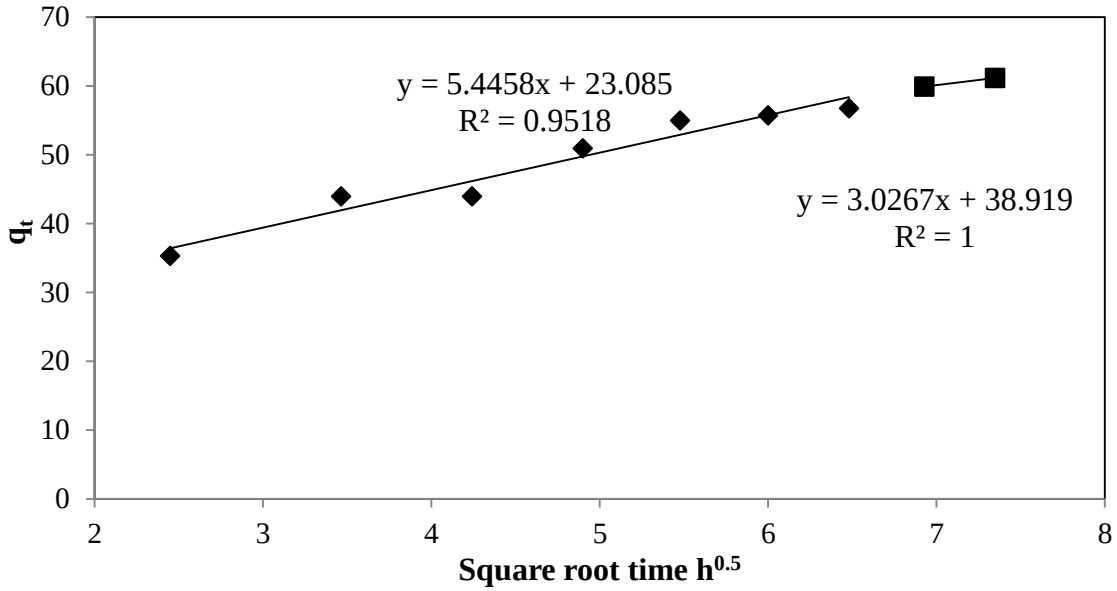

(a)

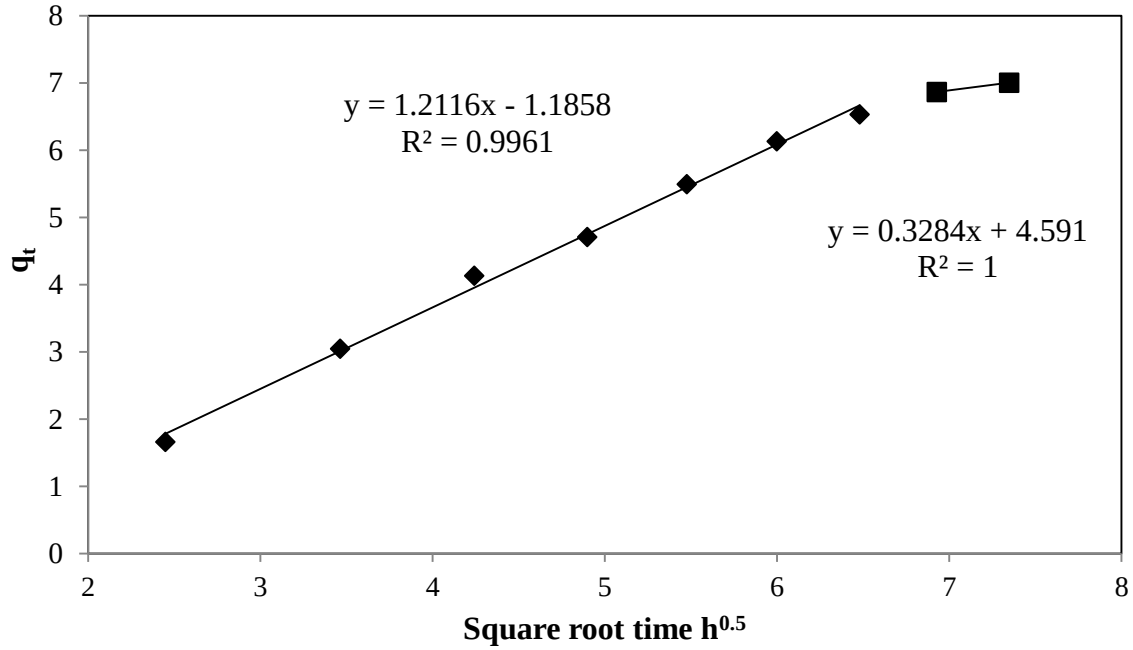

(b)

Figure 6.53: Intraparticle plot of (a) phenol and (b) cyanide SAB using Rice Husk (RH)

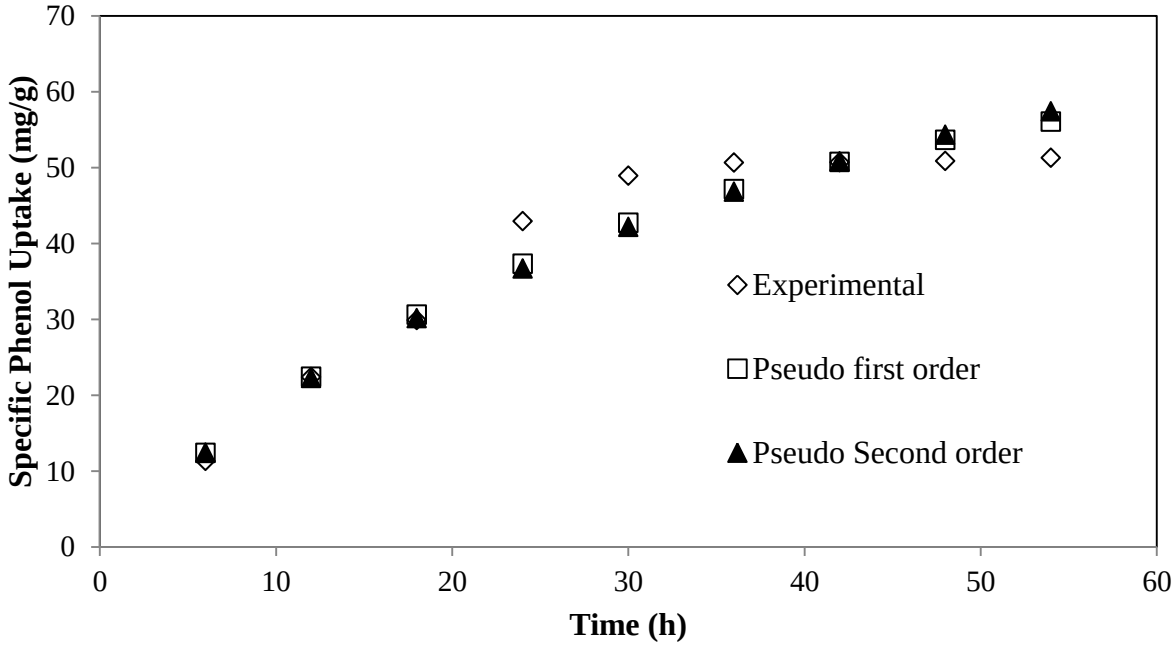

(a)

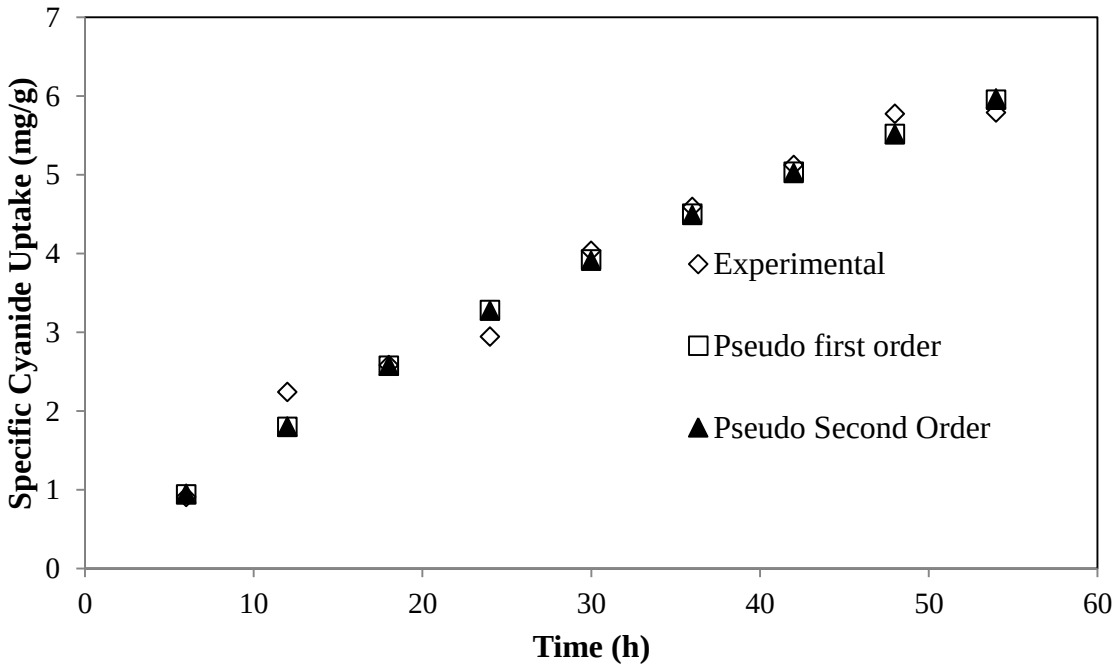

(b)

Figure 6.54: Kinetic modelling of SAB of (a) phenol and (b) cyanide at reaction conditions using Corn Husk Leaves (CHL)

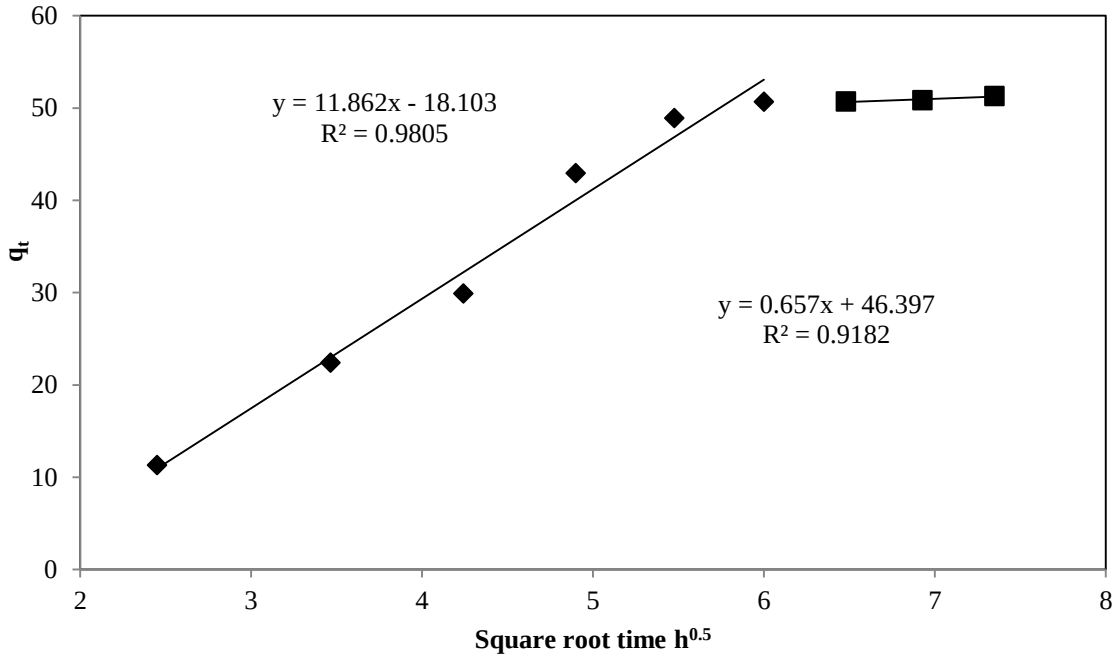

(a)

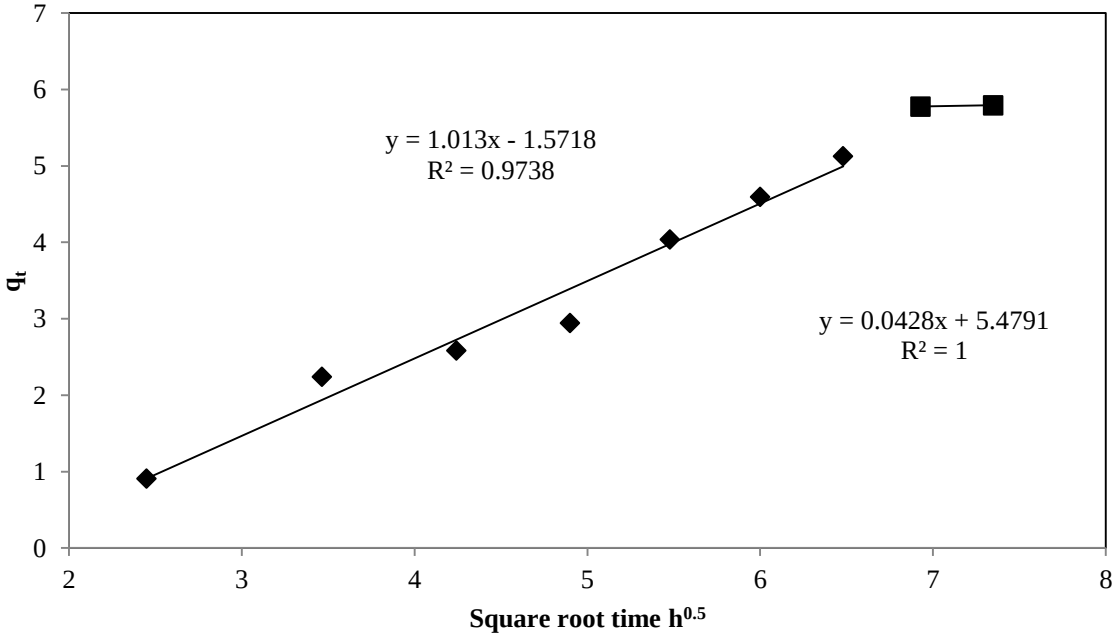

(b)

Figure 6.55: Intraparticle plot of (a) phenol and (b) cyanide SAB using Corn Husk Leaves (CHL)

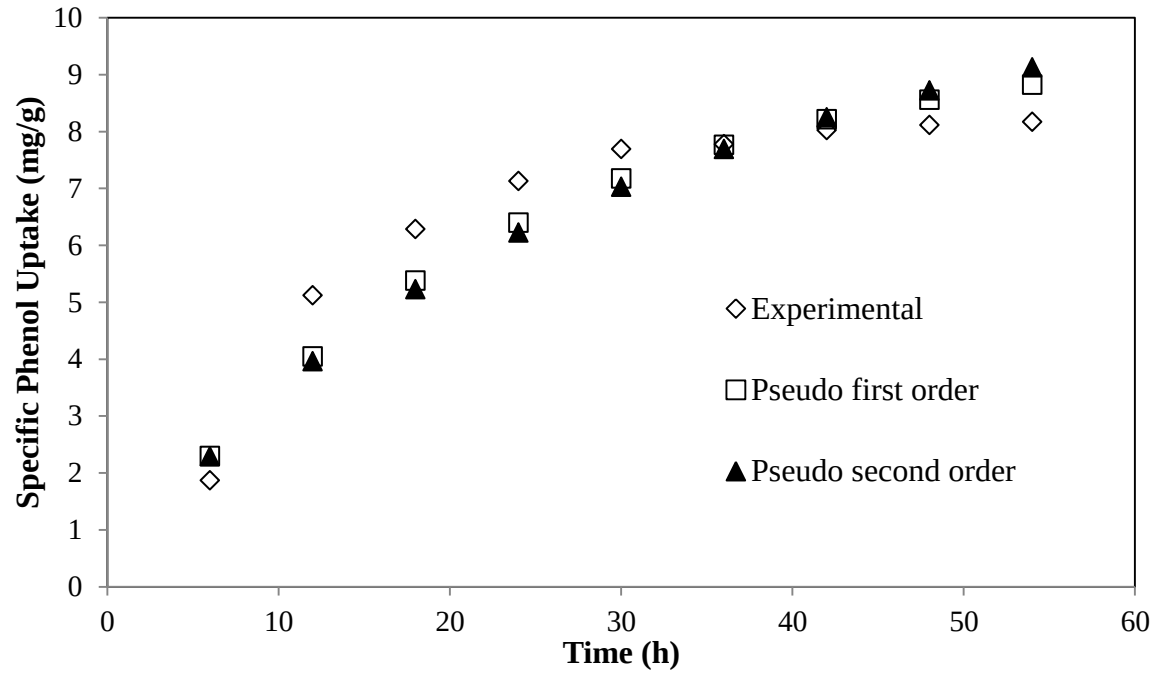

(a)

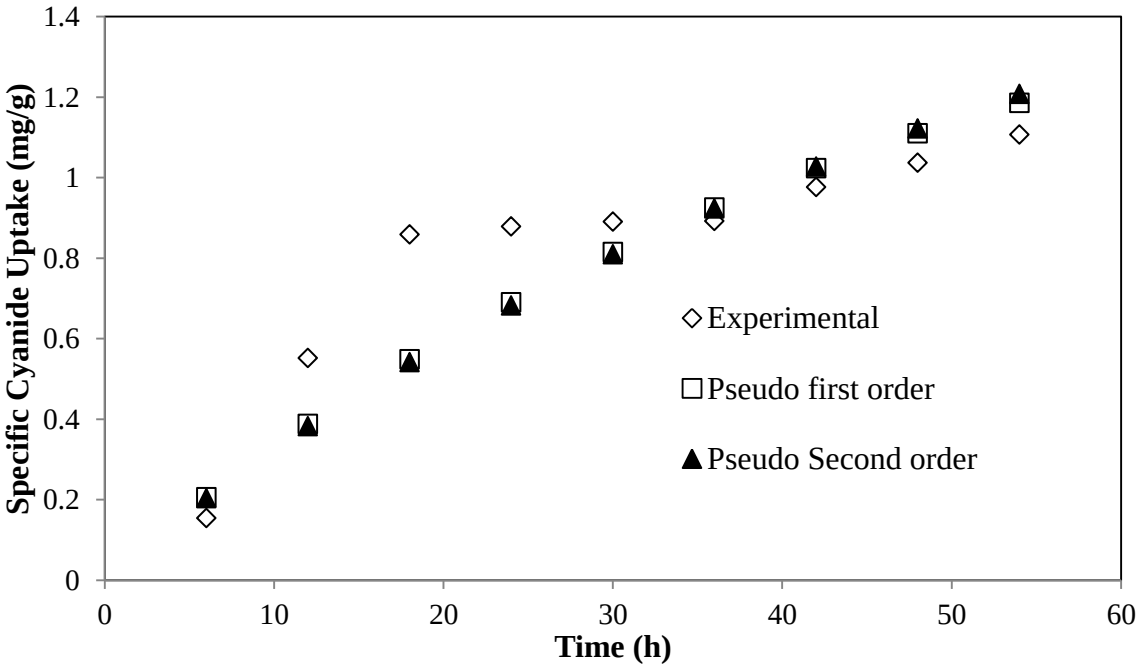

(b)

Figure 6.56: Kinetic modelling of SAB of (a) phenol and (b) cyanide at reaction conditions using Egg Shells (ES)

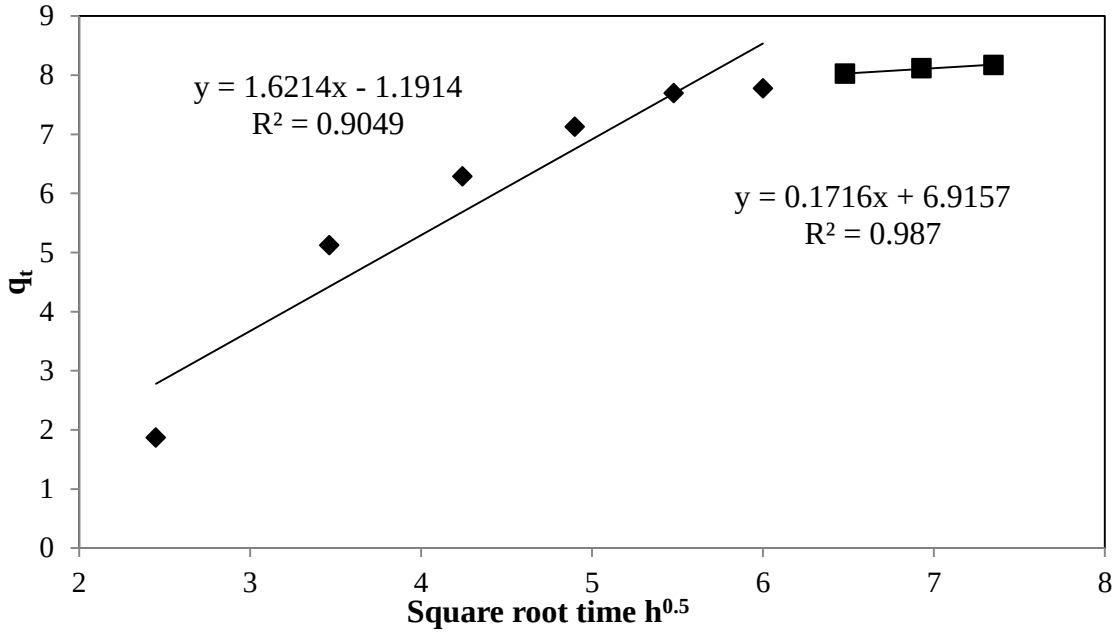

(a)

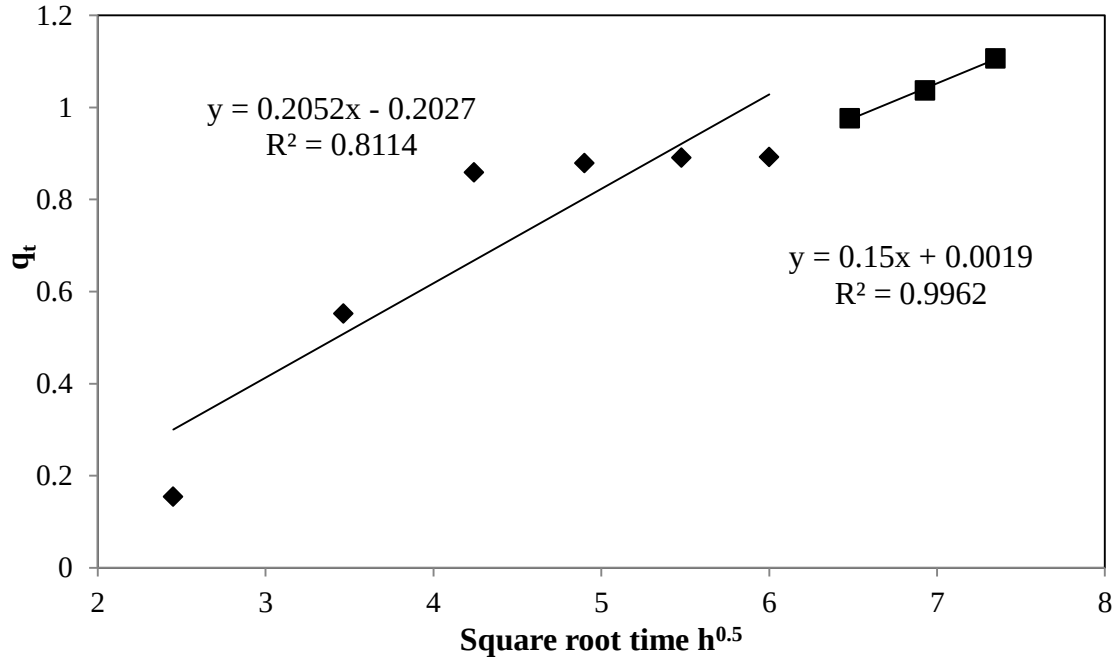

(b)

Figure 6.57: Intraparticle plot of (a) phenol and (b) cyanide SAB using Egg shells (ES)

Both pseudo first order and second order models were best fitted to the SAB process with all the three adsorbents.

6.1.6 THERMODYNAMIC STUDIES:

Thermodynamic parameters estimated for SAB of both phenol and cyanide for all the three biosorbents are shown in table 6.7 and the subsequent plots are shown from figure 6.58 to 6.60.

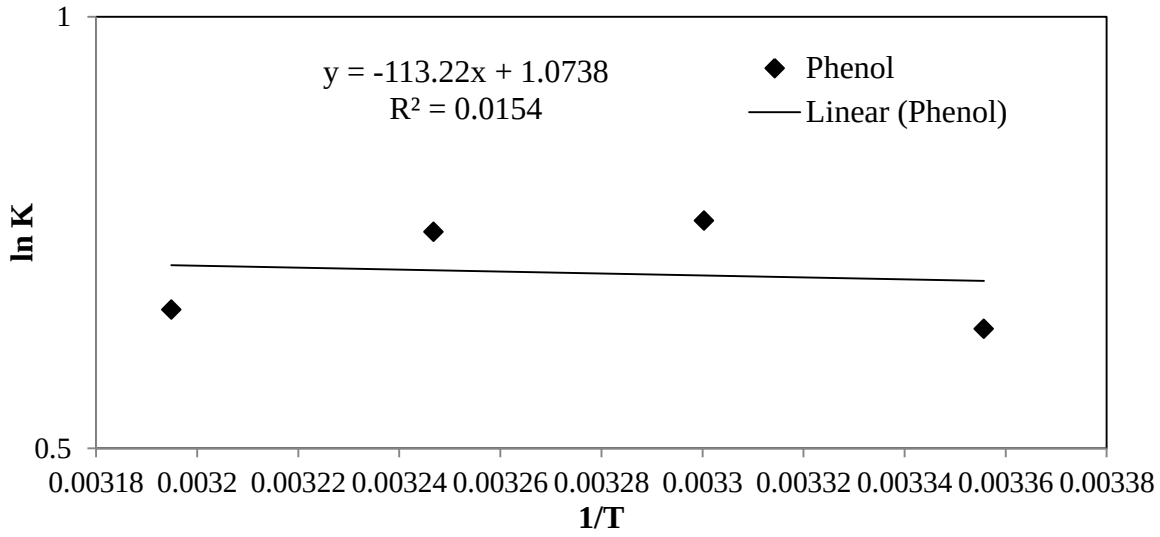

(a)

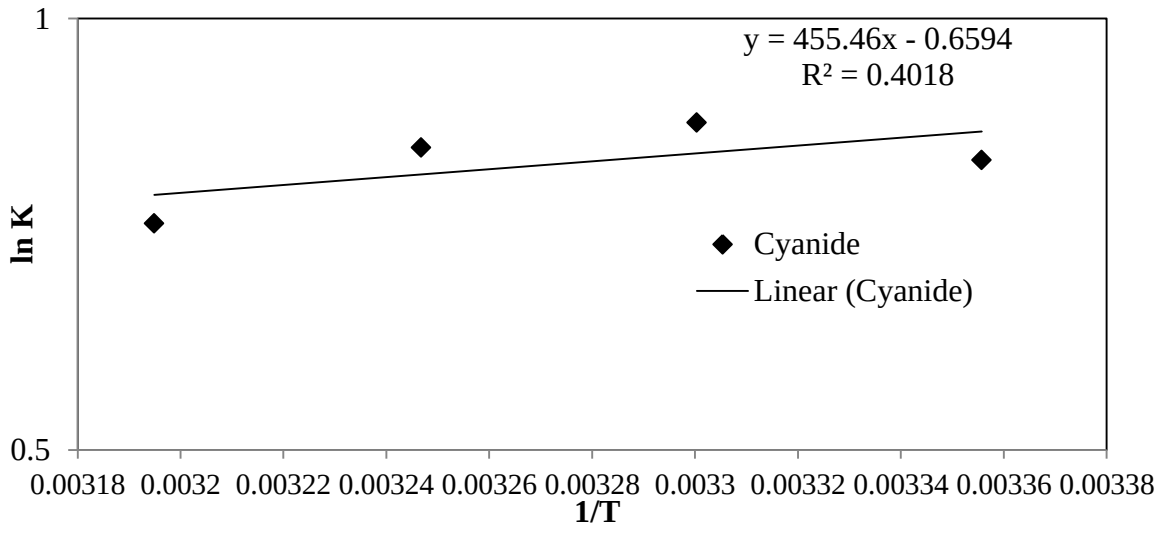

(b)

Figure 6.58: Study of thermodynamic parameters for SAB of (a) phenol and (b) cyanide using Rice Husk

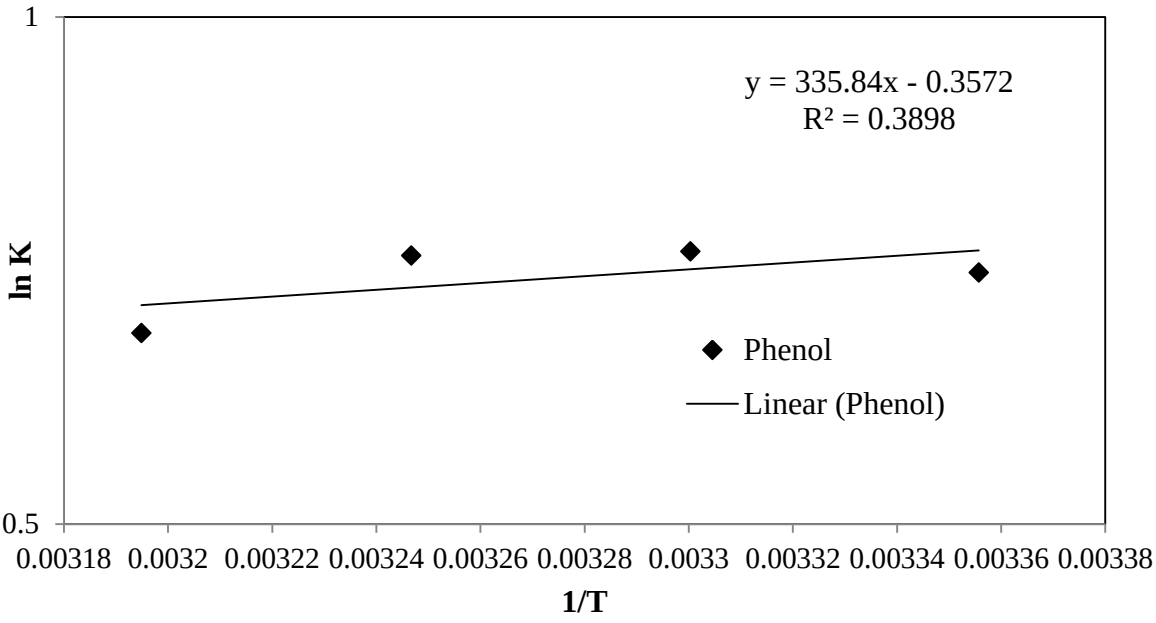

(a)

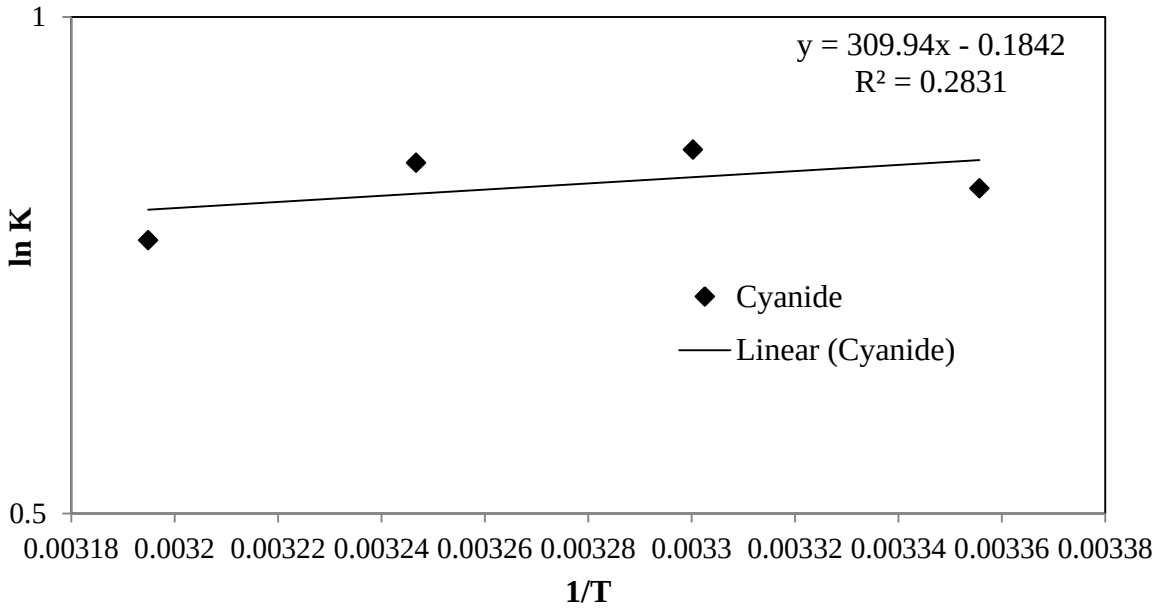

(b)

Figure 6.59: Study of thermodynamic parameters for SAB of (a) phenol and (b) cyanide using Corn Husk Leaves

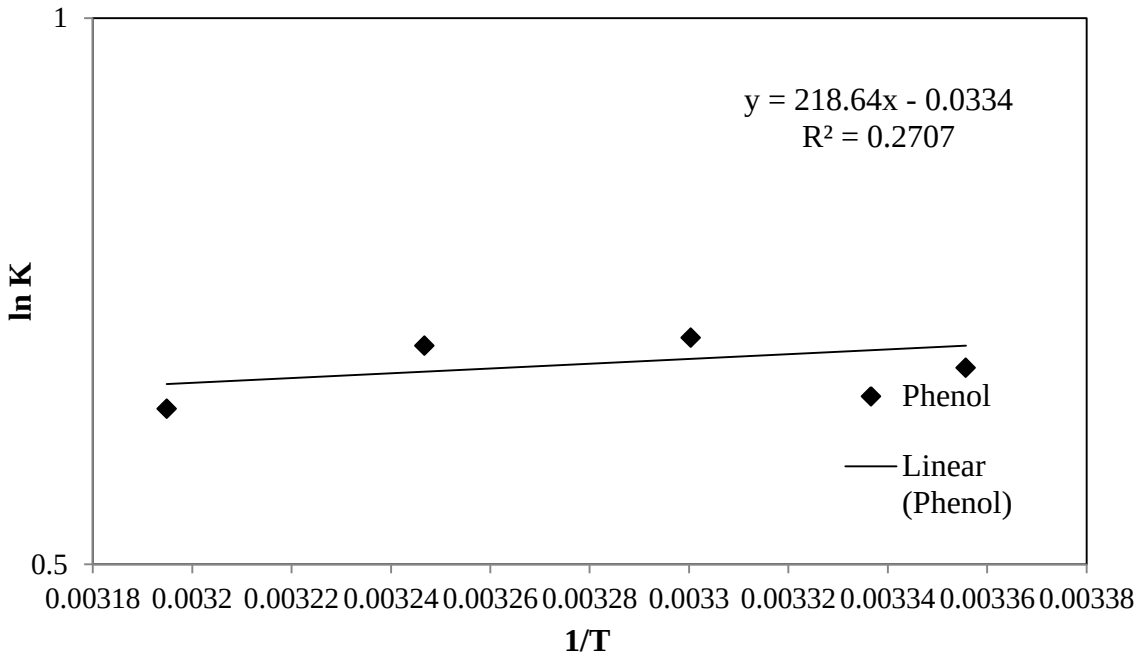

(a)

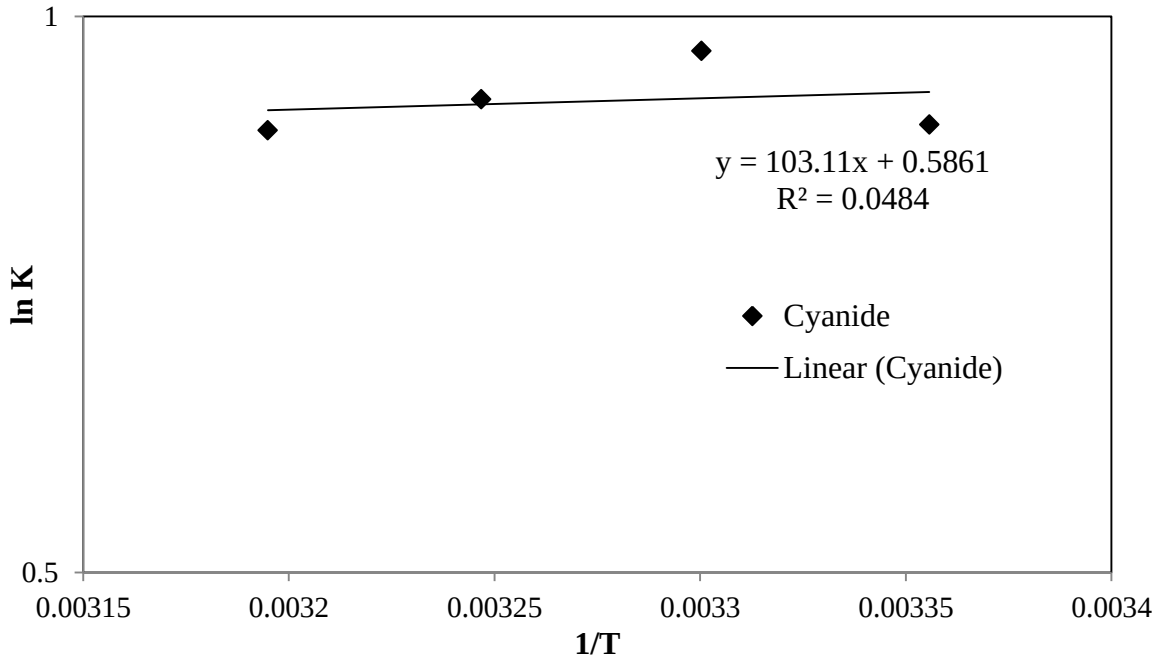

(b)

Figure 6.60: Study of thermodynamic parameters for SAB of (a) phenol and (b) cyanide using Egg Shells

Table 6.21: Summary of thermodynamic parameters for SAB of phenol and cyanide

Temperature	Thermodynamic Parameters					
	Rice Husk					
	Phenol			Cyanide		
	ΔG^0 kJ/mol	ΔH^0 kJ/mol	ΔS^0 J/mol.K	ΔG^0 kJ/mol	ΔH^0 kJ/mol	ΔS^0 J/mol.K
25	-1.580	0.9413	8.927	-2.071	-3.787	-5.482
30	-1.923			-2.215		
35	-1.921			-2.178		
40	-1.718			-1.984		
	Corn Husk Leaves					
	ΔG^0 kJ/mol	ΔH^0 kJ/mol	ΔS^0 J/mol.K	ΔG^0 kJ/mol	ΔH^0 kJ/mol	ΔS^0 J/mol.K
25	-1.853	-2.792	-2.969	-2.050	-2.577	-1.531
30	-1.936			-2.181		
35	-1.958			-2.185		
40	-1.791			-2.017		
	Egg Shells					
	ΔG^0 kJ/mol	ΔH^0 kJ/mol	ΔS^0 J/mol.K	ΔG^0 kJ/mol	ΔH^0 kJ/mol	ΔS^0 J/mol.K
25	-1.685	-1.817	-0.277	-2.237	-0.857	-4.87
30	-1.782			-2.441		
35	-1.792			-2.369		
40	-1.691			-2.336		

The value of ΔG^0 is negative for both phenol and cyanide for all the three adsorbents showing a feasible and spontaneous adsorption process. The value of ΔG^0 does not change much with increase in temperature showing that there is not much change in the adsorption process with increasing temperature. For rice husk in case of phenol the value of ΔH^0 is positive indicating an endothermic process and an increase in randomness at the solid/liquid interface but for cyanide the value of ΔH^0 is negative indicating an exothermic process and decrease in randomness at the solid/liquid interface. For corn husk leaves and egg shells SAB

of both phenol and cyanide is an exothermic process with a decrease of randomness at the solid/liquid interface.

6.2 CONTINUOUS STUDIES FOR SIMULTANEOUS ADSORPTION AND BIODEGRADATION OF PHENOL AND CYANIDE:

6.2.1 WORKING VOLUME OF REACTOR:

The working volume as calculated by the procedure discussed in the previous chapter was 2900 mL for the RTD studies. The working volume of GAC and rice husk packed column was estimated as 2800 mL and 2500 mL respectively.

6.2.2 RESIDENCE TIME DISTRIBUTION (RTD) STUDIES OF THE REACTOR:

The flow pattern of the reactor which is an important aspect in optimizing SAB of phenol and cyanide was estimated by estimating RTD studies on the reactor. Water was run in the packed bed reactor with glass beads packing. NaOH was used as a tracer to conduct RTD studies in the reactor. The concentration of tracer was measured at a specific time interval and further studies were conducted. RTD studies were conducted for four different case studies. The RTD data for different case studies were fitted for axial dispersion model. The different case studies and their results are discussed in the table 6.8 given below.

Table 6.22: Experimental data for the RTD studies

					Axial Dispersion Model				
S. No.	Pump rpm	Tracer input	Agitation	Flow rate mL/min	Mean Residence Time ($\boldsymbol{\tau}$), Min	Mean of C-Curve (t_m), min	σ_θ^2	D/uL	Difference (t_m-$\boldsymbol{\tau}$), min
1	25	Random	No	176	17	23	3.343	1.671	6
2	25	Pulse	No	176	17	53	0.131	0.066	36
3	25	Pulse	Yes	128	23	100	0.15	0.07	77

4	50	Pulse	No	260	11	18	4 0.23 9	7 0.11 9	7

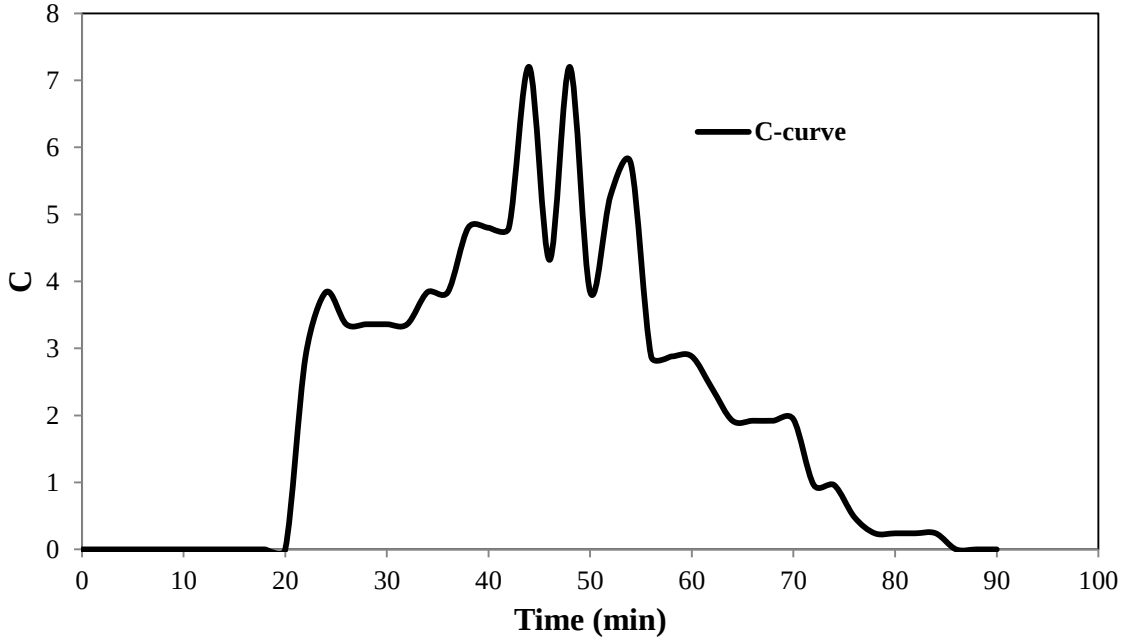

Figure 6.61: C-Curve for Random tracer input at 25 rpm

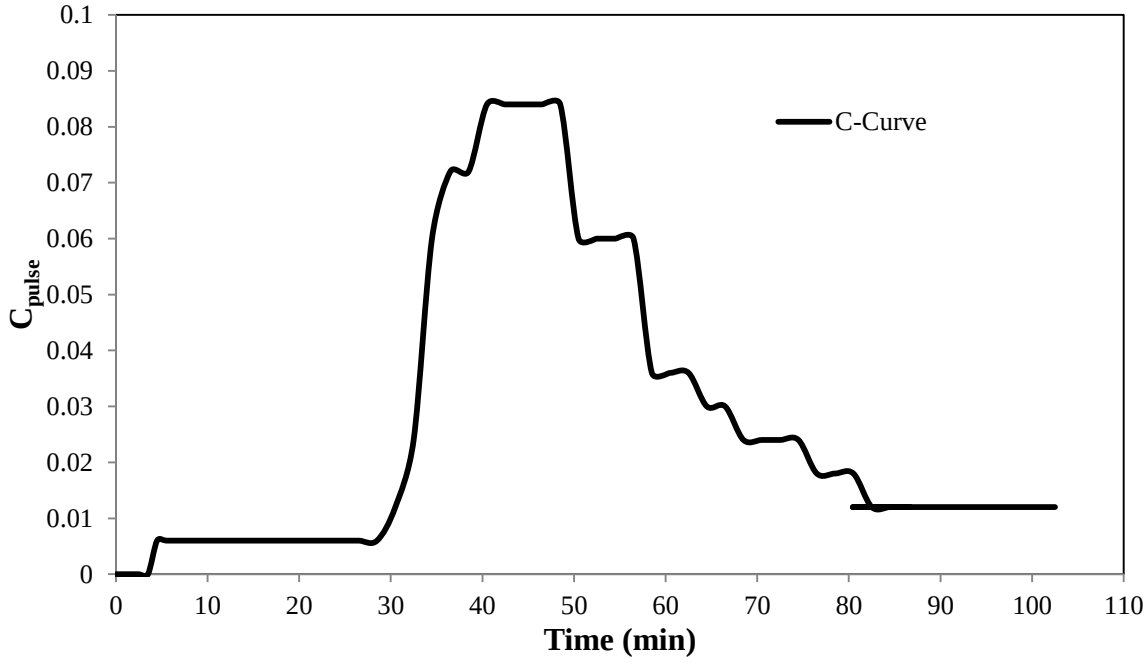

Figure 6.62: C-Curve for Pulse tracer input at 25 rpm

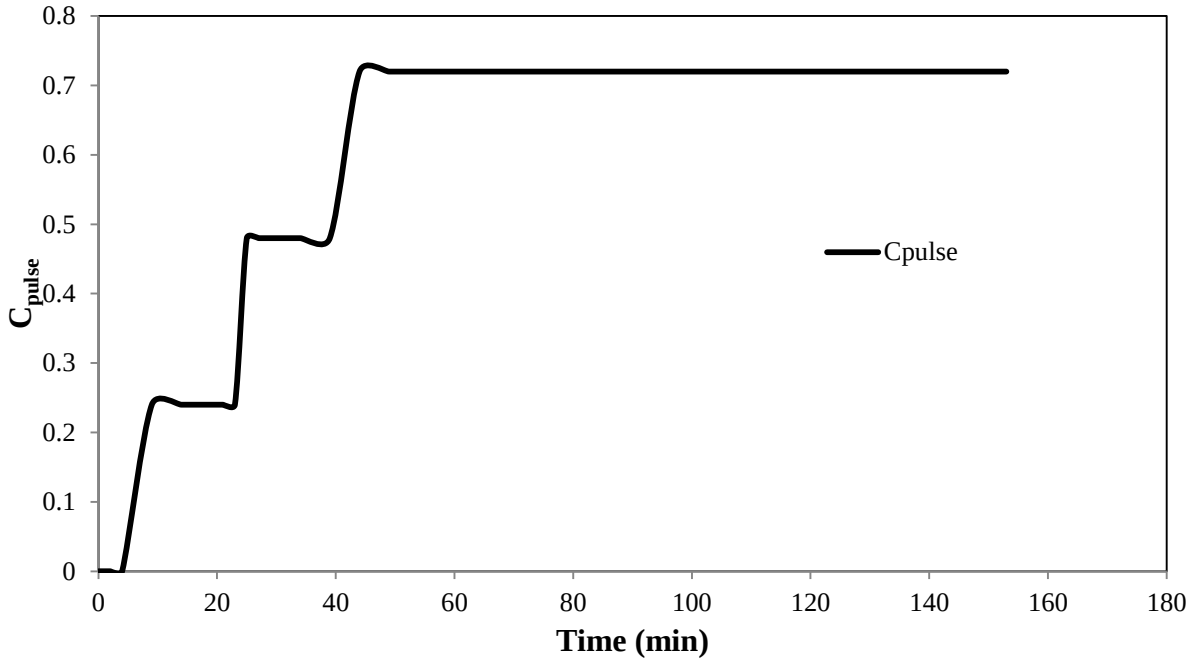

Figure 6.63: C-Curve for Pulse tracer input at 25 rpm with an agitation produced in the inlet tank

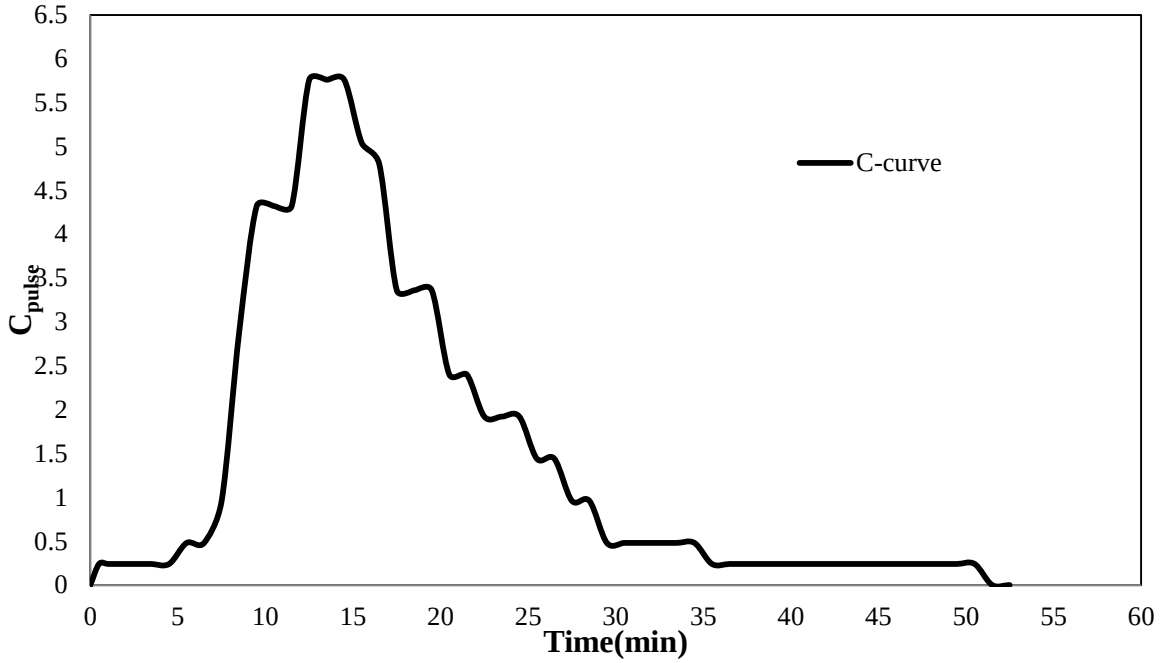

Figure 6.64: C-Curve for Pulse tracer input at 50 rpm

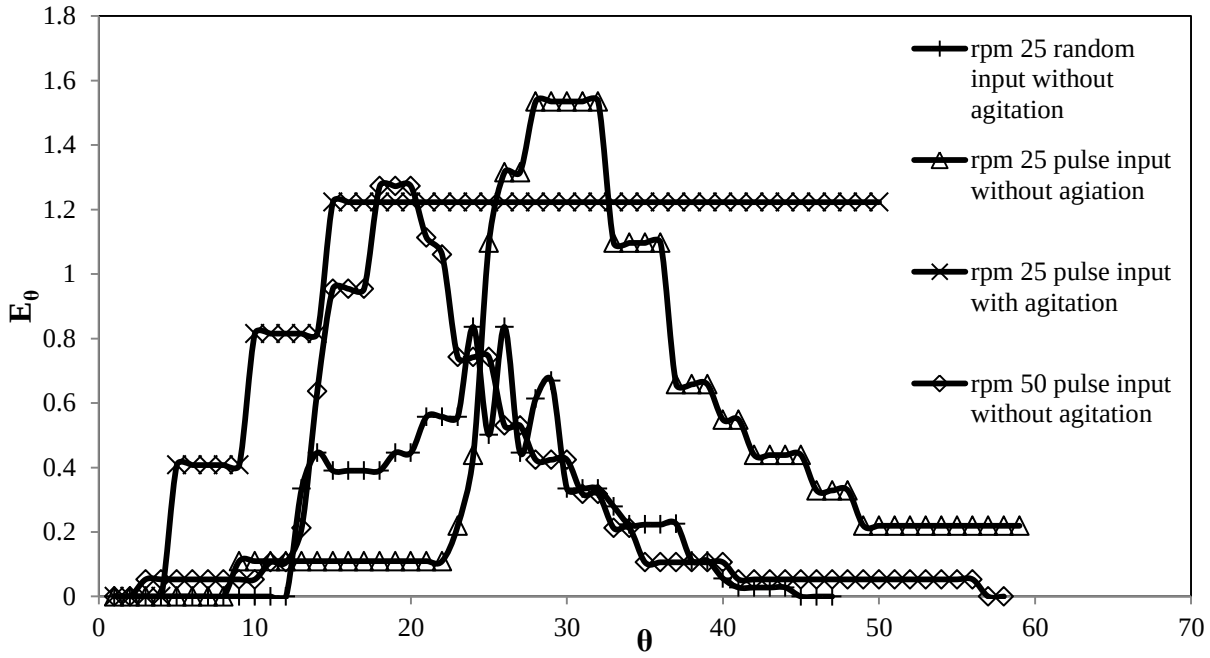

Figure 6.65: E_θ Curve for different conditions

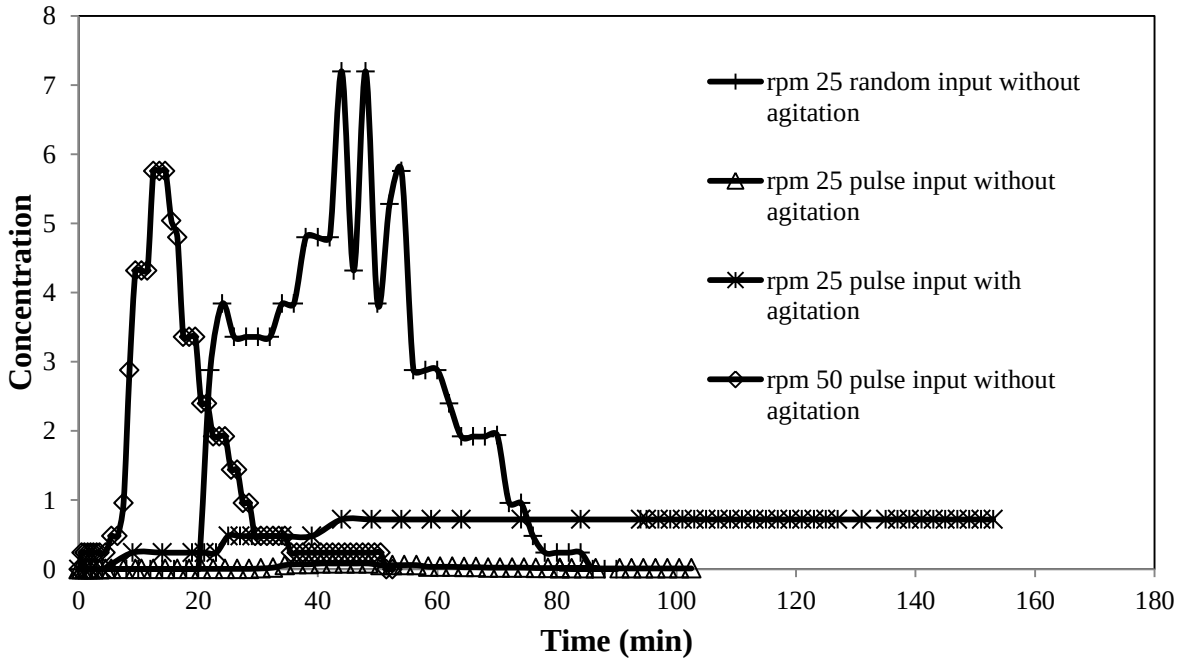

Figure 6.66: C-Curve for different conditions

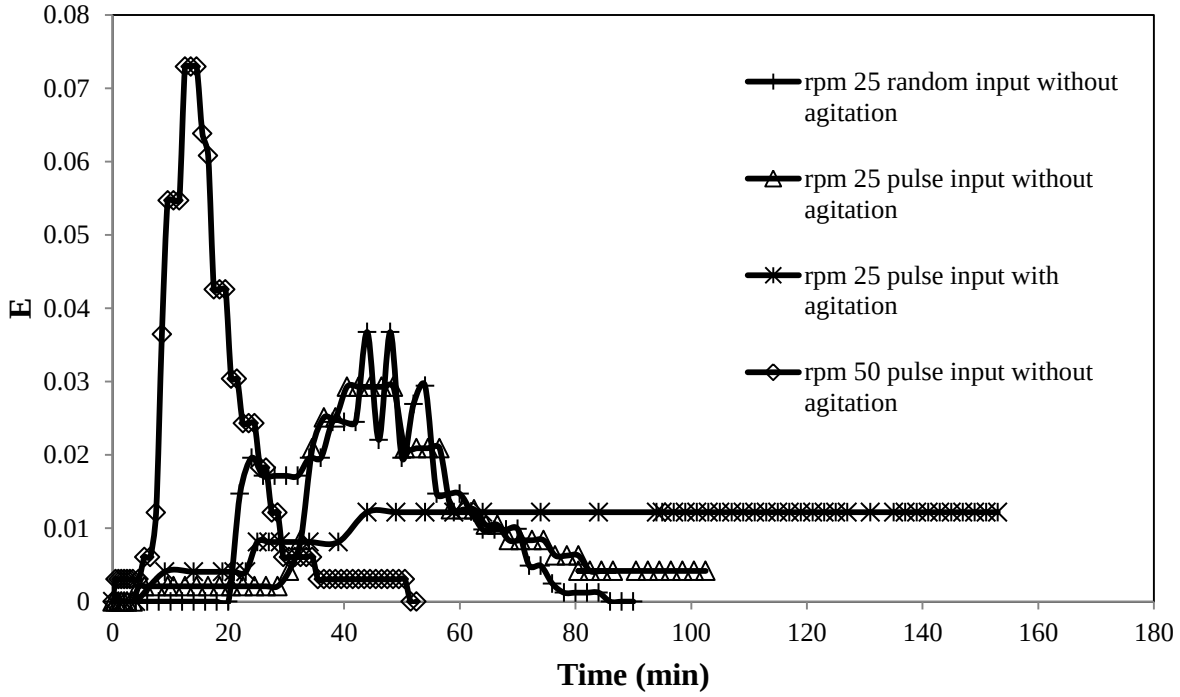

Figure 6.67: E curve for different conditions

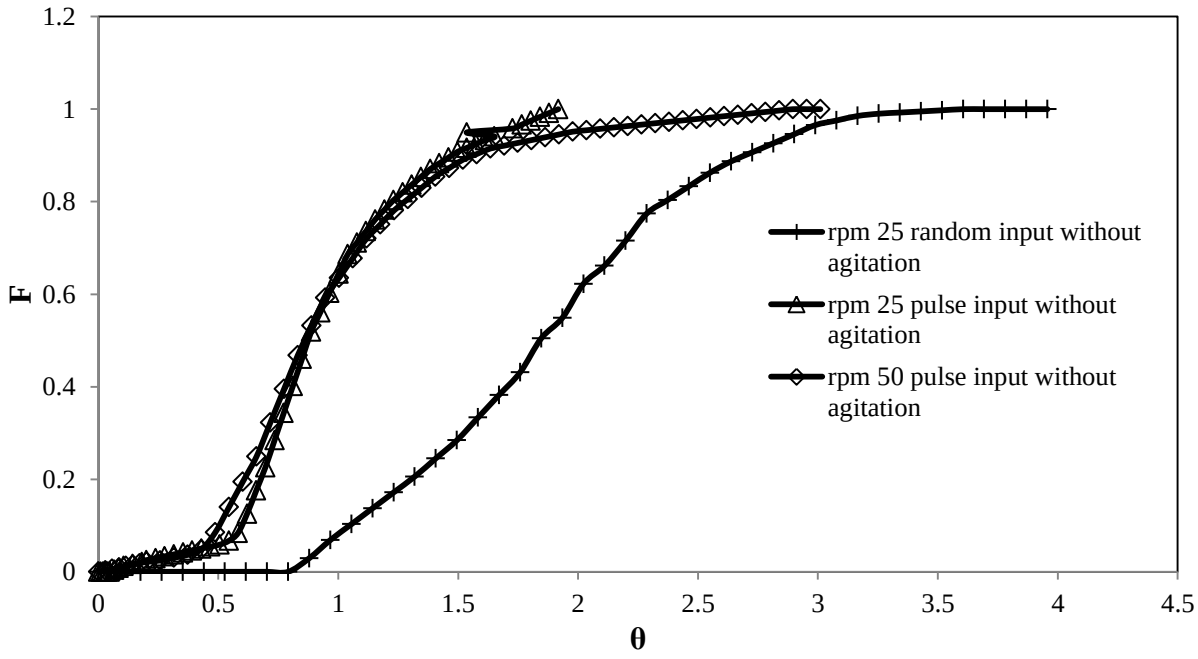

Figure 6.68: F-Curve for different cases

Figure 6.61 to figure 6.68 follows the plots for Concentration curve (C-Curve), Exit age distribution curve (E-Curve), E_θ- Curve and Cumulative distribution curve (F-Curve) for the tracer at different pump rpm and for different input method. From the data of table 6.8 and the following plots it is clearly seen that the maximum variance of 3.343 and dispersion

number of 1.671 appears for random tracer input which clearly shows the presence of huge dispersions inside the reactor. But the maximum difference in the mean of C-Curve and the mean residence time or the theoretical and experimental mean residence time is maximum for the case in which agitation is introduced in the inlet feed tank which also shows the presence of axial dispersion as well as presence of dead and stagnant zones. For rest of the cases there is a presence of moderate dispersion in the reactor. The study of axial dispersion model for all the four case studies reveal that the flow behaviour of the packed bed reactor is more inclined to plug flow. The studies also reveals that for low flow rates or low flow rates the behaviour of the more inclined towards plug flow but there can be presence of stagnant or dead zones in the reactor whereas for a high flow rate the dispersion number can be high but there are less chances for the formation of stagnant and dead zones.

6.2.3 SELECTION OF ADSORBENT:

Batch studies were conducted on three adsorbents namely rice husk, corn husk leaves and egg shells. The optimized parameters and the adsorbent dose of 40 g/L taken from literature (Agarwal et.al.) were taken for performing the batch experiment for granular activated carbon. This experiment was taken as control for the continuous studies of simultaneous adsorption and biodegradation of phenol and cyanide in their synthetic simulated binary solution.

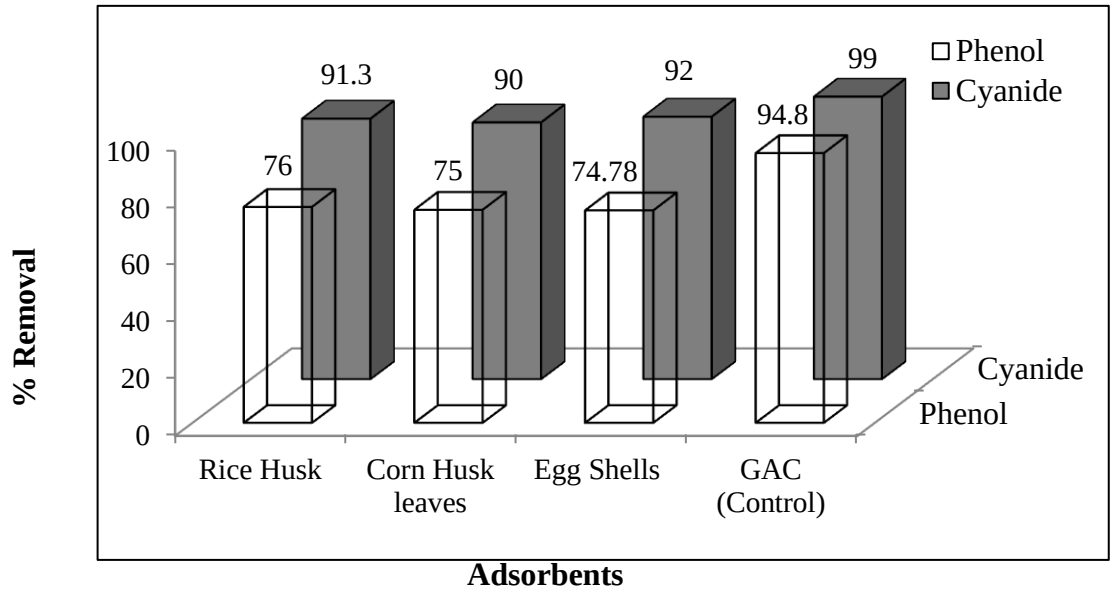

Figure 6.69: Comparative plot of percentage removal of Phenol and Cyanide using Rice Husk, Corn Husk Leaves, Egg Shells, Granular Activated Carbon

From the results of batch studies as shown in figure 6.69 it can be seen that amongst all the biosorbents used rice husk showed the maximum removal of 76 % for phenol and 91.3 % for cyanide. Thus the continuous studies were performed taking Granular activated carbon (GAC) and Rice Husk as adsorbents or packing materials for the packed bed continuous reactor.

6.2.4 Continuous Studies for Simultaneous Adsorption and Biodegradation of Phenol and Cyanide using Granular Activated Carbon:

The experiments for the continuous removal of phenol and cyanide by SAB process was studied for granular activated carbon for two different EBCTs of 5 h and 2.5 h. At an EBCT of 5 h the flow rate as measured by using a stop watch and a measuring cylinder was 9.828 mL/min and that for EBCT 2.5 h was to be 19.656 mL/min. The results for SAB studies of both phenol and cyanide are shown in the figures and table that follow.

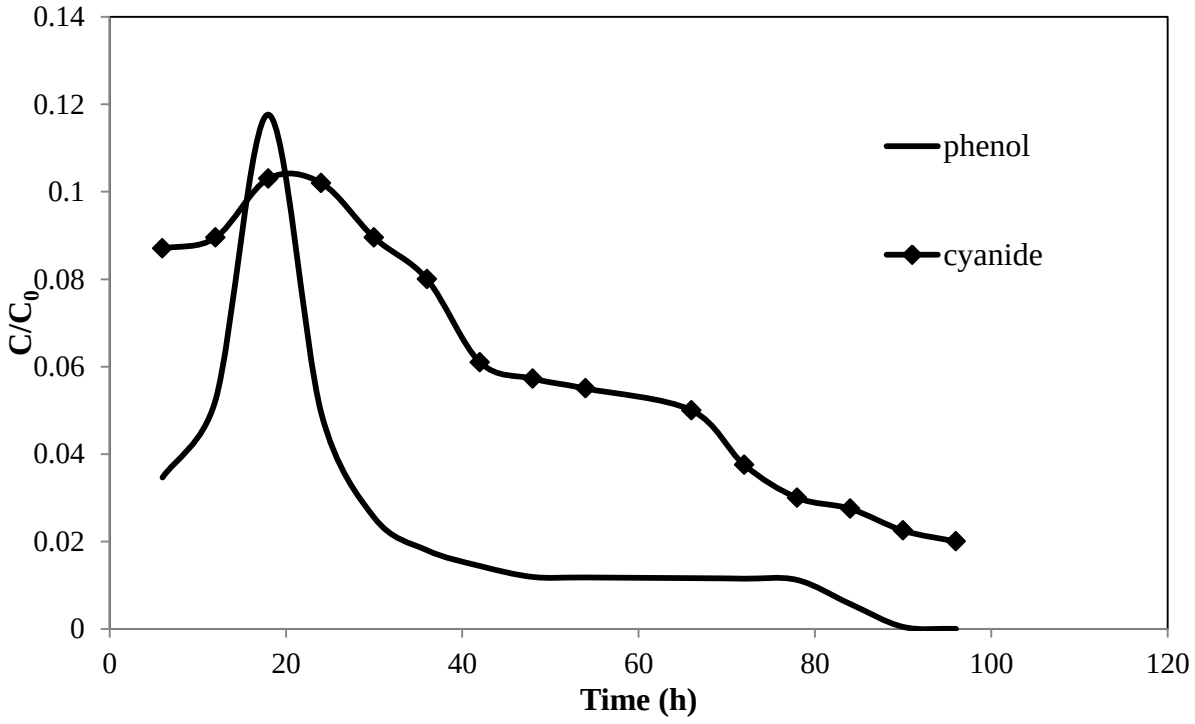

Figure 6.70: Normalised concentration curve for SAB of phenol and cyanide using a column reactor with granular activated carbon packing at an initial phenol concentration : 400 mg/L, initial cyanide concentration : 40 mg/L, EBCT : 5 h, pH=7

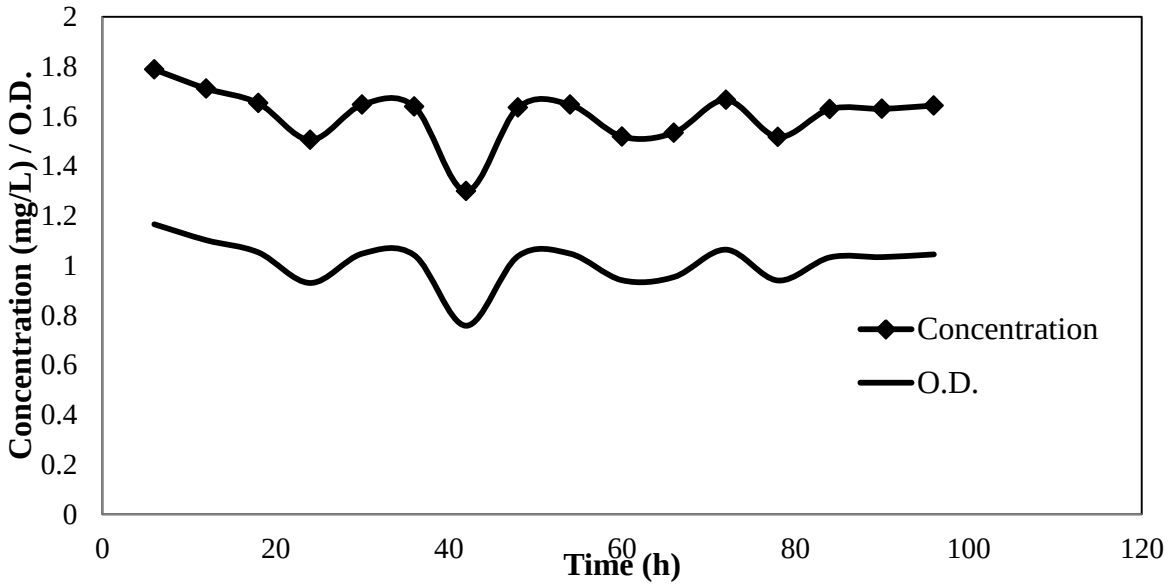

Figure 6.71: Biomass Concentration (mg/L) and Optical Density plot for a GAC packed column at an initial phenol concentration: 400 mg/L, initial cyanide concentration: 40 mg/L, EBCT: 5h, pH=7

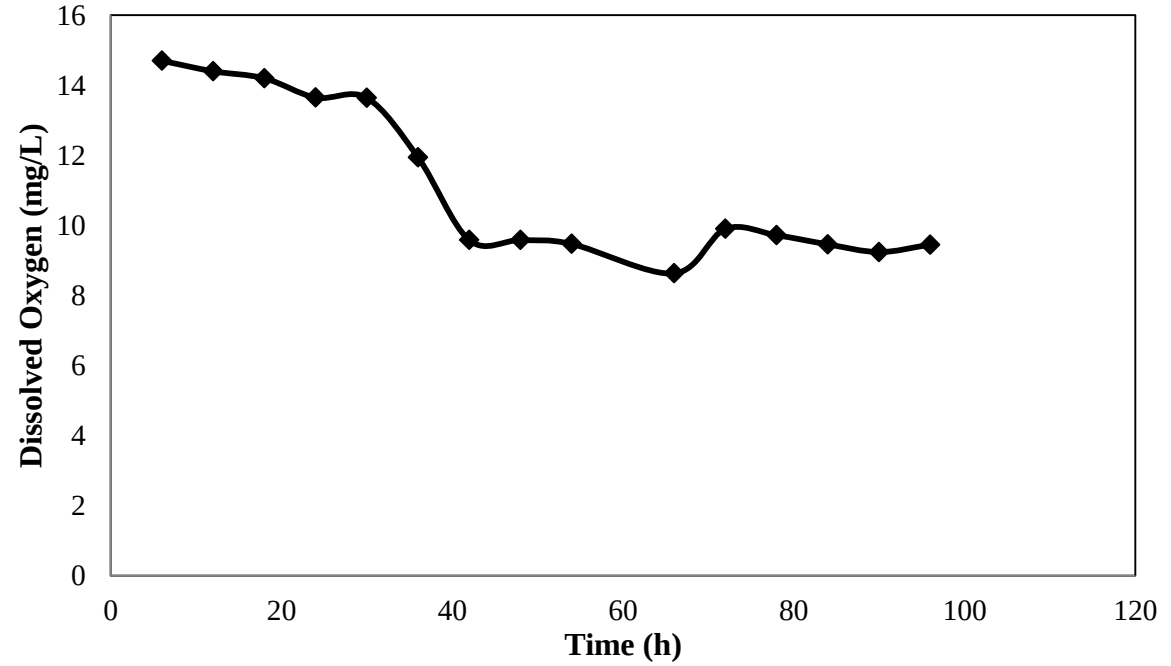

Figure 6.72: Dissolved Oxygen (mg/L) variation for a GAC packed column at an initial phenol concentration: 400 mg/L, initial cyanide concentration: 40 mg/L, EBCT: 5h, pH=7 for SAB of phenol and cyanide for 96 h

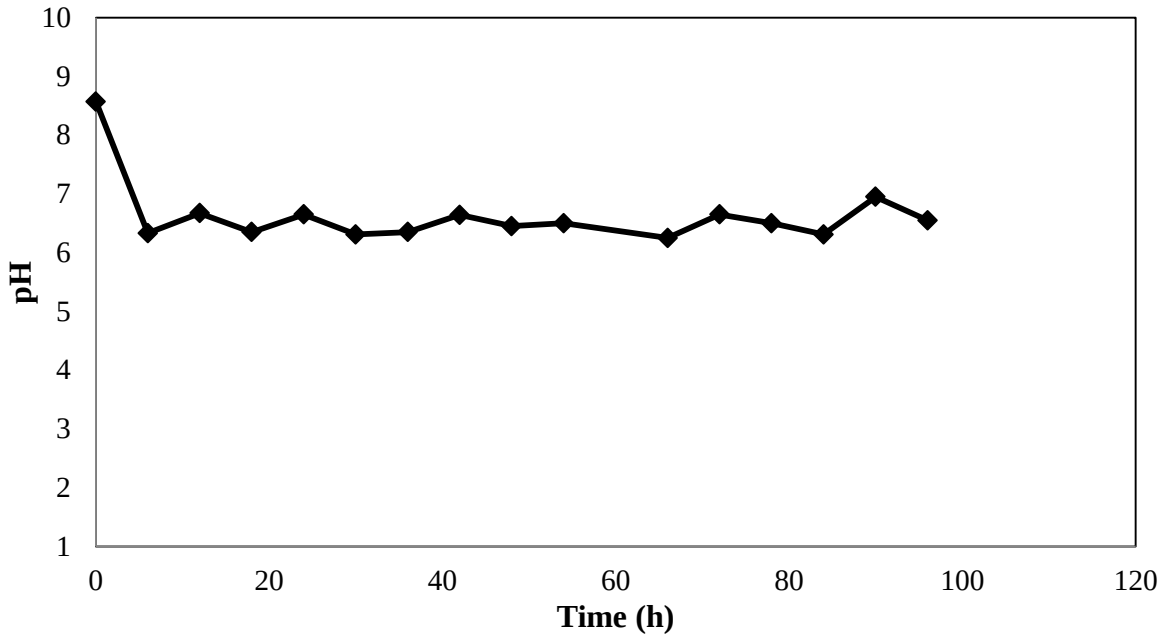

Figure 6.73: Variation of pH for a GAC packed column at an initial phenol concentration: 400 mg/L, initial cyanide concentration: 40 mg/L, EBCT: 5h, pH=7 for SAB of phenol and cyanide for 96 h

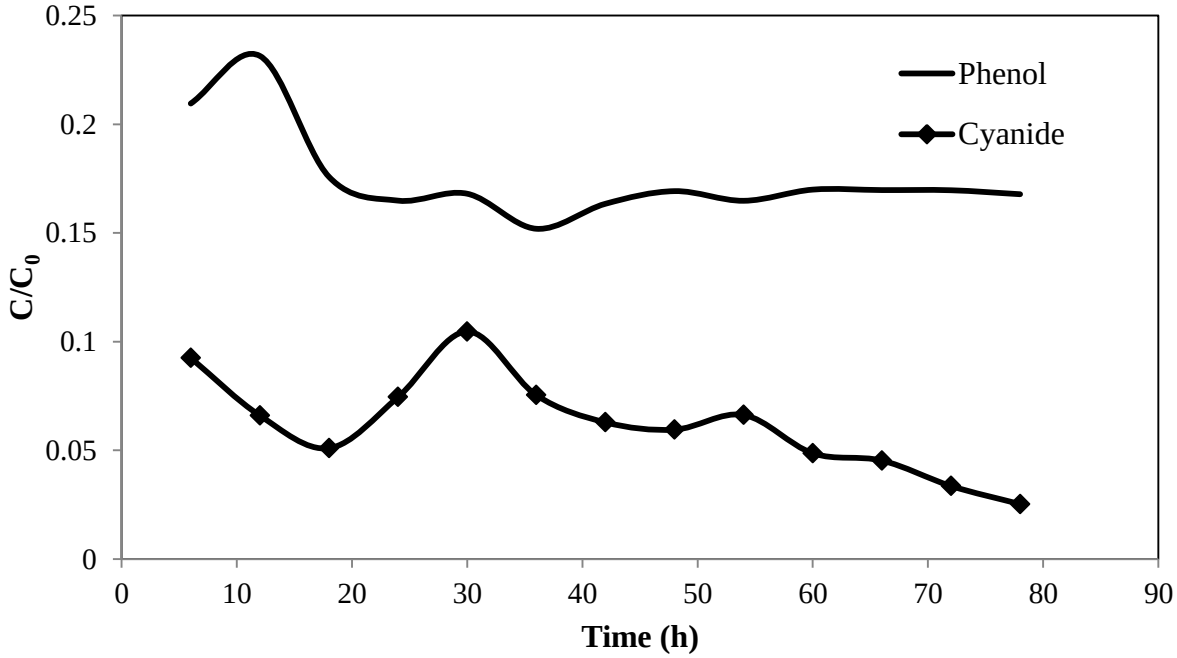

Figure 6.74: Normalised concentration curve for SAB of phenol and cyanide using a column reactor with granular activated carbon packing at an initial phenol concentration : 400 mg/L, initial cyanide concentration : 40 mg/L, EBCT : 2.5 h, pH=7

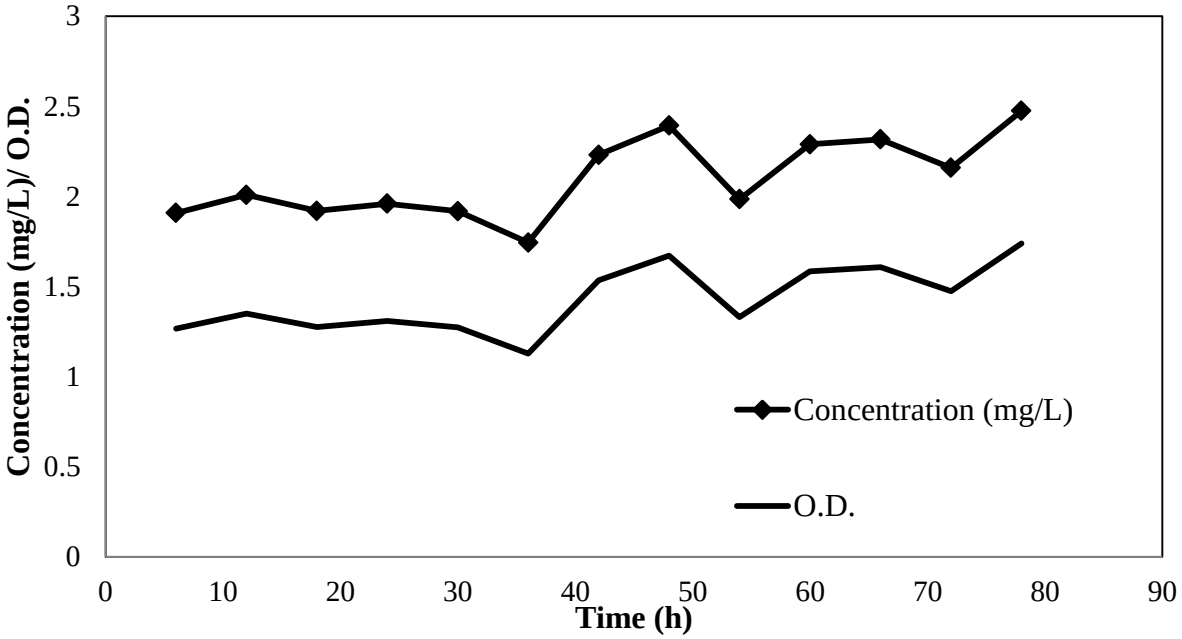

Figure 6.75: Biomass Concentration (mg/L) and Optical Density plot for SAB of phenol and cyanide using a column reactor with granular activated carbon packing at an initial phenol concentration : 400 mg/L, initial cyanide concentration : 40 mg/L, EBCT : 2.5 h, pH=7

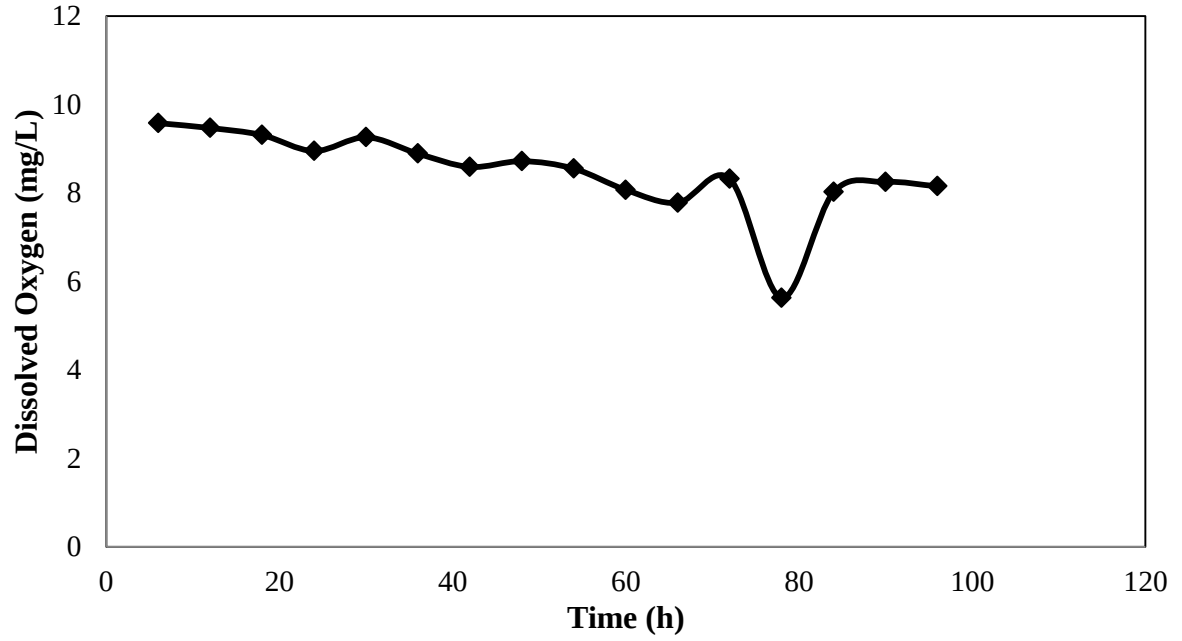

Figure 6.76: Dissolved Oxygen (mg/L) variation for SAB of phenol and cyanide using a column reactor with granular activated carbon packing at an initial phenol concentration : 400 mg/L, initial cyanide concentration : 40 mg/L, EBCT : 2.5 h, pH: 7 for 96 h

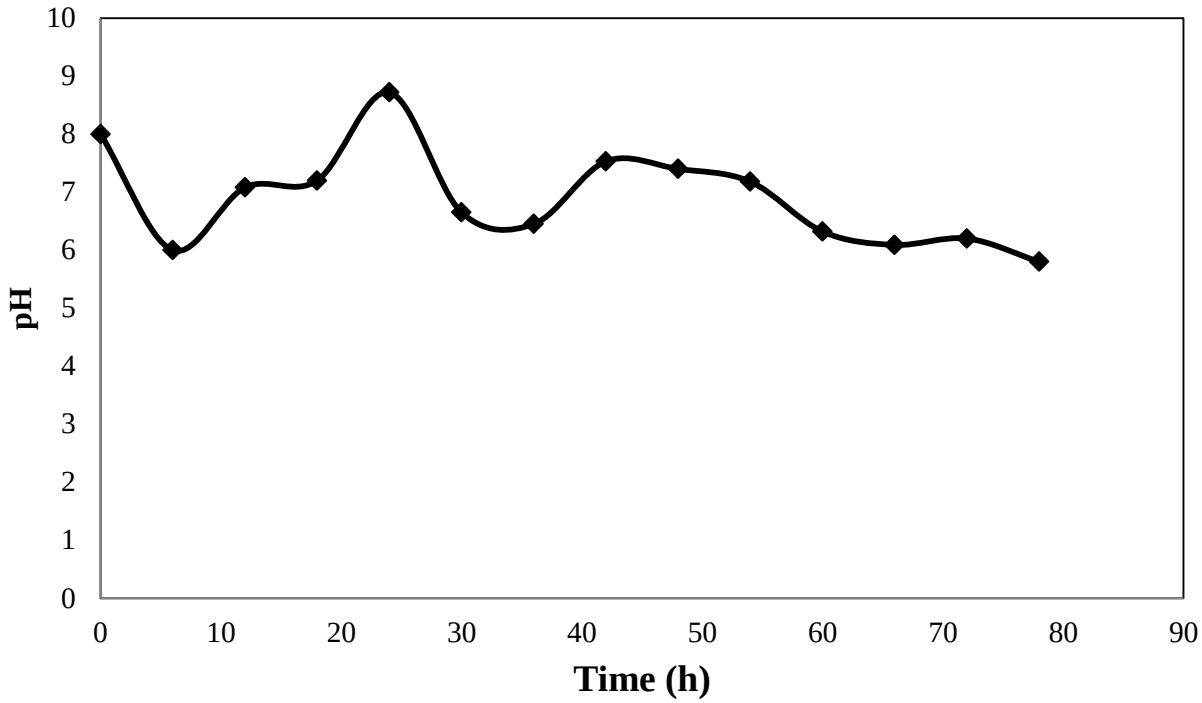

Figure 6.77: pH variation for SAB of phenol and cyanide using a GAC packed column reactor at an initial phenol concentration: 400 mg/L, initial cyanide concentration: 40 mg/L, EBCT: 2.5 h, pH: 7 for 96 h

Table 6.23: Percentage removal of phenol and cyanide in a GAC packed column by simultaneous adsorption and biodegradation

SAB Studies for Removal of phenol and cyanide in a continuous packed bed tubular reactor						
EBCT (h)	**RPM of the Peristaltic pump**	**Flow Rate (mL/min)**	**Initial Concentration (mg/L)**		**% Removal**	
			Phenol	**Cyanide**	**Phenol**	**Cyanide**
5	7.28	9.828	400	40	99.99	98.85
2.5	3.64	19.656	400	40	82.48	93.80

The figures 6.70 and 6.74 are the plots of normalised concentration versus time for both phenol and cyanide at an EBCT of 5 h and 2.5 h respectively. Table 6.9 shows the data for the SAB studies in a continuous reactor. From the data shown in table 6.9 it can be clearly seen that the percentage removal increases with decreasing flow rate or simply it can be said that with increase in the peristaltic pump rpm the percentage removal of phenol and cyanide

decreases. This behaviour can be attributed to the fact that with a low EBCT the contact time of the pollutant with the adsorbent bed decreases which in turn decreases the percentage removal of the pollutant from the waste water. Therefore amongst both the EBCTs selected for the continuous studies of phenol and cyanide removal by the process of SAB, EBCT of 5 h turns out to be the optimum EBCT. The pH of the process remained between 6 and 7 in the entire time duration for both the EBCTs which are in accordance to the optimum pH estimated from the batch studies. The biomass concentration in the process ranged between 1.52 mg/L to 1.8 mg/L for the EBCT 5 h and that for EBCT 2.5 h it ranged between 1.908 mg/L to 2.2 mg/L. The dissolved oxygen also decreased from 14 mg/L to 8 mg/L and then remained constant at 8 mg/L due to the utilisation of oxygen by the anaerobic facultative bacteria.

For an EBCT of 5 h GAC shows a phenol and cyanide removal of 99.9 and 98.85 % respectively which meets the MCL of phenol and is almost close to the MCL of cyanide as 0.5 mg/L and 0.2 mg/L for phenol and cyanide respectively.

6.2.5 Breakthrough Curve for Simultaneous Adsorption and Biodegradation of Phenol and Cyanide using Granular Activated Carbon:

The granular activated carbon bed which was simultaneously regenerated due to the simultaneous biodegradation of the adsorbed phenol and cyanide was freed of the bacteria by starving them to death for 4-5 days and then washing it twice or thrice to remove the biomass left in the reactor, was used for plotting the breakthrough curve for the co-adsorption of phenol and cyanide on the regenerated bed. The breakthrough curve i.e. the plot between normalised concentration (C/C_0) and time as obtained for co-adsorption of phenol and cyanide by granular activated carbon is shown in figure 6.76 and figure 6.77.

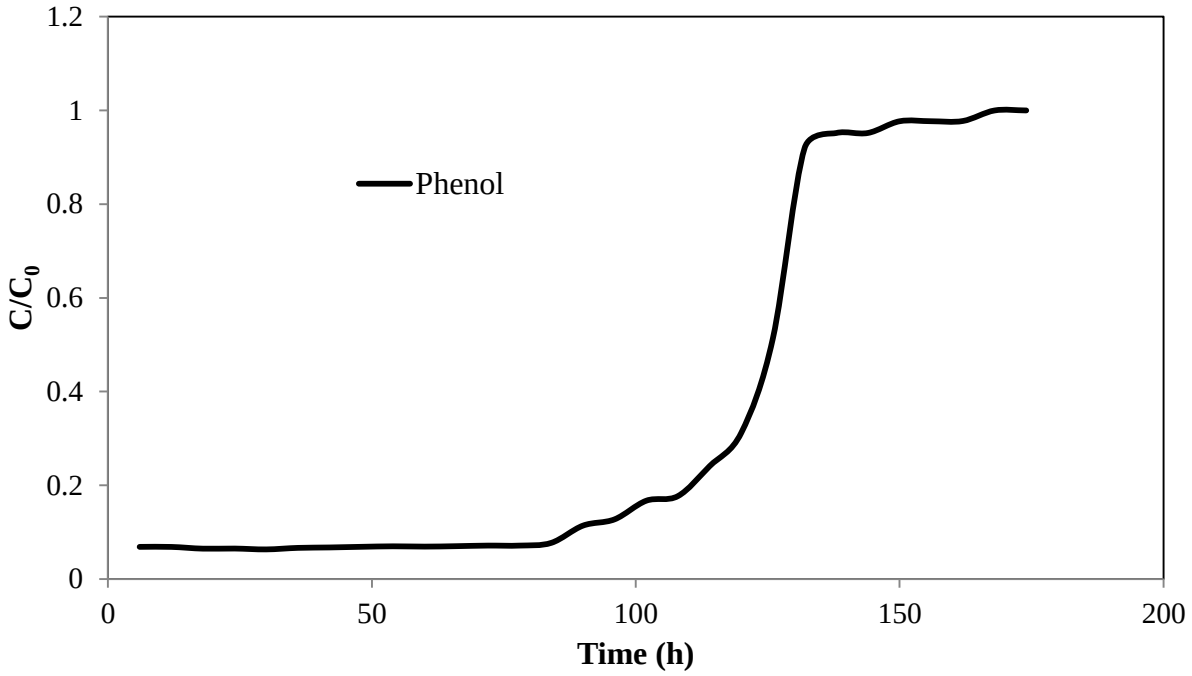

Figure 6.78: Breakthrough Curve of phenol removal using regenerated GAC column at an EBCT of 5 h

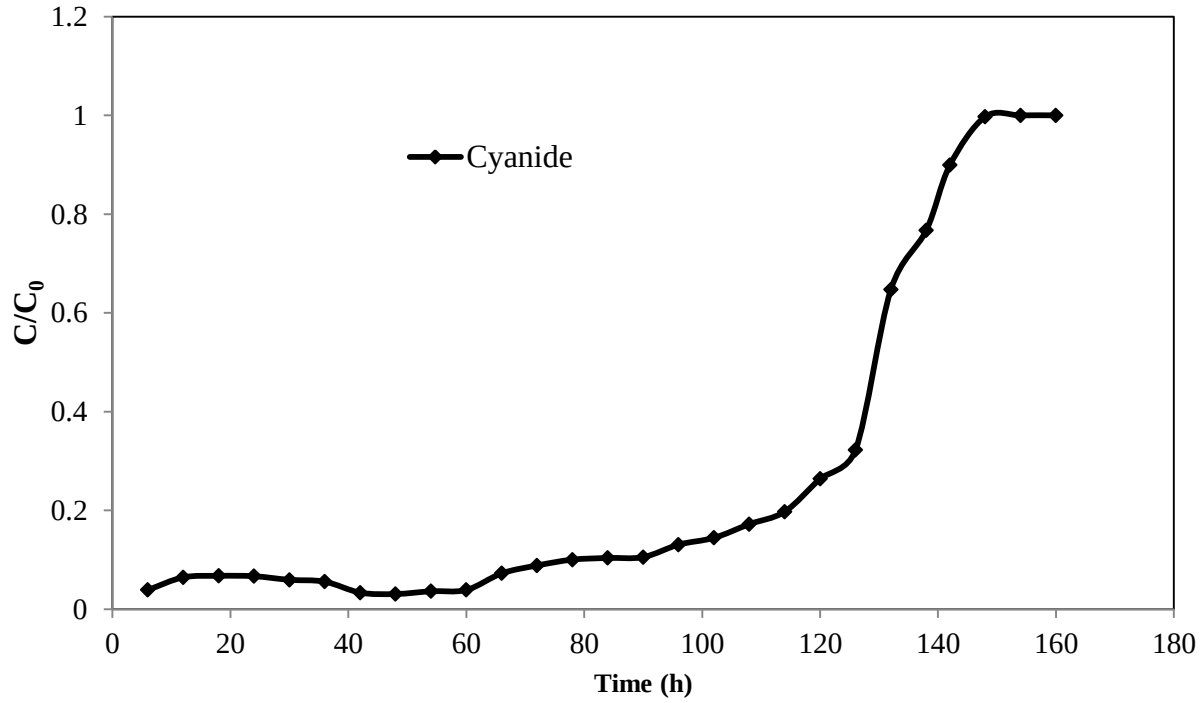

Figure 6.79: Breakthrough Curve of cyanide removal using regenerated GAC column at an EBCT of 5 h

The total flow time i.e. the time of complete bed exhaustion for phenol was 174 h and that for cyanide was 160 h. The percentage removal for both phenol and cyanide were calculated as 64.24 and 73.12 % respectively. Maximum column capacity for phenol and cyanide is 21.97 mg/g and 2.29 mg/g respectively. The data of normalised concentration versus time was fitted to the kinetic models of Adams Bohart, Wolborska, Thomas and Yoon and Nelson model to understand the dynamic response of the packed bed reactor. The data for all the models is given below in table 6.10.

Table 6.10: Parameters predicted from various kinetic model for the multicomponent adsorption of phenol and cyanide using GAC column

	Adams Bohart Model						
	C_0 (mg/L)	**Q (mL/min)**	**$k_{AB} \times 10^{-5}$ (L/min mg)**	**N_0 (mg/L)**	**R^2**	**ε^2**	**χ^2**
Phenol	400	9.828	.1675	6891.12	0.9646	39.82	0.00406
Cyanide	40	9.828	1.279	769.57	0.977	32.85	0.01289
	Wolborska Model						
	C_0 (mg/L)	**Q (mL/min)**	**β_a (min^{-1})**	**N_0 (mg/L)**	**R^2**	**ε^2**	**χ^2**
Phenol	400	9.828	0.0115	6891.12	0.9646	39.82	0.00406
Cyanide	40	9.828	0.0098	769.57	0.977	32.85	0.01289
	Thomas Model						
	C_0 (mg/L)	**Q (mL/min)**	**$k_{Th} \times 10^{-5}$ (L/min mg)**	**q_0 (mg/g)**	**R^2**	**ε^2**	**χ^2**
Phenol	400	9.828	0.219	260	0.9314	42.56	0.0337
Cyanide	40	9.828	1.625	2.88	0.968	41.58	0.0663
	Yoon and Nelson Model						
	C_0 (mg/L)	**Q (mL/min)**	**$k_{YN} \times 10^{-4}$ (min^{-1})**	**τ (h)**	**R^2**	**ε^2**	**χ^2**

Phenol	400	9.828	8.75	132	0.9314	49.58	0.00226
Cyanide	40	9.828	6.5	146.84	0.968	41.58	0.0167

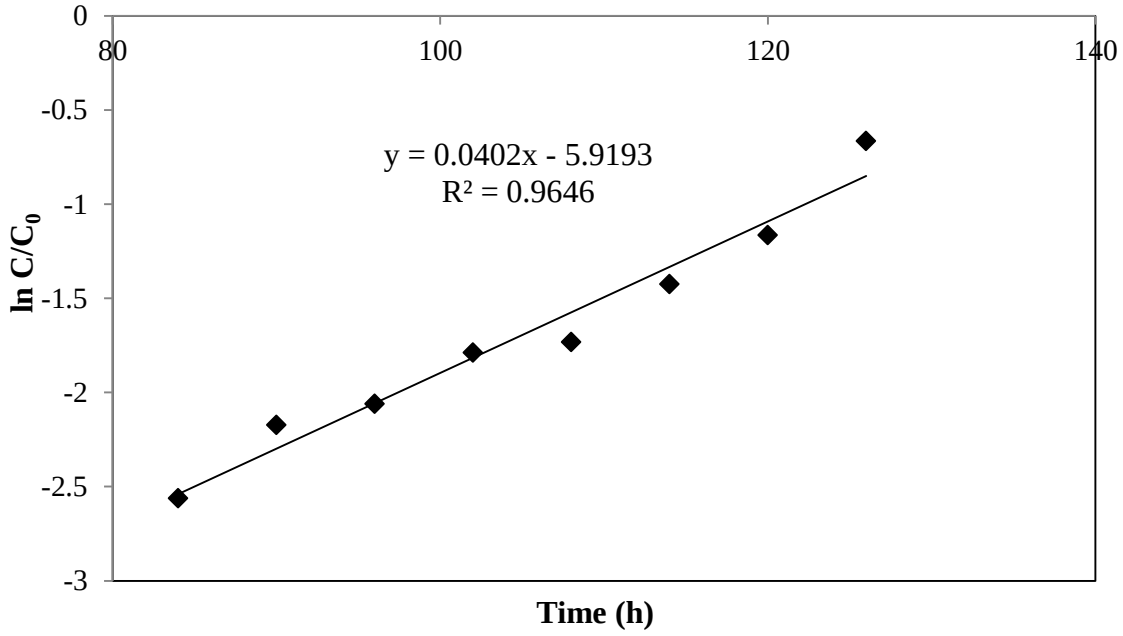

(a)

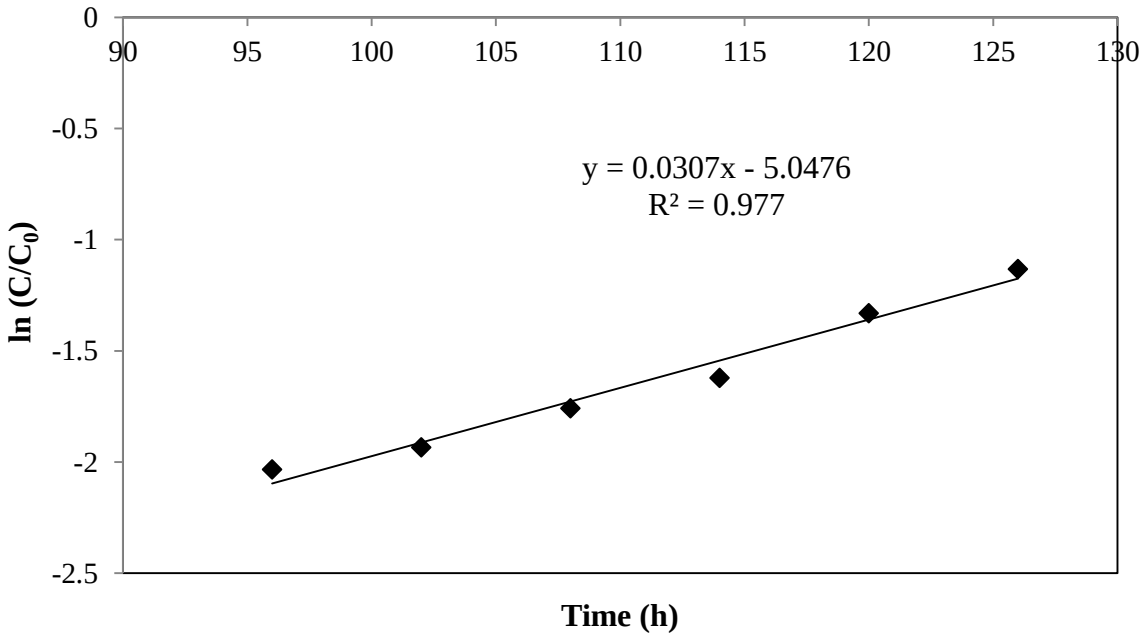

(b)

Figure 6.80 Plots for Adams Bohart and Wolborska Model for phenol (a) and cyanide (b)

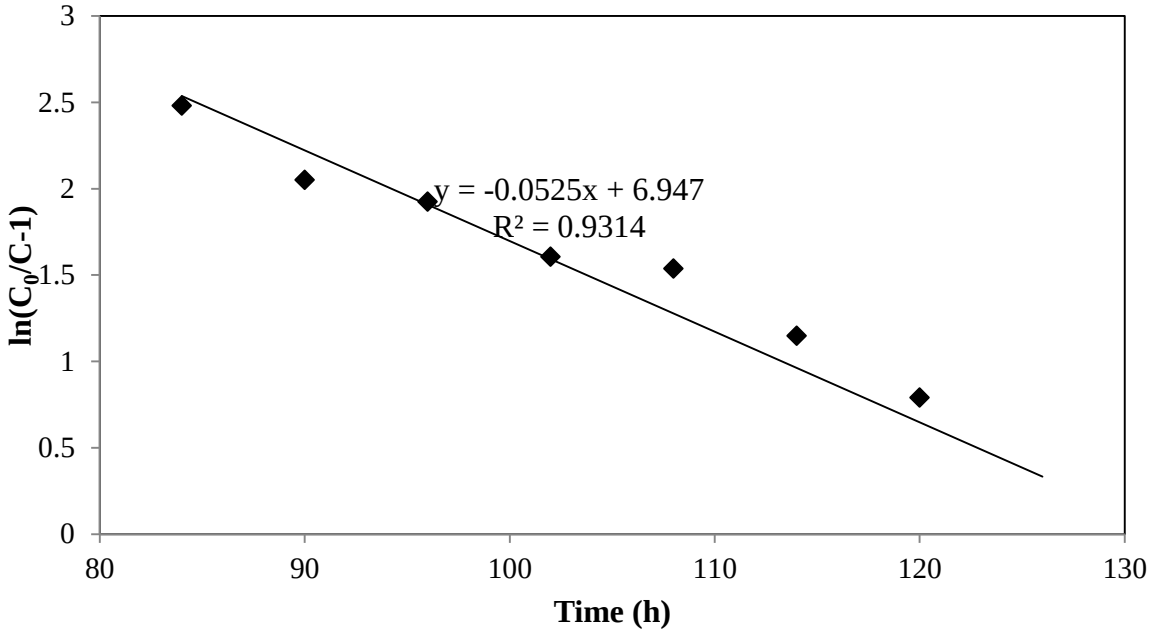

(a)

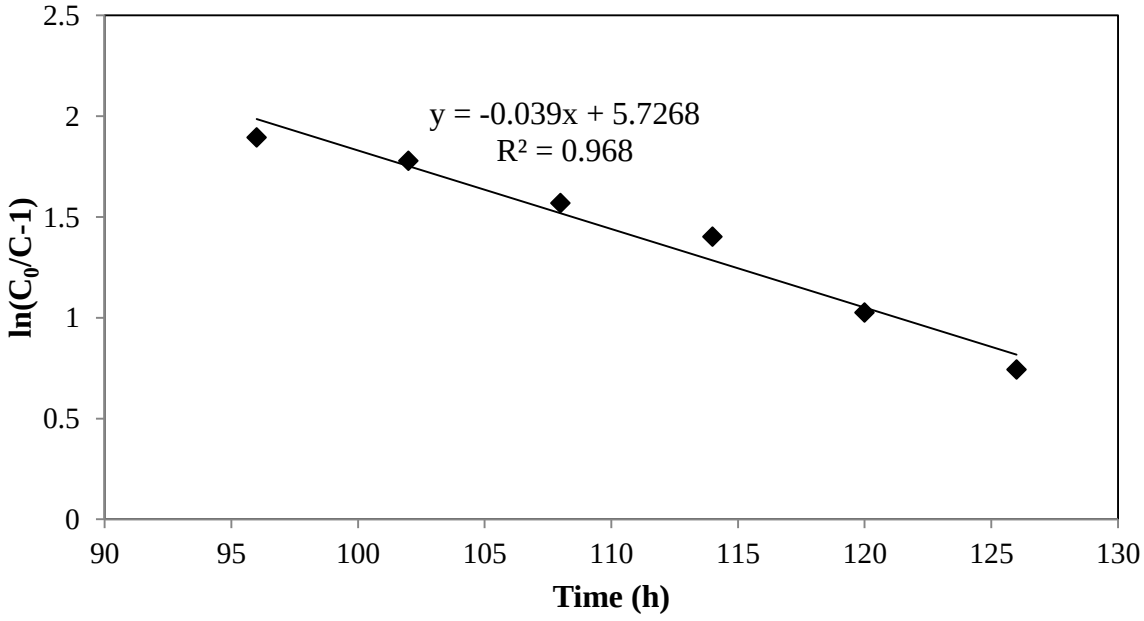

(b)

Figure 6.81 Plots of Thomas model for phenol (a) and cyanide (b)

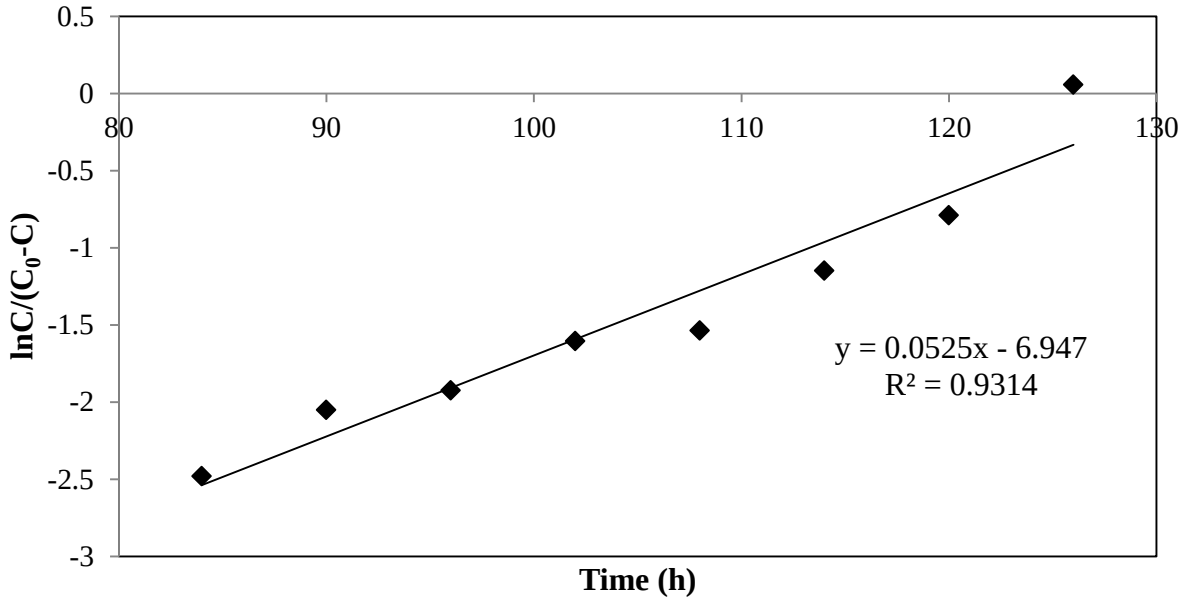

(a)

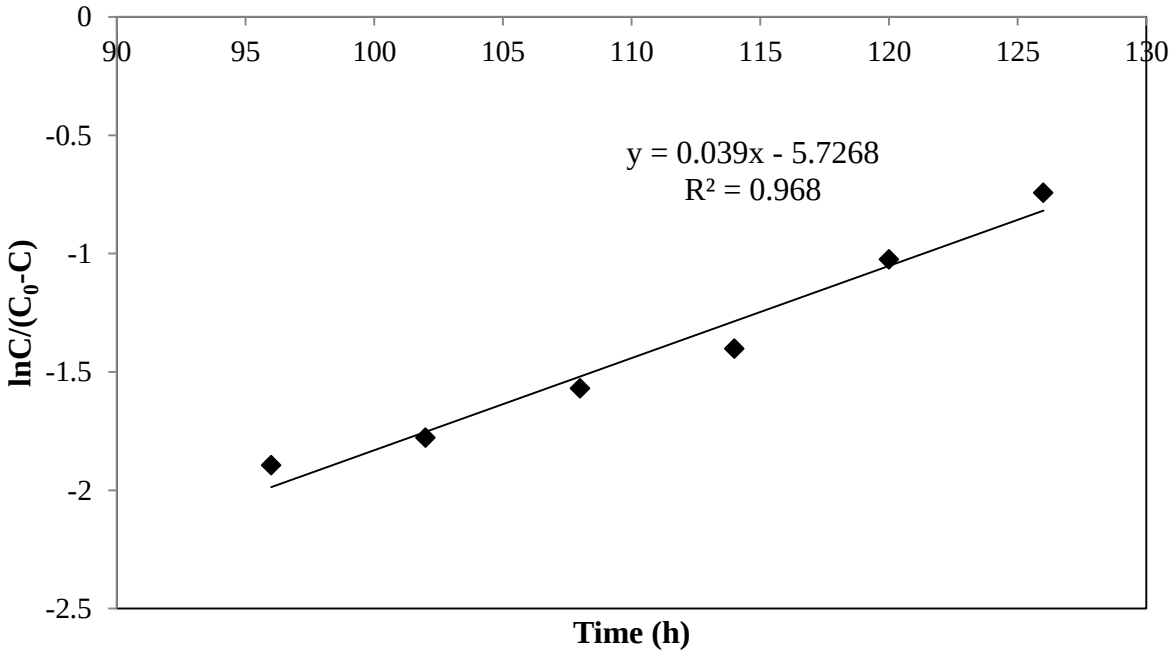

(b)

Figure 6.82 Plots of Yoon and Nelson model for phenol (a) and cyanide (b)

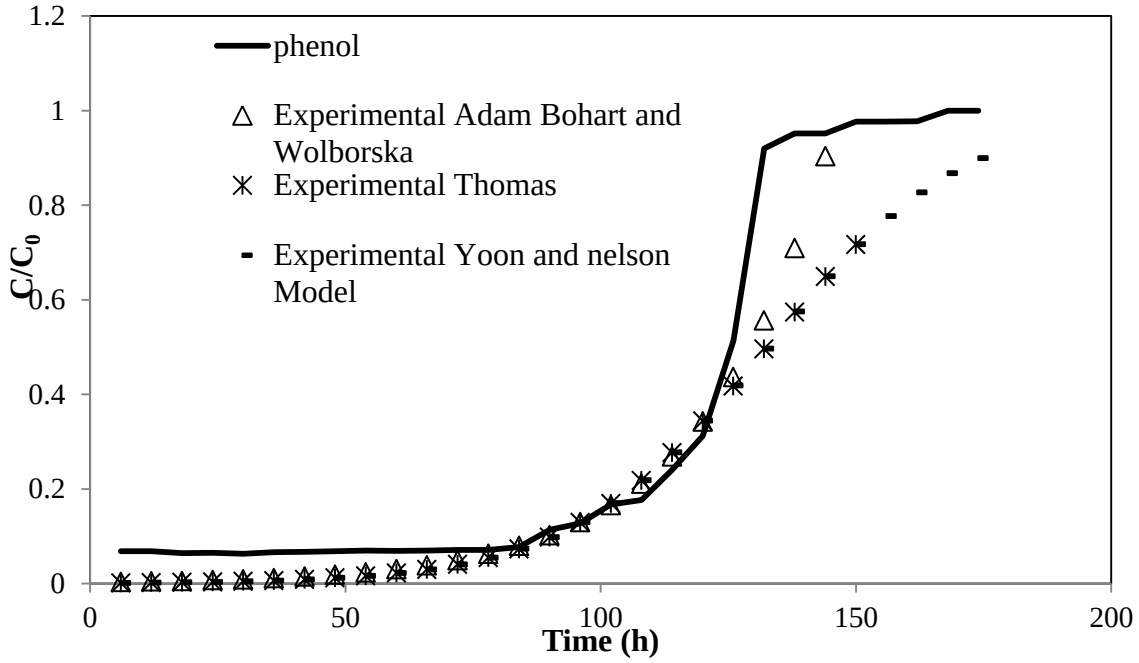

Figure 6.83: Graph showing the experimental breakthrough curve and the curves obtained by Adams Bohart, Wolborska, Thomas and Yoon and Nelson model for phenol uptake by GAC column

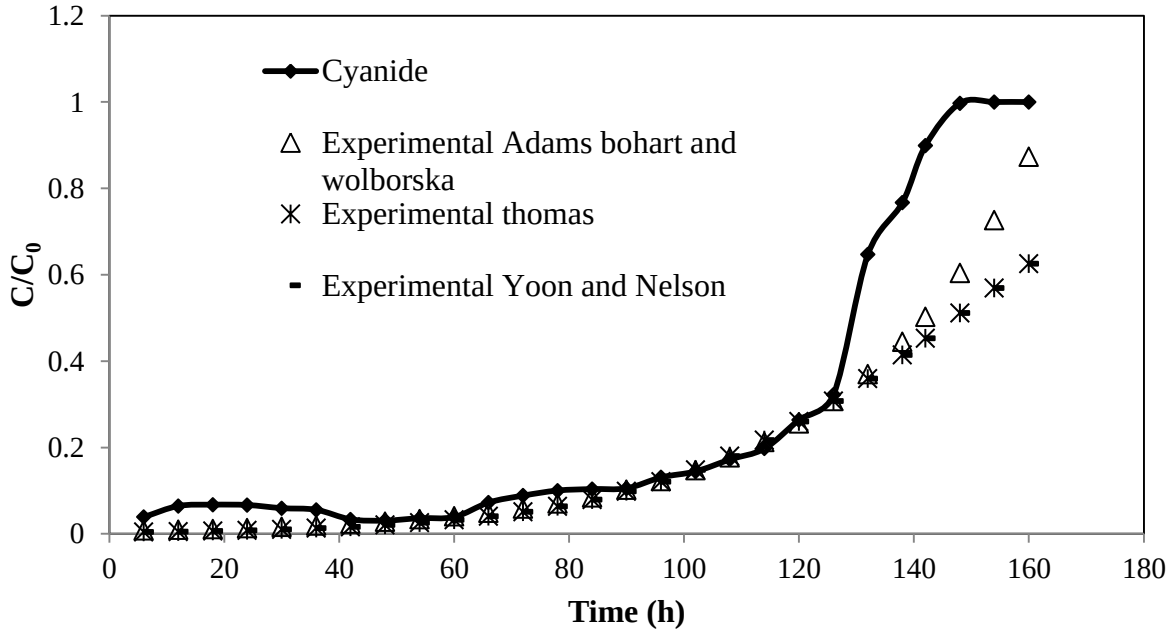

Figure 6.84: Graph showing the experimental breakthrough curve and the curves obtained by Adams Bohart, Wolborska, Thomas and Yoon and Nelson model for cyanide uptake by GAC column

Adams Bohart model and Wolborska best predicts the data for co-adsorption of phenol and cyanide on granular activated carbon column. Therefore the adsorption rate of both phenol and cyanide is directly proportional to adsorbent and adsorbate's residual capacity. Mass transfer zone(MTZ) studies were also carried out for the co-adsorption of phenol and cyanide on granular activated carbon column. The effect of bed height on the MTZ was also analysed. The data in Table 6.11 showed that with increase in bed height the mass transfer zone height increased along with the rate of movement of mass transfer zone along with the time taken to reach the total bed capacity also increases (Mishra et. al. and Degs et.al.)

Table 6.24: Effect of bed height on the Mass Transfer Zone predictions for the column reactor

Bed Height = 100 cm		
	Phenol	**Cyanide**
T_v (h)	107.39	112.83
T_c (h)	111.78	116.97
MTZ (cm)	3.92	3.54
q_{th} (mg/g)	21.12	2.22
q_s (mg/g)	21.97	2.29
χ^2_{th}	0.00166	0.00134
χ^2_s	0	0
$V_{0.9}$ (L)	77.83	83.73
$V_{0.2}$ (L)	64.86	67.22
RMTZ (m/h)	1.78	1.26
Bed Height = 87.5 cm		
T_v (h)	103.26	95.02
T_c (h)	111.50	104.72
MTZ (cm)	6.47	8.11
q_{th} (mg/g)	23.19	2.13
q_s (mg/g)	25.05	2.35
χ^2_{th}	0.00279	0.00596
χ^2_s	0.01509	0.00051
$V_{0.9}$ (L)	77.83	81.37
$V_{0.2}$ (L)	53.07	55.43

RMTZ (m/h)	1.54	1.84
Bed Height = 62.5 cm		
T_v (h)	77.41	80.15
T_c (h)	81.63	83.96
MTZ (cm)	3.23	2.84
q_{th} (mg/g)	24.34	2.52
q_s (mg/g)	25.67	2.64
χ^2_{th}	0.0095	0.0077
χ^2_s	0.0208	0.0167
$V_{0.9}$ (L)	64.86	67.22
$V_{0.2}$ (L)	44.81	38.92
RMTZ (m/h)	0.95	0.59
Bed Height = 37.5 cm		
T_v (h)	52.46	45.43
T_c (h)	59.38	47.45
MTZ (cm)	4.37	1.59
q_{th} (mg/g)	27.49	2.38
q_s (mg/g)	37.13	2.49
χ^2_{th}	0.0401	0.00118
χ^2_s	0.0865	0.00569
$V_{0.9}$ (L)	53.07	42.45
$V_{0.2}$ (L)	16.51	17.69
RMTZ (m/h)	0.70	0.38

6.2.5 CONTINUOUS STUDIES FOR SIMULTANEOUS ADSORPTION AND BIODEGRADATION OF PHENOL AND CYANIDE USING RICE HUSK:

The continuous studies for simultaneous adsorption and biodegradation of phenol and cyanide were also carried out using NaOH treated rice husk as the packing material. The experiments were carried out at an EBCT of 5 h which gave the maximum removal for granular activated carbon as the packing material. The flow rate obtained at this EBCT was 9.867 mL/min. The plots for normalised concentration versus time are shown below in figure 6.85. There is a sudden increase in the outlet concentration of both phenol and cyanide due to

the shock load studies which were conducted after 74 h. The concentration was suddenly raised to 800 mg/L and 80 mg/L phenol and cyanide respectively which increased the level of toxicity for the bacteria. The concentration then started to decrease which is due to the adaptation of the bacteria to the sudden increase in concentration of both the pollutants. The percentage removal of both phenol and cyanide for simultaneous adsorption and biodegradation using NaOH treated rice husk was calculated as 81.43 % and 90.80 % respectively.

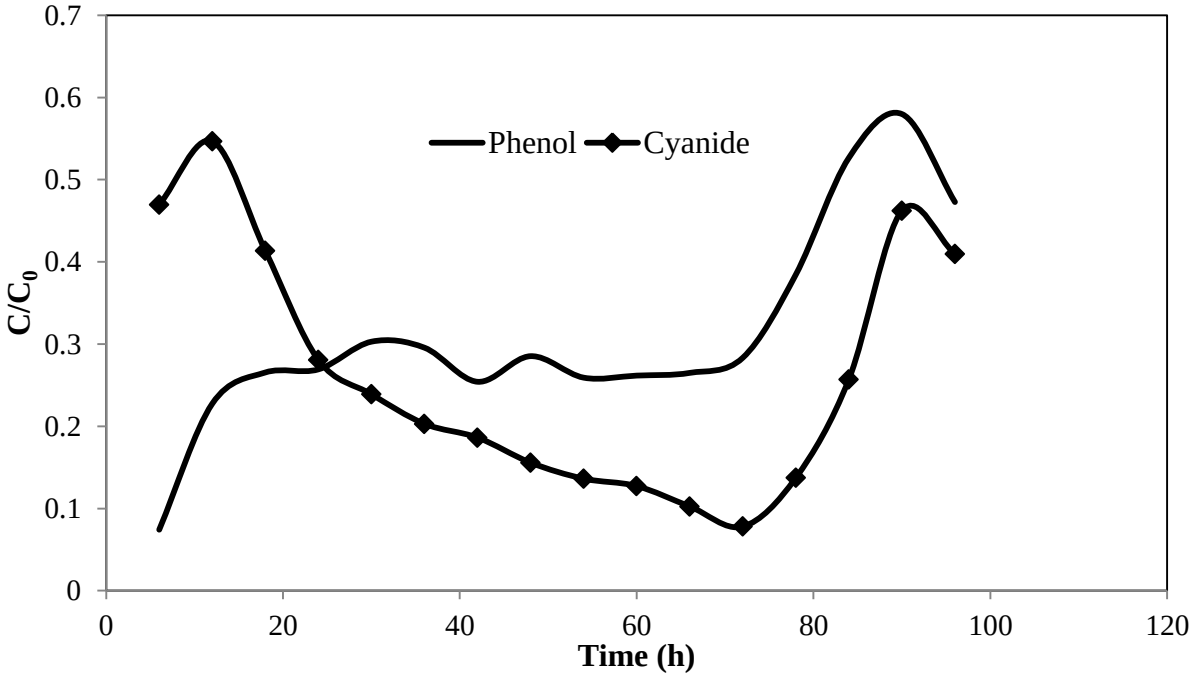

Figure 6.85: Normalised concentration curve for SAB of phenol and cyanide using a column reactor with rice husk at an initial phenol concentration: 400 mg/L, initial cyanide concentration : 40 mg/L, EBCT : 5 h, pH: 7

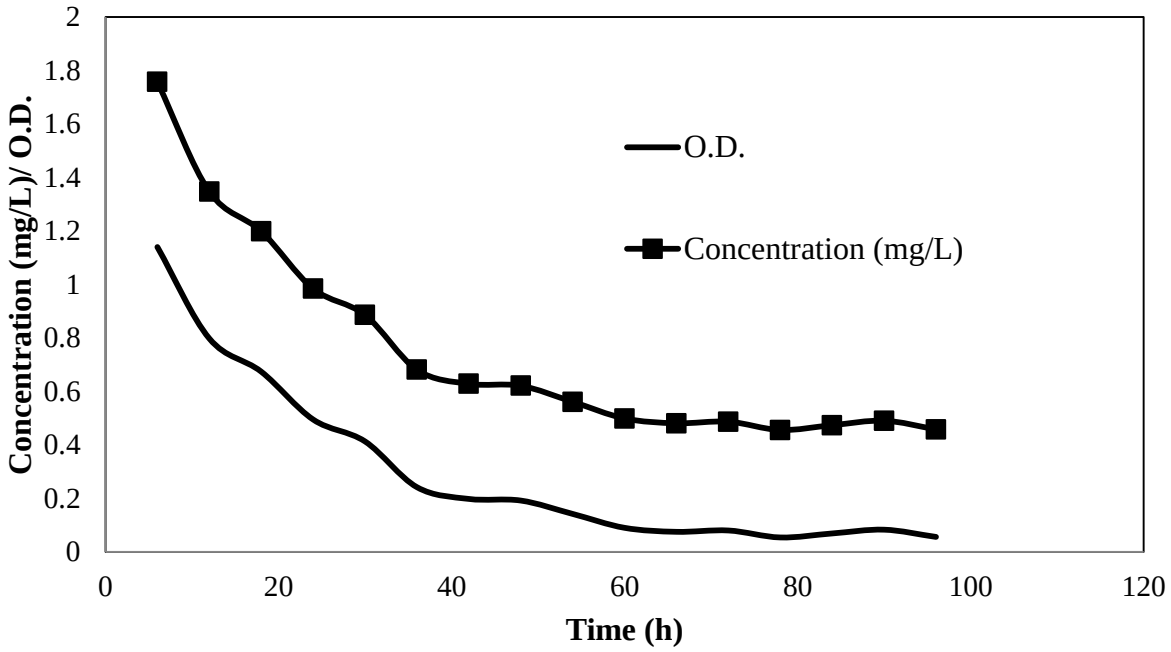

Figure 6.86: Biomass Concentration (mg/L) and Optical Density plot for SAB of phenol and cyanide using a rice husk packed column at an initial phenol concentration : 400 mg/L, initial cyanide concentration : 40 mg/L, EBCT : 2.5 h, pH: 7 for 96 h

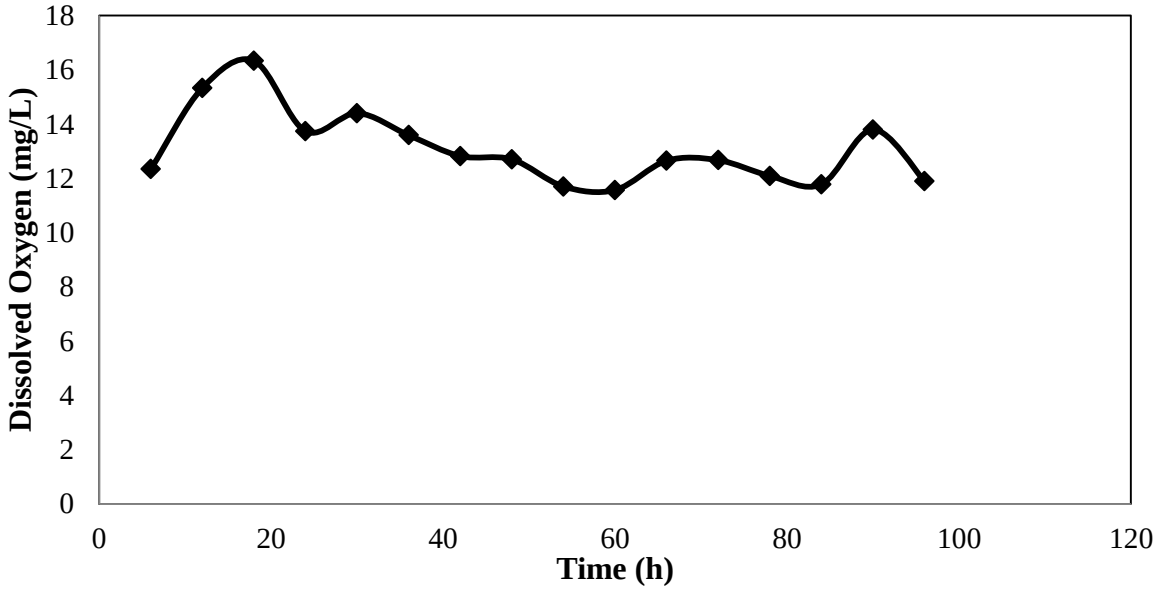

Figure 6.87: Dissolved Oxygen (mg/L) plot for SAB of phenol and cyanide using a rice husk packed column at an initial phenol concentration: 400 mg/L, initial cyanide concentration: 40 mg/L, EBCT : 2.5 h, pH=7 for 96 h

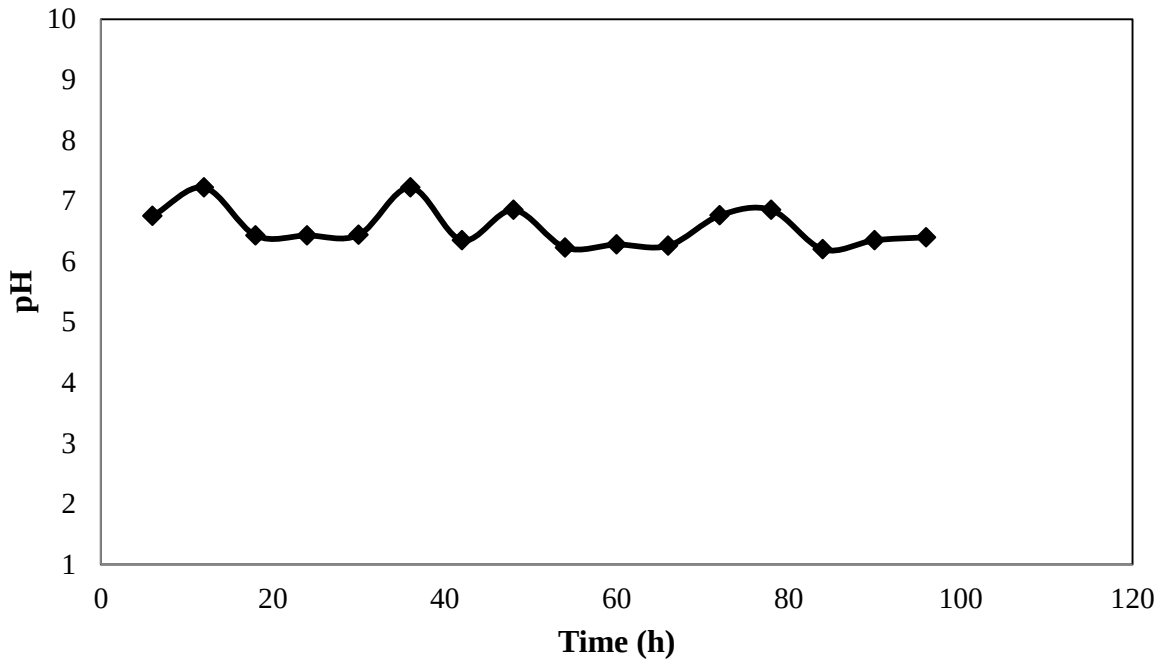

Figure 6.88: pH variation plot for SAB of phenol and cyanide using a rice husk packed column at an initial phenol concentration: 400 mg/L, initial cyanide concentration: 40 mg/L, EBCT : 2.5 h, pH:7 for 96 h

The biomass concentration and O.D. is continuously decreasing in case of Rice husk packed columns which is due to the antibacterial nature of rice husk (reference). The removal percentage is slightly less for the rice husk column that the GAC column which can also be attributed to the dying bacteria in rice husk column. The pH in this case also remains between 6 and 7. There is an increase in the dissolved oxygen which is due to life extermination inside the reactor. The decrease in percentage removal of phenol and cyanide in the reactor is due to the inability of the pores on the rice husk surface to get simultaneously regenerated due to biodegradation as the bacterial life is exterminating in the reactor environment.

CHAPTER 7

CONCLUSIONS

In the present study co-removal of phenol and cyanide using simultaneous adsorption and biodegradation has been carried out using three biosorbents rice husk, corn husk leaves and egg shells in the batch studies. Column studies were also carried out using granular activated carbon and rice husk. The results of the batch and column studies performed are as follows:

- SAB process of phenol and cyanide are dependent of pH of the process. The optimum pH for the process for all the adsorbents comes out to be 7. The bacteria showed no visible growth in extreme acidic and extreme alkaline pH.
- The adsorption of both phenol and cyanide took place in their undissociated forms.
- The optimum adsorbent dose for rice husk was 5 g/L, for corn husk leaves was 6 g/L and that for egg shells was 35 g/L.
- The temperature in the entire process was maintained at 30 ^{0}C.
- Both pseudo first order and second order models were best fitted to the SAB process with all the three adsorbents.
- The equilibrium isotherms that were best fit were either non modified Langmuir or extended Langmuir for phenol adsorption onto the three adsorbents and the isotherms that best fitted cyanide data was modified Langmuir isotherm.
- There is not much change in the SAB process with increase in temperature. ΔG^0 is negative showing the feasibility of the process. For rice husk SAB of phenol is an endothermic process with an increase in randomness at the solid/liquid interface but SAB of cyanide is an exothermic process with decrease in randomness at the solid/liquid interface. For corn husk leaves and egg shells SAB of both phenol and cyanide is an exothermic process with a decrease of randomness at the solid/liquid interface.
- RTD studies were performed on the reactor which showed its behaviour to be close to plug flow.
- Column studies were carried out taking rice husk and granular activated carbon.
- Effective bed contact time of 5 h showed a higher removal percentage and column capacity for simultaneous adsorption and biodegradation in the GAC column.
- The percentage removal of phenol and cyanide for the continuous GAC column by simultaneous adsorption and biodegradation was estimated as 99.99 %and 98.85 %.

- The percentage removal for co-adsorption of phenol and cyanide by regenerated GAC columns were 64.24 % and 73.12 %.
- The breakthrough curve obtained showed a better fit to the Adams Bohart and Wolborska Model.
- The percentage removal of phenol and cyanide for the continuous rice husk column by simultaneous adsorption and biodegradation was estimated as 81.43 % and 90.80 %.

- A more detailed study on the co-removal of phenol and cyanide concentrating more on the potential of cheap biosorbents.
- Surface modifications of the adsorbents can be done to increase the removal percentage and optimize the process.
- The applicability of the process should be tested by carrying out the investigation for real industrial waste water.
- Genetically modified micro-organisms should be used that should only concentrate on target fulfillment.

PUBLICATIONS

International Referred Journals

- **Sengupta P.** and Balomajumder C., (2014) IJRET: International Journal of Research in Engineering and Technology EISSN: 2319-1163 PISSN: 2321-7308
  "Potential of Corn Husk Leaves for the Co-Removal of Phenol and Cyanide from Waste Water using Simultaneous Adsorption and Biodegradation"
- Agarwal B., **Sengupta P.** and Balomajumder C., (2013) World Academy of Science, Engineering and Technology International Journal of Chemical, Materials Science and Engineering Vol:7 No:11, 2013
  "Equilibrium, Kinetic and Thermodynamic Studies of Simultaneous Co-Adsorptive Removal of Phenol and Cyanide Using Chitosan"
- **Sengupta P.** and Balomajumder C., (2014) The Canadian Journal of Chemical Engineering, Communicated, Manuscript ID CJCE-14-0355
  "*Co-adsorption of phenol and cyanide by Granular activated carbon in a continuous packed bed reactor: A modeling approach"*
- **Sengupta P.**, Agarwal B. and Balamajumder C., (2014) Research Journal of Chemical Sciences, Communicated, Manuscript ID ISCA-RJCS-2014-97
  "*A study of accuracy of multicomponent analysis of phenol and cyanide in their binary solution by colorimetric method"*

National Conference

- **Sengupta P.** and Balomajumder C. (2014) National Seminar on "Recent Advances in Pollution and Abatement"
  "*Simultaneous Adsorption and Biodegradation of phenol and cyanide in their binary solution by egg shells"*

APPENDIX-A

Calibration Curve of phenol and cyanide in water and nutrient media

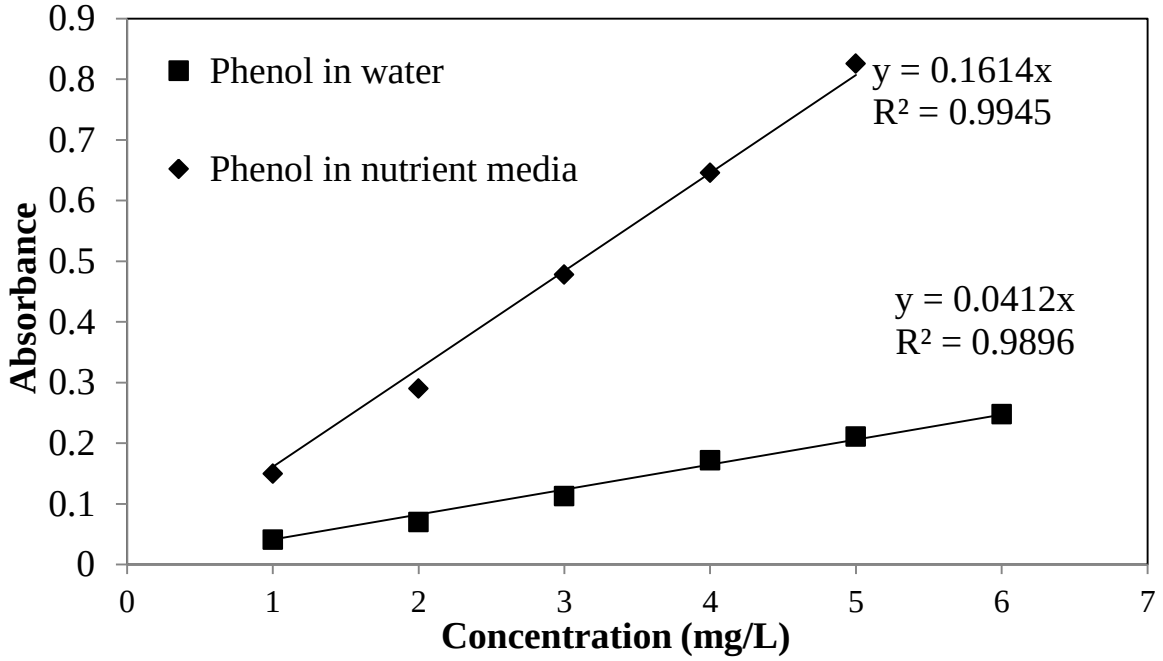

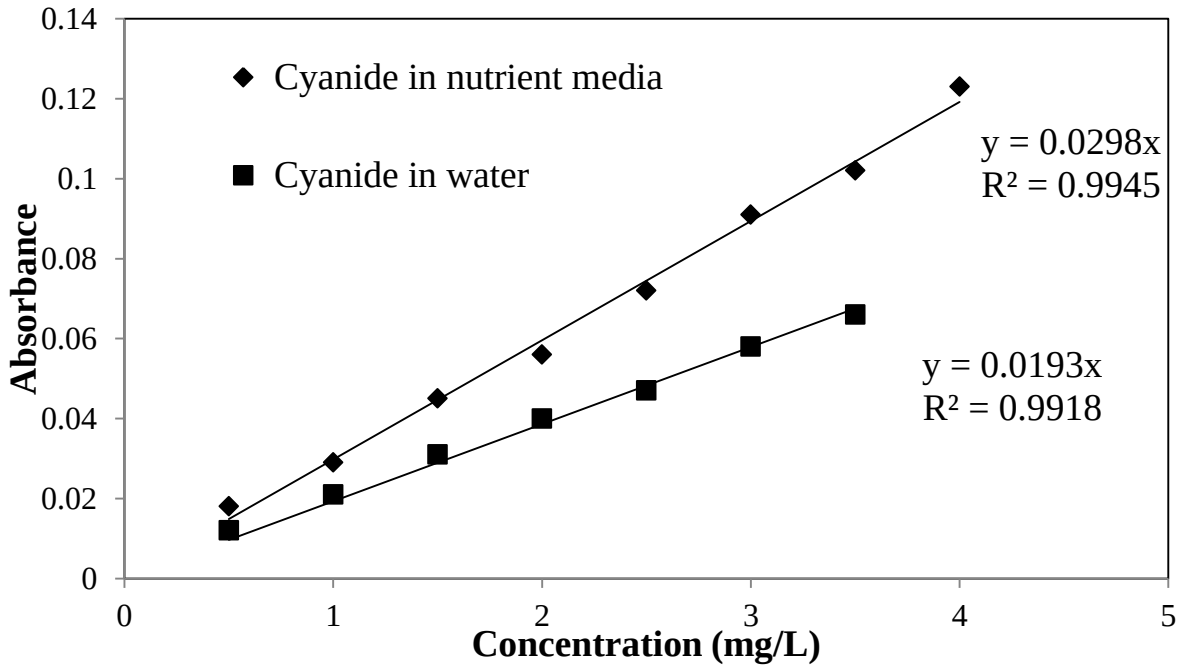

APPENDIX-B

Biomass Concentration (mg/L) Vs. O.D. Plot for *S. odorifera*

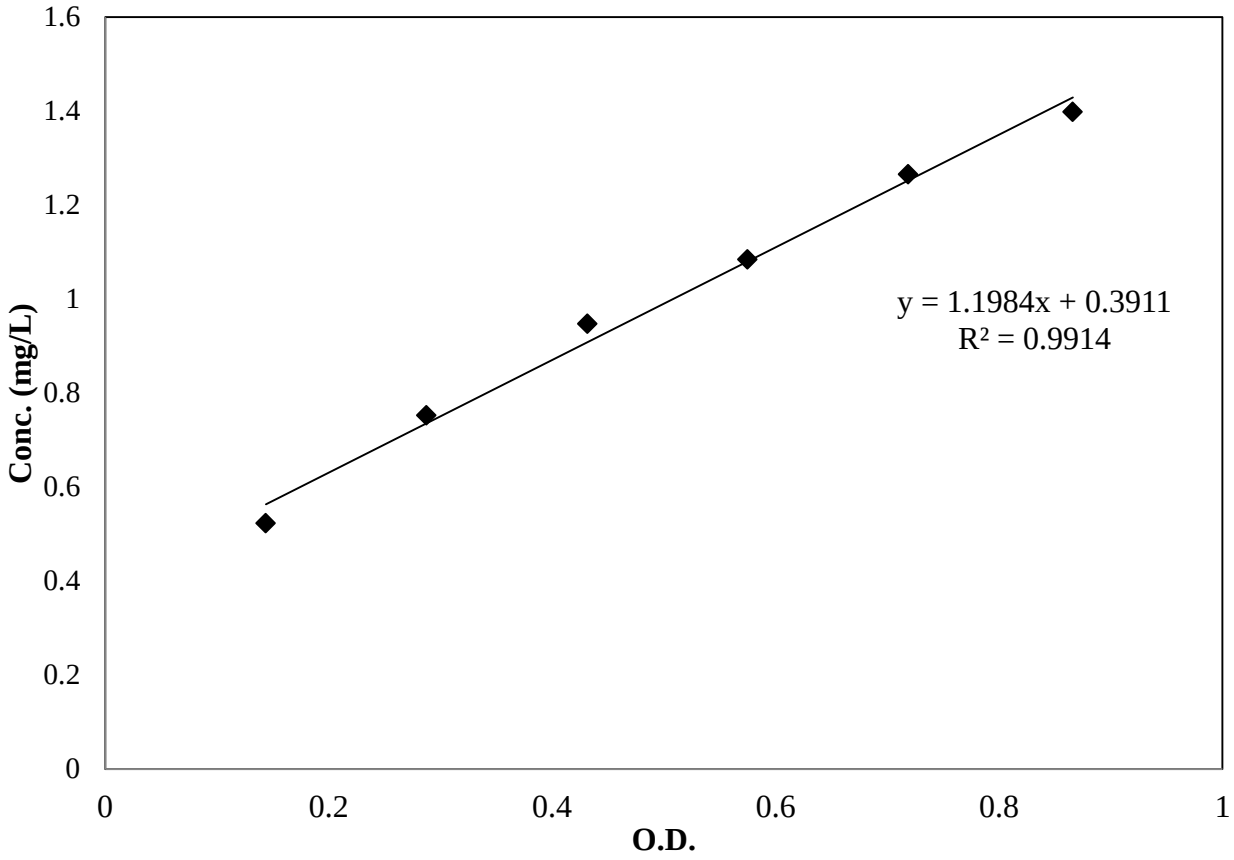

APPENDIX-C

DETAILS OF ANALYTICAL INSTRUMENTS USED AND PROCEDURE FOR ANALYSIS

Name of instrument and its use	Model & make	Operating conditions	Remarks
FTIR (spectra of various adsorbent)	Thermo FTIR , model AVATR 370 Csl coupled with EZOMNIC software (version 6.2)	KBR Plate method, around 10 mg of dried sample was dispersed in 100 mg of spectroscopic grade	Detection limit: Able to detect qualitatively the presence of few µg of element in sample.
Thermogravimerty (TG) of adsorbents	EXSTER TG/DTA 6300	Reference name: Alumina Powder Gas1 : Air (200 ml/min) PAN : Alumina Temperature program: 35 to 1200 Cel Cel / min : 10	Able to observe the loss of weight of adsorbent with change in temperature.
Scanning electron microscope (scanning electron micrographs (SEM) of adsorbents)	LEO Electron Microscopy Ltd., England	ACC voltage: upto 30 kV, Resolution: 4 nm in HV and 6 nm in VP	Magnification range: 10X to 300000X
Surface analyser (Surface area and porosity measurement)	Micromeritics, model ASAP 2010	Nitrogen was used as cold bath at . 77 K	Brunauer-Emmett-Teller (BET) method was used
UV- Visible Spectrophotometer (measurement of optical density)	Perkin Elmer Lamda 35	λ : 540 nm Power requirement: 100-240 V	Wave length accuracy: • ± 0.1 nm Wave length reproducibility: • ± 0.1 nm
X-Ray Diffractometer (Pattern of adsorbents)	Model D8 Advance, BRUKER AXS	Cu target X-ray diffraction with 2θ: 5-100 degree, Working voltage: 10-100 kV, Tube current: 4 to 80 mA	Can work within 2θ: 0-150 deg

REFERENCES

Adhoum N. and Monser L., "Removal of cyanide from aqueous solution using impregnated activated carbon", Chemical Engineering and Processing ,41,17–21,2012.

Adjei M.D., and Ohta Y., "Factors affecting the biodegradation of cyanide by Burkholderia Cepacia Strain C-3", Journal of Bioscience and Bioengineering Vol. 89, No. 3, (2000) 274-277.

Agarwal B., Sengupta P., Balomajumder C., "Equilibrium, Kinetic and Thermodynamic Studies of Simultaneous Co-Adsorptive Removal of Phenol and Cyanide Using Chitosan" Int. J. Chem., Mater. Sci. Eng. (2013) Vol:7 No:11

Agarwal B.,Majumder C.B. and Thakur P.K., "Simultaneous co-adsorptive removal of phenol and cyanide from binary solution using granular activated carbon", Chemical Engineering Journal 228 (2013) 655–664.

Aksu Z., and Gonen F. "Binary biosorption of phenol and chromium(VI) onto immobilized activated sludge in a packed bed: Prediction of kinetic parameters and breakthrough curves", Sep. Purif. Technol. 49 (2006) 205–216.

Aksu Z., Gonen F.,"Biosorption of phenol by immobilized activated sludge in a continuous packed bed: prediction of breakthrough curves", Process Biochemistry 39 (2004) 599–613

Al-Degs Y.S., Khraisheh M.A.M., Allen S.J., and Ahmad M.N. "Adsorption characteristics of reactive dyes in columns of activated carbon". J. Hazard. Mater. 165 (2009) 944–949.

Alonso-González a O., Nava-Alonso F., Uribe-Salas A. and Dreisinger D., "Use of quaternary ammonium salts to remove copper–cyanide complexes

Banat F.A., Al-Bashir B., Al-Asheh S. and Hayajneh O., "Adsorption of phenol by bentonite", Environmental Pollution 107 (2000) 391-398.

Banerjee A. and Ghoshal A.K., "Phenol degradation performance by isolated Bacillus cereus immobilized in alginate", International Biodeterioration & Biodegradation 65 (2011) 1052-1060.

Barclay M., Hart A., Knowles C.J., Meeussen: and Tetdl V.A., "Biodegradation of metal cyanides by mixed and pure cultures of fungi" Enzyme and Microbial Technology 22 (1998) 223-231.

Behnamfard A. and Salarirad M.M., “Equilibrium and kinetic studies on free cyanide adsorption from aqueous solution by activated carbon”, Journal of Hazardous Material, 170 (2009)127-133.

Bischoff, K.B.; McCracken E.A. Trcaer Test in Flow Systems. Ind. Eng. Chem. Res. 1966, 58, 18-31.

Bodzek M.,Bohdziewicz J.and Ma/gorzata Kowalska, “Immobilized enzyme membranes for phenol and cyanide decomposition”,J. Membrane Sciences 113 (1996) 373-384.

Boyadzhiev L., Bezenshek E. and Lazarova Z. “Removal of phenol from waste water by double emulsion membranes and creeping film pertraction”, Journal of Membrane Science, 21 (1984) 137-144.

Cacace D., Ashbaugh H., Kouri N., Bledsoe S., Lancaster S., Chalk S., Spectrophotometric determination of aqueous cyanide using a revised phenolphthalin method. Anal. Chim. Acta., 589, 137-141 (2007)

Chen C.Y., Kao C.M. and Chen S.C., “Application of Klebsiella oxytoca immobilized cells on the treatment of cyanide wastewater”, Chemosphere 71 (2008) 133–139.

Chinaka S., Tanaka S., Takayama N., Tsuji N., Takou S., Ueda K.,High-Sensitivity Analysis of Cyanide by Capillary Electrophoresis with Fluorescence Detection. Anal. Sci., 17, 649-652 (2001)

Cho J., Moon J., Seong K. and Park K., “ Antimicrobial activity of 4-Hydroxybenzoic acid and trans 4-Hydrocynammic Acid isolated and identified from Rice Hull.” Biosci. Biotechnol. Biochem., 62 (11) 1998 2273-2276

Da¸browski A, Podkos´cielny P., Hubicki Z., Barczak. M., “Adsorption of phenolic compounds by activated carbon—a critical review”, Chemosphere 58 (2005) 1049–1070

Danckwerts, P.V. Continous Flow Systems Distribution of Residence Times. Chem. Eng. Sci. 1953, 2, 1-18.

Dash R.R., Majumder C.B. and Kumar A., “Treatment of metal cyanide bearing wastewater by simultaneous adsorption and biodegradation (SAB)”, Journal of Hazardous Materials 152 (2008) 387–396.

Depci T., “Comparison of activated carbon and iron impregnated activated carbon derived from Golbas¸ lignite to remove cyanide from water”, Chemical Engineering Journal ,181– 182 ,467– 478, 2012.

Deveci H., Yazic E.Y., Alp I. and Uslu T., “Removal of cyanide from aqueous solutions by plain and metal-impregnated granular activated carbons”, Int. J. Miner. Process, 79, (2006),198–208.

Dıaz-Nava M.C., Olguın M.T., Solache-Rıos M., “Adsorption of phenol onto surfactants modified bentonite”, J Incl Phenom Macrocycl Chem (2012) 74:67–75 DOI 10.1007/s10847-011-0084-6.

Djokic L., Narancic T.,Biocanin M.,Saljnikov E., Casey E.,Vasiljevic B., Nikodinovic-Runica J., “Phenol removal from four different natural soil types by Bacillus sp.PS11” , Applied Soil Ecology 70 (2013) 1– 8.

Duda A.M., Addressing nonpoint sources of water pollution must become an international priority, Wat. Sci. Tech., 28, 1-11(1993)

Dursun A.Y. and Kalayci C.S., “Equilibrium, kinetic and thermodynamic studies on the adsorption of phenol onto chitin”, Journal of Hazardous Materials ,B123, 2005,151–157.

Ezzi M.I., Lynch J.M., “Biodegradation of cyanide by Trichoderma spp. and Fusarium spp.”, Enzyme and Microbial Technology 36 (2005) 849–854.

Fialov A., Boschke E. and Bley T., “Rapid monitoring of the biodegradation of phenol-like compounds by the yeast Candida maltosa using BOD measurements”, International Biodeterioration & Biodegradation 54 (2004) 69 – 76.

Fisher F. B., Brows J. S., Colorimetric Determination of Cyanide in Stack Gas and Waste Water. Anal. Chem., 24, 1440-1444 (1952)

Folin O., Denis W., A Colorimetric Method for the determination of Phenols (and Phenol Derivatives) in Urine. J. Biol. Chem., 22, 305-308 (1915)

Genieva S. D., Ch. Turmanova S., Dimitrova A. S.and L. T. Vlaev, “Characterization Of Rice Husks and the products of its Thermal Degradation in Air or Nitrogen Atmosphere” Journal of Thermal Analysis and Calorimetry, Vol. 93 (2008) 2, 387–396

Gholamreza Moussavi, Rasoul Khosravi, “Removal of cyanide from wastewater by adsorption onto pistachio hull wastes: Parametric experiments, kinetics and equilibrium analysis”, Journal of Hazardous Materials ,183, (2010) 724–730.

Gholamreza Moussavi, Sadegh Talebi, “Comparing the efficacy of a novel waste-based adsorbent with PAC for the simultaneous removal of chromium (VI) and cyanide from electroplating wastewater, chemical engineering research and design ,9 0, (2012) 960–966,.

Girods P., Dufour A., Fierro V., Rogayume Y., Zoulalian A., Celzard A., " Activated carbon prepared from wood particleboard waste : Characterisation and phenol adsorption capacities" , J. Hazardous Materials 166(2009) 491-501.

Gondal M.A., Sayeed M.N., Seddigi Z., "Laser enhanced photo-catalytic removal of phenol from water using p-type NiO semiconductor catalyst", Journal of Hazardous Materials 155 (2008) 83–89.

Gonz´alez P.S., Capozucca C.E., Tigier H.A., Milrad S.R. and Agostini E., "Phytoremediation of phenol from wastewater, by peroxidases of tomato hairy root cultures", Enzyme and Microbial Technology 39 (2006) 647–653.

Gulbeyi Dursun , Handan C¸ ic¸eka, Arzu Y. Dursun, "Adsorption of phenol from aqueous solution by using carbonised beet pulp", Journal of Hazardous Materials, B125, (2005)175–182.

Guotong Qin, Yuan Yao, Wei Wei, Tao Zhang, "Preparation of hydrophobic granular silica aerogels and adsorption of phenol from water", Applied Surface Science, 2013.

Gupta N., Balomajumder C. and Agarwal V.K., "Adsorption of cyanide ion on pressmud surface: A modeling approach", Chemical Engineering Journal, 191, 548– 556, 2012.

Hameed B.H. and Rahman A.A., "Removal of phenol from aqueous solutions by adsorption onto activated carbon prepared from biomass material", Journal of Hazardous Materials 160, 2008, 576–581.

Han B., Shen z. and Wickramasinghe S.R., "Cyanide removal from industrial wastewaters using gas membranes", Journal of Membrane Science 257 (2005) 171–181.

Han R., Ding D., Xu Y., Zou W.,Wang Y., Li Y., Zou L. "Use of rice husk for the adsorption of congo red from aqueous solution in column mode", Biores. Techno. 99, (2008) 2938–2946.

Haque M. R., Bradbury J. H., Total cyanide determination of plants and foods using the picrate and acid hydrolysis methods. Food Chem., 77, 107-114 (2002)

Hasan B. S., Ozdes D., Gundogdu A., Duran C. and Soylak M., "Removal of phenol from aqueous solutions by adsorption onto organomodified Tirebolu bentonite: Equilibrium, kinetic and thermodynamic study", Journal of Hazardous Materials ,172, (2009) 353–362.

Huanosta-Gutierrez T., Dantas R.F., Ramirez-Zamora R.M. and Esplugas S., "Evaluation of copper slag to catalyze advanced oxidation processes for the removal of phenol in water", Journal of Hazardous Materials 213– 214 (2012) 325– 330.

Kilic M., Apaydin-Varol E. and E. Putun, “Adsorptive removal of phenol from aqueous solutions on activated carbon prepared from tobacco residues: Equilibrium, kinetics and thermodynamics”, Journal of Hazardous Materials 189 (2011) 397–403.

Kiran R.V. and Balomajumder C., “Simultaneous Adsorptive Removal of Cyanide and Phenol from Industrial Wastewater: Optimization of Process Parameters”, *Res.J.Chem.Sci* Vol. 1(4), 30-39, July (2011).

Kuch H., Chmiter K. B., Determination of Endocrine-Disrupting Phenolic Compounds and Estrogens in Surface and Drinking Water by HRGC-(NCI)-MS in the Picogram per Liter Range. Environ. Sci. Technol., 35, 3201-3206 (2001)

Larsen M., Trapp S. and Pirandello A., “Removal of cyanide by woody plants”, Chemosphere 54 (2004) 325–333.

Levenspiel, O. Chemical Reaction Engineering, 3rd ed.; John Wiley, USA, 1999

Lin K., Pan J., Chen Y., Cheng R. and Xu X., “Study the adsorption of phenol from aqueous solution by solvent extraction”, Minerals Engineering 23 (2010) 765–770.

M.D. Adams, “ Removal of cyanide from solution using activated carbon”, Minerals Engineering, Vol. 7, No. 9, 1165-1177, 1994.

Ma J., Ding Z., Wei G., Zhao H., Huang T., Sources of water pollution and evolution of water quality in the Wuwei basin of Shiyang river, Northwest China. J. Environ. Manage., 90, 1168-1177 (2009)

Malkoc E., Nuhoglu Y., and Dundar M. “Adsorption of Chromium (VI) on pomace—An olive oil industry waste:Batch and column studies”, J. Hazard. Mater. B138 (2006) 142–151.

Maniyam M.N.,Sjahrir F., Ibrahim1 A.L, Anthony E.G., “Biodegradation of cyanide by Rhodococcus UKMP-5M”, Biologia 68/2: 177—185, 2013 Section Cellular and Molecular Biology DOI: 10.2478/s11756-013-0158-6 .

Metcalf & Eddy, Inc. Wastewater Engineering Treatment and Resuse, 4th ed.; Tata McGraw Hill, New Delhi, 2010.

Michałowicz J. and Duda W., “Phenols – Sources and Toxicity”, Polish J. of Environ. Stud. Vol. 16, No. 3 (2007).

Mishra V., Balomajumder C., and Agarwal V. K. “Simultaneous Adsorption and Bioaccumulation: A Study on Continuous Mass Transfer in Column Reactor”. Environ. Prog. Sustain. Energ. (Vol.32, No.3) (2012) DOI 10.1002.

Montedoro G., Servili M., Baldioli M., Miniati E., Simple and Hydrolyzable Phenolic Compounds in Virgin Olive Oil. 1. Their Extraction, Separation, and Quantitative and Semiquantitative Evaluation by HPLC, J. Agric. Food Chem., 40 1571-1576 (1992)

Moran R., "Cyanide Uncertainties, Observations on the Chemistry, Toxicity, and Analysis of Cyanide in Mining-Related Waters", Mineral Policy Center *Protecting Communities and the Environment* 1998.

Murthy Z.V.P, Gupta S.K., "Sodium cyanide separation and parameter estimation for reverse osmosis thin film composite polyamide membrane", Journal of Membrane Science 154 (1999) 89-103.

Ning P., Qiu J.,Wang X.,Liu W. and Chen W., "Metal loaded zeolite adsorbents for hydrogen cyanide removal", Journal of Environmental Sciences 2013, 25(4) 808–814.

Pavia D. L., Lampman G. M., Kriz G. S, Vyvyan J.R., Spectroscopy, Brooks/Cole, 2007.

Polat H., Molva M. and Polat M., "Capacity and mechanism of phenol adsorption on lignite", Int. J. Miner. Process, 79, (2006) 264–273.

Rengaraj S., Moon S., Sivabalan R., Arabindoo B. and Murugesan V.,"Agricultural solid waste for the removal of organics: adsorption of phenol from water and wastewater by palm seed coat activated carbon", Waste Management, 22, 543–548, 2002.

Rockfln R. D., Johnson E. L., Determination of Cyanide, Sulfide, Iodide, and Bromide by Ion Chromatography with Electrochemical Detection. Anal. Chem., 55, 4-7 (1983)

Sag Y., Atacoglu I., and Kutsal T. "Equilibrium parameters for the single- and multicomponent biosorption of Cr (VI) and Fe (III) ions on *R. arrhizus* in a packed column", Hydrometallurgy 55 (2000) 165–179.

Samiotakis M., Ebbs S.D., "Possible evidence for transport of an iron cyanide complex by plants", Environmental Pollution 127 (2004) 169–173.

Schmidt P. C., Glombitza B. W., Quantitative multicomponent analysis of aspirin and salicylic acid in tablets without separation of excipients by means of principal component regression and a classical least squares algorithm. Trends Anal. Chem., 14, 45-49 (1995)

Sengupta P., Balomajumder C. "Potential of Corn Husk Leaves for the co-removal of Phenol and Cyanide from Waste Water using Simultaneous Adsorption and Biodegradation". Inter. J. Research Eng. Tech. (2014) eISSN: 2319-1163 , pISSN: 2321-7308.

Si-Hyun Do, Young-Hoon Jo, Ho-Dong Park, Sung-Ho Kong, "Synthesis of iron composites on nano-pore substrates: Identification and its application to removal of cyanide", Chemosphere 89 (2012) 1450–1456.

Singh S., Melo J.S., Eapen S. and D'Souza S.F., "Potential of vetiver (Vetiveria zizanoides L. Nash) for phytoremediation of phenol", Ecotoxicology and Environmental Safety 71 (2008) 671–676.

Srihari V. and Das A., "Comparative studies on adsorptive removal of phenol by three agro-based carbons: Equilibrium and isotherm studies", Ecotoxicology and Environmental Safety, 71 ,274–283, 2008.

Srivastava V.C., Swamy M.M., Mall I.D., Prasad B. and Mishra I.M., "Adsorptive removal of phenol by bagasse fly ash and activated carbon: Equilibrium, kinetics and thermodynamics", Colloids and Surfaces A: Physicochem. Eng. Aspects, 272 , 89–104, 2006.

Suh Y-J., Park J.M., Yang J-W., "Biodegradation of cyanide compounds by Pseudomonas fluorescens immobilized on zeolite", Enzyme and Microbial Technology Volume 16, Issue 6, June 1994, Pages 529–533.

Susarla S., Medina V.F., McCutcheon S.C., "Phytoremediation: An ecological solution to organic chemical contamination", Ecological Engineering 18 (2002) 647–658.

The Priority List of Hazardous Substances, Substance Priority List (SPL), from the Comprehensive Environmental Response, Compensation, and Liability Act (CERCLA) section 104 (i), as amended by the Superfund Amendments and Reauthorization Act (SARA).

Tiitto R. J., Phenolic Constituents in the Leaves of Northern Willows: Methods for the analysis of certain Phenolics. J. Agric. Food Chem., 33, 213-217 (1985)

Tracqui A., Raul J.S., Geraut A., Berthelon L., Ludes B., Determination of Blood Cyanide by HPLC-MS. J. Aal. Toxicol., 26, 144-148 (2002)

Tsai W.T., Yang J.M., Lai C.W., Cheng Y.H., Lin C.C. and Yeh C.W., "Characterization and adsorption properties of eggshells and eggshell membrane", Bioresource Technology 97 (2006) 488–493

Viraraghavan T., Alfaro F., "Adsorption of phenol from waste water by peat, fly ash and bentonite, Journal of Hazardous Materials, 57,59-70, 1998.

Wei . and Cao X., "Adsorption and catalytic processes of cyanide solutions and acid washed activated carbon", Carbon Vol. 31, No. 8. (1993)1319-1324.

White D.M., Pilon T.A. and Woolard C., "Biological treatment of cyanide containing wastewater", Wat. Res. Vol. 34, No. 7, Pp. 2105-2109, 2000.

Ye X., Kuklenyik Z., Needham L. L., Calafat A. M., Automated On-Line Column-Switching HPLC-MS/MS Method with Peak Focusing for the Determination of Nine Environmental Phenols in Urine, Anal. Chem., 77, 5407-5413 (2005)

Yeddou A.R., Nadjemi B., Halet F., Ould-Dris A. and Capart R., "Removal of cyanide in aqueous solution by oxidation with hydrogen peroxide in presence of activated carbon prepared from olive stones", Minerals Engineering ,23 (2010) 32–39.

Zhang W., Huang G., Wei J., Li H., Zheng R. and Zhou Y. "Removal of phenol from synthetic waste water using Gemini micellar-enhanced ultrafiltration (GMEUF)", Journal of Hazardous Materials 235– 236 (2012) 128– 137

Zhang W., Liu W., Lv Y., Li B. and Ying W., "Enhanced carbon adsorption treatment for removing cyanide from coking plant effluent", Journal of Hazardous Materials, 184,135–140, 2010.